Middle Atmosphere Program

HANDBOOK FOR MAP VOLUME 29

Edited by
J. Laštovička, Part 1
T. Miles and A. O'Neill, Part 2

ICSU

International Council of Scientific Unions

SCOSTEP

Scientific Committee on Solar-Terrestrial Physics
J. G. Roederer, President
W. I. Axford, Vice President
C. H. Liu, Scientific Secretary

MAP ORGANIZATION

MIDDLE ATMOSPHERE PROGRAM STEERING COMMITTEE

S. A. Bowhill, SCOSTEP, Chairman
K. Labitzke, COSPAR, Vice Chairman
C. H. Liu, SCOSTEP, Secretary

H. S. Ahluwalia, IUPAP
R. D. Bojkov, WMO
A. D. Danilov, COSPAR
J. C. Gille, COSPAR
I. Hirota, IUGG/IAMAP
A. H. Manson, SCOSTEP
T. Nagata, SCAR
R. G. Roper, IUGG/IAMAP
P. C. Simon, IAU
J. Taubenheim, IUGG/IAGA
T. E. VanZandt, URSI
R. A. Vincent, URSI

MAP STANDING COMMITTEES

Data Management -- G. Hartmann and I. Hirota, Co-Chairmen
Publications -- Belva Edwards, Chairman

MAP STUDY GROUPS

MSG-5 Ions and Aerosols, F. Arnold and M. P. McCormick, Co-Chairmen
MSG-8 Atmospheric Chemistry, G. Witt, Chairman
MSG-9 Measurement of Middle Atmosphere Parameters by Long Duration Balloon Flights, J. E. Blamont, Chairman

MAP PROJECTS

	Coordinator		Coordinator
AMA:	T. Hirasawa	MAC-SINE:	E. V. Thrane
ATMAP:	J. M. Forbes	MAE:	R. A. Goldberg
DYNAMICS:	K. Labitzke	MASH:	A. O'Neill
GLOBMET:	R. G. Roper	NIEO:	S. Kato
GLOBUS:	J. P. Pommereau	OZMAP:	D. F. Heath
GOSSA:	M. P. McCormick	SSIM:	P. C. Simon
GRATMAP:	D. C. Fritts	SUPER CAMP:	E. Kopp
MAC-EPSILON:	E. V. Thrane	WINE	U. von Zahn

MAP REGIONAL CONSULTATIVE GROUP

Europe: M. L. Chanin, Chairman

MIDDLE

ATMOSPHERE

PROGRAM

HANDBOOK FOR MAP

Volume 29

Part 1:
Extended Abstracts
International Symposium on Solar Activity
Forcing of the Middle Atmosphere
Part 2:
MASH Workshop, Williamsburg, 1986

Edited by
J. Laštovička, Part 1
T. Miles and A. O'Neill, Part 2

September 1989

Published for the ICSU Scientific Committee on Solar-Terrestrial Physics (SCOSTEP) with financial assistance from the National Aeronautics and Space Administration under the 1988 Middle Atmosphere Program Management Contract and Unesco Subvention 1988-1989.

Copies available from SCOSTEP Secretariat, University of Illinois, 1406 W. Green Street, Urbana, Illinois 61801.

PREFACE

The symposium "Solar Activity Forcing of the Middle Atmosphere" held on 3-8 April 1989 in the Castle of Liblice, Czechoslovakia was organized by the IAGA Working Group II.D "External Forcing of the Middle Atmosphere" (co-chairmen J. Laštovička and R.F. Donnelly) and by the Geophysical Institute of the Czechoslovak Academy of Sciences (director Prof. V. Bucha, past Vice-president of IAGA), and co-organized by the ICMUA/IAMAP Working Group on Solar-Terrestrial Relations. R.F. Donnelly, J. Laštovička (convenors), A. Ebel (ICMUA/ IAMAP) and J. Taubenheim (IAGA) were members of the Programme Committee. The Organizing Committee was chaired by J. Laštovička. The symposium was sponsored by IAGA and co-sponsored by the MAP Steering Commitee and by ICMUA/IAMAP.

80 scientists from 12 countries and 4 accompanying persons took part in the symposium. All facilities, including accommodation and board, were provided at the Castle.

19 invited, 26 contributed and 7 poster papers were presented at the symposium. The symposium consited of 8 blocks: 1. "Related" papers. 2. Influence of Quasi-Biennial Oscillation. 3. Influence of solar electromagnetic radiation variability. 4. Solar wind and high energy particle influence. 5. Circulation. 6. Atmospheric electricity. 7. Lower ionosphere. 8. "Solar" posters.

"Related" papers. Donnelly showed that for solar cycle 21, the maximum of the soft X-ray and ultraviolet solar flux, of the He I 1083 nm equivalent width and the net line-of-sight magnetic flux magnitude was attained in the second half of 1981, in R it was attained in late 1979, F10.7 displayed both peaks and the total solar irradiance appeared to decline since early 1979. Short-term variations of solar UV flux are very well measured and fairly well modelled. The observed UV changes during a part of solar cycles 21-22 represent about 30% of the observed variations of the total solar irradiance (London et al.). Bucha demonstrated the effects of geomagnetic activity on troposheric processes by implications to meteorological processes in Europe. Schuurmans presented some earlier results on proton flare influence on meteorological processes and their interpretation in the light of new findings in the Sun-atmosphere relationships.

A group of papers treated the role of Quasi-Biennial Oscillation (QBO) which seems to be of vital importance for long-term effects of solar activity on the atmosphere. Chanin used an extended set of data and demonstrated the opposite correlation of stratospheric (but not mesospheric) parameters with the solar cycle for west and east phases of QBO. This conclusion was confirmed by the analysis of rocket temperature profiles from Thumba, Volgograd and Molodezhnaya (Mohana kumar) and by the analysis of rocket and ionospheric observations by Taubenheim and Entzian, who also showed a direct solar-cycle control above 55 km (mesosphere). Kidiarova and Fomina demostrated combined solar cycle and QBO effects on the propagation of planetary wave energy. The 3-D model results of Dameris and Ebel show significant differences of the dynamical response of the middle atmosphere to weak external (solar) forcing for west and east phases of QBO. Tinsley pointed out the role of

galactic cosmic rays as carriers of solar variability to the lower ionosphere and introduced the QBO influence into this mechanism. Mohanakumar demonstrated the interrelated role of the solar cycle and QBO in the weather in South India.

Solar UV-flux variability and the middle atmosphere. This was the largest block (14 papers). A systematic depletion of ozone related to 27-day UV-variation is detected near 70 km, which is attributed to Lyman-alpha photodissociation of water vapour and to unexpectedly strong temperature/UV response (Keating). Chandra claims that the solar induced perturbations in temperature between 2-70 mb are too weak to be detected against the background dynamical temperature variations. Hood summarized some current work on measurement and interpretation of stratospheric ozone and temperature responses to observed short-term solar ultraviolet variations - there is clear correlative evidence of such a response at tropical latitudes where planetary wave amplitudes are relatively small. Danilin and Kouznetsov obtained from a 1-D photochemical model the maximum O_3 response to solar forcing at the equator in summer. Krivolutsky obtained theoretically the solar induced wave corresponding to a selected Rossby-Haurwitz mode (s=1, n=-5) and found strong evidence for the solar origin of the 27 day wave in the 30-mb level height. Krivolutsky and Loshkova found invariance of phase of the 27-day wave with height. Kidiyarova found a systematic difference between temporal variations of total ozone in spring in the 20th and 21st solar cycles. Chakrabarty et al. deduced NO concentrations in the mesosphere near the equator to be higher by a factor of about 5 in solar maximum compared with solar minimum based on electron density measurements at Thumba. Prasad et al. demonstrated total ozone influence on solar UV-B ground-based measurements.

The proposed physical mechanisms of solar induced variations in the middle atmosphere are often controversial in their physical consequences, which is among other things due to the complexity and non-linearity of the atmospheric response to comparatively weak solar activity forcing (Ebel). Zadorozhny et al. presented results of 1-D photochemical model studies of atmospheric response to solar forcing for clean versus anthropogenically polluted atmosphere. Atmospheric effects of the solar cycle in the UV-flux and particle precipitation were treated by Dyominov with the use of a 2-D model.

Solar wind and corpuscular effects in the middle atmosphere were reviewed by Laštovička, who e.g. presented a morphological model of the occurrence of the IMF sector boundary effects in the middle atmosphere. He considers the role of highly relativistic electrons to be the most important recent finding and the geomagnetic storm to be the most important disturbing factor of solar wind origin. Model computations by Jackman et al. indicate fairly good agreement with ozone data for the solar proton event-induced ozone depletion caused by NO_y species connected with the August 1972 events. Kudela claims that the main components of corpuscular radiation contributing to the energy deposition in the middle atmosphere are cosmic ray nuclei (galactic and solar) and high energy electrons, mainly of magnetosphe ric origin. The model calculations by Sosin and Skryabin yield an ozone content increase near 80 km about 3 days after an intense electron precipitation event, which coincides with observations. A new improved model of

(except for "solar" posters) appear in this issue of Handbook for MAP. The authors themselves are responsible for scientific level, language quality and mostly for technical level of camera-ready manuscripts published in this issue.

The successful symposium provided a relatively complex overview of the effects of solar activity influences on the middle atmosphere. Lively discussions of individual papers as well as many discussions outside of the meeting hall helped improve international collaboration.

cosmic ray - middle atmosphere interaction was pre sented by Vellinov and Mateev. Mateev et al. presented some model results on the penetration of MHD-waves detected in ionospheric cusps into the middle atmosphere.

Circulation. The best detected effects of solar activity in winds at heights of about 80-100 km are those of geomagnetic storms (short-term) and of solar cycle (long-term), as shown by Kazimirovsky. Gaidukov et al. observed interrelated solar and meteorological control of lower thermospheric winds near Irkutsk (Eastern Siberia).

The effects of solar activity on atmospheric electricity were reviewed by Reiter including historical development of this problem. Tyutin and Zadorozhny found a distinct dependence of the height profile of the electric field in the mesosphere at high latitudes on the magnitude of geomagnetic disturbance. Zhuang and Lu demonstrated the influence of the solar cycle, solar flares and the IMF sector structure on the occurrence frequency of thuderstorms and, thus, on atmospheric electricity in the Beijing area and the Northeast region.

A review of the effects of solar activity on the lower ionosphere was given by Danilov. He claims the direct positive influence of solar activity to be at least partly compensated by the indirect one through the effect of solar activity on the middle atmosphere as a whole. Satori found that the ionospheric effect of a Forbush-decrease of galactic cosmic rays could cause a decrease of electron density peaking near 70-72 km. The lower ionospheric plasma appears to be markedly controlled by the structure of IMF at high, auroral and sub-auroral latitudes (Bremer), the effect being less important in middle latitudes. Shirochkov presented a survey of the current knowledge of the PCA effects at polar latitudes. A considerable part of the 27-day oscillations in radio wave absorption in the lower ionosphere seems to be of meteorological (= neutral atmosphere) origin after Pancheva and Laštovička. De la Morena et al. state that if the solar Lyman-alpha flux variability is very well developed, then it dominates in the lower ionospheric variability; if it is developed rather poorly, the lower ionospheric variability is dominated by variations of meteorological origin.

Morozova proved the parameters of the statistical model of the SID occurrence to be dependent on the phase of the solar cycle. Křivský presented several delayed effects of solar proton qflares (starting a few hours after the flare occurrence), which were interpreted in terms of an enhanced flux of particles of subcosmic range. Murzaeva suggested a method of diagnostics of solar flare X-ray flux by means of multifrequency ground-based VLF measurements. On the basis of ionospheric data, Boška and Pancheva found the equatorward boundary of the auroral zone to have been shifted to geomagnetic latitudes below 50°N during and just after the extremely severe geomagnetic storm of February 1986. Zelenkova et al. calculated from riometric absorption the integral flux of precipitating electrons ($E > 40$ keV) and electron density profiles. Eliseev et al. observed disturbances of night-time high-latitude VLF propagation interpreted as a consequence of the influence of magnetospheric convection electric field on electron density in the lower ionosphere.

Extended abstracts (or abstracts) of all of the papers

PART 1

INTERNATIONAL SYMPOSIUM

"SOLAR ACTIVITY FORCING OF THE MIDDLE ATMOSPHERE"

Castle of Liblice, Czechoslovakia
3-8 April 1989

Preface iii
Table of Contents vii

RELATED PAPERS

R. F. Donnelly: Solar UV variability 1
J. London, J. Pap, G. J. Rottman: Observed solar near UV variability: a contribution to variations of the solar constant 9
V. Bucha: Effects of corpuscular radiation on weather and climate 13
C. J. E. Schuurmans: The tropospheric response pattern to solar activity forcing 22

QUASI-BIENNIAL OSCILLATIONS

M. L. Chanin: A review of the 11 year solar cycle, the QBO, and the atmosphere relationship 27
P. Keckhut, M. L. Chanin: Seasonal variation of the 11 year solar cycle effect on the middle atmosphere; role of the quasi-biennial oscillation 33
K. Mohanakumar: Influence of solar activity on middle atmosphere associated with phases of equatorial quasi-biennial oscillation 39
J. Taubenheim, G. Entzian, G. von Cossart: Solar activity influence on interannual climatic variations of mesosphere and stratosphere in mid-latitudes 43
V. G. Kidivarova, N. N. Fomina: The planetary waves dynamics and interannual course of meteorological parameters in the high latitude stratosphere and mesosphere of the Northern and Southern Hemispheres during the 20th and 21st solar cycles and different phases of QBO 47
M. Dameris, A. Ebel: The QBO and weak external forcing by solar activity: a three dimensional model study 49
B. A. Tinsley, G. M. Brown, P. H. Scherrer: Solar activity, the QBO, and tropospheric responses 53
K. Mohanakumar: A search for a solar related change in tropospheric weather 62

SOLAR ELECTROMAGNETIC RADIATION EFFECTS

G. M. Keating: The mesospheric response to short-term solar ultraviolet variability 67
S. Chandra: Response of the middle atmosphere to solar UV and dynamical perturbations 68
L. L. Hood: Stratospheric effects of solar ultraviolet variations on the solar rotation time scale 76
M. Yu. Danilin, G. I. Kouznetzov: Gases of the middle atmosphere and short-term solar radiation variations 82
A. A. Krivolutsky: Atmospheric planetary waves induced by solar rotation 86
A. A. Krivolutsky, O. A. Loshkova: Resonant Rossby waves and solar activity 92
I. N. Ivanova, A. A. Krivolutsky, V. N. Kuznetsova: On the relationship between the phases of 27-day total ozone and solar activity indices in different latitudinal zones 96
V. G. Kidiarova: Total ozone time variations during the spring reversals in the high latitudinal stratosphere and mesosphere of the Northern and Southern Hemispheres during the 20th and 21st solar cycles and different phases of QBO 100
G. A. Kokin, N. I. Brezgin, I. N. Ivanova, V. N. Kuznetsova, E. M. Larin, V. V. Sazonov, A. F. Chizhov, O. V. Shtirkov: The vertical ozone distribution during maximum and minimum solar activity 104
D. K. Chakrabarty, S. V. Pakhomov, G. Beig: Variation of D-Region nitric-oxide density with solar activity and season at the dip equator 108
B. S. N. Prasad, H. B. Gayathri, B. Narasimhamurty: Diurnal and temporal variation of UV-flux and its dependence on stratospheric ozone 112
A. Ebel: Physical mechanisms of solar activity effects in the middle atmosphere 116
A. M. Zadorozhny, I. G. Dyominov, G. A. Tuchkov: Numerical simulation of the middle atmosphere chemical composition and temperature under changing solar conditions 117
I. G. Dyominov: An influence of solar activity on latitudinal distribution of atmospheric ozone and temperature in 2-D radiative-photochemical model 118

SOLAR WIND AND CORPUSCULAR EFFECTS

J. Laštovička: Solar wind and high energy particle effects in the middle atmosphere 119

C. H. Jackman, A. R. Douglass, P. E. Meade: The effects of solar particle events on the middle atmosphere 129
K. Kudela: Energy deposition of corpuscular radiation in the middle atmosphere 135
I. I. Sosin, N. G. Skryabin: A change of mesospheric ozone content under electron precipitation influence 142
P. I. Vellinov, L. N. Mateev: Solar activity influence on cosmic ray penetration in the middle atmosphere 147
L. N. Mateev, P. I. Nenovski, P. I. Vellinov: Intensive MHD-structures penetration in the middle atmosphere initiated in the ionospheric cusp under quiet geomagnetic activity 151

CIRCULATION

E. S. Kazimirovsky: Lower thermosphere (80-100 km) dynamics response to solar and geomagnetic activity 156
V. A. Gaidukov, E. S. Kazimirovsky, E. I.Zhovty, M. A. Chernigovskaya: Solar activity effects in dynamical regime of the middle atmosphere over Eastern Siberia 164

ATMOSPHERIC ELECTRICITY

R. Reiter: Solar activity influences on atmospheric electricity and on some structures in the middle atmosphere 168
A. A. Tyutin, A. M. Zadorozhny: Measurements of mesospheric electric field under various geomagnetic conditions 178
H.-C. Zhuang, Yi.-C. Lu: Relationship between solar activities and thunderstorm activities in the Beijing area and the Northeast region of China 179

LOWER IONOSPHERE

A. D. Danilov: General overview of the solar activity effects on the lower ionosphere 183
G. Satori: Electron density profiles in the background of LF absorption during Forbush-decrease and PSE 192
J. Bremer: The influence of IMF on the lower ionospheric plasma in high and middle latitudes 196
A. V. Shirochkov: Solar cosmic ray effects in the lower ionosphere 203
D. Pancheva, J. Laštovička: Solar or meteorological control of lower ionospheric fluctuations (2-15 and 27 days) in middle latitudes 210

B. A. de la Morena, J. Laštovička, Z. Ts. Rapoport, L. Alberca: The 27-day versus 13.5-day variations in the solar Lyman-alpha radiation and the radio wave absorption in the lower ionosphere over Europe 215
L. P. Morozova: The probability of SWF occurrence in relation to solar activity 219
L. Křivsky: Post-flare effects in the lower ionosphere of middle latitudes 223
N. N. Murzaeva: Natural VLF emissions as a tool of diagnostics of X-ray flux of solar flares 227
J. Boška, D. Pancheva: Ionospheric effects of the extreme solar activity of February 1986 231
L. V. Zelenkova, V. A. Soldatov, J. V. Arkhipov, V. F. Laikova: On the relation between the electron content of the ionospheric D-region, variations of the riometer absorption, and the H-component of the geomagnetic field 236
A. Yu. Eliseev, Yu. V. Kashpar, A. A. Nikitin: Influence of non-stationary field of magnetospheric convection on the D-region 240

AUTHOR INDEX, Part 1 244

PART 2

MASH WORKSHOP - WILLIAMSBURG, VIRGINIA - APRIL 1986

T. Miles, A. O'Neill: Comparison of satellite derived dynamical quantities in the stratosphere of the Southern Hemisphere 245

PART 1

SOLAR UV VARIABILITY

Richard F. Donnelly

NOAA Air Resources Laboratory, Boulder, Colorado, U.S.A.

UV TRIAD

A new era in research of the temporal variations of solar UV radiation started on Nov. 7, 1978, with nearly daily measurements of the relative temporal variations of the solar UV flux in the 160 - 400 nm wavelength range by the Solar Backscatter Ultraviolet (SBUV) instrument on the NIMBUS7 satellite (HEATH, 1980). Similar SBUV/2 monitors have been operating on NOAA9 since April 1985 (DONNELLY, 1988b) and on NOAA11 since Nov. 1988, and are scheduled to fly on several more future NOAA satellites. The SBUV measurements form one part of a triad that is providing a major improvement in our understanding of solar UV flux variations.

The second part of the triad is the independent measurement of the solar UV flux in the 115 - 305 nm range from the SME satellite starting in October 1981 (ROTTMAN et al., 1982), which is still operating. A similar instrument is scheduled to fly on the UARS satellite in late 1991 as well as a SUSIM instrument (VANHOOSIER et al., 1981). These instruments are optimized for solar observations and include in-flight calibrations and reference components that are not routinely exposed to the space environment and solar UV radiation in order to detect instrument drift in the components used to make the daily measurements.

The triad's third part involves modeling the full-disk UV flux from spatially resolved measurements of solar activity (LEAN et al., 1982). This complements the corroborating measurements by providing a better physical understanding of why the UV variations have their observed temporal and wavelength dependences. Currently, quite crude scaled data of plage areas, brightness and location are used while an evolution toward more quantitative spatially-scanned data in the Ca K line from ground-based observatories is in progress.

UV instruments flown in space usually have problems with instrumentation drifts. Besides in-flight calibrations, rarely exposed reference components, occasional heating of some optical components to drive off surface contaminants and stowing of optical components when not in use, two other approaches to determine long-term variations are being used, namely: (1) relative photometry to increase long-term relative precision, like the Mg II core-to-wing ratio (HEATH and SCHLESINGER, 1986) and (2) shuttle-flight measurements of the solar UV spectral irradiance with excellent absolute flux accuracy using both SUSIM and also Simon's UV section of the European Spacelab instrument (LABS et al., 1987). These latter measurements are sometimes referred to as re-calibration measurements for the satellite monitors; or the satellite measurements may be viewed as providing the short-term (days, weeks) and intermediate-term (months) relative variations in the vicinity of these shuttle flight measurements to aid the interpretation of the long-term (years, solar cycle) changes.

SOLAR CYCLE VARIATIONS

Figure 1 shows several long-term trends during solar cycle 21. The measurements of the total solar irradiance (S) show daily data where the narrow lines extending 0.1 to 0.2% below the longer-term trend are dips caused by sunspot darkening and the long-term decline is interpreted as a decrese in

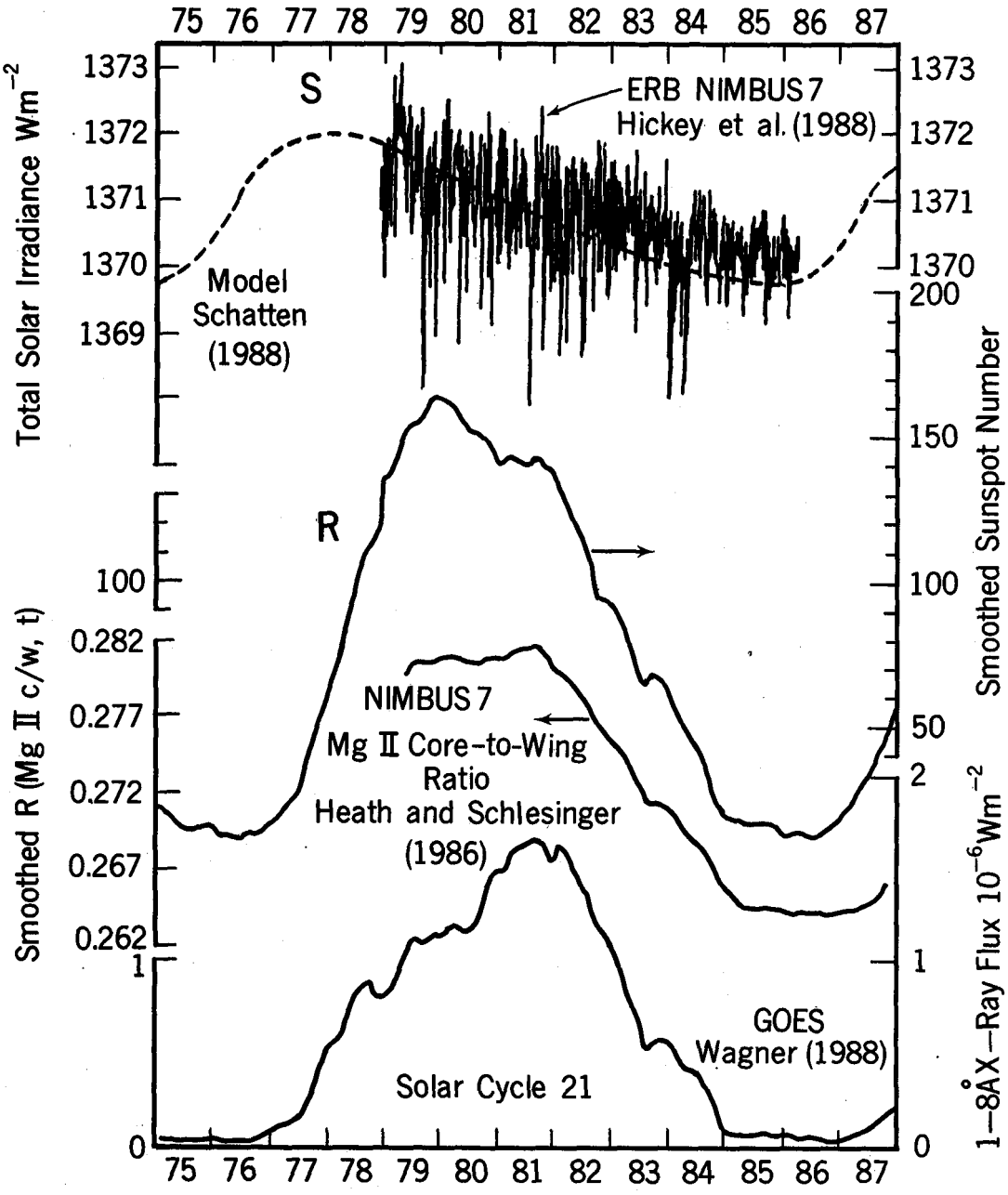

Figure 1. Solar cycle variations for the total irradiance, sunspot number, Mg II and soft X-rays. The bottom three curves are monthly values of annually smoothed data.

white-light facula brightening. The measurements suggest that the long-term maximum occurs either in early 1979 or before the measurements started. Either way, S peaks distinctly before the cycle maxima for the other three curves. Schatten's model for S(t) places the maximum for S almost two years earlier than that for the sunspot number (R). His model stresses the importance of the high contrast for white-light faculae at large solar central angles (60 - 90°) and such low contrast at small central angles (0 - 30°) that it is difficult to observe or detect faculae near the center of the disk. Schatten's model includes polar faculae, which have high central angles, contributing a peak effect after solar minimum, during the fast rise and early peak of his S(t) model. Also, the butterfly diagram of solar activity shows that regions tend to emerge at higher solar latitudes early in the cycle (30°) and progress toward the solar equator at the end of the cycle; so the contrasts of facula tend to be higher early in the cycle because their solar central angles are higher on average during their apparent passage across the solar disk. Conversely, sunspots have their maximum darkening as seen at Earth when they are at small solar central angles. Thus the solar cycle dependence of the active latitudes coupled with the white light contrasts for facula brightening and sunspot darkening and foreshortening of areas as a function of central angle cause the peak of the solar cycle dependence of S to occur earlier than for chromospheric and photospheric UV fluxes. Considering that the UV fluxes are not a negligible portion of S(t), and that the UV flux peaks later in the cycle, future revised models for S(t) will probably not peak quite as early as the dashed curve in Figure 1. Nevertheless, S appears to have a dull saw tooth appearance with a fast rise, early blunt peak and long slow decay with numerous narrow cracks caused by sunspot darkening.

The sunspot number R peaks in late 1979, about two years earlier than the UV flux; however R is strongly dominated by the number of groups of sunspots. The number of sunspots, excluding the number of groups, peaks about two years later than R and has a flatter peak (WILSON et al., 1987), which is more like the Mg II UV data in Figure 1. The chromospheric and upper photospheric UV flux variations caused by active regions are only weakly influenced by dark sunspots, filaments, etc., and are dominated by bright plages, plage remnants and numerous small active network features (LEAN et al., 1982). The solar central angle dependence of these features, combining contrast and foreshortening, has a fairly flat peak at small central angles or at the center of the sun viewed at Earth, dropping to about 40% near 60° and near zero at the limb (90°). This makes the solar UV flux at Earth slightly less sensitive to the high latitude regions at the start of a new cycle but fairly insensitive to the latitudes of the regions throughout the rest of the cycle. Note that the shape of the solar cycle curve for the UV Mg II ratio is fairly flat in 1985 and 1986.

The soft X-ray flux has a much higher peak in late 1981 than its level in late 1979 than do the UV fluxes observed by NIMBUS7 in the 170 - 300 nm range. This implies the net emission measure of hot cornal plasma at $T > 3 \times 10^6$ °K is significantly higher in late 1981, which implies higher emission of the coronal Fe XV line at 284 A and Fe XVI line at 335 A in late 1981 than in late 1979. RYBANSKI et al. (1988) showed that the Fe XIV green line coronal index also has a much higher long-term peak in late 1981 than in late 1979. Although AE-E measurements of the Fe XV and XVI EUV lines in 1977-1980 were closely correlated with the Ottawa 10.7 cm flux (F10) during the early rise of solar cycle 21, these soft X-ray and green line results imply the AE-E measurements significantly missed the solar cycle peak fluxes for EUV coronal lines. F10, which will be shown below to have a solar cycle shape like that for the chromospheric Mg II data, does not have a solar cycle shape like that for the coronal soft X-ray flux and green line; therefore, F10 does not represent well the temporal

shape of solar cycle variations of coronal emissions. In Figure 1, note the low flat levels at solar cycle minimum for the soft X-rays in 1975, 1976, 1985 and 1986, i. e. the hot coronal emission ($T > 3x10^6$ K) drops to negligible low levels for about two years at the solar cycle minimum.

The main purpose of Figure 1 is to illustrate that the solar cycle shape of solar fluxes and activity indices varies from an early peak in S(t) to much later peaks in the UV flux and soft X-rays. Secondly, the ratio of the maximum flux to minimum is about 0.1% for S(t), 7% for the UV Mg II core-to-wing ratio to more than 85x's for the 1 - 8 A soft X-rays for annually smoothed data.

Figure 2 shows daily values of F10 (the best of the currently available ground-based daily measures of solar activity), Lyman alpha flux (the best measure of solar activity in the top of the chromosphere and base of the transition region from the SME satellite) and the combined Mg II core-to-wing ratio from the NIMBUS7 and NOAA9 satellites for solar cycle 21 and the rise of cycle 22 (used here as being representative of the temporal shape of the UV flux variations in the 175 - 285 nm range, HEATH and SCHLESINGER, 1986; DONNELLY, 1988b). Notice the very flat background (excluding the occasional solar-rotational spike) in 1985 and 1986 in F10, a quite flat background but with a little more curvature in the Mg II UV data (with more numerous short-term spikes), and the even greater long-term curvature in the Lyman alpha data. So we see minor differences in the long-term variations or shape of the solar cycle among these three data sets. R(MgIIc/w) reached 60% higher in Jan. 1989 (not shown) than the highest values shown in mid 1988 relative to the solar minimum values in Sept. 1986, which is already as high as being just below the annual average for the peak of solar cycle 21. So we expect solar cycle 22 to have as strong or stronger UV and EUV emission as in cycle 21.

INTERMEDIATE-TERM VARIATIONS

Intermediate-term variations last from about 4 to 11 months and may be considered to be of two types. An example of the first type can be seen in all three data sets in Figure 2, peaking in early 1984 and lasting about 11 months. Other such variations are evident in 1982 and 1983. They are also present in 1978 - 1981, but one may want to smooth out the solar rotational variations to see them more clearly. Neglecting the short-term variations, notice how similar in temporal shape the intermediate-term variations are in these three data sets and how their amplitude relative to the solar cycle minimum-to-maximum amplitude is about the same. Notice that these intermedite-term variations are very weak or absent in F10 and quite weak in the Mg II UV data in 1985 and 1986 during solar cycle minimum but fairly strong throughout 1978 through mid 1984. These variations are related to increases and decreases in the number of active regions where the regions are widely distributed in solar longitude so that the average per rotation varies.

Figure 3 shows short-term solar rotational variations and a mixture of the two types of intermediate variations. The second type of intermediate variation involves a modulation of the solar-rotational amplitudes over a four to nine month interval. For example, after the tick marked May 30, there is a small rotational peak (at the time of a dip in S from sunspot darkening) followed by two giant ones and then three medium solar rotational peaks. That train of peaks spaced fairly evenly in time is then followed by new peaks at a different phase in the solar rotation. Note that the giant peak in July is partly so large because the amplitude of the rotational minima has been decreasing for several rotations. The two types of intermediate-term variations involve the same physical process of the emergence and evolution of groups of active regions; they are analogous to mathematically separating the longitudi-

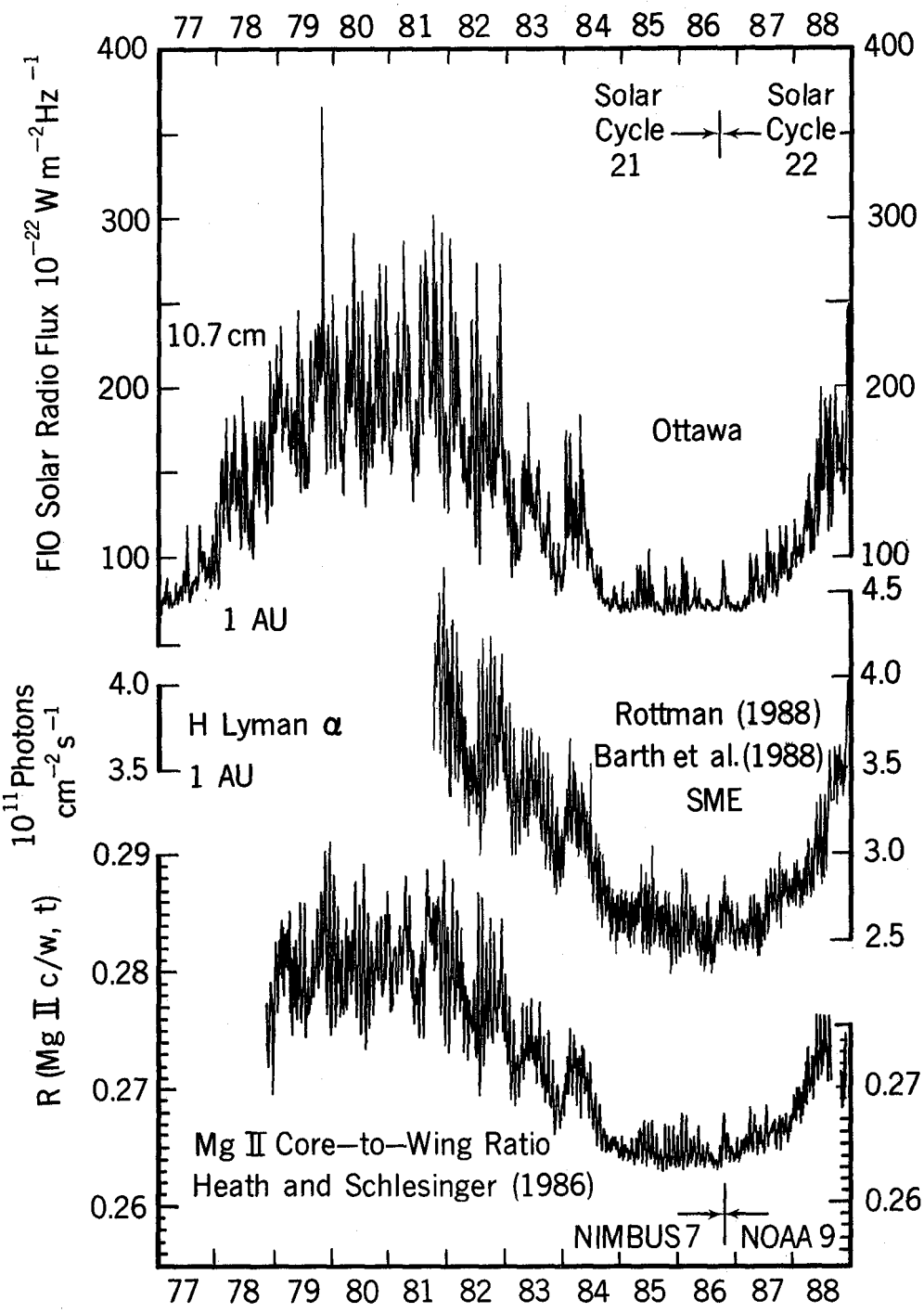

Figure 2. Solar cycle 21 and the rise of cycle 22 for F10, H Lyman alpha, and R(MgIIc/w), first from NIMBUS7 and then from NOAA9 after Oct. 1986.

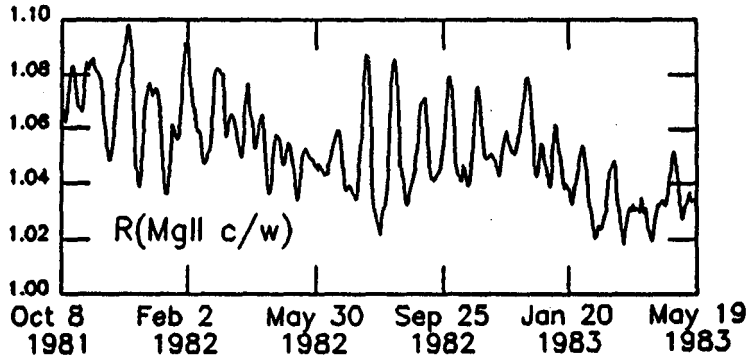

Figure 3. The NIMBUS7 Mg II core-to-wing ratio normalized to the monthly average of Sept. 1986 at the solar cycle minimum.

nal distribution of activity into a rotational average value and the deviations from the average. Sometimes two of the second type appear to form one of the first type as follows. For example, an episode of major activity emerged in August 1979. As the amplitudes of the rotational peaks rose and then decayed, the amplitude of the rotational minima steadily rose. Another episode of major activity then emerged in November 1979. While its rotational peaks rose and then decayed, the rotational minima also rapidly decreased in amplitude. See Figure 2. There is a tendency to think that rapid flux changes are only related with the emergence of new activity and the influence of plage remnants leads to slower decreases in flux. However, quite large decreases in flux do occur from one rotation to the next probably due to a rapid decrease in the rate of emergence of activity.

One difference in the two types of intermediate term variations is that for the second type, the amplitude modulation of the solar rotational variations caused by a major group of active regions, F10 rises more rapidly, peaks earlier and decays faster than for the UV fluxes (DONNELLY et al., 1983). For example, just above the dividing line between NIMBUS7 and NOAA9 data in Figure 2, one sees an isolated peak in F10 but several small subsequent solar rotational variations in Mg II and Lyman alpha. In 1985 and 1986, there are fewer solar-rotational peaks in F10 than in the UV data. Conversely, there is good agreement for F10, Lyman alpha and Mg II in the size and shape of the first type of intermediate-term variation relative to the solar-cycle amplitude.

So far, research of the atmospheric effects of solar UV variations has concentrated on the short-term variations because they were the first data available, the consequent effects in ozone and temperature could be clearly identified in stratospheric measurements, and interesting complications between the early model results and the observed effects were discovered. Analysis of these intermediate-term variations will likely be the next area of active research, although CHANDRA (1989) has shown it will be difficult to identify their stratospheric effects. Note that their durations vary significantly from one to another in Figure 2, i. e. they are not a simple periodicity.

SHORT-TERM VARIATIONS

Solar UV fluxes vary over days to weeks due to the evolution of active regions and the strong modulation caused by the combination of solar rotation and the strong decrease in UV flux emission with increasing solar central angle for the location of the region as viewed from Earth. The solar rotation modulation causes the time series in Figure 3 to be full of narrow peaks. The

fact that no two of these peaks are of equal amplitude or are identical in relative shape is a consequence of the combined effects of the temporal evolution of several active regions. Note that the amplitude of these short-term variations are quite large, frequently about as large as half the smoothed solar cycle increase. See Figure 2. The amplitude of the giant solar-rotational variation in the center of Figure 3 is more than 80% of the smoothed solar cycle amplitude. Figure 3 shows weak 13-day periodicity (two peaks per rotation) mixed with 27-day periodicity in March and April 1982, and in Dec. 1982 and Jan. 1983, which is a common occurrence in UV fluxes.

The short-term variations differ significantly in F10 relative to those in the UV flux, e. g. the lack of 13-day periodicity in F10, the faster rise, earlier peak and quicker decay in F10 of episodes of 27-day solar rotational variations caused by major groups of active regions (DONNELLY et al., 1983), a larger half-maximum width of the 27-day solar rotational variations for F10, and the larger amplitude of the short-term variations relative to the smoothed solar cycle amplitude in F10 (DONNELLY, 1987). Some authors refer to a good agreement between F10 and UV fluxes while others emphasize the disagreements; the former are usually refering to comparisons of long-term variations and the latter to short-term variations.

Mg II CORE-TO-WING RATIO

The short-term variations of the solar UV flux within the 175 - 285 nm range have been shown to be highly uniform in temporal shape, although the percentage amplitude varies with wavelength (HEATH and SCHLESINGER, 1986; DONNELLY, 1988b). This uniformity is interpreted to be caused by the solar central angle dependence of active region emission and the strength of one region relative to another as a function of time being uniform over this wavelength range because the source regions are essentially the same. This uniformity does not extend to all wavelengths, which is drastically evident in Figure 1. But within this limited wavelength range, the uniformity of souce regions and emission and absorption mechanisms suggests that the intermediate and long-term variations also have uniform temporal shapes, which is the assumption used when applying the Mg II core-to-wing ratio to estimate the long-term variations of the UV flux within the 175 - 285 nm range. Indeed, in the cases of F10 and Lyman alpha, where large and small differences, respectively, are known to occur for short-term variations with respect to the UV flux within the 175 - 285 nm range, the long- and intermediate-term variations for both F10 and Lyman alpha are fairly similar to those of the Mg II line in Figure 2.

GROUND-BASED MEASURES OF SOLAR ACTIVITY

The correlation coefficient for the NIMBUS7 or NOAA9 Mg II core-to-wing ratio with respect to the Ca K 1A index is about 0.98. It appears to be the best ground-based measure for estimating solar UV fluxes. Unfortunately, it is not available daily. The He I 10830 A data is probably not as closely related to the UV flux variations, but it is available almost daily and will be useful for occasionally estimating UV fluxes missing in the satellite measurements. F10 is useful for estimating the short-term variations of coronal EUV fluxes. For chromospheric EUV fluxes and chromospheric and upper photospheric UV fluxes, F10 is helpful for long-term and intermediate-term variations, but not for short-term variations. Figure 1 show that sunspot numbers are not very useful for estimating UV flux variations. The calcium plage index is helpful only for short-term variations; it fails for intermediate- and long-term variations because of numerous small bright features not included in the scaled data that are important for the UV flux. Digitized raster-scans of the solar disk in the Ca-K line should overcome the shortcomings in the older plage index.

CONCLUSIONS

Twenty years ago, we knew the general spectral shape of solar UV fluxes but not much about their temporal variations. Today, several satellites provide daily solar UV measurements and better instruments will soon be flown. (It is amazing there are no monitoring measurements of the solar EUV flux below 115 nm!) Short-term variations are very well measured and fairly well modelled. Intermediate-term variations are the next active area for intercomparing different satellite measurements, modeling the UV fluxes and researching their stratospheric effects.

REFERENCES

Barth, C.A., W.K. Tobiska, and G.J. Rottman, Comparison of the solar Lyman alpha flux with the solar 10.7 cm radio flux, EOS, 69, 1354, 1988.

Chandra, S., Response of the middle atmosphere to solar and dynamical perturbations, this volume, 1989.

Donnelly, R.F., D.F. Heath, J.L. Lean and G.J. Rottman, Differences in the temporal variations of solar UV flux, 10.7-cm solar radio flux, sunspot number, and Ca-K plage data caused by solar rotation and active region evolution, J. Geophys. Res., 88, 9883, 1983.

Donnelly, R.F., Temporal trends of solar EUV and UV full-disk fluxes, Solar Phys., 109, 37-58, 1987.

Donnelly, R.F., The solar UV Mg II core-to-wing ratio from the NOAA9 satellite during the rise of solar cycle 22, Adv. Space Res., 8, (7)77-(7)80, 1988a.

Donnelly, R.F., Uniformity in solar UV flux variations important to the stratosphere, Annales Geophys., 6, 417-424, 1988b.

Heath, D.F., A review of observational evidence for short and long term ultraviolet flux variability of the sun, Sun and Climate, CNES, 18 Ave. Edouard - Belin, 31055 Toulouse Cedex, France, 447-471, 1980.

Heath, D.F., and B.M. Schlesinger, The Mg 280-nm doublet as a monitor of changes in solar ultraviolet irradiance, J. Geophys. Res. 91, 8672, 1986.

Hickey, J.R., B.M. Alton, H.L. Kyle, and D. Hoyt, Total solar irradiance measurements by ERB/NIMBUS-7. A review of nine years, Space Sci. Rev., 48, 321-342, 1988.

Labs, D., H. Neckel, P. C. Simon and G. Thuillier, Ultraviolet solar irradiance measurement from 200 to 358 nm during Spacelab 1 mission, Solar Phys., 107, 203-219, 1987.

Lean, J.L., O.R. White, W.C. Livingston, D.F. Heath, R.F. Donnelly, and A. Skumanich, A three-component model of the variability of the solar ultraviolet flux: 145-200 nM, J. Geophys. Res., 87, 10307-10317, 1982.

Rottman, G.J., Observations of solar UV and EUV variability, Adv. Space Res., 8, (7)53-(7)66, 1988.

Rottman, G.J., C.A. Barth, R.J. Thomas, G.H. Mount, G.M. Lawrence, D.G. Rusch, R.W. Sanders, G.E. Thomas and J. London, Solar spectral irradiance, 120 - 190nm, October 13, 1981 - January 3, 1982, Geophys. Res. L., 9, 587, 1982.

Rybansky, M., V. Rusin, and E. Dzifcakova, Coronal index of solar activity, V. Years 1977-1986, Bull. Astron. Inst. Czechosl., 39, 106-119, 1988.

Schatten, K.H., A model for solar constant secular changes, Geophys. Res. L., 15, 121-124, 1988.

VanHoosier, M.E., J.-D.F. Bartoe, G.E. Brueckner, D.K. Prinz, and J.W. Cook, A high precision solar ultraviolet spectral irradiance monitor for the wavelength region 120-400 nm, Sol. Phys., 74, 521-530, 1981.

Wagner, W.J., Observations of 1-8A solar x-ray variability during solar cycle 21, Adv. Space Res., 8, (7)67-(7)76, 1988.

Wilson, R.M., D. Rabin, and R.L. Moore, 10.7-cm solar radio flux and the magnetic complexity of active regions, Solar Phys., 111, 279-285, 1987.

OBSERVED SOLAR NEAR UV VARIABILITY: A CONTRIBUTION TO VARIATIONS OF THE SOLAR CONSTANT

Julius London[1], Judit Pap[1], and Gary J. Rottman[2]

University of Colorado, Boulder, CO 80309 USA
[1]Department of Astrophysical, Planetary and Atmospheric Sciences
[2]Laboratory for Atmospheric and Space Physics

Abstract

Continuous Measurements of the Solar UV have been made by an instrument on the Solar Mesosphere Explorer (SME) since October 1981. The results for the wavelength interval 200–300 nm show an irradiance decrease to a minimum in early 1987 and a subsequent increase to mid–April 1989. The observed UV changes during part of solar cycles 21–22 represent approximately 35 percent (during the decreasing phase) and 25 percent (during the increasing phase) of the observed variations of the solar constant for the same time period as the SME measurements.

Solar irradiance received by the earth–atmosphere system and its latitude distribution represents the ultimate driving force for the ocean/atmosphere circulation and long–term climate of the system. How the system generally responds to the imposed external driving force is reasonably well known. However, many of the details of this response are not as well understood. They originate, from complex spatial interactions and multiprocess non–linear feedbacks, both positive and negative (see, for instance HANSEN et al., 1984). Some theories of solar induced climate variations are based, in part, on whether perturbations of the solar irradiance are effective primarily at the earth's surface (sea surface) (e.g., REID and GAGE, 1988) or in the middle atmosphere (e.g., RAMANATHAN, 1982).

Many models of climate variability involve changes of the total solar irradiance, the solar constant, without regard to the wavelength dependence of such changes. The atmospheric penetration of solar radiation, however, is a significant function of wavelength. It is, therefore, important to determine the spectral distribution of the different contributions to observed solar constant variations. As far as we know, measurements of the time variations of these contributions are currently available only for UV wavelengths. If the recent suggestion (KUHN et al., 1988) of latitude–dependent solar surface temperature variations contribute significantly to the observed solar constant changes, it should be possible to verify this contribution by monitoring the solar irradiance spectral distribution in the visible and near–infrared. Although solar irradiance below 300 nm represents only 1.1 percent of the solar constant, time variations of its relative energy are significantly larger than those of the solar constant (see, for instance, LONDON et al., 1984).

Estimates of the solar constant and its temporal changes have been made using ground–based, balloon, rocket, and satellite measurements (e.g., FRÖHLICH, 1977). The most consistent set of time monitored measurements made so far are the results of satellite observations from two different cavity radiometer type experiments: the Earth Radiation Budget (ERB) Nimbus–7 (e.g., HICKEY et al., 1988) and the Active Cavity Radiometer Irradiance Monitor, Solar Maximum Mission (ACRIM I SMM) (e.g., WILLSON et al., 1986; WILLSON and HUDSON, 1988) programs. Each instrument is capable of observing the total solar irradiance over a spectral range that extends from the short UV to the far IR. The ERB Nimbus–7 measurements started in November 1978, the ACRIM I SMM measurements started in February 1980. Both programs continue to function as of 1 March 1989. For the time period 1980–1987 they each reported approximately 300 mean daily measurements per year. Although there is an average 0.2 percent difference in reported solar constant values, the data from the two systems track each other quite well over the long period of overlapped observations. When the data were subjected to an 81–day smoothing filter, the correlation between the two observation sets was +0.93 for the period Jan 1980–May 1986, largely as a result of the consistent downward trend shown by the two data sets. For the early period of solar cycle 22, (Jun 1986–Oct 1987) the correlation fell to +0.71. For the daily means, the correlations were +0.79 and +0.22 for the two periods respectively. The 81–day smoothed

data sets are shown for the period Jan 1980–May 1988 in Fig. 1. Additional ACRIM I data to mid–1988 (WILLSON and HUDSON, 1988), not shown in Fig. 1, also indicate a continued sharp increase in solar constant values starting in early 1987.

Measurements of the time variations of solar UV irradiance have been recently reviewed by (LEAN, 1987). The most relevant observations available for estimating the contribution of long period UV irradiance variations to those of the solar constant are observations derived from the UVS Solar Mesosphere Explorer (SME) instrument. These SME measurements cover the wavelength interval 120–300 nm. The observations started in October 1981 and were terminated in mid–April 1989. Details of the SME experiment, including relative accuracies at different wavelengths are discussed in ROTTMAN, 1987 and references therein. An estimate of UV (175–400 nm) variations (HEATH and SCHLESSINGER, 1984) is also derived from measurements from the Solar Backscatter Ultraviolet (SBUV) instrument on Nimbus–7.

The observed day–to–day solar constant measurements are quite noisy, and we, therefore, used an 81–day running mean as a filter for both the SME and ERB Nimbus–7 data sets covering the time interval 1 Jan 1982 to 30 Apr 88, the coincident period for which data from both programs are available.

The 81–day smoothed time variations of the SME total solar irradiance for the spectral interval 200–300 nm and the ERB Nimbus–7 solar constant values for the 6–1/3 year period are shown in Fig. 2. The UV values show an average decrease from Jan 1982 to a minimum in mid–March 1987. During this period there is an indicated oscillation with an average period of about 230 days and decreasing amplitude up to the time of minimum. This oscillation is found at almost all of the 5 nm subintervals contributing to the total SME curve given in Fig. 2. with very good coherence in phase. The ERB Nimbus–7 solar constant data show long–term decreasing values up to early 1986, some increase to mid–1987 and then a pronounced rise in the solar constant values consistent with the UV increase. There is, however, only a loosely corresponding shorter period oscillation analogous to that seen with the solar UV data.

Slope of Trend Line for SME UV Solar Irradiance(*10(-4) W/m^2 yr):

Wavelength (nm)	Slope (a)	Slope (b)
200-205	-4.9	10.9
205-210	-9.2	13.1
210-215	-10.7	31.2
215-220	-16.6	32.5
220-225	-37.5	26.3
225-230	-17.9	46.8
230-235	-29.0	24.7
235-240	-25.1	64.5
240-245	-33.9	29.2
245-250	-16.8	30.3
250-255	-17.8	35.5
255-260	-36.0	36.7
260-265	-32.5	26.4
265-270	-60.5	76.8
270-275	6.0	117.5
275-280	-52.1	434.3
280-285	-38.6	42.1
285-290	-41.6	117.7
290-295	-101.3	76.8
295-300	-38.6	105.3
200-300	-609.1	1406.8
ERB (SC)	-1797.0	6189.0
ACRIM (SC)	-1957.7	531.5

(a) 1 Jan 1982 - 30 May 1986
(b) 1 Jan 1987 - 30 Apr 1988

The UV and solar constant data sets were divided into two intervals covering the joint descending and ascending period of the observed irradiance values in each set. SME observed data were averaged over 5 nm intervals. The computed slope for each 5 nm interval for the two different period as well as the total spectral variation (200–300 nm) and the associated

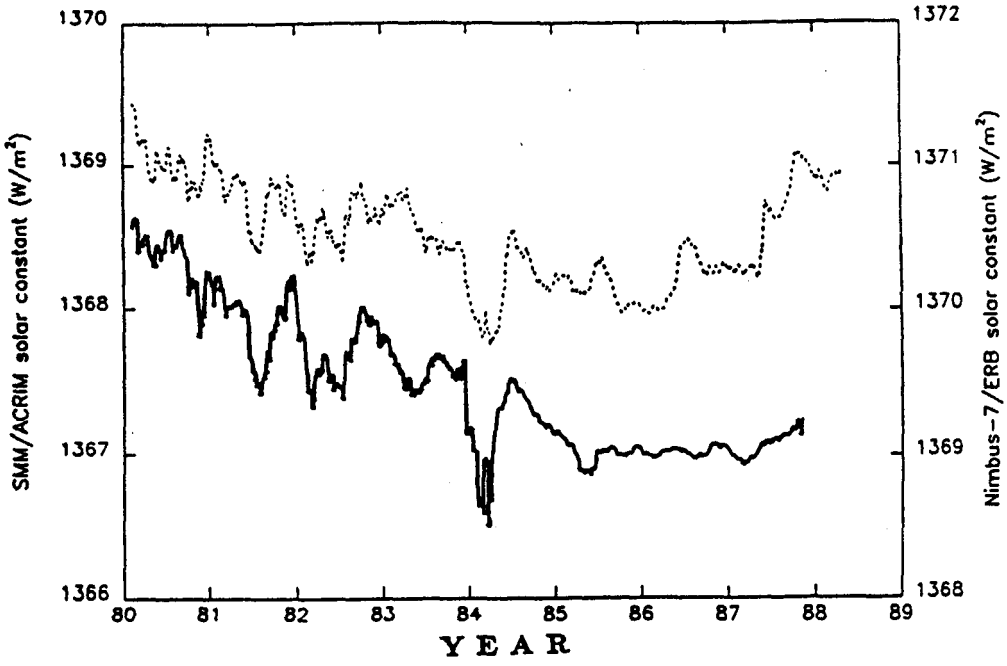

Fig. 1. **Solar constant observations, 81-day running means, from the ACRIM I (heavy line) and ERB (dashed line) experiments.**

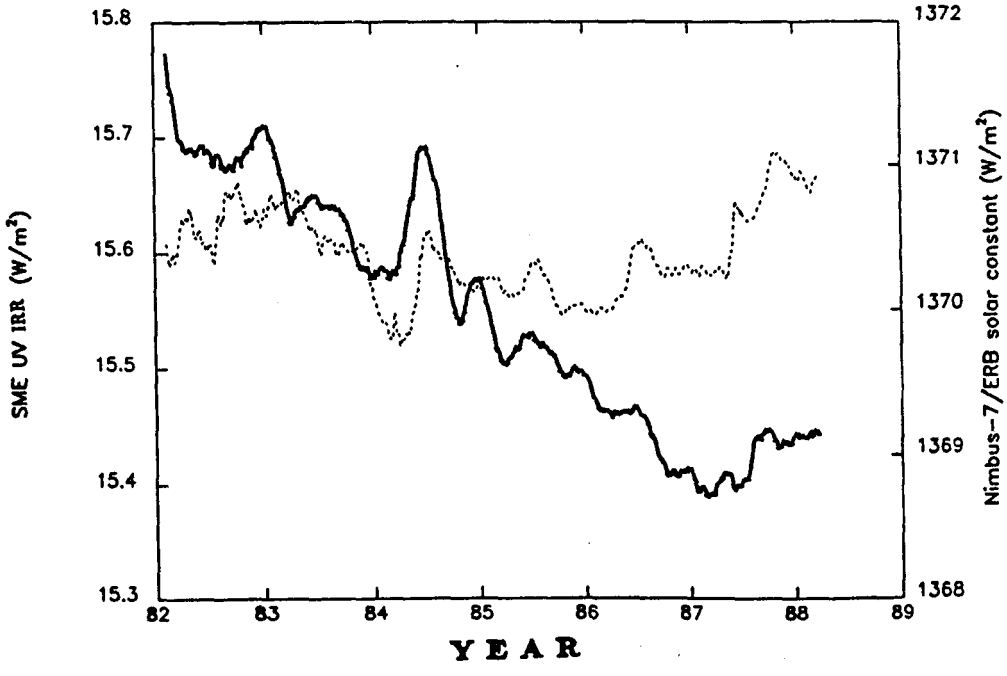

Fig. 2. **Solar UV (200-300 nm) (heavy line) and ERB solar constant measurements (dashed line) 81-day running means for the period starting Jan 1982. (See text for details).**

ERB change for each period are given in Table 1. For the negative phase of solar cycle 21 the UV decrease is about –0.06 $Wm^{-2}yr^{-1}$. The observed solar constant decrease is about 0.180 $Wm^{-2}yr^{-1}$ (ERB) or 0.196 $Wm^{-2}yr^{-1}$ (ACRIM) giving an average UV contribution to the solar constant change during this period of about 32 percent. For the relatively short period shown for the increasing phase of cycle 22, the values are 0.14 $Wm^{-2}yr^{-1}$ and 0.62 $Wm^{-2}yr^{-1}$ (ERB), giving a percent contribution of the UV irradiance to the observed solar constant increase of about 22.7 percent. As can be seen from the results shown in Table 1, most of the large contributions are contained in the wavelength region 265–300 nm, although, for reasons unknown to us at present, there is a small increase in the spectral interval 270–275 nm. Most of the UV energy beyond 265 nm is absorbed in the lower and middle stratosphere (20–40 km) (see, for instance, BRASSEUR AND SOLOMON, 1986). Thus, we see that a significant portion (~25–35 percent) of the observed solar constant variation is absorbed at levels above the troposphere where there may be important effects on the time varied radiation budget. These effects need to be included in models of solar influences on climate variations.

Acknowledgements

We would like to thank H. Lee Kyle and R. C. Willson for making available to us the solar constant data used in our analysis. We also thank Kristin Hoyer and Barry Knapp for programming assistance. One of us (J.P.) acknowledges with appreciation partial support as a grant–in–aid from the Graduate School (CRCW), University of Colorado. This study was supported by research grants NSG 5153 and UARA/NAS5–27263 from the National Aeronautics and Space Administration. The SME project is supported by NASA under contract number NASW–4091.

References

Brasseur, Guy and Susan Solomon, 1986. *Aeronomy of the Middle Atmosphere.* Dordrecht: D. Reidel Publishing Co.

Fröhlich, C., 1977: *Solar Constant in the Solar Output and Its Variation.* Oran W. White (ed.), Boulder: Colorado Associated University Press, 93–109.

Hansen, J., A. Lacis, D. Rind, G. Russels, P. Stone, I. Fung, R. Ruedy, and J. Lerner, 1984: *Climate Sensitivity: Analysis of Feedback Mechanism*, J. E. Hansen and T. Takahashi, eds., Am. Geophys. Union, 130–163.

Heath, Donald F. and Barry M. Schlesinger, 1984: Temporal Variability of UV Solar Spectral Irradiance from 160–400 nm over Periods of the Evolution and Rotation Regions from Maximum to Minimum Phases of the Sunspot Cycle. *Proceedings of the International Radiation Symposium*, G. Fiocco, ed., Perugia, Italy, August 1984, 315–319.

Hickey, John R., 1988: Total Solar Irradiance Measurements by ERB/Nimbus 7. A Review of Nine Years. *Sp. Science Rev.*, **48**, 3211–342.

Kuhn, J. R., K. G. Libbrecht, and R. H. Dicke, 1988: The Surface Temperature of the Sun and Changes in the Solar Constant, *Science*, **242**, 908–911.

Lean, Judith L., 1987: Solar Ultraviolet Irradiance Variations: A Review. *J. Geophys. Res.*, **92**, 839–868.

London, J., G. G. Bjarnason, and G. J. Rottman, 1984: 18 Months of UV Irradiance Observations from the Solar Mesosphere Explorer, *Geophys. Res. Lett.*, **11**, 54–56.

Ramanathan, V., 1982: Coupling through Radiative and Chemical Processes, in *Solar Variability, Weather and Climate.* Studies in Geophysics. Nat. Res. Counc., 83–91.

Reid, George C. and Kenneth S. Gage, 1988: The Climatic Impact of Secular Variations in Solar Irradiance. Sec. Sol. and Geomag. Var. Stephenson, R. F. and N. V. Wolfendale (eds.), Kluwer Acad. Publ., 225–243.

Rottman, Gary J., 1987: Results from Space Measurements of Solar UV and EUV Flux, Proceedings of Workship, *Solar Radiative Output Variations*, Peter Foukal, ed., NCAR, Boulder, CO, 71–86.

Willson, R. C., H. S. Hudson, C. Fröhlich, and R. W. Brusa, 1986: Long–Term Downward Trend in Total Solar Irradiance, *Science*, **234**, 1114–1117.

Willson, Richard C. and H. S. Hudson, 1988: Solar Luminosity Variations in Solar Cycle 21. *Nature*, **332**, 810–812.

EFFECTS OF CORPUSCULAR RADIATION ON WEATHER AND CLIMATE

V. Bucha

Geophysical Institute, Czechosl. Acad. Sci., Boční II, 141 31 Praha 4, Czechoslovakia

INTRODUCTION

HARRY VAN LOON and JEFFERY C. ROGERS (1978) have investigated the wellknown tendency for winter temperatures to be low over northern Europe when they are high over Greenland and the Canadian Arctic, and conversely (Fig. 1).Well-defined pressure anomalies over most of the Northern Hemisphere are associated with this regional seesaw in temperature, and these pressure anomalies are so distributed that the pressure in the region of the Icelandic low is negatively correlated with the pressure over the North Pacific Ocean and over the area south of 50°N in the North Atlantic Ocean, Mediterranean and Middle East, but positively correlated with the pressure over the Rocky Mountains. Since 1840 the seesaw, as defined by temperatures in Scandinavia and Greenland, occurred in more than 40% of the winter months and the occurrences are seemingly not randomly distributed in time as one anomaly pattern would be more frequent than the other for several decades. For this reason the circulation anomalies in the seesaw come to play an important part in deciding the level of regional mean temperatures in winter and thus in deciding the long-term temperature trends. These regional temperature trends are then closely associated with changes in frequency of atmospheric circulation types, and it is therefore unikely (VAN LOON, ROGERS, 1978) that the trends are caused directly by changes in insolation or in atmospheric constituents and aerosols.

RESULTS

Changes in winter temperature (Nov. Dec. Jan. Feb.) in Oslo have a similar character as in Prague. Fig. 2 shows a comparison of changes in geomagnetic activity (C indices) with winter temperatures at several sites, Prague and Oslo which are positively correlated, and Jakobshavn and Walla-Walla which are negatively correlated. Very expressive is the positive correlation between the geomagnetic activity and temperature in Prague (c.c.0.63) . This seems to be in favour with the fact that the increased corpuscular (geomagnetic) activity is connected with the prevailing zonal type of atmospheric circulation (r.h.s. of Fig. 2 bottom) leading to the warming in Prague and Oslo. On the other hand at the time of low corpuscular activity the meridional type prevails (r.h.s. of Fig. 2 top) and causes the cooling in Prague and Oslo due to the prevailing flow from the North during low geomagnetic activity at these sites, while Jakobshavn and Walla - Walla are at the same time under the influence of warm air from the south along the western side of mighty high pressure areas.

This relation can be seen also in Fig. 3 showing that below normal temperatures in Prague (10 cases) occurred at the time of low geomagnetic activity and above normal temperatures (10 cases) correspond to high geomagnetic activity.

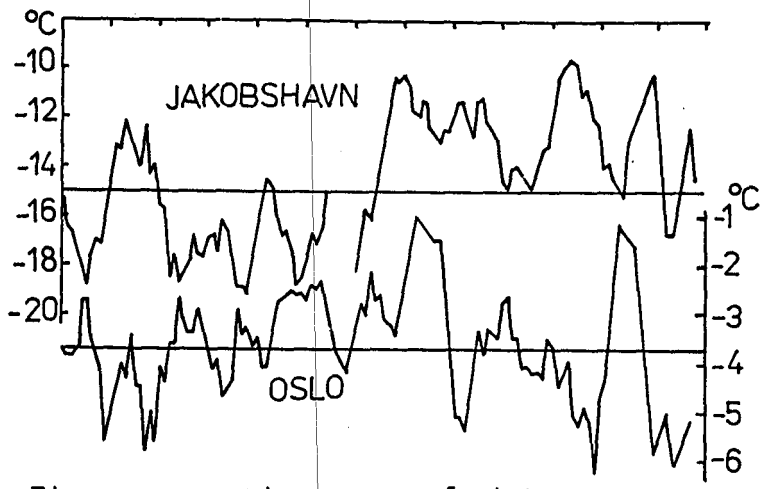

Fig. 1. Five-year running means of winter temperature at Jakobshavn and Oslo (°C) (H.VAN LOON and J.C.ROGERS,1978).

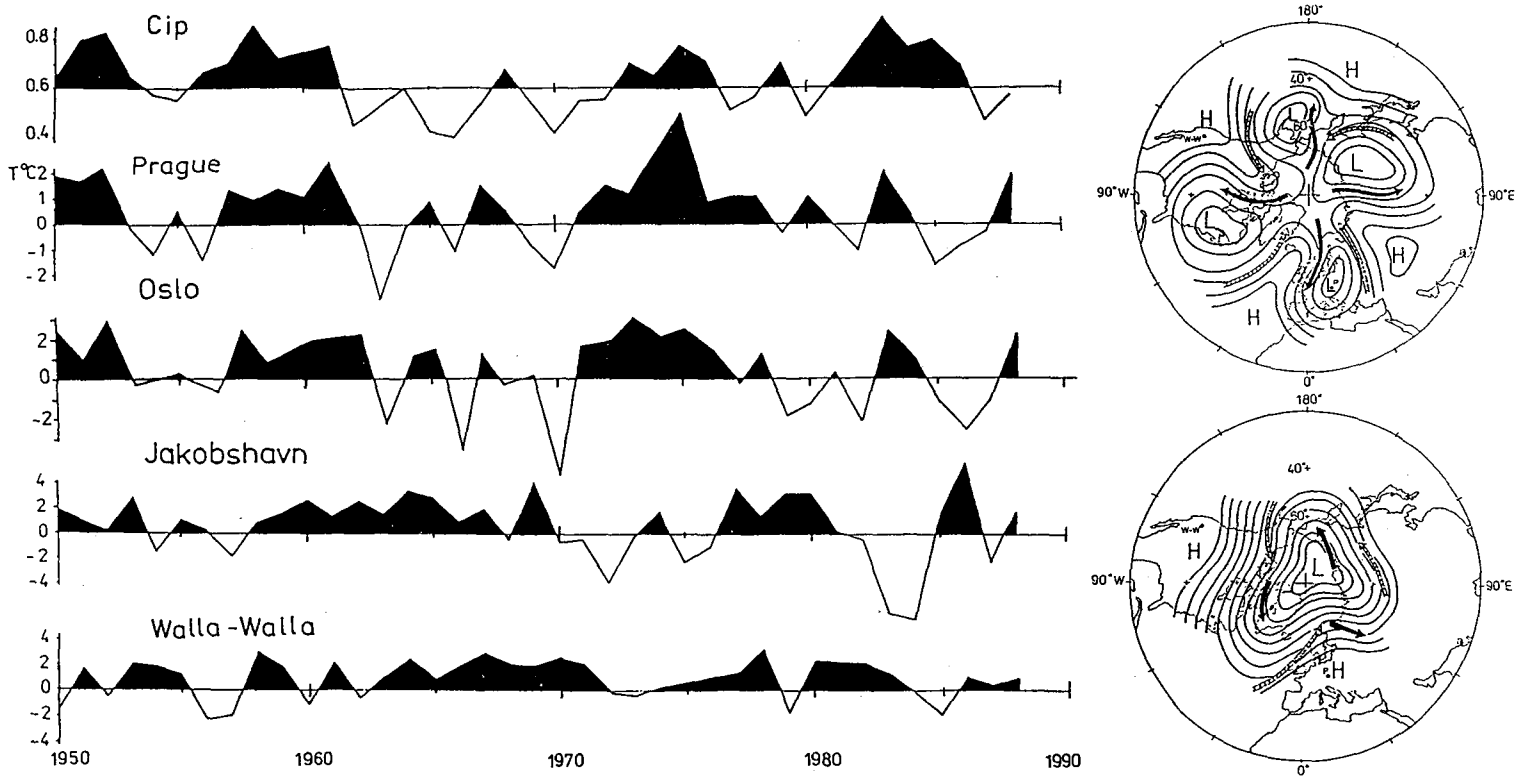

Fig. 2. Changes in geomagnetic activity (C indices - averages for months November,December, January,February) and in temperature for Prague and Oslo showing positive correlation and for Jakobshavn (Greenland) and Walla-Walla (Washington) showing negative correlation with geomagnetic activity. Meridional type of circulation - r.h.s.,top, zonal type - r.h.s. bottom.

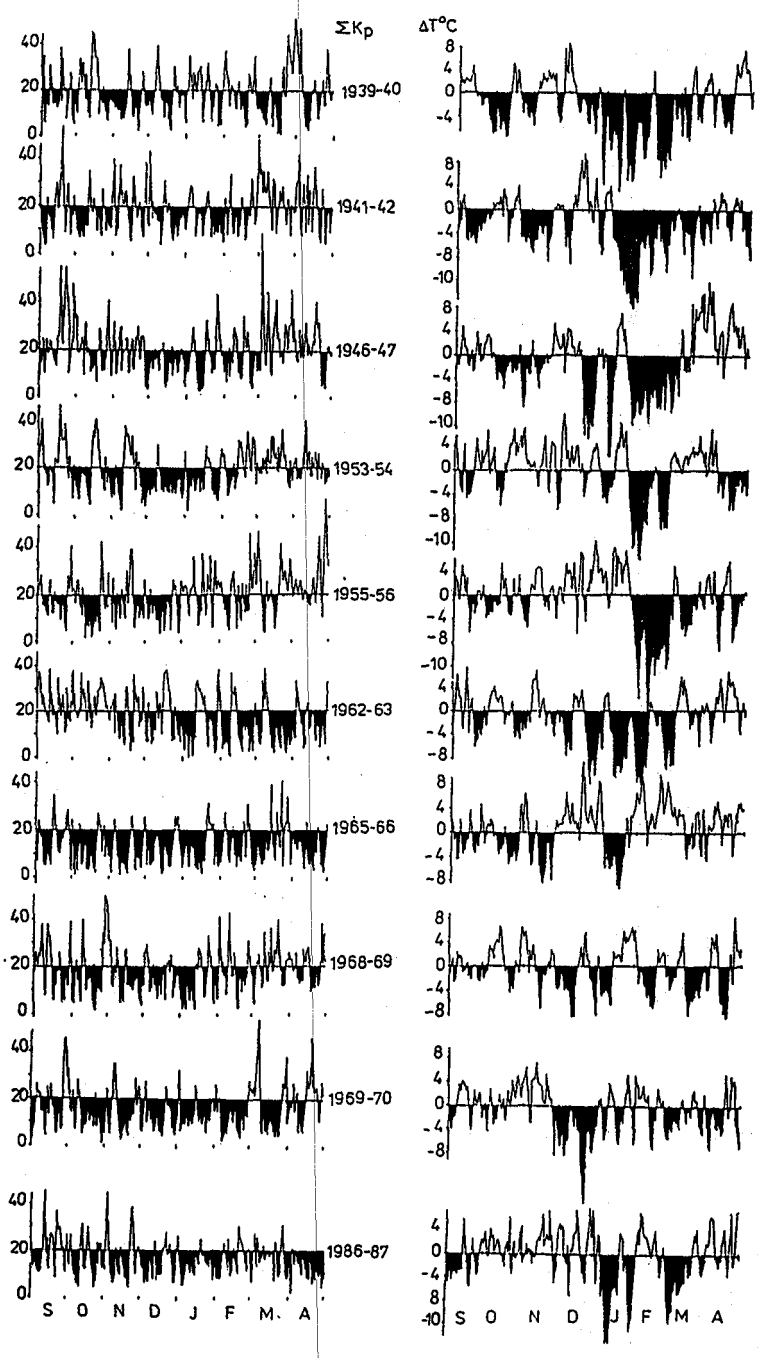

Fig. 3 a Changes of the diurnal values of geomagnetic activity (ΣKp indices l.h.s.) and of temperature (deviations from the normal) in Prague - r.h.s. for the period September-April. Severe winters correspond to very low values of geomagnetic activity - Fig. 3.a, mild winters occurred at the time of enhanced geomagnetic activity - Fig. 3.b

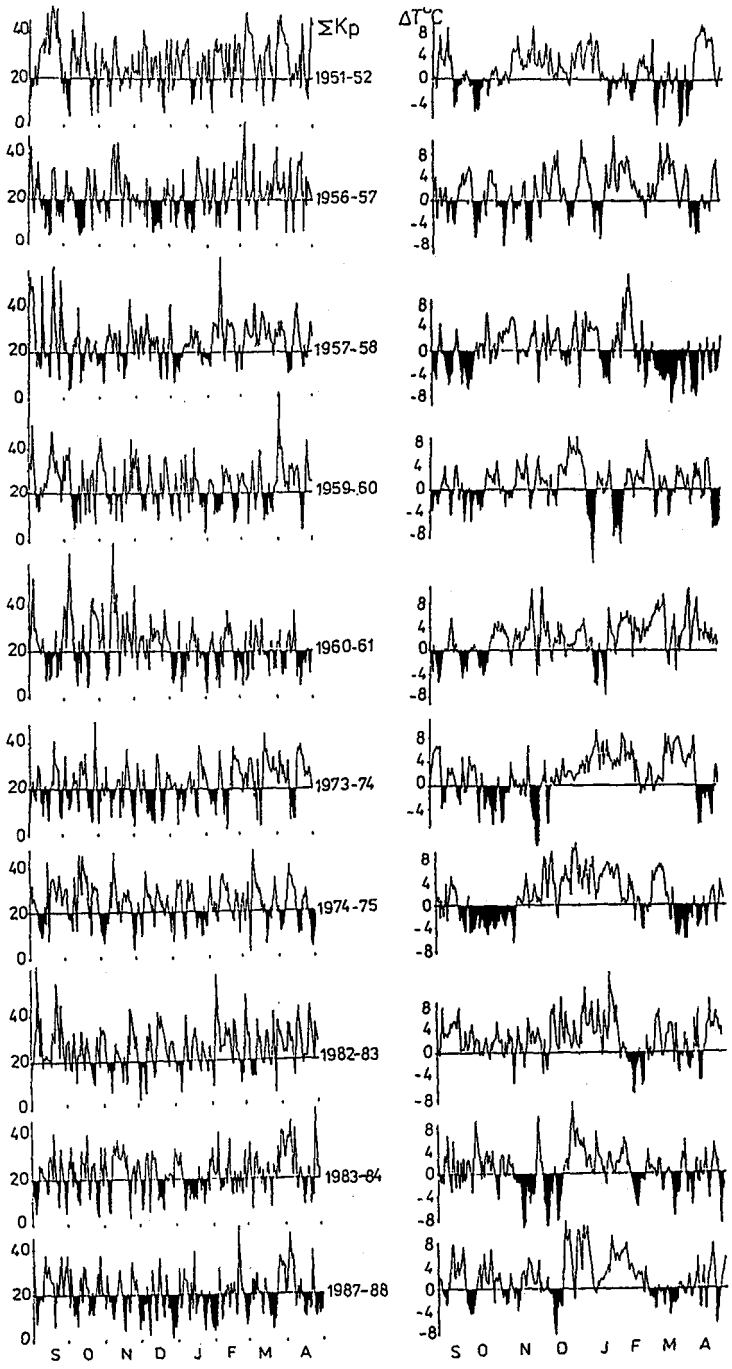
ΣKp
ΔT°C
1951-52
1956-57
1957-58
1959-60
1960-61
1973-74
1974-75
1982-83
1983-84
1987-88
S O N D J F M A
S O N D J F M A

Fig. 3 b

Somebody can object why at the time of extremely low geomagnetic activity (1965-66) the winter in Prague was not so severe. This seems to be connected with a different type of atmospheric circulation as described earlier (BUCHA, 1988).

The cross-correlation of daily changes K_p and T in Prague showed the time lag of 27 days between the increase resp. decrease in geomagnetic activity and increase resp. decrease of temperature in Prague to be the most frequent in the period 1932 - 1985 (BUCHA, HEJDA, 1988). In this way these connections as given in Figs. 1,2,3 seem to confirm the effect of corpuscular radiation on the intensification of processes in the auroral oval and on the increase of temperature leading to the occurrence of zonal type of circulation.

One possibility how to explain the peculiar behaviour of the atmospheric circulation is the intensification of processes which take place along the auroral oval at the time of enhanced corpuscular (geomagnetic) activity characterized by the penetration of energetic particles and bremsstrahlung as far as the lower stratosphere (BUCHA,1986) resulting in the sudden formation of cirrus clouds, in direct increases of temperature and pressure even in the troposphere, and causing the zonalization of atmospheric flow to increase (BUCHA 1984,1988). According to other mechanisms (HINES, 1974) stratospheric and mesospheric winds play a dominant role in determining the "refractive index" for planetary waves (e.g., see CHARNEY and DRAZIN, 1961; MATSUNO 1970; and SCHOEBERL and GELLER, 1976) which will, in turn, determine the transmission-reflection properties of these waves. Thus, changes in the middle atmosphere flow due to corpuscular radiation might lead to changes in the tropospheric amplitudes and phases of planetary waves that propagate to this level. The energetics of these changes are such that relatively small amounts of energy may give rise to significant effects in the upper atmosphere where the density is low, and these upper atmosphere effects merely act to modulate the effect of fixed energy sources in the troposphere. According to BATES (1977) the amplitude and phase of the tropospheric planetary waves as well as the resulting meridional heat flux were found to vary significantly when the tropospheric forcing remained fixed but the stratospheric wind and/or static stability fields were altered.

The three main dissipation mechanisms operative in the stratosphere and mesosphere are radiative damping acting through carbon dioxide and ozone, mechanical dissipation which is presumed to act through the turbulent mixing that results from the "breaking" of waves and tides, and the possible absorption of wave momentum at critical levels.

GELLER and ALPERT´s modeling study indicated (1980) that if solar disturbance effects lead to changes in the mean zonal middle stratospheric flow of 20 %, then changes in the strengths of the high-latitude quasi-stationary troughs and ridges amounting to 20% of the observed range of variability may occur. They believe that they have demonstrated the viability of the HINES (1974) mechanisms for solar effects on the troposphere and have given an idea of the magnitudes of the effects to be anticipated if the stratospheric mean zonal winds vary with solar cycle below an altitude of 35 km.

Furthermore, GELLER and ALPERT´s results indicate (1980) that the tropospheric planetary wave response to solar-induced changes in the zonal mean state of the stratosphere occur regionally, that is to say, they may be much more evident at some lo-

ngitudes and latitudes than at other locations where they may be absent altogether.

It is known that the zonal flow steadily prevails in the southern hemisphere, while periods with zonal or meridional flow alternativaly occur in the northern hemisphere as a result of the corpuscular radiation effect (BUCHA,1988) . The orographic effect due to continents and oceans seems to influence the flow to such degree that we should consider the meridional flow with atmospheric blocking (Fig. 2, r.h.s. top) to be basic in the middle latitudes of the northern hemisphere and not the zonal flow as was presented till now. During several winter periods, when the geomagnetic activity was low, e.g. 1962-65, 1976-80,the meridional circulation together with expresive blocking high pressure areas prevailed in the northern hemisphere with cold winters in Europe and North America. On the other hand, at the time of high geomagnetic activity, e.g. 1959, 1960, 1974, 1975, 1982,1983 the zonal flow with a high index cycle persisted practically during the whole winter period. This again seems to confirm our conclusions that the processes in the auroral oval due to the corpuscular radiation lead to the zonalization of atmospheric circulation (BUCHA, 1983) .

Changes in carbon dioxide concentration are believed to be one of the main factors which influenced and influence the temperature fluctuations on the globe; high concentration of CO_2 was at the time of interglacials and low CO_2 during glacials. But it is of course also possible that the solar activity influenced global temperature which could cause changes in the CO_2 concentration.

CONCLUSION

There is no doubt that the antropogenic effect, especially during the past 40 years, plays an important role. Our task,however, is to distinguish between antropogenic effect in the atmosphere due to human activities and natural climatic fluctuations influencing biological systems. As can be seen in Fig. 4, the increase in global temperature during the past 100 years is in relatively good coincidence with the increase in geomagnetic (corpuscular) activity. That's why we can conclude that it could have been the increase in temperature on the northern hemisphere, due to the processes occurring in the auroral oval under enhanced corpuscular radiation (BUCHA, 1988) which led to an increased atmospheric concentration of CO_2 in the past. Both processes, i.e. antropogenic and solar activity effects, should be therefore intensively studied due to their important role for elucidating the past and present global change mainly in temperature, climate and biological systems.

REFERENCES

Bates, J. R., Dynamics of Stationary Ultra-Long Waves in Middle Latitudes. Quart.J.Roy.Meteor.Soc., 103,397-430, 1977.
Bucha, V., Direct Relations between Solar Activity and Atmospheric Circulation, its Effect on Changes of Weather and Climate, Studia geoph. et geod., 27, 19-45, 1983.
Bucha, V., Mechanism for Linking Solar Activity to Weather-Scale Effects, Climate Changes and Glaciations in the Northern Hemisphere,in Climatic Changes on a Yearly to Millennial Basis,Eds. N.A.

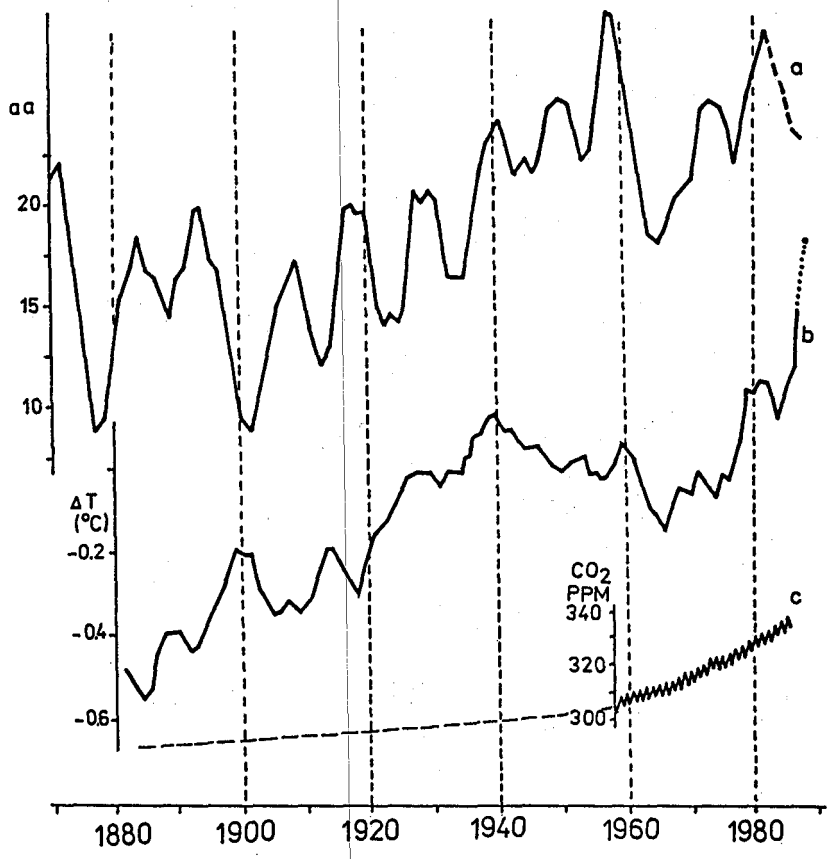

Fig. 4

a/ Changes in geomagnetic activity (aa indices) - five years gliding averages.

b/ Global surface air temperature change (five year running mean) for the past century, with zero point defined as the 1951-1980 mean. The 1988 point compares the January-May 1988 temperature to the mean for the same 5 months in 1951-1980(HANSEN)

c/ Changes in the atmospheric CO_2 concentration,observed increase in atmospheric carbon dioxide,resulting in part from human activities.

Mörner and W. Karlén, D.Reidel Publ. Co., 415-448, 1984.
Bucha, V., Causes of Climate Changes, Adv. Space Res., 6,10,77-82, 1986.
Bucha, V., Influence of Solar Activity on Atmospheric Circulation Types, Annales Geophysicae, 6,5, 513-524, 1988.
Bucha, V. and P. Hejda, Vazby mezi krátkodobými změnami geomagnetické aktivity a teploty, Vztahy Slunce-Země III, 155-160, Praha 1988.
Charney, J.G., and P. G. Drazin, Propagation of Planetary Scale Disturbances from the Lower into the Upper Atmosphere, J.Geophys. Res., 66, 83-109, 1961.
Hines, C. O., A Possible Mechanism for the Production of Sun-Weather Correlations, J. Atmos.Sci., 31, 589-591, 1974.
Loon,H. V. and J. C. Rogers, The Seesaw in Winter Temperatures between Greenland and Northern Europe. Part I: General Description, Mon.Wea.Rev. 106, 296-310, 1978.
Matsuno, T., Vertical Propagation of Stationary Planetary Waves in the Winter Northern Hemisphere, J. Atmos.Sci., 27, 871-883, 1970.
Schoeberl, M. R., and M. A. Geller, The Structure of Stationary Planetary Waves in Winter in Relation to the Polar Night Jet Intensity. Geophys. Res. Lett., 3, 177-180, 1976.

THE TROPOSPHERIC RESPONSE PATTERN TO SOLAR ACTIVITY FORCING

C.J.E. Schuurmans

Royal Netherlands Meteorological Institute
De Bilt, The Netherlands

INTRODUCTION

Twenty years ago (SCHUURMANS and OORT, 1969) the northern hemispheric response pattern of the height of the 500 mb level to strong solar flares was published. Although comparisons were possible for limited areas (see later on), full hemispheric comparisons for independent data have never been made. Recently, however, VAN LOON and LABITZKE (1988) published the results of an association between the 11-year solar cycle, the QBO and the northern hemisphere 700 mb height. Surprisingly, their Figure 12b, presenting lines of equal correlation between the 700 mb height and the 10.7 cm solar clux, for easterly QBO winter months, shows a pattern which is very similar to the one we found for the change of the 500 mb level after strong solar flares.

Of course, pattern similarity alone does not prove anything. According to studies on atmospheric teleconnections and low frequency fluctuations.

Such patterns do seem to be quite common and do not need an external cause for their excitation. Furthermore, VAN LOON and LABITZKE's result describes a possible long-term variation, while the effect of solar flares is essentially a short term reaction.

Notwithstanding this critizism it is tempting to speculate on the possibility that solar flares sometimes are the initial cause of an atmospheric disturbance, which cumulative effect may give rise to a correlation at the 11-year timescale.

HORIZONTAL PATTERN

The response pattern of the 500 mb level to solar flares referred to above is shown in Fig. 1. Like Fig. 2 and 3 it is reprinted form SCHUURMANS and OORT, 1969. Fig. 1 does show positive anomalies in the latitude belt 40-70 °N, with maxima over Europe, Eastern Asia-Western Pacific and Californian area, and negative anomalies over the polar regions, much like the pattern of positive correlations between the 700 mb height field and the 10.7 cm solar flux for easterly QBO, shown by VAN LOON and LABITZKE (1988). Why it is the east phase of QBO which correlates best with our flare results, remains a problem. The 81 flare cases are from the IGY-period (June 1957 till December 1959). It may be possible that during most of this period the QBO was in its east phase (which according to preliminary data available seems to be true). Comparison with results of other studies, however, shows that the reaction pattern at 500 mb after solar flares, above Europe always seems to be of positive sign. Here I refer to the pioneering studies of DUELL and DUELL (1948) and of the Czechoslowakian VALNICEK (1953), which for the area limited to the Eastern Atlantic and Europe, a positive height change of the 500 mb level observed as an average response to some 50 flares, occurring during 1936-41 and 1949-50, respectively.

Subsamples of the 81 flares used in our case, invariably showed a nearly the same reaction pattern, even for a subdivision of flare cases in winter and summer (SCHUURMANS, 1979).

VERTICAL PROFILE

The vertical profile of positive height changes after solar flares shows a maximum at about 300 mb (Fig. 2). In areas of negative height changes at 500 mb the vertical variations were found to be negligible. For this reason further study of the solar flare impact was concentrated upon the areas of positive height change. The warming of the troposphere, which could be expected from the observed height rises of constant pressure levels (on the basis of the assumption of hydrostatic equilibrium) was verified on the basis of observed temperature changes after solar flares. As clearly indicated in Fig. 3 tropospheric warming with a maximum at 500 mb does take place, along with a pronounced cooling of the lower stratosphere. Statistically this cooling is more strongly signficant than the warming of the troposphere.

DEVELOPMENT IN TIME

The changes discussed above occur within 24 hours after a flare. In fact 24-hour time changes were studied, always taking the difference between the first observation after a flare and the aerological observation 24 hours earlier. So on average the reaction pattern refers to a time-lag which is even less than 12 hours! In order to see the development of the effect in time several individual cases were studied. In Fig. 4 an example of this is given. The immediate response is clearly indicated as well as its continuation for at least 36 hours. The 24-hour temperature change at the first observation after the flare is also given. Note the nearly tenfold larger effect as for the sample average presented in Fig. 3. It should be pointed out that the flare case of June 1, 1960, to which Fig. 4 refers is not included in the IGY-sample of 81 flare cases.

MECHANISM

In search for an explanation of the observed reaction profile after solar flares I have tried a model consisting of a vertical circulation system (Fig. 5) forced from above. Following my computations (SCHUURMANS, 1969) some source of diabatic cooling in the lower stratosphere, causing horizontal convergence of air and consequently downward motions in the troposphere, may explain the observed (adiabatic) warming of the troposphere. The mechanism causing the diabatic cooling source, however, remained obscure. The very short time lag between the flare and the observed response is certainly not in favor of an electromagnetic radiation process. Rather, some at present still unknown process, involving energetic solar particle radiation has to be explored.

CONCLUDING REMARKS

Reporting of just old results is certainly not elegant. Reasons to reconsider the possible relevance of solar flare response studies are stated in the introduction. The discovery of the apparently decisive role of the QBO in establishing the atmospheric response pattern to solar forcing may throw new light on some of the earlier published relations. Re-analysis of old data in some cases may be advisable.

The purpose of this paper was to show that data on solar flares and their effects on the earth's atmosphere might be a promising candidate for this.

REFERENCES

DUELL, B. and G. DUELL, The behaviour of barometric pressure during and after solar particle invasions and solar ultraviolet invasions. Smiths. Misc. Coll., 110, no. 8, 1948.

SCHUURMANS, C.J.E. and A.H. OORT, A statistical study of pressure changes in the troposphere and lower stratosphere after strong solar flares. Pure and Applied Geophysics, 75, 233-246, 1969.

SCHUURMANS, C.J.E., The influence of solar flares on the tropospheric circulation. Royal Netherlands Meteorological Institute, Mededelingen en Verhandelingen, no. 92, 1969.

SCHUURMANS, C.J.E., Effects of solar flares on the atmospheric circulation. In: Solar-Terrestrial Influences on Weather and Climate, p. 105-118, D. Reidel Publ. Comp., 1979.

VALNICEK, B., Les éruptions chromosphériques et le temps. Bull. Astron. Inst. of Czechoslowakia, 4, 179, 1953.

VAN LOON, H. and K. LABITZKE, Assocation between the 11-year solar cycle, the QBO, and the atmosphere. Part II: Surface and 700 mb in the Northern Hemisphere in Winter. J. of Climate, 1, 905-920, 1988.

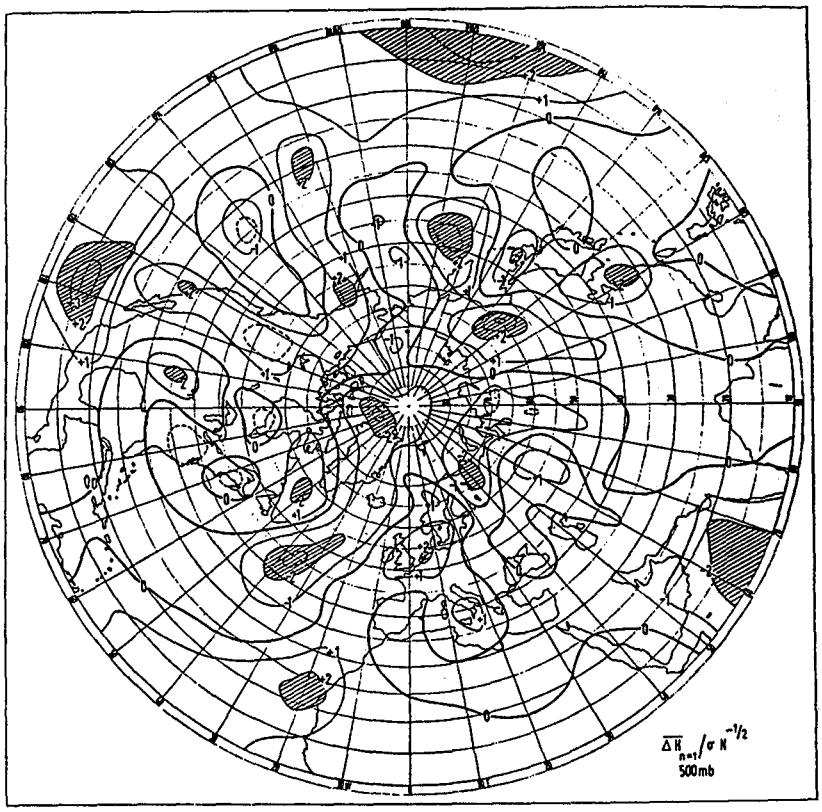

Fig. 1. Mean height change of the 500 mb level after solar flare outbursts. The map gives isolines of the mean change in 24 hours after 81 flares, divided by the standard error of the mean.

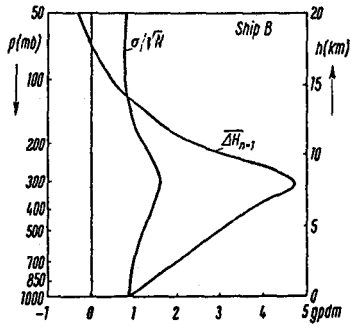

Fig. 2. Mean 24-hr height change of pressure levels after solar flares at Ship B (56°30'N, 51°W).

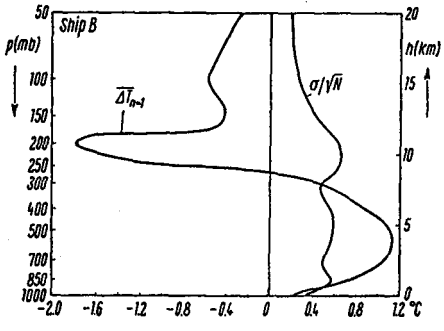

Fig. 3. The same as Fig. 2 for temperature changes.

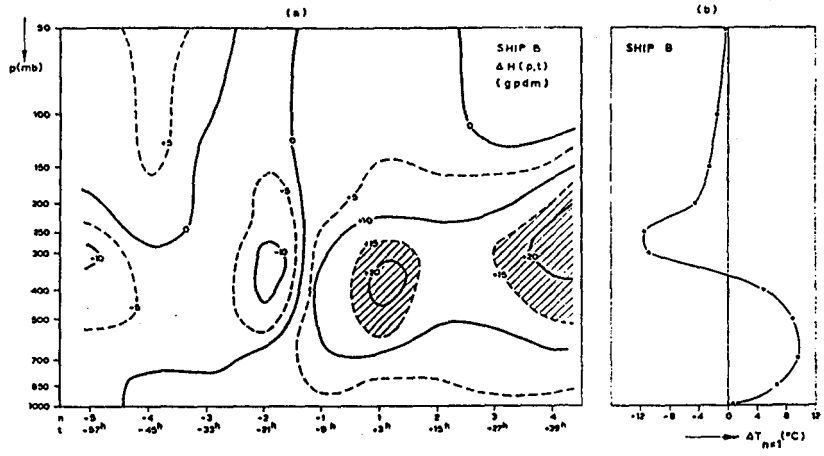

Fig. 4. Height and temperature changes at Ship B, related to the solar flare of June 1, 1960.

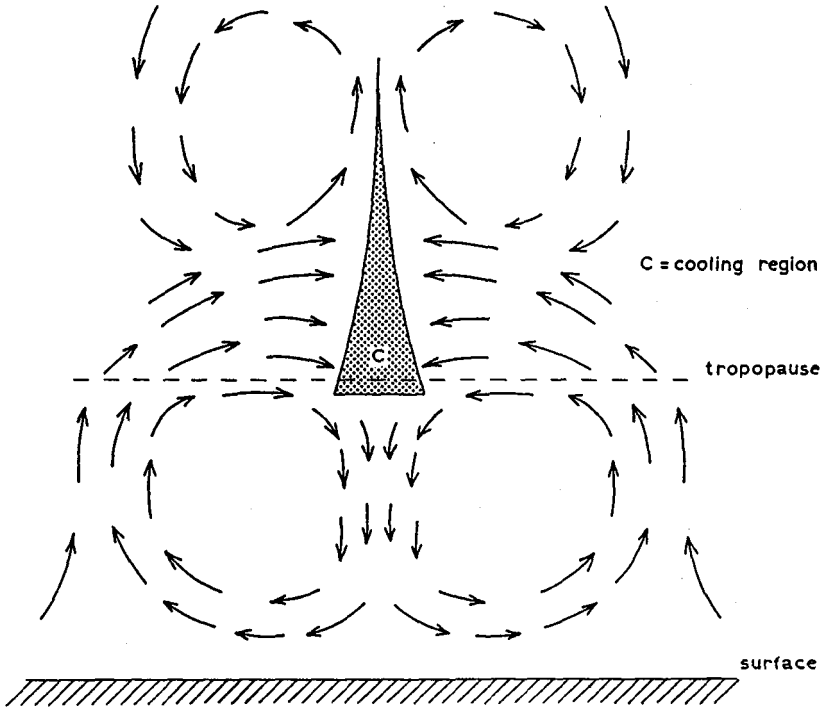

Fig. 5. Proposed circulation system, initiated by a solar particle induced heat sink a the tropopause.

A REVIEW OF THE 11-YEAR SOLAR CYCLE, THE QBO, AND THE ATMOSPHERE RELATIONSHIP

M.L. Chanin

Service d'Aéronomie du CNRS
BP 3
91371 Verrières le Buisson CEDEX - France

1. Introduction

The papers published by LABITZKE (1987) and by LABITZKE and VAN LOON (1988, hereafter referred to as LvL) indicated that the separation of Winter stratospheric data according to the phase of the Quasi-Biennial Oscillation (Q.B.O.) led to a largely improved relationship with the 11-year solar cycle. Since then, this possible relationship has been studied and extended from the surface to the lower thermosphere and its extension to other seasons is in progress. This workshop provides an opportunity to review the state of the problem and to attempt to give a general view of the experimentally observed responses of the atmosphere to solar activity, when considering the phases of the Q.B.O. After a brief recall of the relationship firstly discovered in the winter stratosphere, its extension downwards, upwards and to the other seasons will be successively reviewed.

2. The winter stratosphere and high troposphere

The separation of the stratospheric data according to the phase of the QBO (defined at 40-50 mb) during winter (January and February) first introduced by LABITZKE (1987) for the North Pole and by LVL for the Northern Hemisphere, was at the start of a regained interest in the field of solar terrestrial relationship. It is assumed that the reader is familiar with these now two famous papers, in which was pointed out for the first time a high correlation with solar activity in the low atmosphere (correlation coefficient above 0.8 at 30 mb at the North Pole. However the major results are briefly recalled :

- The data set (consisting on monthly mean temperature and geopotential height) starts in 1953 and cover then three complete solar cycles for the Northern Hemisphere. There is no way to characterize the QBO phase beyond that year, and therefore no direct way to extend the period of study in the past; but it is worth mentionning that data from the two recent winters are in agreement with the above mentionned association. They are used to update figure 1 of LvL and presented in the Figure 1 of this paper (from LABITZKE private communication).
- The signs of the correlation with solar activity are found to be opposite between the polar region and the mid and low latitudes and between the westerly and easterly phases of the QBO. This last point explains why the effect had been masked when considering the whole data set without separating the data according to the phase of the QBO.
- The atmospheric response at the different atmospheric levels from 500 to 30 mb, though variable in shape, have a pattern very similar with quasi-stationary planetary waves.
- While the first papers only dealt with the Northern Hemisphere, it was shown recently, (LABITZKE and VAN LOON 1989a), that the same high level of positive correlation is found for the South pole, but only for the easterly phase of the QBO. Recent results from the Southern high latitude rocket station of Molodezhnaya (69°S 46°E) seem to indicate that the correlation become negative in the high stratosphere for both phases of the QBO (MOHANAKUMAR, 1989). This is confirmed by the study of KIDIYAROVA and FOMINA (1989).

3. The surface and low troposphere

Using the same approach, VAN LOON and LABITZKE (1988) extended the correlation down to the surface, with significant correlation for sea level pressure and surface air temperature

(R ~ 0.6) which were proved to be statistically meaningful (figure 2). The correlation pattern at 700 mb was found to be similar to the teleconnection pattern and this was interpreted as a sign that the observed effect was related to atmospheric internal dynamics. The suggestion that the solar cycle modulates the weather, attracted, as expected, some scepticism even though it was submitted successfully to the adequate statistical tests; but several other results of solar related dependences have been obtained on storm tracks (TINSLEY 1988) and tropical sea surface temperature (BARNETT 1989) which may bring more confidence in this result and help to understand the mechanism involved.

4. Extension to the upper atmosphere

Using two regions which according to LvL presented an opposite behaviour at 30 mb : Heyss Island (81°N, 58°E) and 2 close-by sites in France (44°N, 6°E and 45°N, 2°E)), a study of the solar dependence of the temperature was performed first up to 80 km (LABITZKE and CHANIN 1989) and later up to the lower thermosphere (CHANIN et al. 1989). It showed that the response of the upper atmosphere, even though already present when using the whole data, was amplified by sorting out the data set according to the QBO. It also put into a new light some already published results indicating a negative solar dependence in a region of the atmosphere which was though to be positively related with solar activity. The alternance of positively and negatively correlated regions extending from ground level to 150 km, with vertical structures of the order of 40 km, as seen on figure 3, strongly suggest an influence of planetary waves generated at the surface or in the low troposphere and modulated by the QBO. In the region above 50 km we interpret the observed results as a superposition of a direct radiative effect due to the UV absorption and a dynamically induced effect related to the pattern observed at lower levels.

5. Extension to other seasons

Because of the filtering of upward propagating planetary waves by stratospheric winds, it is expected that the dynamically induced contribution will maximize in winter, while the radiative contribution should present a maximum in summer (~ 70 km). Then the relative importance of both contributions should vary with the seasons and one could expect the response of the stratosphere to solar activity to be weaker in summer than in winter. On the other hand in the mesosphere a positive response is expected for all seasons; it has been observed from a number of sites with a solar dependence of much larger amplitude than predicted from radiative models (see review in CHANIN et al. 1987).

The results of LABITZKE and VAN LOON (1989b) in the Northern summer stratosphere indicate that it was not necessary to group the data according to the QBO to obtain a statistically significant response to solar activity : this response was found to be positive at 30 mb for all the north hemisphere and mostly significant in a belt between 20 and 45 N. Recent results pointed out that a significant negative response is found in the height range 30-50 km and that the correlation with solar flux is amplified for some sites if separating the data according to the QBO. This is observed in summer and autumn at the French lidar station (44°N, 6°E) for easterly QBO (KECKHUT and CHANIN 1989) and during summer in THUMBA (8°N, 77°E) for westerly QBO as reported by MOHANAKUMAR (1989) in this workshop. On the other hand the QBO do not seem to play any role in this altitude range at the site of Molodezhnaya (69°S, 46°E) where the correlation is strongly negative for both phases of the QBO and at Volgograd (49°N, 44°E) where it is below significance for both phases during summer.

The common feature in all of these results is that the responses to solar activity at some levels within the altitude ranges 20-40 km and 60-80 km are found to be of opposite signs at all sites and independently of the season: i.e negative in the stratosphere and positive in the mesosphere. The altitude of the reversal of sign, the importance in the role of QBO and the amplitude of the solar dependence are anyhow variable from onesite to another.

6. Discussion

Before the LABITZKE (1987) paper, the solar influence on atmospheric parameters was searched for by averaging data either globally or on zonal mean, by using all available years independently of the QBO, and in some case by restricting the data set to summer periods to avoid the high winter variability. The experimental results could be summarized as follows :

- no conclusive result in the troposphere
- a small amplitude effect (1 to 2 K) around 40 km for a solar cycle
- a positive relationship with up to 10 K amplitude around 70 km

a well documented positive dependence in the high thermosphere which was thought to start around 120 km, as included in the empirical models.

On the other hand, the radiative photochemical models, taking into account the effect of a change in UV flux and its consequences on the ozone distribution and the radiative budget, predicted changes for a solar cycle of + 2 to + 2.5 K at the most with a maximum effect at 70-75 km (GARCIA et al. 1984, BRASSEUR et al. 1987). Results from one-dimensional radiative transfer model indicates an even smaller effect (0.8 K at 50 km). Such changes are difficult to differenciate from trends of other origins. However the predictions of the models were known to disagree with the data which in the mesosphere led to an amplitude around 5 to 10 K.

The fact to look at data locally, their separation according to QBO, and furthermore the selection of winter data where the effect was found to be stronger, brought a completely new set of results which could be summarized as follows :

- in winter periods, strong correlations with solar activity of opposite signs for easterly and westerly QBO and from pole to mid and low latitude in the region below 30 km and down to the surface
- a reversal of the sign of the correlation between part of the stratosphere and the mesosphere, with the influence of the QBO decreasing with altitude
- a planetary-wave type structure both horizontally and vertically in the atmospheric response to solar activity
- in all the height range the amplitudes of the solar dependence much larger than any model prediction by at least one order of magnitude.

7. Conclusion

The existing models are not adequate rightnow to represent the solar influence as they only take into account the change in UV flux, but before being able to take into account the large scale dynamics in a coupled radiative-photochemical model, one needs to understand the mechanism able to explain the forcing from the lower atmosphere or the surface which could be induced by a change in solar activity. Some of the possible mechanisms are described in this issue (EBEL, 1989).

References

Barnett T.P., A solar-ocean relation : fact or fiction ?, *to be submitted* 1989.

Brasseur G., A. de Rudder, G.M. Keating and M.C. Pitts, Response of middle atmosphere to short term solar ultraviolet variations, 2 theory, *J. Geophys. Res., 92*, 903-914, 1987.

Chanin M.L., N. Smires, A. Hauchecorne, Long-term variation of the temperature of the middle atmosphere at mid-latitude : dynamical and radiative causes, *J. Geophys. Res.*, 933-941, 1987.

Chanin M.L., P. Keckhut, A. Hauchecorne and K. Labitzke, The solar activity - QBO effect in the lower thermosphere, *Accepted Ann. Geophs.*, 1989.

Ebel A., Physical mechanisms of solar activity effects in the middle atmosphere. *Map Handbook,* 1989 (this issue)

Garcia R.R., S. Solomon, R.G. Roble and D.W. Rusch, A numerical response in the middle atmosphere to the 11 year solar cycle, *Planet. Space Sci., 32*, 411-423, 1984.

Keckhut P. and M.L. Chanin, Seasonal variation of the solar activity - QBO effect in the middle atmosphere, *Map Handbook* (this issue), 1989.

Kidiyarova V.G. and N.N. Fomina, The planetary waves dynamics and interannual course of meteorological parameters of the high latitude stratosphere and mesosphere of the northern and southern hemispheres during the 20th and 21th solar cycles and different phases of QBO, *Map Handbook*, 1989 (this issue).

Labitzke K., Sunspots, the QBO and the stratospheric temperature in the north polar region, *Geophys. Res. Lett., 14*, 535-537, 1987.

Labitzke K. and M.L. Chanin, Changes in the middle atmosphere in winter related to the 11-year solar cycle, *Ann. Geophys.*, 6, 643-644, 1988.

Labitzke K. and H. Van Loon, Associations between the 11-year solar cycle, the QBO, and the atmosphere. Part 1 : the troposphere and stratosphere on the northern hemisphere in winter, *J. Atm. Terr. Phys., 50*, 197-206, 1988.

Labitzke K. and H. Van Loon, Association between the 11-year solar cycle, the QBO, and the atmosphere. Part III : aspects of the association, *J. of Climate*, 1989a (in press).

Labitzke K. and H. Van Loon, The 11-year solar cycle in the stratosphere in the Nortern Summer. *Ann. Geophys.* 1989 b (in press)

Mohanakumar K., Influence of solar activity on middle atmosphere associated with phases of equatorial QBO, *Map Handbook* (this issue), 1989.

Tinsley B.A., 1988, The solar cycle and the QBO influences on the latitude of storm tracks in the north Atlantic, *Geophys. Res. Letters, 15*, 409-412, 1988.

Van Loon and K. Labitzke, Association between the 11-year solar cycle, the QBO and the atmosphere. Part II : surface and 700 mb in the northern hemisphere in winter, *J. of Climate, 1*, 9, 905-920, 1988.

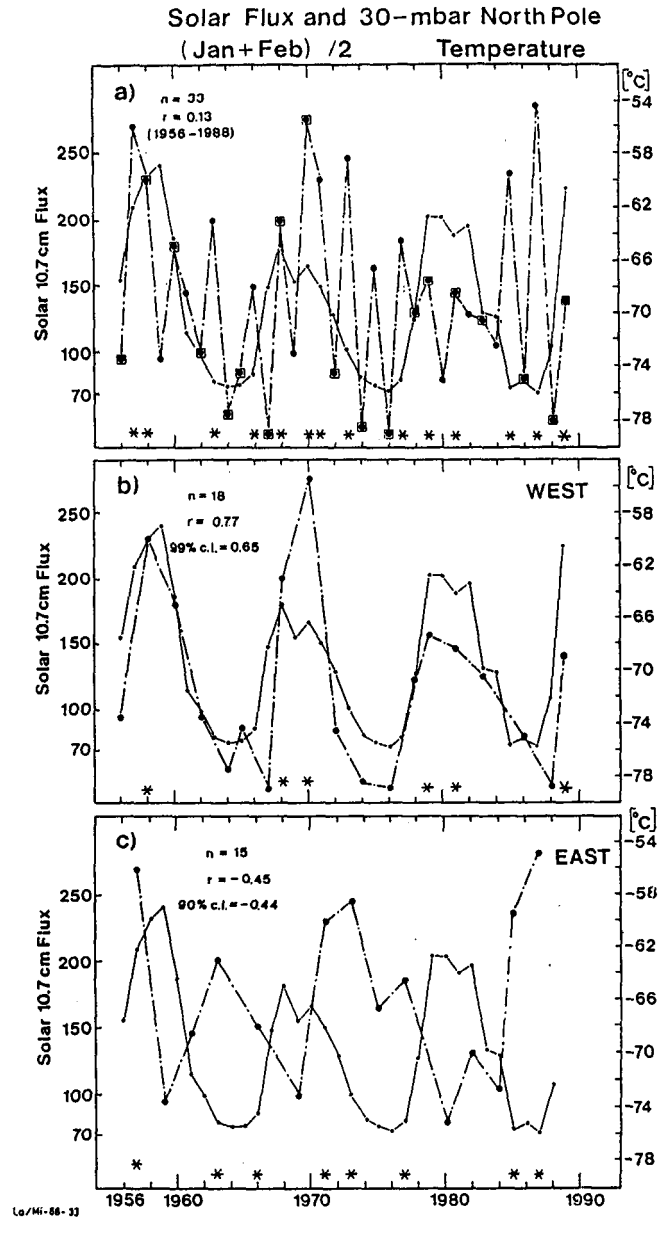

Figure 1: Time series of the 10.7 cm solar flux (units are 10 -22 W m-2 Hz-1) for (Jan.+ Feb./2; and of the mean 30mb temperature (°C) at the North Pole for (Jan. + Feb.)/2. From LvL, updated 1989 (LABITZKE, Private communication)

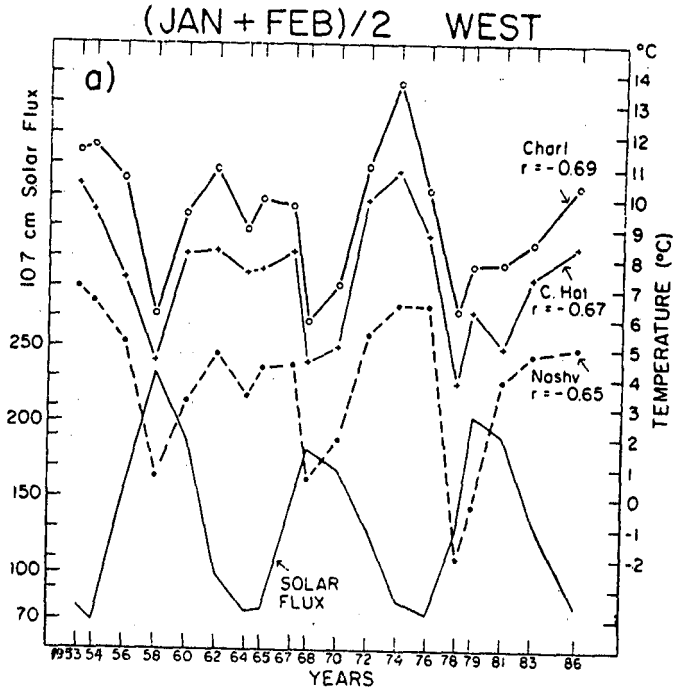

Figure 2: Time series for January-February in the West phase of the QBO of the 10.7 cm solar flux for all years (dashed line) and of surface air temperature at 3 U.S. stations. The correlation coefficiets r are indicated. (VAN LOON and LABITZKE 1988)

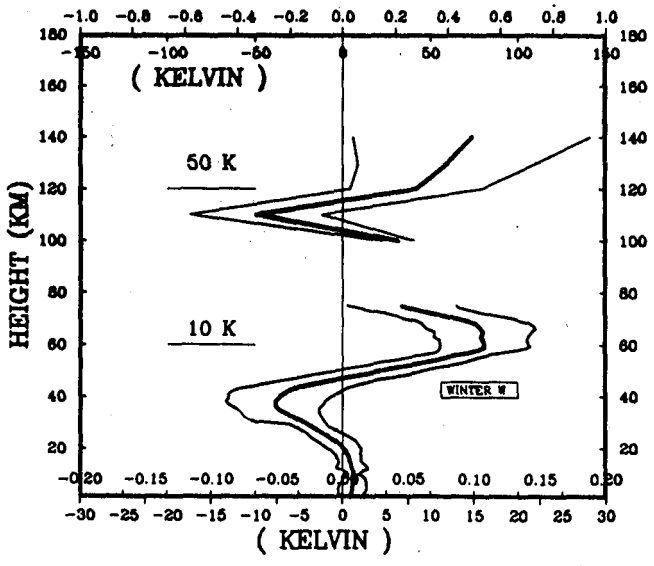

Figure 3: Amplitude of the solar temperature dependence over Southern France expressed in Kelvin and in Kelvin by unit of solar flux. (Note the different scale for top and bottom part). From CHANIN et al. 1989.

SEASONAL VARIATION OF THE 11 YEAR SOLAR CYCLE EFFECT ON THE MIDDLE ATMOSPHERE; ROLE OF THE QUASI BIENNIAL OSCILLATION

611603

6 Pgs

P. Keckhut and M.L. Chanin

Service d'Aéronomie du C.N.R.S.
BP 3
91370 Verrières-le-Buisson CEDEX-FRANCE

1. Introduction

Before the introduction of the Quasi Biennial Oscillation (Q.B.O.) in the study of the solar-atmosphere relationship by LABITZKE (1987) and LABITZKE and VAN LOON (1988), the only region of the atmosphere where an effect of a change in solar activity was generally admitted was the mesosphere. The response of the mesosphere, in phase with the solar activity, was found to be about one order of magnitude above model expectancy (around 10 to 20 Kelvin). It was observed independently of the season and maximized around 70 km (Chanin et al. 1987). On the other hand, from the same study, it was shown that the response of the stratosphere of opposite sign, clearly seen during winter and autumn, was at the threshold of detection in spring and summer. In the stratosphere, it was shown later that the separation of the data taking into account the sign of the Q.B.O. amplifies the negative correlation of the stratospheric temperature with solar activity in winter; it then becomes more significantly negative for the East phase of the Q.B.O. than when the data are all mixed (Labitzke and Chanin 1988). The studies of the seasonal response of the atmosphere to solar effect is crucial to understand the possible mechanism responsable of such a solar activity-Q.B.O. relationship, knowing that the global dynamic circulation is quite different according to the seasons. The purpose of this paper is to inquire if such separation of the data according to the phase of the Q.B.O. has any impact on the solar response of the middle atmosphere for seasons other than winter.

2. Description of the data set

The data used for this study are the temperature profiles obtained from the Rayleigh lidar which has been in operation at the Observatory of Haute-Provence (O.H.P. FRANCE, 44°N-6°E) for the period 1979-1988 and at Biscarrosse (44°N-1°E) for the period 1986-1988. The method has been already described in several publications (Chanin and Hauchecorne 1984) but it is worth noticing that the performances in term of range and accuracy have been largely improved since 1984. The height range reached from both stations is nowadays 90 km instead of 75 km before 1984. However the stratospheric data were disturbed in the post El Chichon period (from April 1982 to February 1984) in the height range 30-34 km and even up to 38 km at the time immediately after the eruption; therefore, for this analysis, the data corresponding to the altitudes where aerosols were present were eliminated from the data set. The downward extension from 30 km to ground level is obtained by using the data from the two near-by radio sonde stations. The quantity which is considered here is the temperature deviation of each monthly averaged value from the corresponding mean value calculated for the whole period of 1979 to 1988. The 10.7 cm radio solar flux is used as the solar activity index. Even it is not the best solar parameter, the other ones (i.e. the UV flux around 205 nm) are not available during the whole period and the 10.7 cm radio solar flux has been shown to be reasonnably well correlated with the solar UV flux, when looking for long term variation (LONDON et al. 1984).

The data were grouped according to the sign of the Q.B.O. from the classification of LABITZKE and VAN LOON (1988), and in 4 periods of 3 months each: December-January-February (DJF) for Winter, March-April-May (MAM) for Spring, June-July-August (JJA) for Summer, and September-October-November (SON) for Autumn. The number of temperature monthly means used in this study was 112 using a total number of 799 profiles.

3. Seasonal variation

The response of the atmosphere to change in solar activity is given for different seasons in Figure 1 for the Westward phase of the Q.B.O. and in Figure 2 for the Eastward phase. As expected, the atmosphere responds positively in the mesosphere in all cases even though with different amplitudes. The largest amplitudes between the minimum and maximum of the solar activity are observed in Winter and Summer for both Q.B.O. signs, as already shown when the data were not sorted out according to Q.B.O. (Chanin et al. 1987).

In the stratospere, the Spring and Winter correlations are identical and negative for Q.B.O. West, whereas Summer and Autumn correlations are positive; for the Q.B.O. East, the Spring is the only season where the response is positive. The amplitudes around 40 km of the negative dependence for Q.B.O. East are decreasing from Winter to Autumn and Summer but are larger in general than Q.B.O. West.The only periods for which the correlation coefficient is significant above the 95% confidence level in the stratosphere are the Autumn and Winter for Q.B.O. East (Figures 3 and 4) and the Spring for Q.B.O. West (Figure 5) and the larger correlation coefficient is found in Autumn for Q.B.O. East: 0.78. The more noticeable feature is the opposite behaviour of the Spring responses for the two different signs of the Q.B.O., which should be related to the way the atmosphere recovers after the final warning. The response of the stratosphere may then be partly smoothed out when all the data are used independently of the Q.B.O..

At that point it is worth comparing these results with the ones obtained in summertime by LABITZKE and VAN LOON (1989 b). They conclude from the analysis performed at 30 mb that it was not necessary to sort out the data to obtain a positive statistically significant response to solar activity. This is not in contradiction with the results of Figures 1 and 2 where the response for both Q.B.O. responses are shown to be positive at 24 km (30 mb). However figures 6 and 7 indicate that a more significantly positive value is observed at this altitude for Q.B.O. West than for Q.B.O. East. There is therefore an indication that the behaviour in the stratosphere is sensitive to the sign of the Q.B.O., even though differently for each season, and the regular alternance of positive and negative responses as a function of altitude seen during winter is not always observed for the other seasons.

4. Mean annual dependence

As the signs of the solar dependency are not systematically opposite for the East and West phases of the Q.B.O. one can wonder what is the response of the atmospheric temperature to solar activity when all the seasons are considered and all the years are taken into account independently of the sign of the Q.B.O.. The answer is given in Figures 8 and 9 in terms of correlation coefficient and solar dependence. The correlation coefficient in the stratosphere varies from +0.25 to -0.25 from 20 to 40 km, to reach +0.6 in the mesosphere. These values are much lower than the ones mentionned before, but due to the large quantity of data, they are above the 95% confidence level. The amplitude of the response for minimum to maximum are about +2 K at 20 km, -4 K at 40 km, and +10 K at 65 km. This value are not negligeable compared to the temperature trends observed for a

decade, which are close to -0.5 K at 20 km and -2 K at 40 km. Theses results obtained at a specific site is not expected to be valid on a global mean if, as shown by LABITZKE and VAN LOON, the response to solar activity follows a regional pattern. However it is an indication that the data have to be used carefully when looking at long term trend unless the data set covers several solar cycles and allows a separation of both solar and long term effect. It is yet to be seen if a solar cycle response exists on a global mean, in the upper stratosphere and mesosphere: the long series of data available for such a study are mainly provided by the existing rocket stations, which are known not to be uniformely spread, even in the North hemisphere, and we feel that those data cannot be used safely to estimate global temperature trends.

5.Conclusion

A more complete study of the response of the whole middle atmosphere to changes in solar activity is needed to get a global view of the solar influence on the stratosphere, and to conclude about the role of the Q.B.O.. From this study, it seems that significant negative or positive responses of the stratosphere are Q.B.O. dependent, while the systematic positive response of the mesosphere is only slightly amplified for Q.B.O. East. The role of the Q.B.O. in summer and autumn periods is puzzling as the filtering role of the stratospheric winds, existing in Winter and slightly less in Spring, is less likely to be of any importance during the rest of the years. A result which could be important for stratospheric trend study is the indication that a significative influence of the 11 year solar cycle is seen, at least at some specific sites, which, as it is likely due to dynamics, have not be expected from the models.

References

Chanin M.L., N. Smires, A. Hauchecorne, Long-term variation of the temperature of the middle atmosphere at mid-latitude: dynamical and radiative causes, *J. Geophys. Res..*, 933-941, 1987.

Chanin M.L., P. Keckhut, A. Hauchecorne and K. Labitzke, The solar activity-QBO effect in the lower thermosphere, *Accepted Ann. Geophys.*, 1989.

Chanin M.L., A review of the 11-years solar cycle, and the atmosphere relationship, *Handbook for Map* (this issue), 1989.

Labitzke K., Sunspots, the QBO and the stratospheric temperature in the north polar region, *Geophys. Res. Lett.* , 14, 535-537, 1987.

Labitzke K.and Chanin, Changes in the middle atmosphere in winter related to the 11-year solar cycle, *Ann. Geophys.* , 6, 643-644, 1988.

Labitzke K. and H. Van Loon, Association between the 11-year solar cycle, the QBO, and the atmosphere. part I: the troposphere and stratosphere on the northern hemisphere in winter, *J. Atm. Terr. Phys.*, 50, 197-206, 1988.

Labitzke K. and H. Van Loon, Association between the 11-year solar cycle, the QBO, and the atmosphere. part III: aspects of the association, *J.of Climate*, 2, 6, 554-565, 1989a.

Labitzke K. and H. Van Loon, The 11-year solar cycle in the stratosphere in the northern summer., *Ann.Geophys.* 1989b (in press).

London J.G., Bjarnason and G.J. Rottman, 18 months of u.v. irradiance observation from the solar mesosphere explorer, *Geophys. Res. Lett.*, 11, 54-56, 1984.

Van Loon H. and K. Labitzke, Association between the 11-year solar cycle, the QBO and the atmosphere, Part II: surface and 700 mb in the northern hemisphere in winter, *J. of Climate*, 1, 9, 905-920, 1988.

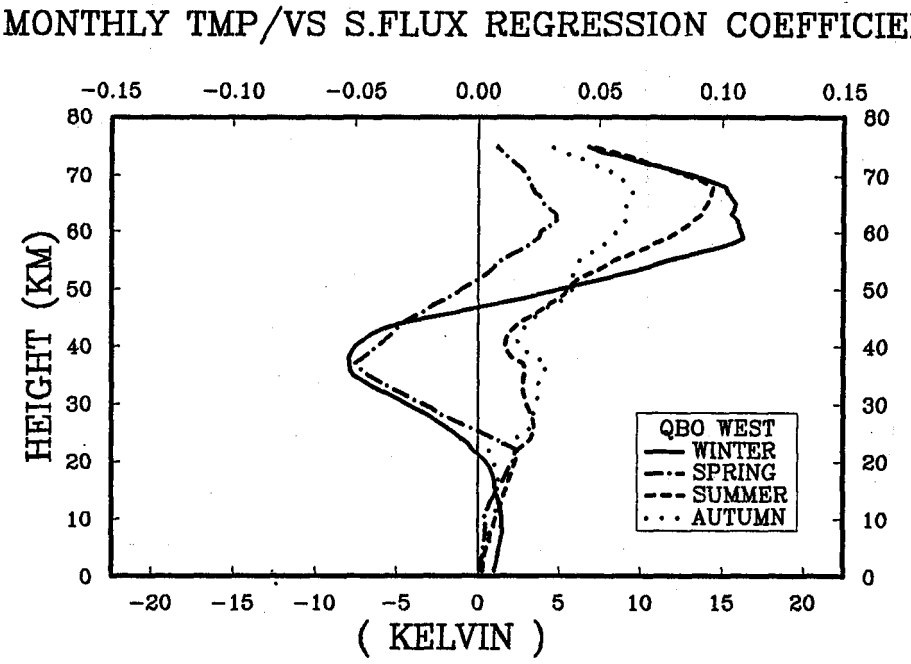

Figure 1: Seasonal amplitude of the solar temperature dependence over Southern France expressed in Kelvin and in Kelvin by unit of solar flux given for the **Westward** phase of the Q.B.O..

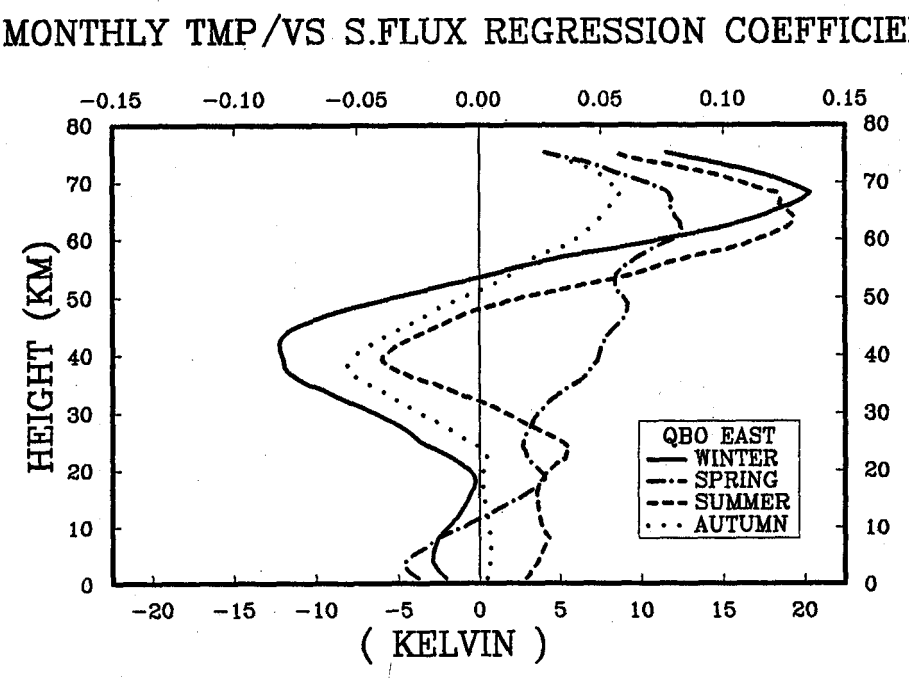

Figure 2: Same as Figure 1 given for the **Eastward** phase of the Q.B.O..

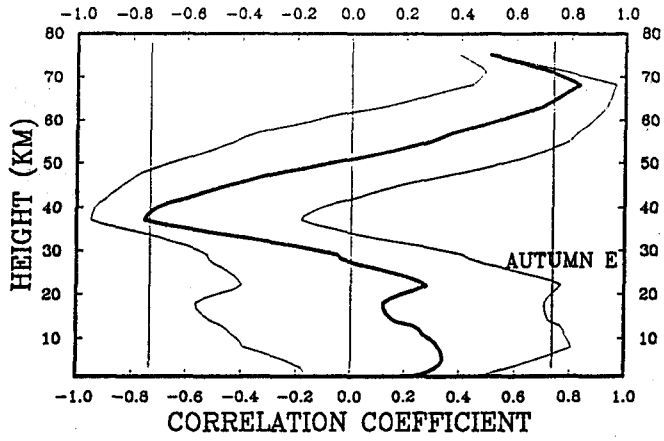

Figure 3: Correlation coefficient between **Autumn** temperature variations and the 10.7 cm solar flux for the **East** phase of the Q.B.O.. The vertical lines indicate the 95% confidence level.

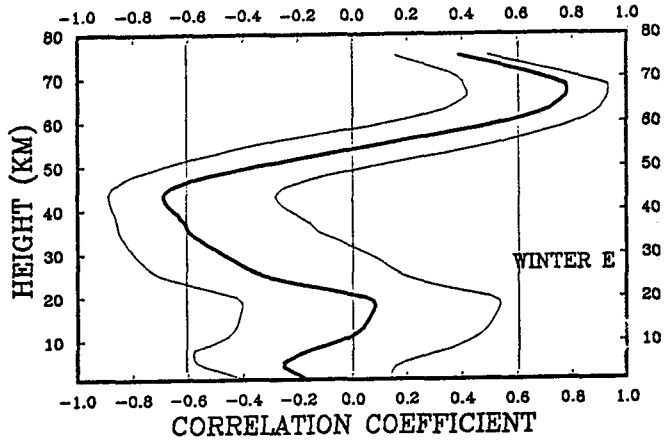

Figure 4: Same as Figure 3 given for **Winter** and for the **East** phase of the Q.B.O..

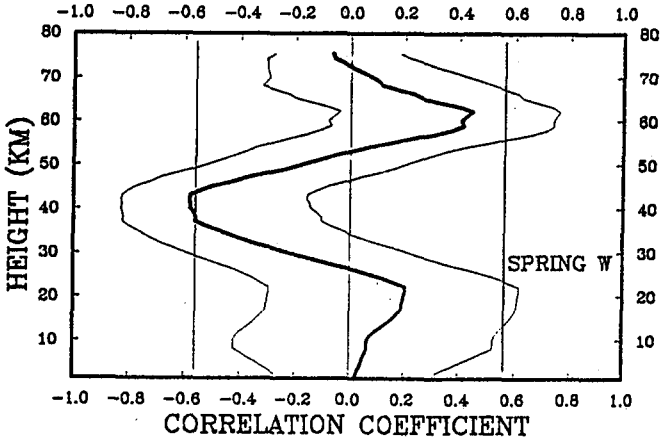

Figure 5: Same as Figure 3 given for **Spring** and for the **West** phase of the Q.B.O..

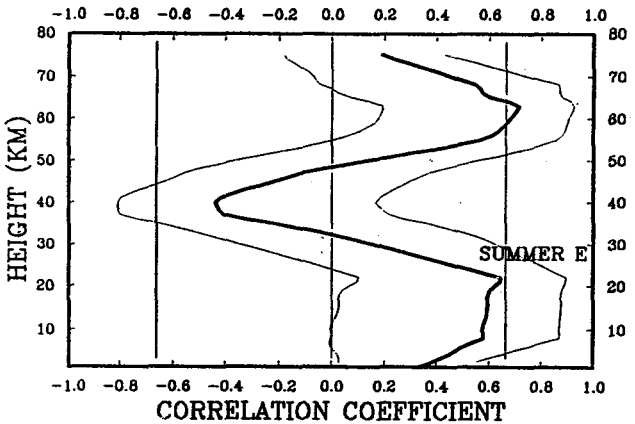

Figure 6: Same as figure 3 for **Summer** and for the East phase of the Q.B.O..

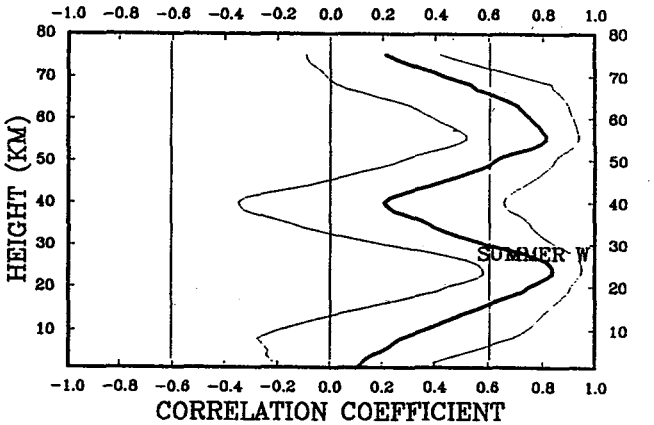

Figure 7: Same as figure 3 for **Summer** and for the West phase of the Q.B.O..

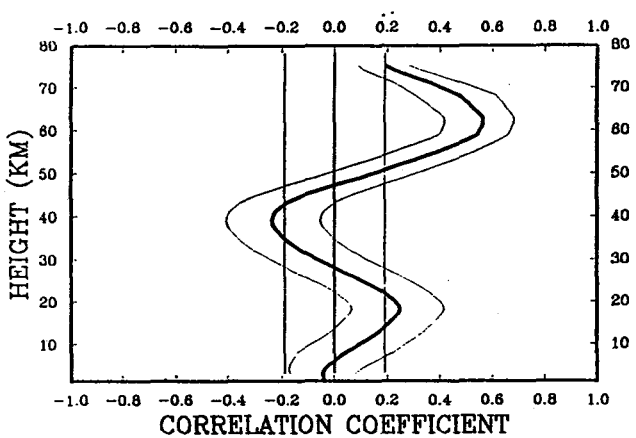

Figure 8: Same as figure 3 for all seasons and independently of the Q.B.O..

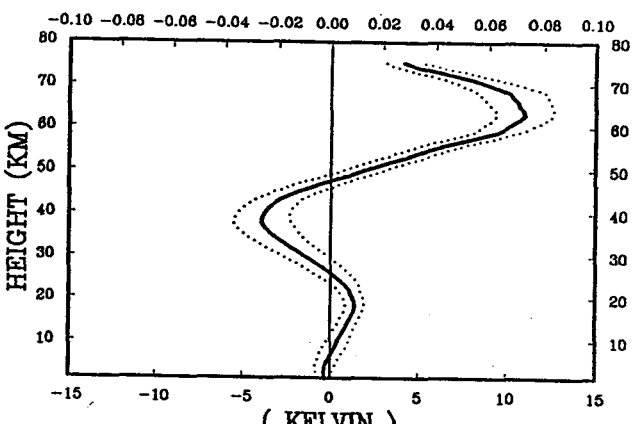

Figure 9: Amplitude of the solar temperature dependence expressed in Kelvin and in Kelvin by unit of solar flux for all seasons and independently of the Q.B.O..

INFLUENCE OF SOLAR ACTIVITY ON MIDDLE ATMOSPHERE ASSOCIATED WITH PHASES OF EQUATORIAL QUASI-BIENNIAL OSCILLATION

K. Mohanakumar

School of Marine Sciences
Cochin University of Science and Technology
Cochin 682 016, India

Earlier studies on the influence of solar activity variations within a 11-year solar cycle on temperature changes in the middle atmosphere revealed that while the temperature in the mesosphere showed strong response to changes in solar activity, the stratosphere remained almost unaffected (MOHANAKUMAR, 1985; 1987; 1988). Recent studies (LABITZKE, 1987; LABITZKE and VAN LOON, 1988; LABITZKE and CHANIN, 1988) showed that when the temperature data were grouped into east or west phase of the equatorial quasi-biennial oscillation (QBO) in stratospheric zonal wind, significant relationships of temperature in the lower stratosphere and troposphere could be obtained with 10.7 cm solar radio flux. Positive correlations in high latitude regions and negative correlations in mid-latitude and tropical regions were obtained during winter when the QBO was in its west phase. During the east phase, converse relationships were indicated. These interesting results inspired the present study on the response of solar activity in 11-year cycle on the temperature structure of the middle atmosphere in the two phases of equatorial QBO of zonal wind at 50 mb, in tropics, mid-latitude and antarctic regions

Soviet M-100 rocketsonde-derived temperature data collected from Thumba (8°N, 77°E) in tropics, Volgograd (49°N, 44°E) in mid-latitude and Molodezhnaya (69°S, 46°E) in antarctic for a 14-year period from 1971 to 1984 were used for the present study. The temperature data at every 5 km interval from 15 to 80 km altitude region were selected for the above three stations. The winter-time temperature was obtained by averaging the data during January and February, and the summer-time temperature by averaging data during July and August for the two Northern Hemispheric stations, whereas, for the antarctic station, the months representing these two seasons are just reverse. These were then grouped according to the periods of easterly and westerly phases of QBO at 50 mb. 10.7 cm solar radio flux was taken as the solar activity parameter for the corresponding periods.

The linear correlation coefficients computed for every 5 km levels between the solar radio flux and temperatures at the three stations are shown in Fig.1. Scattergrams of solar radio flux and temperatures for few selected levels in the stratosphere are also given in the figure to highlight the effect of solar activity on temperature in the two phases of QBO.

During both the seasons, the temperatures in the tropical stratosphere show strong negative correlation with solar radio flux during the westerly phases of QBO and positive or weak negative correlation during the easterly phases. Below 20 km, over tropics, strong positive correlations are obtained during both the seasons and the two phases of QBO. The scattergrams at 30 and 40 km altitude over Thumba indicate that the temperature changes during the westerly phases of QBO are consistently out-of-phase with the changes in solar activity, while during the easterly phase, the variations are inconsistent.

In mid-latitude and antarctic regions, the lower stratospheric temperatures in summer show positive correlation during the easterly phases and negative correlation during the westerly phases of QBO. During winter, on the other hand, lower stratospheric temperature register positive correlation during the westerly phases and negative correlation during the easterly phases. Changes in the slope of the regression line in the scatter diagrams further indicates the lower stratospheric circulation pattern modulates the solar induced changes in the stratospheric thermal structure.

The response of mesospheric temperature to the solar activity is not at all altered by the variations in equatorial stratospheric zonal winds. During both the phases of QBO, the temperatures in mesosphere indicate a direct association to the solar activity at all the three stations. The altitude of maximum response to solar variations is found to be a function of season. The thermal response to solar variations attains its peak value in lower mesosphere (55-60 km) during winter and in middle mesosphere (65-70 km) during summer. The summertime temperature in mesosphere shows a better relation with the solar activity than during winter, irrespective of the change in phases of QBO.

Middle atmospheric temperature departures from the long period (14 year) mean, computed for January and July at every 5 km intervals, over the three stations are illustrated in Fig.2. The vertical arrows in the lower part of Fig.2 depict the periods of quasi-biennial west wind maximum. Periods of high and low solar activity are indicated on the upper part of the Fig.2.

During both summer and winter, consistent and marked cooling is observed in mesosphere in association with the period of low solar activity. The maximum cooling is observed when the solar activity attains its minimum. Maximum cooling occurs slightly early in winter than in summer. As the solar activity increases from minimum to maximum, the temperatures in mesosphere steadily increases and produces consistent heating. Inwinter, the heating occurs early during solar maximum in the upper mesosphere, whereas, in summer it occurs slightly later during solar maximum in the middle mesosphere. The rate of heating decreases as the solar activity gradually subsides and the mesosphere becomes cooler after 1982.

The heating/cooling regimes in mesosphere, produced during the active/weak phases of solar activity, are transported downwards to the stratosphere. The downward transport of the heating/cooling regimes is slow during winter, whereas, there is a rapid downward spreading observed during summer. The temperature changes in middle stratosphere are found to have an inverse relation with those in mesosphere. The middle and lower stratosphere register cooling during solar maximum and heating during solar minimum in both summer and winter seasons at all the three stations. The rate of heating/cooling observed in stratospheric layers are comparatively lower in magnitude than the mesosphere.

REFERENCES

Labitzke, K. 1987, Geophys. Res. Lett., 8, 187.

Labitzke, K. and Chanin, M.L. 1988, Annales Geophys. 6

Labitzke, K. and van Loon, H. 1988 , J. Atmos. Terr. Phys., 50, 197.

Mohanakumar, K. 1985, Planet. Space Sci., 33, 795.

Mohanakumar, K. 1987 J. Atmos. Terr. Phys., 49, 27.

Mohanakumar, K. 1988 Physica Scripta, 37, 460.

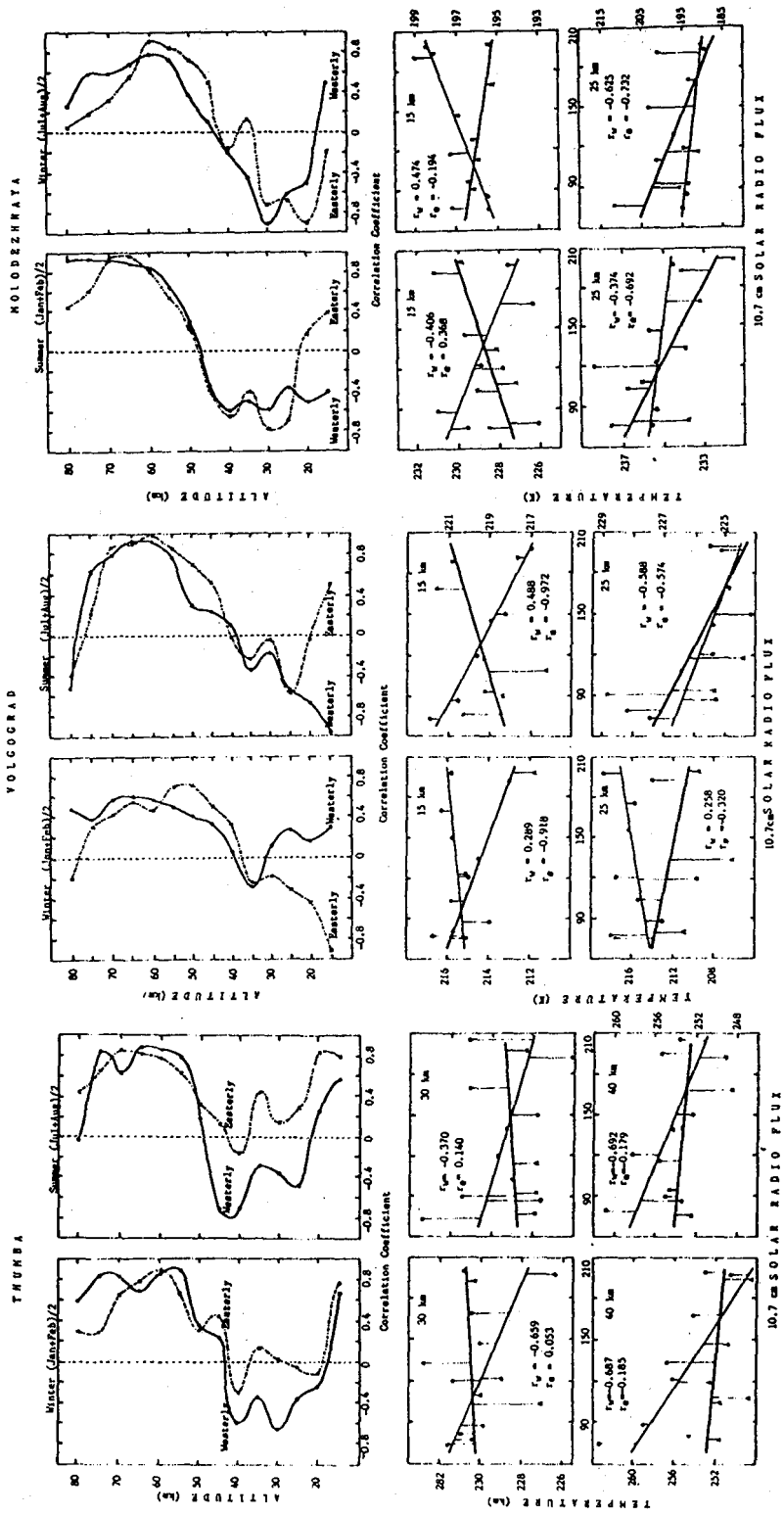

Figure 1. Vertical profiles of correlation coefficients (upper part) and scatter diagrams (lower part).

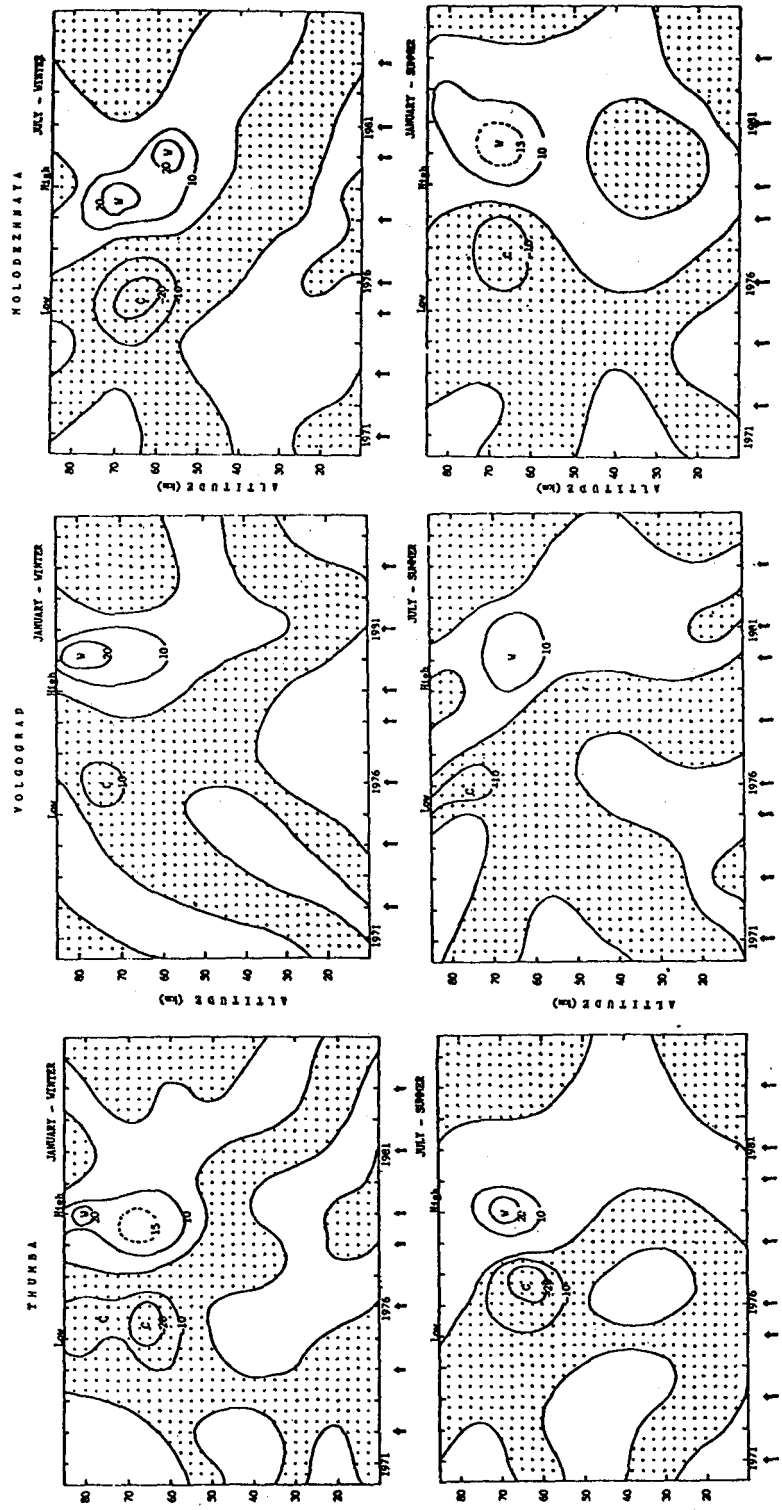

Figure 2. Middle atmospheric heating/cooling associated with solar activity.

SOLAR ACTIVITY INFLUENCE ON CLIMATIC VARIATIONS OF STRATOSPHERE AND MESOSPHERE IN MID-LATITUDES

J. Taubenheim, G. Entzian and G. von Cossart

Heinrich Hertz Institute of Atmosphere Research and Geomagnetism, Academy of Sciences of the GDR, Berlin, DDR-1199

The direct modulation of temperature of the mid-latitude mesosphere by the solar-cycle EUV variation, which leads to greater heat input at higher solar activity, is well established. In an earlier paper (von COSSART and TAUBENHEIM, 1987) we have analyzed more than 500 rocket-measured temperature profiles in the height range 20-80 km over Volgograd (latitude 49 N), covering almost two solar cycles from 1963 through 1983. Averaging over all seasons and times of day, we found a maximum response of temperature to the solar cycle near the altitude level of 65 km, with an amplitude of about 6 K between low (solar 10.7 cm radio flux $F < 100$) and high ($F > 160$) solar activity. With decreasing height in the middle atmosphere, this response falls to zero near 50 km. In an independent, somewhat different evaluation of the same Volgograd rocket data, MOHANAKUMAR (1987) found the same height dependence, but a slightly larger solar-cycle amplitude of 17 K near 65 km. These results have been excellently corroborated by temperature profiles derived by CHANIN et al. (1987) from air density data measured with the Rayleigh Lidar at Haute Provence (latitude 44 N), which again indicate a maximum solar-cycle response near 65 km altitude, but with still larger amplitudes up to about 25 K for winter, and 10 K for spring months.

At heights below 50 km, in the stratosphere, temperatures seem to be negatively correlated with the phase of the solar cycle. The amplitude of this variation is small, statistically not significant in the rocket data (von COSSART and TAUBENHEIM, 1987), but marginally significant with a few K in the Lidar data (CHANIN et al., 1987). Presumably this anti-phase variation of mid-latitude stratosphere temperatures, if it is real, must be produced by the dynamics of middle atmosphere circulation: It is well known that in medium and high latitudes there is an anticorrelation between mesopause and stratopause temperatures, not only in the seasonal variation but also in variations on shorter time scales, e.g., stratospheric warmings (cf. TAUBENHEIM, 1983). It seems not unreasonable to assume that such dynamical compensation mechanism could function on the longer time scale of an 11-yr variation as well.

Middle atmosphere temperature modulation by the solar cycle is independently confirmed by the variation of reflection heights of low-frequency radio waves in the lower ionosphere, which are regularly monitored over about 30 years at our Observatory of Atmosphere Research at Kuehlungsborn (geographic coordinates 52 N, 12 E). As explained elsewhere in detail (TAUBENHEIM and Von COSSART 1987), these reflection heights depend on the geometric altitude of a certain isobaric surface (near 80 k), and on the solar ionizing Lyman-alphe radiation flux. Knowing the solar-cycle variation of Lyman-alpha (e.g.,

ROTTMAN 1988) we can calculate how much the measured reflection heights would be lowered with the transition from solar minimum to maximum, if the vertical baric structure of the neutral atmosphere would remain unchanged. This expected reflection height variation is shown in the first line of the Table below, while the second line gives the observed height change (Von COSSART 1984), which obviously is markedly smaller. This discrepancy between expected and observed height change must be explained by an uplifting of the isobaric level from solar minimum to maximum, caused by the temperature rise in the mesosphere. By integrating the solar-cycle temperature changes over the height region of the middle atmosphere, and assuming that the lower boundary (tropopause) has no solar cycle variation, we can estimate the magnitude of this uplifting. It is given in the last two lines of the table, for the Lidar-derived and for the rocket-measured temperature variations, respectively. Comparison of these figures with those in the third line of the table suggests that the real amplitude of the solar-cycle temperature variation in the mesosphere is underestimated when using the rocket data, but probably overestimated with the Lidar data.

Table 1: Solar minimum-to-maximum change of radio wave reflection heights (in km) in the mid-latitude lower ionosphere

	winter	summer
Calculated from Lyman-alpha variation only	- 1.8	- 1.5
Observed	- 0.8	- 1.0
Difference (interpreted as isobaric level uplifting)	+ 1.0	+ 0.5
Estimated from Lidar data	+ 1.3	+ 0.85
Estimated from rocket data	+ 0.35	+ 0.25

Correlations between solar cycle and stratospheric winter temperatures in dependence on the QBO, as found by LABITZKE (1987) and discussed by LABITZKE and Van LOON (1988) seem to represent quite another kind of interaction between solar activity and middle atmosphere, rather than the direct EUV-induced modulation. This can be seen from fig. 1, where we have plotted the minimum geometric altitudes (in decameters) of the 30 hPa isobaric surface over the Northern Hemisphere in January/February, i.e., the height of the center of the winter polar vortex, versus the Zurich sunspot numbers (R). The data base is the same as used by LABITZKE (Daily maps of the 30 hPa surface, issued by the Institute of Meteorology of the Free University, Berlin-West). Each winter in the period 1961 to 1987 is representd by a symbol 'E' or 'W', indicating the phase of the quasi-biennial oscillation (QBO). These symbols, however, have been put in parenthesis in those cases when a major stratospheric warming occurred in January or

February, leading to enhanced mean temperature of this 2-month interval.

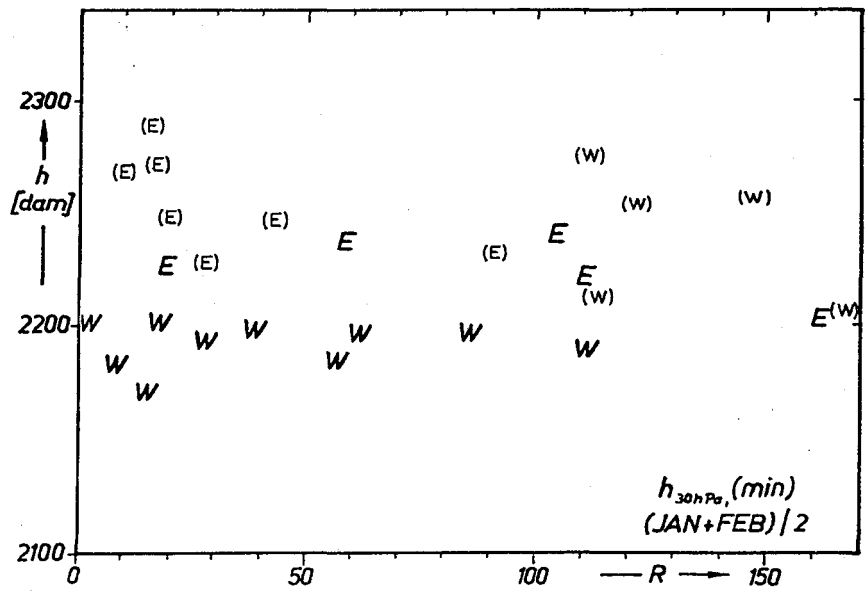

Fig. 1

The symbols 'E' and 'W' without parenthesis are in general accordance with the earlier findings of HOLTON and TAN (1980), that the winter polar vortex is stronger (the vortex center is deeper) during a 'W' phase than during an 'E' phase of the QBO. Obviously, the symbols without parenthesis do not show any significant dependence on solar activity, neither for 'E' nor for 'W' phase, while those in parenthesis generally lie above them, as to be expected in the case of major warming of the stratosphere. From the distribution of symbols with parenthesis in fig. 1, the following relations between major stratospheric warming, QBO, and sunspot numbers become immediately apparent: As pointed out by LABITZKE (1982) already several years ago, the probability of occurrence of major midwinter stratospheric warmings is higher in 'E-phase' than in 'W-phase' winters. This rule, however, holds true only for low and medium solar activity. Higher solar activity seems to 'suppress' the proneness of E-phase winters to major warmings. On the other hand, higher solar activity seems to 'unlock' some destabilizing mechanism, which allows stratospheric warmings to evolve during W-phase winters where they are 'forbidden' at low solar activity. Clearly there is a threshold of solar activity where the occurrence of major warmings switches over from E-phase preference to W-phase preference. Fig. 2 shows the curve of yearly mean Zurich sunspot numbers since 1950, and in the bottom strip, the occurrence of major stratospheric warmings indicated by full and open rectangles for W and E phase winters, respectively. The above-mentioned threshold may be placed near a sunspot number of R = 90, represented by the horizontal line.

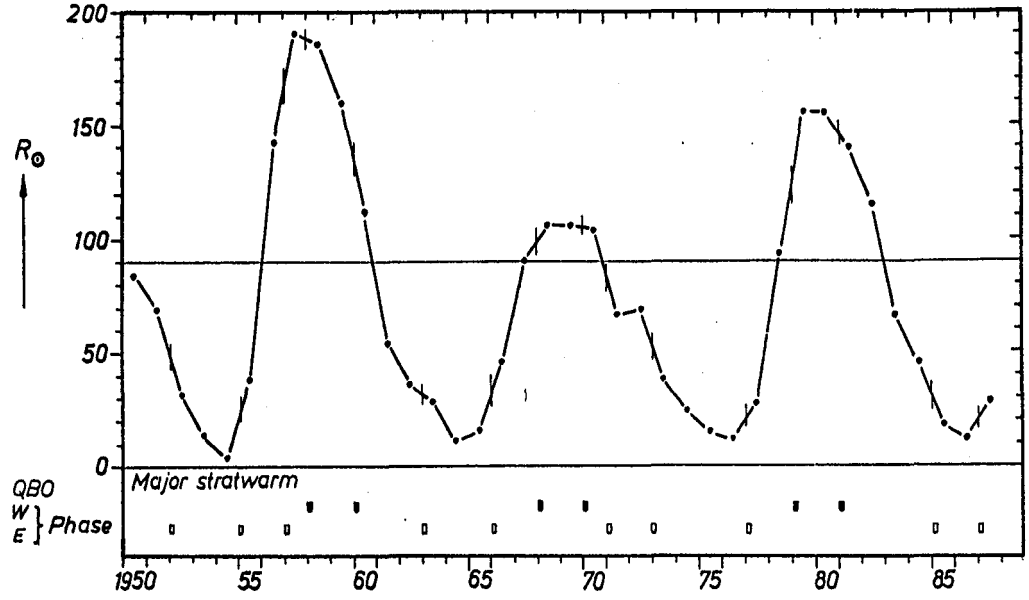

Fig. 2

In conclusion we should like to state that it seems not appropriate to discuss solar forcing of the winter mid-latitude stratosphere in terms of regression or correlation of temperature with solar activity indices. Rather, it might be more helpful to think of a solar activity-dependent 'locking' and 'unlocking' of trigger mechanisms for polar vortex breakdowns.

REFERENCES

Chanin, M.-L., N. Smires and A. Hauchecorne, J.Geophys.Res., 92, 10933, 1987.

Cossart, G. von, Beitr. Geophys., 93, 329, 1984.

Cossart, G. von, and J. Taubenheim, J.atmos.terr.Phys., 49, 303, 1987.

Holton, J.R., and H.-C. Tan, J.atmos.Sci., 37, 2200, 1980.

Labitzke, K., J.Meteor.Soc.Japan, 60, 124, 1982.

Labitzke, K., Geophys.Res.Lett., 14/5, 535, 1987.

Labitzke, K., and H. van Loon, J.atmos.terr.Phys., 50, 197, 1988.

Mohanakumar, K., J.atmos.terr.Phys., 49, 27, 1987.

Rottman, G.J., Adv.Space Res., 8, No. 7, 53, 1988

Taubenheim, J., Space Sci.Rev., 34, 397, 1983.

Taubenheim, J., and G. von Cossart, Beitr.Geophys., 96, 105, 1987.

THE PLANETARY WAVES DYNAMICS AND INTERANNUAL COURSE OF METEOROLOGICAL PARAMETERS OF THE HIGH LATITUDE STRATOSPHERE AND MESOSPHERE OF THE NORTHERN AND SOUTHERN HEMISPHERES DURING THE 20th AND 21st SOLAR CYCLES AND DIFFERENT PHASES OF QBO

V.G. Kidiyarova, N.N. Fomina

CAO, 141700 Dolgoprudny, USSR

The part of energy of the planetary waves which enters the stratosphere depends on conditions of planetary wave generation and propagation through the tropopause, and the part of planetary wave energy which enters the mesosphere depends on conditions of planetary wave propagation through the stratopause. In this report an attempt is made to estimate connections between extratropical middle atmosphere temperature long-term variations and portions of energy of planetary waves which enter the mesosphere and stratosphere during winter seasons in Northern and Southern Hemispheres. Interannual variations of temperatures at the 30 km and 70 km levels are investigated for the central winter months of the period 1970-1986. This period includes the descending branch of the 20th solar cycle and the whole 21st cycle. Calculations are made on the basis of measurements at Heiss Island and Molodezhnaya.

Figure 1 shows interannual temperature courses at heights of 30 km and 70 km over Heiss Island and Molodezhnaya for the central winter months (January and July respectively) during the 1971-1986 period. It can be seen that interannual variations of the mesospheric and stratospheric temperatures are out-of-phase. The long-term variations of temperatures with periods of about 10 years are more visible in the mesosphere. In the northern hemisphere these oscillations are superimposed by oscillations with shorter periods, which may be connected with interannual variations in intensities of stratospheric warmings.

Monthly mean temperatures at 70 km level for central winter months over Molodezhnaya and Heiss Island for west (W) and east (E) phases of QBO for 1970-1976, 1977-1986 and 1970-1986 periods are shown in the Table:

	1970-1976		1977-1986		1970-1986	
	W	E	W	E	W	E
Heiss Isl.	199	190	216	209	207	202
Molodezhnaya	209	210	225	213	219	212

It can be seen that the east phase of QBO is followed by lower mesospheric temperatures.

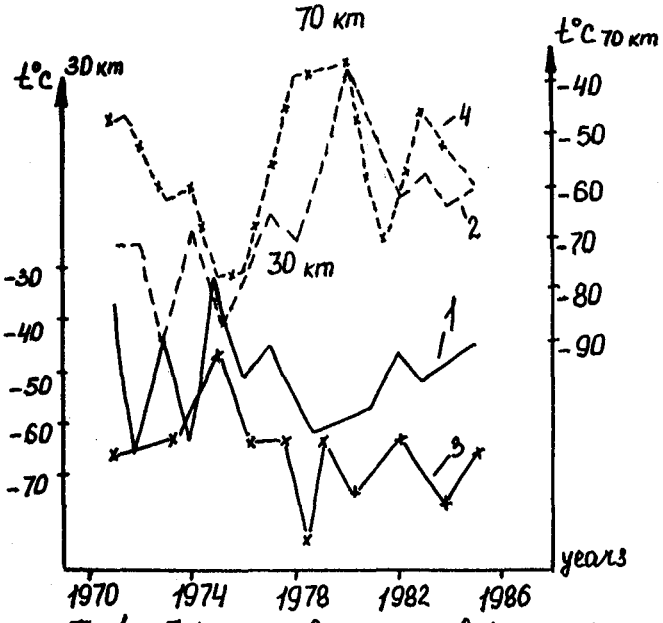

1 – Heiss Jcl. 30 km
2 – Heiss Jcl. 70 km
3 – Molodezhnaja 30 km
4 – Molodezhnaja 70 km

Fig. 1 Interannual courses of temperatures at 30 km and 70 km levels over Heiss Isl. (Januaries) and Molodezhnaja (Julies) for 1970–1986 period.

THE QBO AND WEAK EXTERNAL FORCING BY SOLAR ACTIVITY: A THREE DIMENSIONAL MODEL STUDY

M. Dameris and A. Ebel

Institute for Geophysics and Meteorology
University of Cologne
Albertus-Magnus-Platz
D - 5000 Cologne 41, F.R.G.

Introduction

The goal of this study is a better understanding of the physical mechanisms leading to significant correlations between oscillations in the lower and middle stratosphere and solar variability associated with the sun's rotation. A global 3-d mechanistic model of the middle atmosphere is employed to investigate the effects of minor artificially induced perturbations. The aim is to explore the physical mechanisms of the dynamical response especially of the stratosphere to weak external forcing as it may result from UV flux changes due to solar rotation. First results of numerical experiments dealing about the external forcing of the middle atmosphere by solar activity were presented in a paper by Dameris et al. (1986). Different numerical studies regarding the excitation and propagation of weak perturbations have been continued since then (Dameris, 1987; Ebel et al., 1988).

Description of experiments, Results

The model calculations presented in this paper are made to investigate the influence of the quasi-biennal oscillation (QBO) on the dynamical response of the middle atmosphere to weak perturbations by employing different initial wind fields which represent the west and east phase of the QBO. The initial wind fields used for this study are shown in figure 1: They are characterized by realistic, relatively strong vertical gradients in the tropics between 10 and 40 km height. The conditions at middle to high latitudes are the same for both cases (solstice conditions, north winter, south summer). The global 3-d numerical model taken for this study is the same as described in detail by Dameris et al. (1986) (fully nonlinear, primitive dynamical equations in flux form). Based on the experiments done in the past the external forcing function and the lower boundary conditions are chosen as follows: A weak standing temperature oscillation (zonal wave number 1) centred at 43 km height, 2.5°N is assumed with a maximum amplitude of 1.5 K. The amplitude decreases linearly to half its value in a distance of ± 5.4 km and ± 20°. A period of 13.6 days is employed. Stationary waves of geopotential height have been excited at the lower boundary (10 km). Their characteristics are: Zonal wave number one and two, maximum amplitudes of 100 gpm and 30 gpm, respectively, centred at 60°N (winter), decrease of

amplitudes to zero at 30°N and 80°N. Transient zonal waves are simulated at the lower boundary assuming the latitudinal structure of free westward travelling modes. The following modes were used: (1,4), 16-day wave (max. amplitude 50 gpm); (1,3), 10-day wave (20 gpm); (1,2), 5-day wave (2 gpm).

In the following results of the two model experiments are presented which differ **only** by the definition of the initial wind fields representing the west and the east phase of the QBO. The external forcing and also the lower boundary conditions are the same for both experiments. For a better presentation of the effects of the weak external forcing, control runs without external forcing were also made for otherwise identical conditions. Here only the differences between the experiments with weak external forcing and the respective control run are shown.

Figure 2 shows the horizontal structure of temperature perturbations at 26 km height due to the periodic temperature forcing for both cases (QBO-west, QBO-east) for model day 80, where the differences between the two calculations are most obvious: For the west case two regions of significant response to the assumed temperature perturbation are observed, one in the equatorial region (0.4 K) and the other at high latitudes of the winter hemisphere (0.5 K). The results for the east case indicate significantly stronger amplitudes of the temperature perturbation at high latitudes of the winter hemisphere up to 2.5 K. A similar result is found for the perturbation of the geopotential height field (not shown). For model day 80 maximum amplitudes of 6 gpm are found for the west case instead of 30 gpm for the east case, also observed at high latitudes of the winter hemisphere.

An important tool to analyse the model results and to get an indication why the model reacts in such a way is given by the Eliassen Palm (EP) flux diagnostics. The results shown in figure 3 indicate that there is little or no transport of wave energy across the critical wind line (u=0) into regions where the mean wind is easterly. At model day 76 (here also differences with respect to control run) the meridional cross section of the EP-vector for the west case indicates relatively strong activity at the tropics lower than 30 km height in comparison to the results of the east case. This effect is probably caused by the westerly winds in this region: The wave energy can directly penetrate from the region of main forcing (43 km, 2.5°N) to lower levels. At middle to high latitudes of the stratosphere the EP-vectors (transport of wave energy) are significantly enhanced for the east case. Most of the perturbation energy is bend into the region of westerly winds (winter hemisphere).

Conclusion

The model results show significant differences of the dynamical response of the middle atmosphere to weak external forcing by assuming different initial conditions representing the west and the east phase of the QBO. If the QBO has its easterly phase, solar induced perturbations, which are generated near the equatorial stratopause, lead to stronger

variations in the middle and lower stratosphere than during the west phase of the QBO. Up to now no statistical analysis is available for a comparison with our model results. Statistical analyses which were made in the past, for example by Ebel et al. (1986) must be repeated, but now with regard to the different QBO phases, to get indications if the real atmosphere reacts similar.

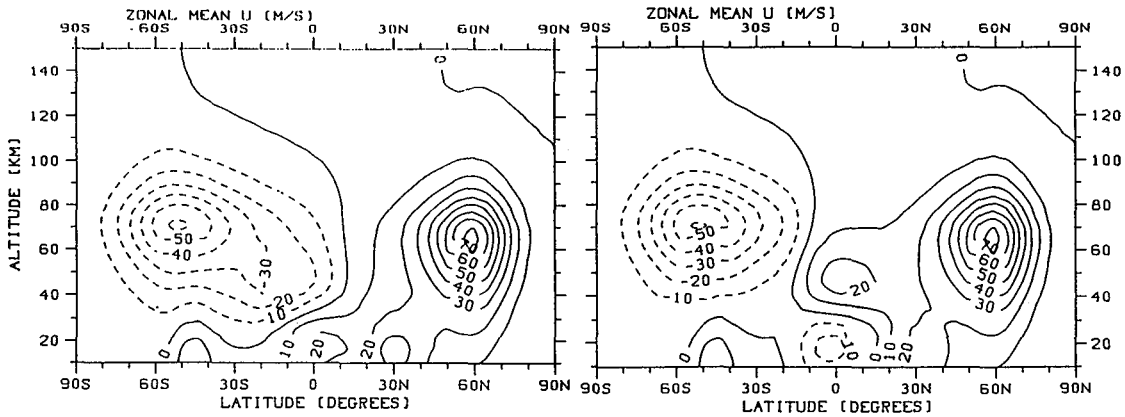

Figure 1: Initial stage of the mean zonal wind field used for the numerical experiments, representing the west phase of the QBO (left), representing the east phase of the QBO (right). Positive and negative values indicate eastward and westward motion, respectively. Units are m/s.

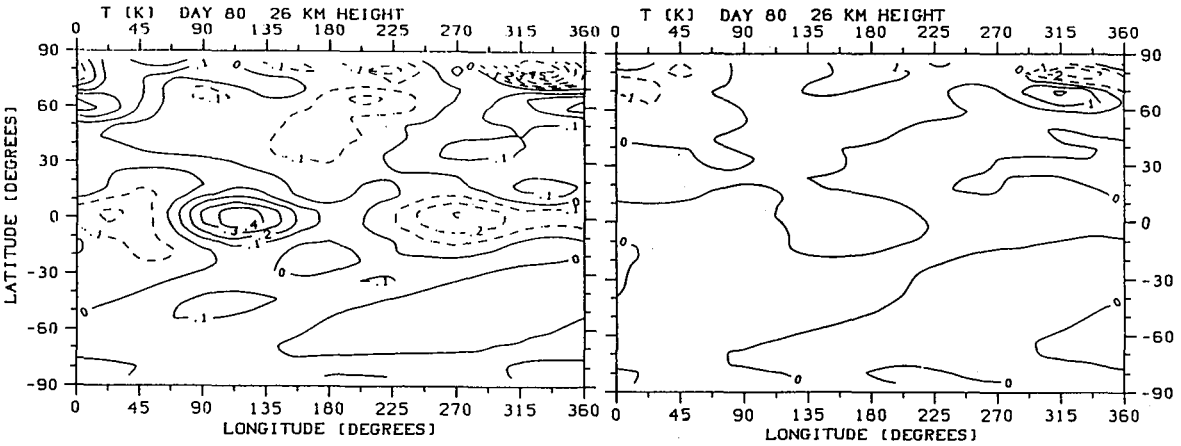

Figure 2: Horizontal structure of the response to periodic temperature forcing centred at 43 km height, 2.5°N with a zonal wave number 1 structure. Temperature perturbations (differences with respect to control run) in K at 26 km height for model day 80. West-case (left-hand side) and East-case (right-hand side). Attention, the contour lines are different for the two cases.

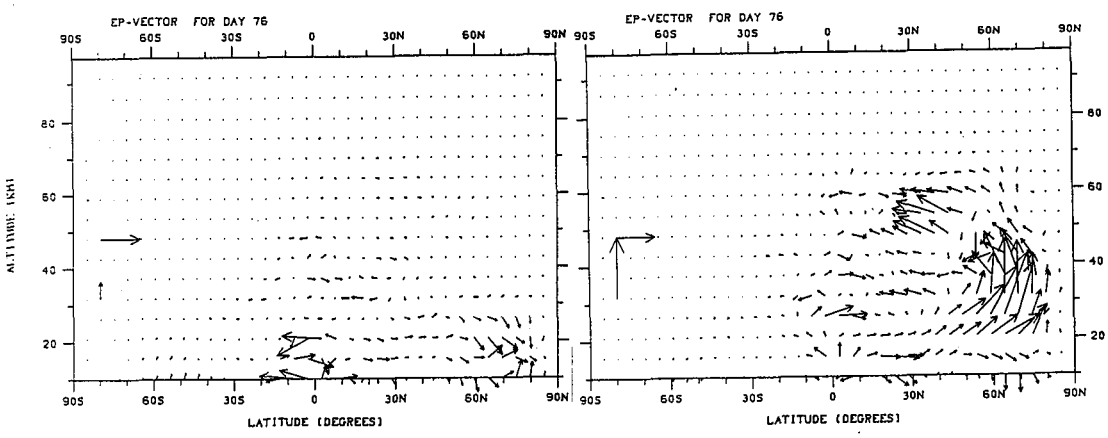

Figure 3: Differences of the EP-vectors (differences with respect to control run) for the West-case (left-hand side) and East-case (right-hand side) for model day 76. The distance occupied by 10° of latitude represents a value $2\ \pi\ a^2\ \rho_s \cdot 7.0 \cdot 10^{-3} m^2 s^{-2}$ of F_ϕ and that occupied by 10 km of pressure-altitude z represents a value $2\ \pi a^3 \rho_s \cdot 6.2 \cdot 10^{-5} m^2 s^{-2}$ of F_z.

References

Dameris M., Die Ausbreitung schwacher solar induzierter Störungen in der mittleren Atmosphäre, Mitteilungen aus dem Institut für Geophysik und Meteorologie der Universität zu Köln, **53**, 1987.

Dameris M., Ebel A., Jakobs H.J., Three-dimensional simulation of quasiperiodic perturbations attributed to solar activity effects in the middle atmosphere, Ann. Geophysicae, **4**, 287-296, 1986.

Ebel A., Dameris M., Hass H., Manson A.H., Meek C.E., Petzoldt K., Vertical change of the response to solar activity oscillations with periods around 13 and 27 days in the middle atmosphere, Ann. Geophysicae, **4**, 271-280, 1986.

Ebel A., Dameris M., Jakobs H.J., Modelling of the dynamical response of the middle atmosphere to weak external forcing: Influence of stationary and transient waves, Ann. Geophysicae, **6**, 501-512, 1988.

SOLAR ACTIVITY, THE QBO, AND TROPOSPHERIC RESPONSES

Brian A Tinsley,
UTD Center for Space Science, MSFO22, Box 830688, Richardson, Texas 75083, USA
Geoffrey M Brown,
UC Wales Physics Department, Aberystwyth, Wales, UK,
Philip H Scherrer
Stanford U Center for Space Science and Astronomy, California, USA

Abstract. The suggestion that galactic cosmic rays (GCR) as modulated by the solar wind are the carriers of the component of solar variability that affects weather and climate has been discussed in the literature for 30 years, and there is now a considerable body of evidence that supports it. Variations of GCR occur with the 11 year solar cycle, matching the time scale of recent results for atmospheric variations, as modulated by the quasibiennial oscillation of equatorial stratospheric winds (the QBO). Variations in GCR occur on the time scale of centuries with a well defined peak in the coldest decade of the "little ice age". New evidence is presented on the meteorological responses to GCR variations on the time scale of a few days. These responses include changes in the vertical temperature profile in the troposphere and lower stratosphere in the two days following solar flare related high speed plasma streams and associated GCR decreases, and in decreases in Vorticity Area Index (VAI) following Forbush decreases of GCR. The occurrence of correlations of GCR and meteorological responses on all three time scales strengthens the hypothesis of GCR as carriers of solar variability to the lower atmosphere.

Both short and long term tropospheric responses are understandable as changes in the intensity of cyclonic storms initiated by mechanisms involving cloud microphysical and cloud electrification processes, due to changes in local ion production from changes in GCR fluxes and other high energy particles in the MeV to low GeV range. The nature of these mechanisms remains undetermined. The height distribution of the tropospheric response and the amount of energy involved and the rapidity of the time response suggest the release of latent heat could be involved. Changes in cloud albedo and absorptivity to infrared radiation are also plausible. Both the release of latent heat and changes in radiative transfer can account for the observed changes in vertical temperature profile, leading to changes in the intensity of cyclonic disturbances that are associated with changes in vorticity area index. Theoretical considerations link such changes to the observed latitudinal movement of the jet stream.

Possible stratospheric wind (particularly QBO) effects on the transport of HNO_3 and other constituents incorporated in cluster ions and possible condensation and freezing nuclei are considered as relevant to the long term variations. This is an abridged version of the full paper that is being published elswhere.

RESPONSE OF TROPOSPHERIC TEMPERATURE PROFILE TO HIGH SPEED PLASMA STREAMS

The atmospheric response to short term solar wind changes near the earth has been examined using the data source of Lindblad and Lundstedt (1981, 1983). From their list of High Speed Plasma Streams (HSPS), defined by an increase in solar wind speed between consecutive days of at least 80 km s^{-1}, a set of stronger events has been selected defined by $dV = (V_m - V_o) > 200$ km s^{-1}, where V_m is the maximum speed of the interplanetary plasma stream in the vicinity of the earth, and V_o is the smallest speed on the first day. Over the period Jan. 1966 through Feb. 1978 there were 55 such HSPS associated with solar flares, and 196 HSPS not associated with flares. The non-

flare streams were mostly associated with coronal holes and were considerably more frequent on the declining phase of the solar cycle, in agreement with the well known preponderance of recurrent magnetic storms during this period. The distinction between the flare and non-flare related HSPS corresponds approximately to the distinction made by Burlaga et al. (1984) between transient shock associated flows and corotating streams. (Nevertheless shock associated flows can sometimes result from coronal mass ejections not associated with flares.) HSPS in general are associated with gradients in the solar wind velocity transverse to the 'garden hose' direction of the large scale magnetic field, whereas the flare related events also include strong gradients along the garden hose direction. A number of terrestrial effects are associated with HSPS events, including magnetic storm related X ray emissions; thermal, chemical and dynamical perturbations of the thermosphere, and penetration of fluctuating large scale electric and magnetic fields to the surface. For many of the flare related events there is in addition the reduction of the flux of GCR that penetrate to varying depths through the atmosphere (Forbush decreases), and for some the precipitation of particles in the MeV to GeV range at high latitudes. These effects of solar wind disturbances have been described for example by Akasofu and Chapman (1972, particularly ch. 7) and more recent reviews are those in the series of US National Reports to the IUGG. Thus there are a number of possible short term carriers of solar variability to the atmosphere, and a detailed analysis is required to identify at least one that has the appropriate time variations to cause the observed tropospheric responses.

It should be stressed that the rather extreme HSPS events selected according to the criterion $dV > 200$ km s^{-1} are relatively rare, only 4 or 5 of the flare related events per year on average, with a maximum occurrence (around solar maximum) of 10 per year. We study these as diagnostics; if short term but rare GCR changes unambiguously affect the troposphere then 11 year and longer term GCR changes may do so also. Of the 196 non flare events, 55 were selected to form a comparison set, with each as far as possible a match by being about the same dV and near to the time of a flare event. In Fig 1 from the top panel down we compare superposed epoch analyses of solar wind velocity (V) in the vicinity of the earth; solar wind magnetic field strength (B); GCR flux at the surface; and tropopause pressure, using the first day of increase of solar wind velocity as the key day (day 0). For the flare related events (solid curve) B increased by about 4nT on average, relative to the previous level of 5-6nT. The peak effect is on day 0. For the non flare events there is an increase over several days preceding day 0, and a drop of 3-4nT afterwards. The third panel shows that the average Forbush decrease in the GCR neutron count rate at Dourbes, Belgium was about 1% for the flare related events. The peak effect is on day +2, and the percentage effect at 5-20 km altitude would have been several times larger (Pomerantz and Duggal, 1974), since the main GCR flux at these heights is at lower energies that are more strongly affected by the interplanetary magnetic field than the higher energy flux that reaches the surface. In the case of the non-flare related events, the GCR change is smaller and of a different shape. This might be considered strange in view of the closeness of the V variations, and some similarities of the B variations in the two data sets. However, as noted earlier, a very important variation in V and B for modulating GCR fluxes is in the gradient along the garden hose direction, associated with shocks and produced by coronal mass ejections mainly associated with solar flares, that are not easily separable from transverse gradients in measurements by spacecraft near the earth. Another difference is that for corotating streams the magnetic field strength increases a day or two before it does for shock associated flows, relative to the increase in solar wind velocity (Burlaga et al., 1984).

The bottom panel shows the response to the HSPS in tropopause pressure measured by radiosondes above Berlin, from the data series Meteorologische Abhandlungen. There is about a 20 mb increase in tropopause pressure on day +2 that is more than two standard deviations above the mean. The response to the non flare-related HSPS is less than one

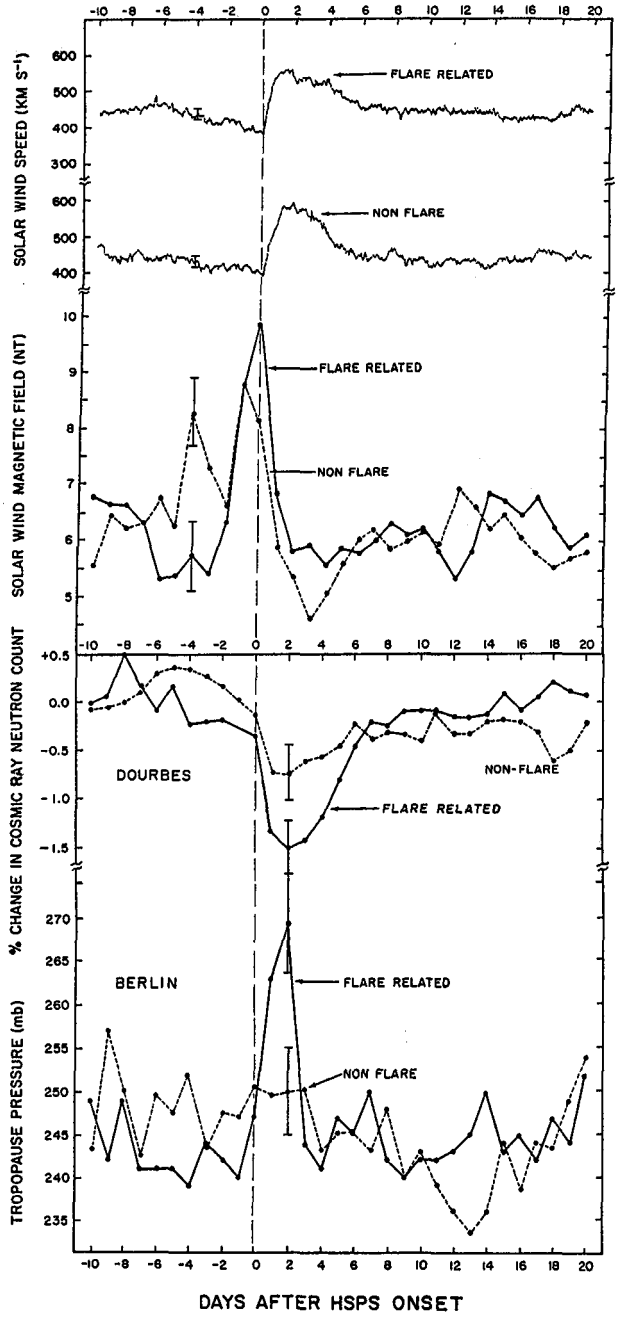

Fig. 1. Superposed epoch analysis for variability of solar-terrestrial parameters associated with 55 flare related and 55 non flare related high speed plasma streams in the solar wind, Jan. 1966 through Feb. 1978. Upper panel, solar wind speed and magnetic field; lower panel, surface neutron monitor countrate and tropopause pressure from European stations. Length of error bars is two standard deviations.

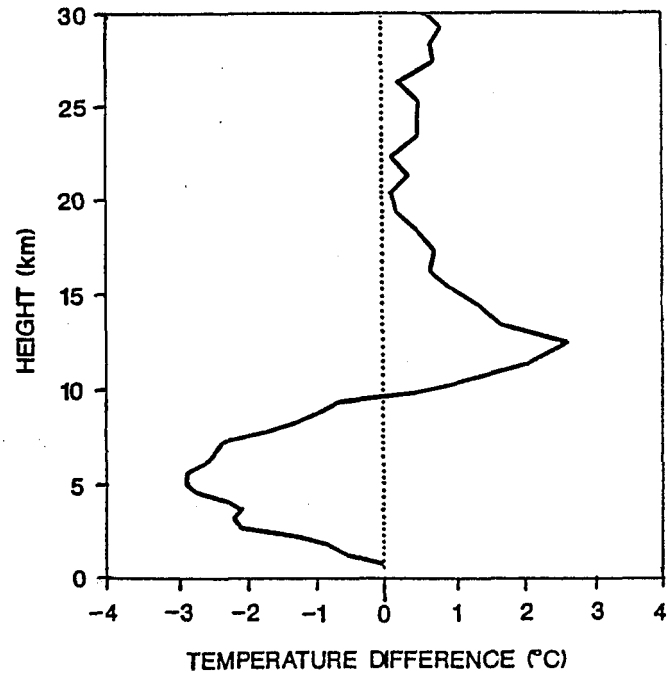

Fig. 2. Average atmospheric temperature change for the 55 flare associated events of Fig. 1, obtained by subtracting the profile for day -1 from the profile for day +2.

standadd deviation. The changes associated with flare related HSPS have not been found for lower speed streams than those selected here. The tropopause response also reveals itself as a change in the vertical temperature profile, and Figure 2 shows the average temperature change for the flare associated events computed as a function of height, obtained by subtracting the profile for day -1 from that of day +2. The response is in the form of a heating by 2-3^{0} C near the tropopause height (~12 km), and a cooling by about the same amount near 5 km, resulting in a decrease in tropopause height of about 0.7 km, that is equivalent to a pressure increase of about 20 mb. These tropopause height and temperature changes have been confirmed by direct examination of the measured parameters.

RESPONSE OF VAI TO FORBUSH DECREASES

In view of the tropospheric responses in Figs 1 and 2 being associated with Forbush decreases, it was decided to use specifically the days of onset of Forbush decreases as key days in a superposed epoch analysis of northern hemisphere VAI responses. A table of Forbush decreases greater than 3% observed by the Mt. Washington neutron monitor was used (NGDC 1985). The energy of the particles monitored lies primarily in the range 1-10 GeV. Actually, a more appropriate GCR flux to use in comparison with VAI variations would be that of about a factor of ten lower in energy, which is the main source of ionization and a source of chemical species in the lower stratosphere and troposphere. The neutron monitor data is used as a proxy for this lower energy GCR flux, which is supplemented at times by particles in the same energy range energised in the sun, the solar wind, and the magnetosphere.
The results of the superposed epoch analysis for 72 events from Nov. 1955 through April 1962, and for 106 events from May 1963 through Feb. 1982 are shown in Figs 3 and 4. The averaged variation of GCR observed with the Climax neutron monitor is shown for the same events. The VAI responses are further separated according to whether the events occurred in the winter months (Nov.-March) or the remainder of the year (April-Oct.), and according to whether they occurred in the QBO W or E phases. The results show that there is in general a reduction in the VAI associated with the reduction in GCR for both the 1955-62 and 1963-82 periods, and that this is deeper in the winter than in the non-winter, and that it is present for both QBO phases. A further subdivision of the winter data into E and W QBO phases (not shown) also resulted in the VAI reduction appearing about equally strongly in each phase. These events were not selected for steady solar wind or absence of sector boundaries or other Forbush decreases preceding or following the event within the epoch used in the analysis, as has been the case in previous VAI analyses, and some of the 'noise' in the VAI may be due to this.

PLAUSIBILITY OF GCR AS CARRIERS OF SOLAR VARIABILITY TO THE LOWER ATMOSPHERE

There are GCR variations that match the meterological and climate responses three different time scales. On the century time scale the decade of the 1690's, in the coldest part of the "little ice age" coincided with a peak in the ^{14}C and ^{10}Be production from GCR; the latter was 70% above levels before and after, from concentrations measured in Greenland ice cores (Attolini, et al.; 1988). There is an 11 year variation by about 50% in the GCR produced ionization at upper troposphere/lower stratosphere heights and an 11 year variation by a factor of about 10 in its day to day variability (Pomerantz and Duggal, 1974). The time variations of GCR and meterological variables in Figs. 1 to 4 show that GCR have appropriate time variations to be carriers of the short term (day to day) solar variability to the lower atmosphere. It is recognized that the presence of a correlation does not demonstrate by itself a physical connection. However the energetic particle hypothesis (low energy GCR and other particles of similar energy from the sun,

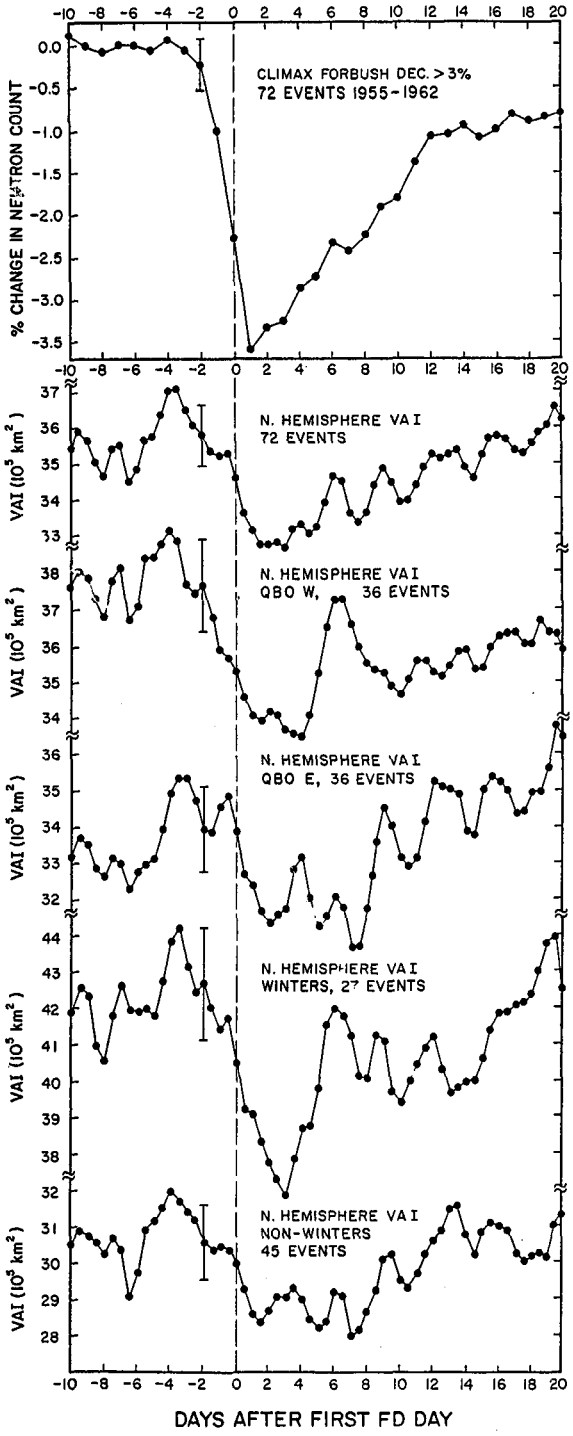

Fig. 3. Superposed epoch analysis of changes in hemispheric vorticity area index and Climax neutron monitor countrate associated with 72 Forbush decreases in Nov. 1955 through April 1962, with breakdown by QBO phase and winter-nonwinter intervals.

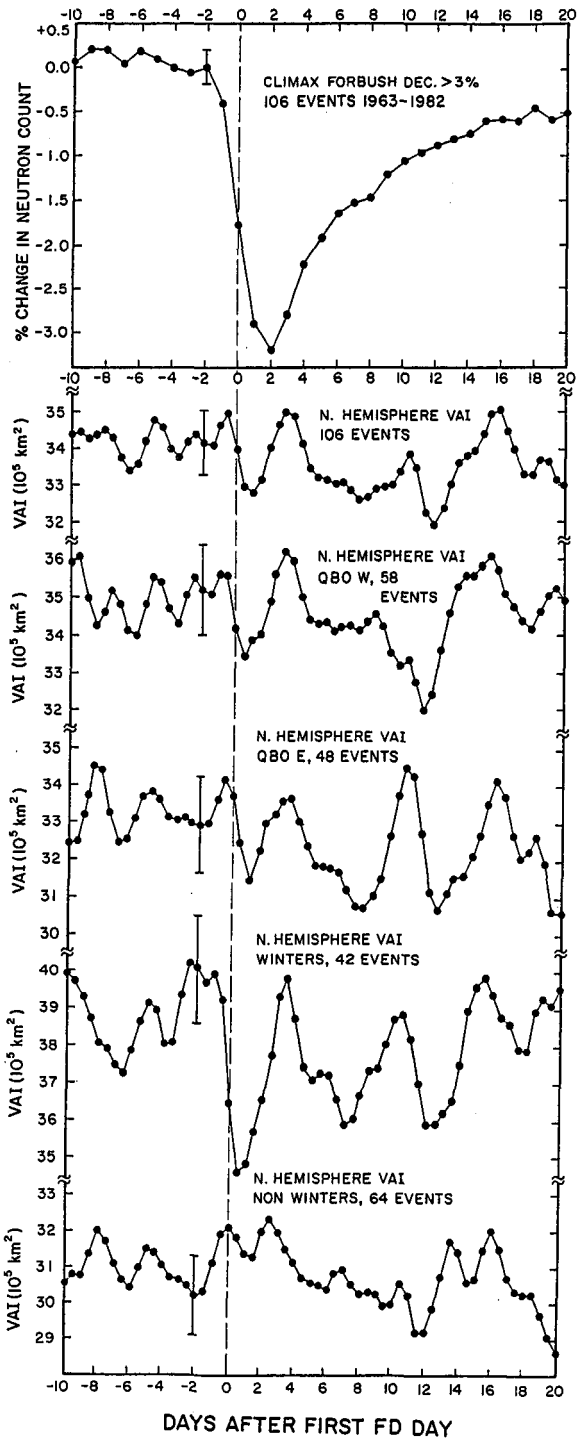

Fig. 4. As for Fig. 3 for 106 Forbush decreases in May 1963 through Feb. 1982.

interplanetary medium, and magnetosphere) seems the most promising one in terms of analyses made to date, and so we will continue to explore it.

The changes in height profile of Fig 2 occurred in the range 2-15 km, maximizing (in terms of energy involved) near 5 km or 500 mb. This is near where the greatest VAI response to sector boundary changes was found by Wilcox (1974) and not far from the 700mb level where Stolov and Shapiro (1974) found that large negative (cyclonic) centers developed in the 4 days following geomagnetic storms. This is the height range where in regions of uplift, associated especially with wintertime cyclonic disturbances, there is latent heat release occurring from conversion of water vapor to liquid and liquid to solid. Pauley and Smith (1988) showed that latent heat release exerted important direct and indirect influences on the development of a synoptic scale wave system containing an extratropical cyclone, particularly below 500mb, with latent heat release producing heating of up to 15^{o}C per day. In the same regions changes in the production of cirrus clouds would affect albedo to visible radiation and absorptivity to infrared. Thus changes in cloud microphysical processes associated with variations in GCR ionization could significantly affect the air temperature and dynamics of a cyclone. Only very small amounts of energy are required to initiate changes in these processes, if changes in condensation nuclei or ice nuclei are involved. If electric fields are involved in the cloud microphysics, then this is the height region where the conductivity is lowest and where only a small amount of energy in the form of a change in ion production has the greatest effect on the conductivity and electric field. The dominant source of ions in the troposphere and lower stratosphere above 1 to 2 km altitude is GCR.

An hypothesis linking the solar wind and cosmic ray changes on both short and long time scales to tropospheric and lower stratospheric changes is that: (a) an increase (decrease) in cosmic ray ion production in this region is reflected in changes in cloud microphysical and cloud electrification processes; so that (b) where there is supercooled liquid water or condensing vapor or evaporating droplets in regions such as cyclonic eddies in the jet stream, there is an increase (decrease) in the release of latent heat associated with the changes of state of water, and changes in cloud albedo and infrared absorptivity; that (c) affect the vertical temperature gradient; that in turn (d) increases (decreases) the intensity of the cyclonic eddies and thus increases (decreases) the vorticity area index. It is likely that: (e) there will be associated changes in wave activity that generate a divergence in the momentum flux in the general circulation; that (f) thereby produce latitudinal shifts in the mean latitude of the jet stream and in averages of storm track latitudes.

For Forbush decreases, a decrease in latent heat release in storms would occur with the above scenario, and this matches the observed reduction in temperature near 5 km as shown in Fig. 2. While changes in latent heat release would generally be associated with individual storms, this is not necessarily the case for changes in cloud albedo and absorbtivity. If these changes occur over a large region, say poleward of the jet stream, they could produce a change in temperature profile in that region that would affect the pressure gradient across the jet stream leading to a change in the average intensity or frequency of cyclonic eddies. There is an increase in the number of low pressure areas crossing 60^{o} W meridian between latitudes 40^{o} and 50^{o} N, for the QBO W phase for minimum solar activity (Labitzke and van Loon, 1988), and this frequency change is associated with a downstream shift in the latitude of the jet stream and storm tracks in the eastern N Atlantic (Brown and John, 1979; Tinsley, 1988). This frequency change may be produced by a localised latent heat release in the storms, or by a distributed effect due to cloud and radiative changes over a large area, and in either case the association with the jet stream latitude shift can be understood theoretically if the increased frequency of lows at solar minimum (that corresponds to about one every 2-3 days, as compared to about one every 4-6 days at solar maximum) leads to a greater divergence of momentum flux, by greater generation of waves, including gravity waves, that propagate out of the region. As discussed, for example by Hoskins (1983, p 190-3),

this will lead to a downstream poleward movement of the jet stream and storm tracks, in accordance with the observations. Also Pauley and Smith (1988) found that the effect of releases of latent heat in their simulated cyclonic disturbances was to intensify the storm and cause the downwind storm track to shift poleward. Both decreases in VAI associated with Forbush decreases, of which more occur at solar maximum, or VAI decreases associated with the lower general level of GCR flux at solar maximum, could account for the more equatorward storm tracks at that time.

In the stratosphere 27 day and longer term variations have been found that can be partially explained in terms of changes in the flux of solar ultraviolet radiation as the carrier (Keating et al., 1987; Brasseur et al., 1987). The energy involved in the stratospheric response is very small compared to that in the tropospheric response, and it is difficult to see how effects could propagate downwards and be amplified rapidly enough to account for tropospheric changes in the time scale of the HSPS and FD responses. On the contrary, it appears more likely that wave energy from tropospheric responses propagates upwards and towards the poles, and accounts for some of the unexplained stratospheric temperature variations.

This work has been supported by the Atmospheric Sciences Division of NSF.

REFERENCES

Akasofu, S-I, and S. Chapman, "Solar-Terrestrial Physics", Oxford University Press, 1972

Attolini, M.R., S. Cecchini, G.C. Castagnoli, M. Galli, and T. Nanni, On the existence of the 11-year cycle in solar activity before the Maunder Minimum, J. Geophys. Res., 93, 12729, 1988.

Brasseur, G, A. De Rudder, G.M. Keating, and M.C. Pitts, Response of Middle Atmosphere to Short-Term Solar Ultraviolet Variations: 2. Theory, J. Geophys. Res., 92, 903, 1987.

Brown, G.M., and J.I. John, Solar cycle influences in tropospheric circulation, J. Atmos. Terr. Phys., 41, 43, 1979.

Burlaga, L.F., F.B. McDonald, N.F. Ness, R. Schwenn, A.J. Lazarus and F. Mariani, Interplanetary Flow Systems Associated with Cosmic Ray Modulation in 1977-80, J. Geophys. Res. 89, 6579, 1984.

Hoskins, B.J., Modelling of the transient eddies and their feedback on the mean flow, in "Large Scale Dynamical Processes in the Atmosphere", Ed. B.J. Hoskins and R. Pearce, Academic Press, 1983.

Keating, G.M., M.C. Pitts, G. Brasseur, and A.De Rudder, Response of Middle Atmosphere to Short-Term Solar Ultraviolet Variations: 1. Observations, J. Geophys. Res., 92, 889, 1987.

Labitzke, and H. van Loon, Association between the 11-year solar cycle, the QBO, and the atmosphere, Part III, Aspects of the association, in press, J. of Climate, 1988.

Lindblad, B.A., and H. Lundstedt, A catalogue of high speed plasma streams in the solar wind, Solar Physics, 74, 197, 1981.

Lindblad, B.A., and H. Lundstedt, A catalog of high speed plasma streams in the solar wind 1975-78, Solar physics, 88, 377, 1983.

NGDC, 'Forbush decreases 1955-1984' in "Solar Geophysical Data", No. 485, Pt. 1, p 91, NOAA, Boulder, 1985.

Pauley, P.M., and P.J. Smith, Direct and indirect effects of latent heat release on a synoptic scale wave system, Mon. Weather Rev., 116, 1209, 1988.

Pomerantz, M.A., and S.P. Duggal, The sun and cosmic rays, Rev. Geophys. and Space Phys., 12, 343, 1974.

Stolov, H.L., and R. Shapiro, Investigation of the responses of the general circulation at 700 mb to solar geomagnetic disturbance, J. Geophys. Res., 79, 2161, 1974.

Tinsley, B.A., The solar cycle and the QBO influences on the latitude of storm tracks in the North Atlantic, Geophys. Res. Lett., 15, 409, 1988.

Wilcox, J.M., P.H. Scherrer, L. Svalgaard, W.O. Roberts, R.H. Olson, and R.L. Jenne, Influence of solar magnetic sector structure on terrestrial atmospheric vorticity, J. Atmos. Sci., 31, 581, 1974.

12

A SEARCH FOR SOLAR RELATED CHANGES IN TROPOSPHERIC WEATHER

K. Mohanakumar

School of Marine Sciences
Cochin University of Science and Technology
Cochin 682 016, India

The possibility that solar variations associated with the 11-year solar cycle may be the cause of the changes in tropospheric weather and climate has been the subject to scientific investigation for several decades (KING, 1975; PITTOCK, 1978). In the light of recent studies (MOHANAKUMAR, 1985; 1987; VON COSSART, 1985; CHANIN et. al, 1987), it has been established that mesospheric temperature is strongly influenced by the solar activity. Recently (LABITZKE, 1987; LABITZKE and VAN LOON, 1988), it has been shown that marked signals of the 11-year solar cycle emergence into the stratosphere and troposphere when the atmospheric data are stratified according to east or west phase of equatorial quasi-biennial oscillation (QBO) of zonal wind in the lower stratosphere. These findings give a revival of interest on studies about the sun-weather relationship.

Meteorologists are greatly concerned with the changes in tropospheric phenomena. In the present study, an attempt has been made to find solar activity related changes in tropospheric weather, by the modulation of the QBO of zonal wind at 50 mb. Rainfall and surface temperature data for a period of about three solar cycles, 1953 to 1988, from various stations in Indian subcontinent have been utilised in this study. The study is further extended to find a possible teleconnection between the temperature changes in middle atmospheric levels and surface temperature when the data are stratified according to east or west phase of the QBO. The temperature data have been averaged for January and February to represent the winter-time temperature and for July and August to represent the summer-time temperature. Since the southwest monsoon is the major rainfall season for many parts of Indian subcontinent, the total rainfall recorded during June to September, represents the rainfall data. 10.7 cm solar radio flux is chosen as the solar activity parameter.

Equatorial quasi-biennial oscillation of zonal wind (ANDREWS et.al, 1987) at 50 mb in July during the years 1953 to 1988 is shown in Fig.1. The long period average rainfall for India during the monsoon season, June 1 to September 30, is about 85 cm. The amount of rainfall is generally classified as deficient (D): less than 10%, normal (N): $\pm$ 10% and excess (E): more than 10%, from the average rainfall and is indicated in Fig.1. High and low solar activity periods, indicated when the solar radio flux for the four months exceeds 600 and is less than 500 respectively are shown in the upper part of Fig.1.

It is evident from Fig.1 that excess rainfall over India is mainly associated with the westerly phases of QBO and when the solar activity is low. Out of 13 excess rainfall recorded during the last 36 years, 10 occurred when QBO was in its westerly phase. Another interesting aspect is that all the above 10 occurrences are reported when the solar activity is low. Only in three cases, excess rainfall is associated with the easterly phase of QBO and this occurred when the solar activity is high. These three excess rainfalls are found prior to 1971 after which no excess rainfall is observed in this phase.

Rainfall is found to be deficient when the QBO was in its easterly phase and the easterly wind speed is less than 10 ms^{-1}. Out of 9 deficient rainfalls recorded, 8 were found to have occurred in the easterly phase and, generally, when the solar activity is low. Only once, deficient rainfall is reported during the westerly phase which occurred when the westerly wind was weak (5 ms^{-1}) and solar activity was normal.

Normal rainfall is also frequent during the westerly phase of QBO. Out of 14 occurrences, 9 were reported in the westerly phase, of which 6 cases occurred when solar activity was high. When the solar activity is low and QBO is in its easterly phase with strong wind speed (above 20 ms^{-1}), the occurrence of normal rainfall is almost certain. There were 4 such cases in which normal rainfall was observed. This type of phenomena occurs once in every 11-year solar cycle.

These results indicate that solar activity exerts some influence on the rainfall pattern through the modulations in the phases of the equatorial stratospheric zonal wind.

Correlation studies between solar activity and surface temperature during winter and summer, after separating the data into easterly and westerly phases of QBO, in three near-equatorial stations, have been carried out and the results are listed in Table 1. The correlation in the westerly phases of QBO is found to be positive and marginally significant, whereas it is negative and statistically insignificant in the easterly phase. During summer, negative and marginally significant correlations are obtained in the westerly phase while positive but insignificant correlations are obtained in the easterly phase except at Calicut. When the data for both the phases are combined, no correlation exists between solar activity and surface temperature.

The study is further extended to find the relationship between temperature at various levels in the middle atmosphere and surface temperature over Trivandrum ($8^{o}N$), where the meteorological rocket launching station, Thumba is situated. Correlation coefficients were computed between surface temperature and the temperatures at every 5 km levels between 25 and 75 km over Thumba, after separating the data according to the two phases of QBO and also averaging for summer and winter seasons. The computed correlation coefficients plotted against height are shown in Fig. 2. The significance of the correlation coefficients is tested with Students t-test and is indicated in Fig. 2.

In winter, in the westerly phases of QBO, the middle atmospheric temperature shows a better association with the surface temperature. Below 30 km, the correlation is found to be opposite in the two phases of QBO. The correlation values during the westerly phase rapidly decrease with height in the stratosphere and become strongly negative at 40 km. The surface temperature, thus has an out-of-phase variation with the temperature at 40 km altitude. The correlation coefficients increase with height and become positive and highly significant between 60 and 70 km altitude. The middle mesospheric temperature shows a direct relation to the surface temperature in the westerly phase. The correlation decreases towards the upper mesosphere. The correlation profiles in the easterly phase also show similar variations in the middle atmosphere, but never become statistically significant.

Correlation profiles during the summer season show somewhat opposite behaviour to that during winter season. Positive correlations in stratosphere and negative correlations in mesosphere are obtained. Upto 35 km height, the correlation in the two phases are opposite in nature. Positive and marginally significant correlations are seen at 30 and 35 km heights, in the westerly phases of QBO. Correlations are not found to be significant at higher levels in summer season.

Fig. 3 shows the scattergrams of solar radio flux temperature at 60 km and temperature at 40 km with surface temperature when the QBO is its westerly phase during winter. For the period 1971 to 1985, the 10.7 cm solar radio flux has a positive correlation of 0.624 with surface temperature, and the regression line has a positive slope. This indicates that the surface temperature in the westerly phases increases with the solar activity. The surface temperature also shows a positive association with the temperature at 60 km, as evident from the strong positive gradient and high correlation (0.810). On the other hand, the surface temperature indicates an inverse relation with the temperature at 40 km altitude. Thus, the winter-time surface temperature in the westerly phases of QBO increases as the stratospheric temperature at 40 km decreases.

The results obtained from the study between surface temperature and temperatures in the middle atmosphere reveal that the middle mesospheric temperature has a direct, and the upper stratospheric temperature has an inverse association with the surface temperature when the QBO is in its westerly phase and during winter. These results suggest that changes in temperature in mesosphere or stratosphere, for example, due to stratospheric warming or mesospheric cooling, may be reflected in surface temperature.

REFERENCES

Andrews, D.G., J.R. Holton and C.B. Leovy. 1987, Middle Atmospheric Dynamics, Academic Press, New York.

Chanin, M.L., N. Smires and A. Hauchecorne. 1987, J. Geophys. Res., 92, 10933.

King, J.W. 1975, Aeronaut. Astronaut., 13, 10.

Labitzke, K. 1987, Geophys. Res. Lett., 14, 535.

Labitzke, K. and H. van Loon. 1988, J. Atmos. Terr. Phys., 50, 197.

Mohanakumar, K. 1985, Planet. Space Sci. 33, 795.

Mohanakumar, K. 1988, Physica Scripta, 37, 460.

Pittock, A.B. 1978, Rev. Geophys. Space Phys., 16, 400.

von Cossart, G. 1985, Gerl. Beitr. Geophys., 93, 329.

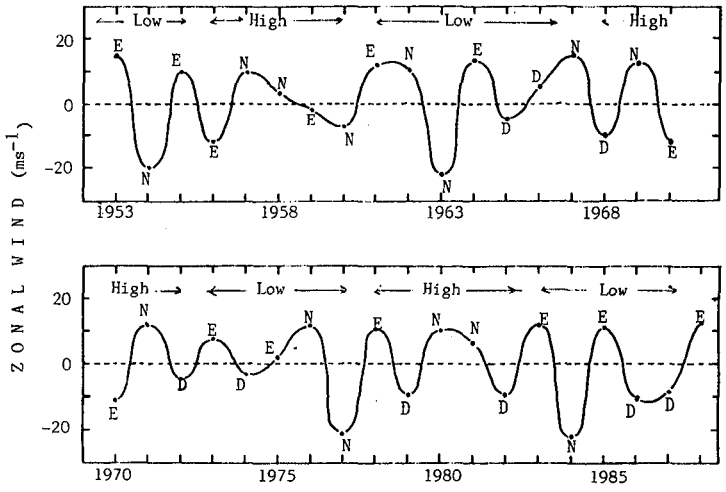

Fig. 1. Equatorial Quasi-biennial Oscillation of zonal wind at 50 mb for July and Southwest Monsoon Rainfall over India (D : Deficient; E : Excess; N : Normal)

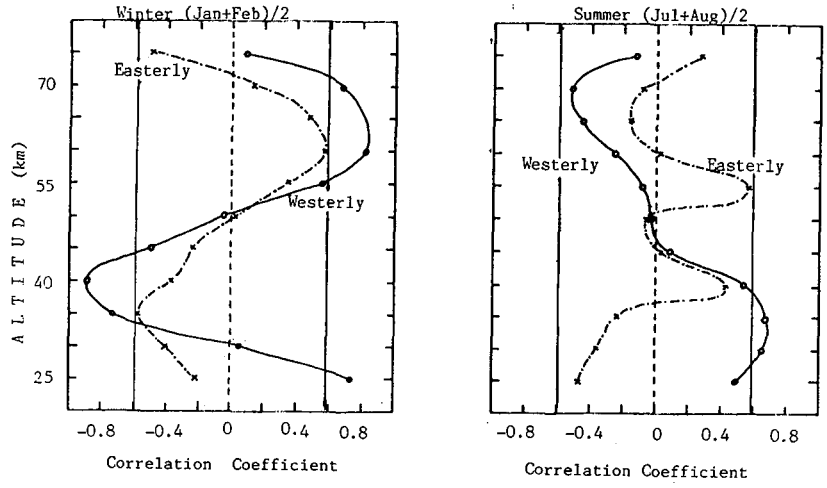

Fig. 2. Vertcal profile of Correlation Coefficient between Surface Temperature and Middle Atmospheric Temperature in Tropics

TABLE 1

CORRELATION COEFFICIENTS BETWEEN
SOLAR ACTIVITY AND SURFACE TEMPERATURE

WINTER (JAN + FEB)/2

Station	Westerly Phase n = 19	Easterly Phase n = 15	Combined n = 34
TRIVANDRUM (8^{o}N)	0.437 (90%)	-0.250 (n.s.)	0.126 (n.s.)
COCHIN (10^{o}N)	0.481 (95%)	-0.309 (n.s.)	0.031 (n.s.)
CALICUT (12^{o}N)	0.614 (98%)	-0.335 (n.s.)	0.213 (n.s.)

SUMMER (JUL + AUG)/2

Station	Westerly Phase n = 19	Easterly Phase n = 15	Combined n = 34
TRIVANDRUM (8^{o}N)	-0.476 (95%)	0.438 (n.s.)	-0.043 (n.s.)
COCHIN (10^{o}N)	-0.502 (95%)	0.385 (n.s.)	-0.102 (n.s.)
CALICUT (12^{o}N)	-0.389 (90%)	0.640 (99%)	0.196 (n.s.)

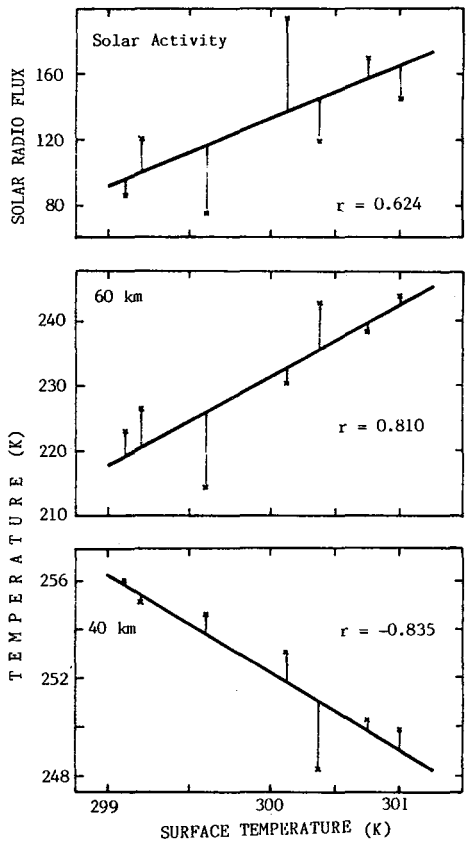

Fig. 3. Scatter diagrams of Surface Temperature with Solar Radio Flux, Temperatures at 60 and 40 km.

THE MESOSPHERIC RESPONSES TO SHORT-TERM SOLAR ULTRAVIOLET VARIABILITY

Gerald M. Keating

Atmospheric Sciences Division, NASA Langley Research Center, Hampton, VA 23665-5225, U.S.A.

The response of mesospheric ozone and temperature to short-term solar ultraviolet variations related to the 27-day rotation of the Sun has been recently detected from analysis of satellite measurements. A systematic depletion of ozone is detected near 70 km, which is attributed to (1) solar Lyman alpha photodissociation of water vapor with subsequent catalytic destruction of O_x by HO_x and (2) temperature feedback effects resulting from the unexpectedly strong temperature/UV response near 70 km. The nature of latitudinal and semiannual variations in the ozone/UV and temperature/UV response have now been isolated. Observed variations are compared to theoretical models.

RESPONSE OF THE MIDDLE ATMOSPHERE TO SOLAR UV AND DYNAMICAL PERTURBATIONS

S.Chandra
Code 616, NASA-Goddard Space Flight Center, Greenbelt, Md., 20771.

INTRODUCTION

Recent studies of solar UV related changes of ozone and temperature have considerably improved our understanding of the solar UV and ozone relationship in the middle atmosphere on time scales of a solar rotation. These studies have shown that during periods of high solar activity, ozone in the upper stratosphere has a measurable response to changes in the solar UV flux in accordance with theoretical predictions. For example, both model predictions and observations suggest that stratospheric response to solar UV perturbations should be maximum at about 2 mb. At this level, the ozone mixing ratio and temperature increase by about 0.4 percent and 0.1 K respectively for 1 percent increase in solar flux in the spectral range of 205 nm (CHANDRA, 1986, BRASSEUR et al., 1987; KEATING et al., 1987; HOOD, 1987 and the references therein). These are relatively weak perturbations compared to dynamical perturbations since the variability in 205 nm over a solar rotation is generally very small (about 1-4 percent) even during periods of high solar activity. The solar induced changes in the stratosphere are often masked by dynamical oscillations with periods between 3-7 weeks (CHANDRA, 1986).

The problem of measuring solar response of the stratospheric ozone and temperature on time scales of a solar cycle is even more difficult. In the altitude range of 2 mb the model based calculations, based on plausible scenarios of solar UV variation, suggest a change of less than 4 percent in ozone mixing ratio and 1-2 K in temperature. In the case of total ozone, the predicted change is less than 1 percent (GARCIA et al., 1984; CHANDRA, 1985; BRASSEUR et al., 1987). Since ozone and temperature data for such studies are limited to 1 or 2 solar cycles, the solar UV related changes over a solar cycle cannot be uniquely separated from inter-annual variabilities and instrument drifts which are often present in data sets extending over a few years. Thus definitive evidence for solar UV and ozone relationship must still come from studying their relations over shorter periods.

In 1971, it was suggested by the author that the periods in solar activity are not limited to 27 days and 11 years but may have additional components in the range of 4-6 months which may influence the seasonal characteristics of the atmospheric parameters (CHANDRA, 1972). It has now become apparent that such periods in solar activity do indeed exist and are intrinsic periods of the Sun (LEAN and BRUECKNER, 1989 and the references therein). LEAN and BRUECKNER (1989) have shown that the solar activity, as inferred from the sunspot blocking function, the 10.7 cm solar radio flux(F10.7), and the sunspot number show a strong periodicity at about 155 days or 5 months. Their studies do not indicate the relative importance of this period with respect to the 27 day period. However, a recent study by HOEGY and WOLFF (1989) suggest that the amplitude of the 5 month period is comparable to the 27 day period in the F10.7 cm data and about 30-40% smaller in the solar Lyman α data obtained from the Solar Mesospheric Explorer. These authors have also reported the existence of a 7 month solar period inferred from the photoelectron current measured by the Langmuir probe on the Pioneer Venus orbiter over the time

period from 1979 to 1987. It is, therefore, of interest to know if the atmospheric parameters respond to changes in solar UV flux at periods other than 27 days and if so, what are their relative sensitivities.

The purpose of this paper is to study the relative response of the middle atmosphere to solar forcing at 155 and 27 day periods as indicated from the spectral analyses of a number of solar indices. As discussed in LEAN and BRUECKNER (1989), the range of the 155 day period varies from 152 days to 160 days depending upon the time interval of data used in the spectral analysis. For convenience, this period will be referred to as a 5 month solar period.

DATA SOURCE AND ANALYSIS

The data used for this study consist of daily values of ozone mixing ratio at 2 mb obtained from the Nimbus-7 SBUV instrument and the daily values of total ozone obtained from the Nimbus 7 TOMS experiment. In addition, temperature data at a number of pressure levels, derived from the NMC analyses(GELMAN et al., 1986), are used as indicators of thermal and dynamical conditions in the middle atmosphere. Both the ozone and temperature data are obtained from the NSSDC (National Space Science Data Center, Greenbelt, Md, 20771) and are zonally averaged in the latitude interval of 10 degrees from -80° S to $+80^{\circ}$ N. Many of the characteristics of these data sets have been extensively discussed in the literature (eg., CHANDRA, 1986, HOOD 1987, and the references therein). The time interval used for this study covers the period of about 6 years from January 1, 1979 to October 1984 and mostly corresponds to periods of high solar activity. The data after 1984 were not included because they correspond to periods of low solar activity and tend to increase the contribution of dynamical signals at the expense of solar signals.

As an index of solar UV flux, we have used the daily values of F10.7, the solar decimeter flux measured at Ottawa, Canada. The 10.7cm index is considered to be one of the best solar indices available for studying the long term characteristics of solar UV flux in the spectral range of 160-400 nm (HEATH and SCHLESINGER, 1986). However, we will discuss some of the implications of using this index as compared to directly measured solar UV flux at 205 nm (F205), also measured from the Nimbus 7 SBUV spectrometer.

For each latitude zone, the most apparent characteristics of ozone and temperature time series are annual and semiannual components which are periodic and generally independent of solar activity. In the case of F10.7, the most apparent feature is the 11 year cycle which is modulated by periods varying from 13 days (one half solar rotation) to several months. For studying the atmospheric response to solar variability on time scales of less than six months, it is useful to remove the longer term periods which may dominate the spectral characteristics of these time series. The most expedient way to remove periods greater than six months is to subtract a 180 day running average from each of the time series. This was found to be adequate for solar indices such as F10.7 and F205 which do not have strong seasonal components. For ozone and temperature time series, subtracting a 180 day running average did not substantially reduce the annual component particularly at middle and high latitudes. The contributions of annual, semiannual and long term trends from ozone and temperature time series were, therefore, first removed using a regression model consisting of annual, semiannual and linear terms. The resulting time series were then treated the same way as F10.7 and F205, i.e., from each of the time series a 180 day running average was subtracted to emphasize periods less than six months.

SPECTRAL CHARACTERISTICS OF SOLAR DATA

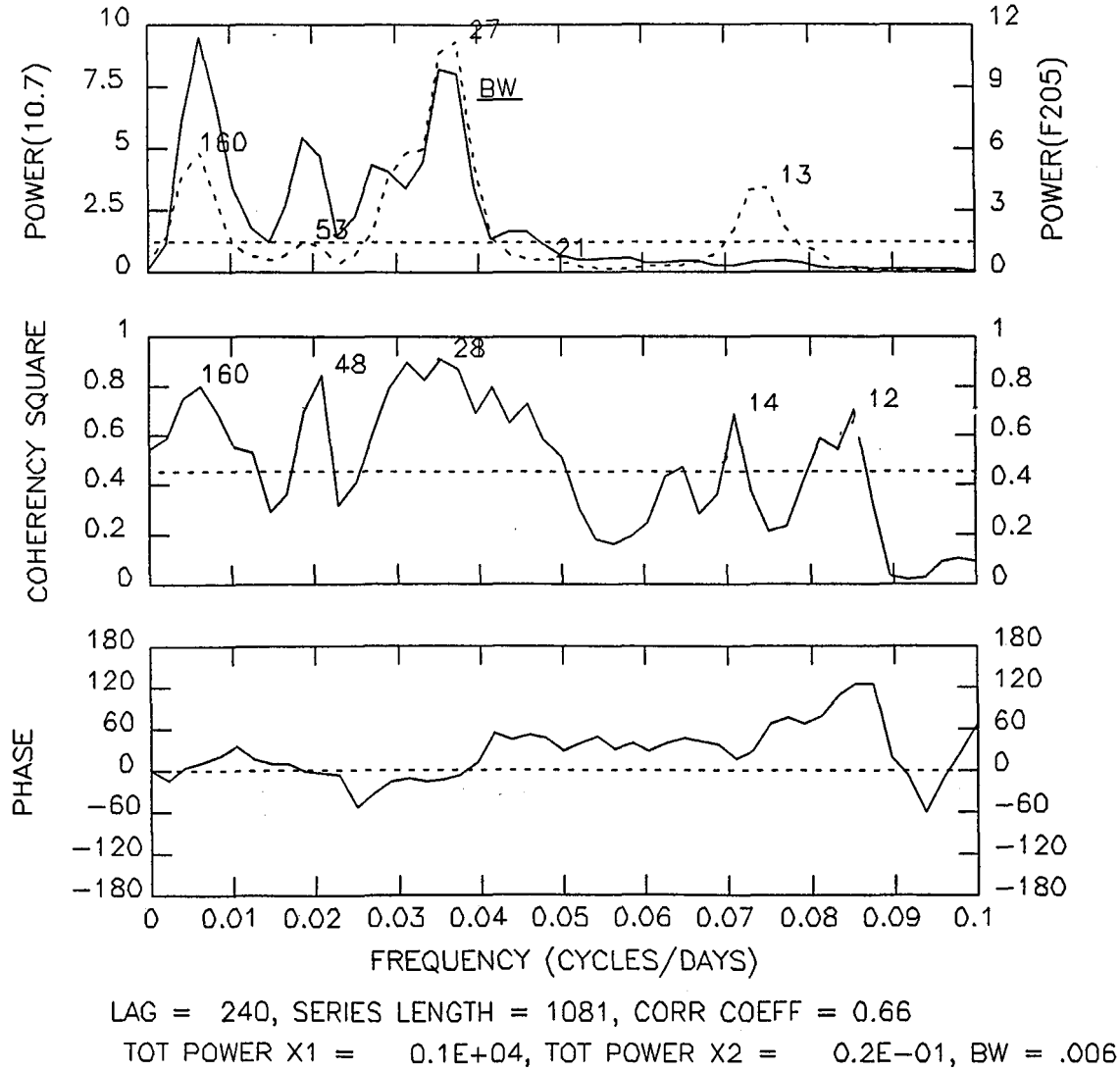

Figure 1. The power spectra of F10.7 and F205 (top panel, solid and dotted lines) and the spectra of their coherency (middle panel) and phase(lower panel). The power spectra are expressed as a percentage of total power for each time series. The horizontal dotted line in the upper panel corresponds to 95 % confidence level (CL) for the spectral estimate of the first series (F10.7). In the middle panel it corresponds to 95 % CL for the coherency spectrum. The spectral bandwidth is indicated by a bar in the upper panel. The figure also lists a number of useful parameters: These are: lag (days), length of the series (days), correlation coefficient of the two series, total power(power) of the first(X1) and the second(X2) series (in arbitrary units) and bandwidth(cycles/day).

The spectral characteristics of F205 and F10.7 for periods less than six months are shown in Figure 1 (upper panel) in the form of the power spectra of the two series covering the time interval from January 79 to June 1982. Shown in this Figure are also the spectra of coherency squared and phase (middle and lower panels) of the two time series. The calculations are based on algorithms described in JENKINS and WATTS (1968) using a Tukey Hanning spectral window of 240 days and lag of the same interval. This results in a bandwidth of .006 cycles/day. Both the spectra are normalized to their respective total powers for visual comparison of the relative powers of significant periods.

Figure 1 clearly shows two major peaks at 28 and 160 days (5 months) respectively. In addition, it shows an intermediate peak at 53 days which is probably a harmonic of the 5 month period (LEAN and BRUECKNER, 1989). These periods are also present in F205. However, their relative powers are very different in F205. For example, in F10.7 the powers in the 5 month and 27 day periods are of equal magnitude. In F205, the 5 month period contains half the power of the 27 day period. The 53 day period is barely significant in F205 and the 13 day period is significant in F205, but not in F10.7. In spite of these differences, the two time series are almost in phase (bottom panel) and show significant coherency at all periods between 27 days and 5 months.

The differences in the spectral characteristics of F205 and F10.7 time series with respect to the 27 and 13.5 day periods have been extensively discussed in the literature and are attributed to the differences in the spatial and temporal characteristics of the active regions which give rise to these emissions (DONNELLY et al., 1983). The origin of the 160 day period is not well understood. It is believed to be associated with those regions of the Sun where magnetic field is concentrated in small areas such as sunspots (LEAN and BRUECKNER, 1989 and the references therein). HOEGY and WOLFF (1989) attribute this period and other longer periods to long lived flux enhancements caused by nonlinear interactions of global oscillation modes in the sun's convective envelope and radiative interior.

SPECTRAL CHARACTERISTICS OF OZONE AND TEMPERATURE

The spectral analyses of the 2 mb ozone mixing ratio and F10.7 or F205 show a measurable response in ozone to changes in solar flux at 27 days at tropical and mid latitudes but not at high latitudes. The 2 mb ozone also shows a strong signal at about 4 months which from the time series analysis can be attributed to winter time planetary wave disturbances. However, this period has no coherency with the 5 month period in F10.7 or F205. The solar response in ozone at 27 days is significantly increased when dynamical signals are minimized by averaging over a latitude band of $\pm 40^{\circ}$. This, however, does not improve the response at 5 months. Figure 2 shows the spectral characteristics of ozone mixing ratio at 2 mb with respect to F10.7 (upper panel), their coherency (middle panel) and phase (lower panel). The two time series cover the time interval from January 1979 to 1984. The data after 1984 were excluded because they correspond to very low solar activity and increase the relative contribution of dynamical signals at the expense of solar signals. In addition, ozone time series are averaged over $\pm 40^{\circ}$ to minimize the interference from dynamical signals. As seen in Figures 2, the normalized power spectrum of F10.7 shows strong peaks at 5 months and 27 days as in Figure 1. The relative magnitudes of these peaks are not changed by including an additional two and half years of data after June 1982. The power spectrum of ozone mixing ratio shows a strong peak at 4 months with considerable overlapping of power with 5 month period of F10.7. In comparison, the 27 day peak is only slightly above the 95% confidence limit. Notwithstanding these differences, the coherency spectrum of the two time series shows a significant peak at 27 days with almost no phase lag. The value of coherency squared at 4 or 5 month

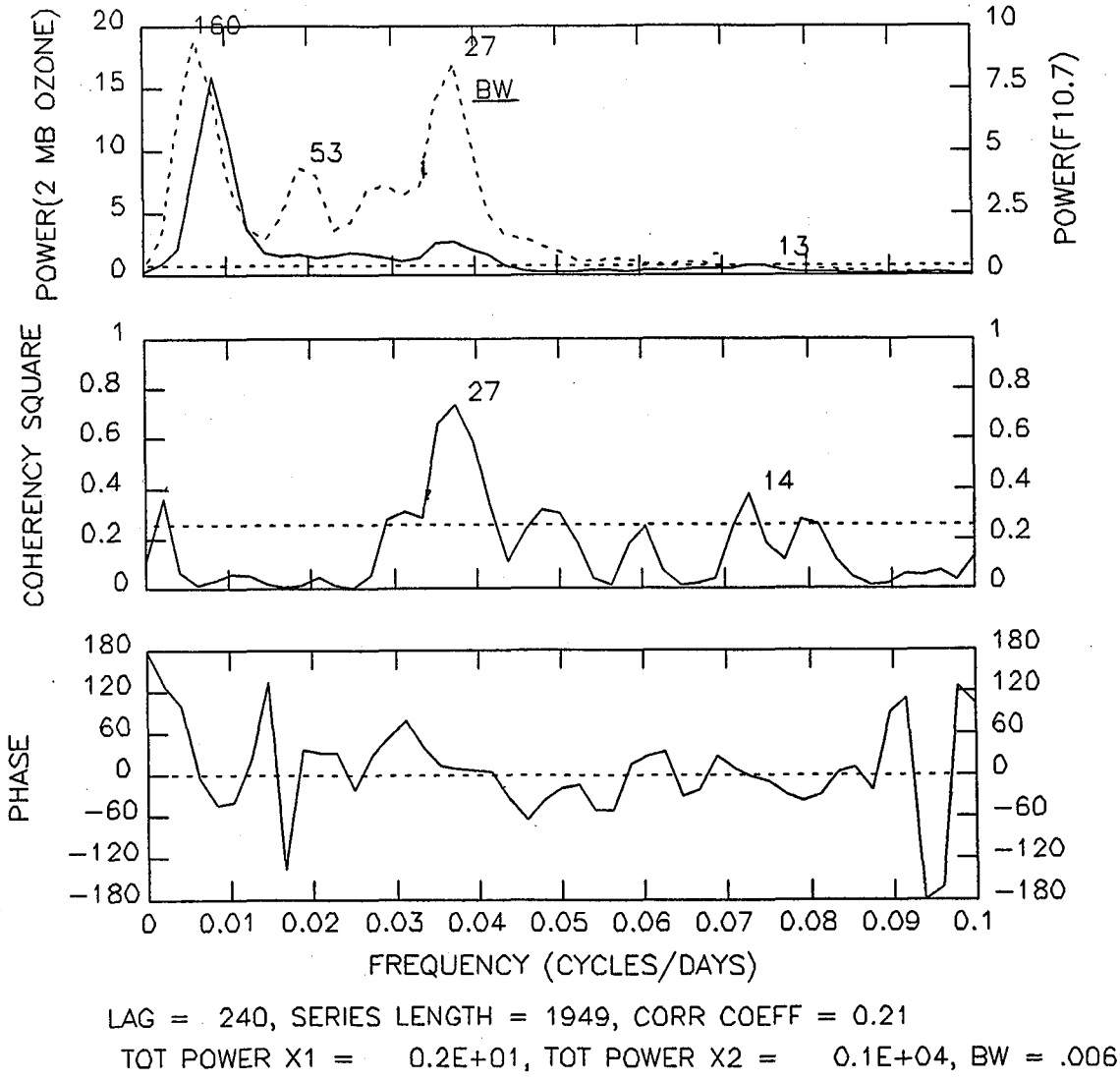

Figure 2. The same as Figure 1 except the spectra correspond to ozone mixing ratio at 2 mb (solid line) and F10.7 (dotted line) respectively. The ozone mixing ratio is averaged between ±40° latitude.

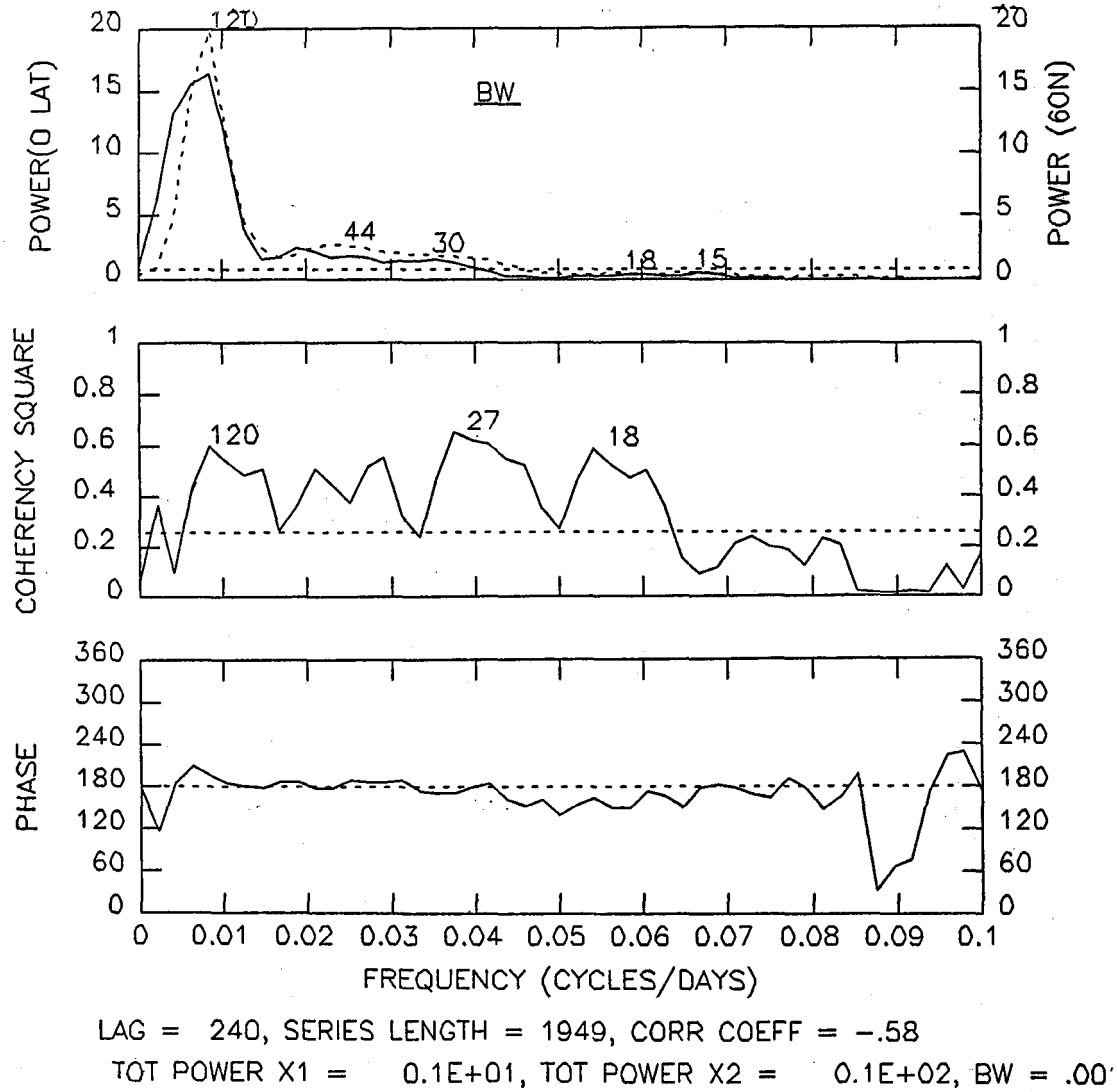

Figure 3. The same as Figure 1 except the spectra correspond to temperatures at 2 mb at the equator (solid) and 60°N.(dotted line)

periods are close to zero. A similar analysis of temperature at 2 mb shows a strong peak at 4 months as in 2 mb ozone. It, however, does not show significant coherency at 27 days or any other period indicating that temperature variances are mostly dynamical in origin and the solar signal, if any, is at a noise level.

The 4 month period seen in ozone and temperature data is a manifestation of increased planetary wave activity during the fall and spring epoches in both the hemispheres and is quasi-periodic in nature. Therefore, unlike the annual and semiannual cycles associated with the seasonal changes, this period cannot be filtered from a given time series by harmonic analysis. It manifests itself in the same way as shorter periods in the range of 3-7 weeks, i.e., it is global in extent and independent of solar activity. Its phase varies with latitude such that oscillations at high and tropical latitudes are 180° out of phase (CHANDRA, 1985 &1986). Figure 3 compares the power spectra of 2 mb temperature at 60°N and the equator and the spectra of their coherency and phase. It shows a strong period at about 4 months in both the time series and relatively broad periods in the spectral range of 3 to 7 weeks. These periods, though statistically significant, are considerably weaker than the 4 month period. The coherency and phase spectra of 2 mb temperature at 60°N and the equator in Figure 3 strongly suggest the dynamical nature of oscillations between 3-20 weeks. All periods in this range show significant coherency and are 180° out of phase with respect to high and low latitude oscillations which are characteristics of dynamical oscillations.

A similar inference about the dynamical nature of the 4 month period can be made by comparing the power spectra of total ozone and ozone mixing ratio and temperature at different pressure levels and latitudes. All these spectra indicate the dominance of a 4 month period unrelated to solar activity. They also show significant coherency between ozone and temperature at all frequencies between 27 days and 4 months both in the upper and the lower stratospheres. Their phase spectra, however, show an in phase relation in the lower stratosphere and an out of phase relation in the upper stratosphere. This phase change reflects a transition from a dynamical control to photochemical control of ozone from the lower to the upper stratosphere as discussed in CHANDRA (1986). The absence of a 5 month solar signal in the ozone data indicates that it is relatively weaker than the 27 day signal and is masked by a strong interference from a dynamical signal of comparable period unrelated to solar activity. Its relative weakness with respect to the 27 day component is consistent with the fact that the solar spectrum in the UV range is also weaker at this frequency compared to the 27 day component as indicated in Figure 1.

CONCLUDING REMARKS

In this paper, we have studied the response of the stratospheric ozone and temperature at time scales of solar periodicities at 27 days and 5 months. The study which was based on six years of data from 1979 to 1984, covered the most active period during solar cycle 21. The spectral and cross spectral analyses of these data showed a significant solar response in ozone mixing ratio at 2 mb at 27 days with a phase lag of less than a day. No such response was observed at the 5 month period. The temperature between 2 and 70 mb did not show significant response to solar forcing at either 27 days or at 5 months. These results are consistent with the earlier conclusions of the author (CHANDRA, 1985 and 1986) that the solar induced perturbations in temperature are too weak to be detected against the background dynamical disturbances which are several times larger and independent of solar activity. The lack of solar UV response in ozone at 5 months may also be attributed to the dominance of a 4 month period in ozone and temperature data whose phase

and amplitude, like other dynamical perturbations, are latitude dependent. This, coupled with the possibility that the UV component of the 5 month period may be weaker than the corresponding 27 day component, makes the detection of a solar response in atmospheric data much more difficult.

References

Brasseur, G., A. De Rudder, G. M. Keating, and M. C. Pitts, Response of middle atmosphere to short term solar ultraviolet variations, 2, Theory, J. Geophys. Res.,92, 903, 1987.

Chandra, S. Qusi-seasonal variations in the Sun, Symposium on Significant Accomplishments in Sciences, Goddard Space Flight Center, Jan, 14, 1971;NASA-SP-286 :pp 164-170, 1972.

Chandra, S., The solar and dynamically induced oscillations in the stratosphere, J. Geophys. Res., 91, 2719, 1986

Chandra, S., Solar induced oscillations in the stratosphere: A myth or reality, J. Geophys. Res, 90, 2331, 1985.

Donnelly, D. F., D. F. Heath, J. L. Lean, and G. J. Rottman, Differences in the temporal variations of solar uv flux, 10.7 cm solar radio flux, sunspot number, and Ca-K plage data caused by solar rotation and active region evolution. J. Geophys Res. 88, 9883, 1983.

Garcia, R. S., S. Solomon, R. G. Roble, and D. W. Rush, A numerical study of the response of the middle atmosphere to the 11 year solar cycle, Planet. Space Sci.,32, 411, 1984.

Gelman, M. E., A. J. Miller, K. W. Johnson and R. M. Nagatani, Detection of long term trends in global stratospheric temperature from NMC analyses derived from NOAA satellite data, Advances In Space Res. 6, 17, 1986.

Heath, D. F., and B. M. Schlesinger, The Mg-280 nm doublet as a monitor of changes in solar ultraviolet irradiance, J. Geophys. Res., 91, 8672, 1986.

Hoegy, W. R., and C. L. Wolff, A seven month solar cycle observed with the Langmuir probe on Pioneer Venus Orbiter, J. Geophys. Res., 1989 (Submitted)

Hood, L. L., Solar ultraviolet induced variations in the stratosphere and mesosphere, J. Geophys. 92, 876, 1988.

Jenkins, G. M., and D. G. Watts, Spectral analysis and its applications, Holden Day, Oakland, Calif., 1968.

Keating, G. M., M. C. Pitts, G. Brasseur, and A. De Rudder, Response of the middle atmosphere to short term solar ultraviolet variations: 1. Observations, J. Geophys. Res. 92, 889, 1987.

Lean, J. L., and G. E. Brueckner, Intermediate-term solar periodicities: 100-500 days, The Astrophys. J., 337, 568,1989

STRATOSPHERIC EFFECTS OF SOLAR ULTRAVIOLET VARIATIONS ON THE SOLAR ROTATION TIME SCALE

L. L. Hood

Lunar and Planetary Laboratory
University of Arizona
Tucson, AZ 85721 USA

The purpose of this paper is to present a summary of some current work on measurement and interpretation of stratospheric ozone and temperature responses to observed short-term solar ultraviolet variations. Although some studies have yielded provisional evidence for a nearly in-phase ozone-solar cycle relationship, they extend at most over only one or two eleven-year cycles so the statistical significance of the correlations is not large. Similarly, the relatively short lengths of individual satellite data sets combined with the problem of estimating the effect of changes in instrument sensitivity (drift) during the observing period have complicated attempts to infer long-term or solar cycle ozone trends. The solar rotation and active region development time scale provides an alternate time scale for which detailed studies of middle atmospheric ozone and temperature responses to solar ultraviolet variability are currently possible using available satellite data sets. At tropical latitudes where planetary wave amplitudes are relatively small, clear correlative evidence for the existence of middle atmospheric ozone and temperature responses to short-term solar ultraviolet variations has been obtained in recent years [GILLE et al., 1984; HEATH and SCHLESINGER, 1985; HOOD, 1984; 1986; KEATING et al., 1985; 1987; CHANDRA, 1986; ECKMAN, 1986; AIKIN and SMITH, 1986; HOOD and CANTRELL, 1988]. These measurements will ultimately allow improved empirical and theoretical calculations of longer-term solar induced ozone and temperature variations at low and middle latitudes.

The satellite remote sensing measurements that are utilized here consist of the Nimbus 7 solar backscattered ultraviolet (SBUV) daily zonal mean profiles and stratosphere and mesosphere sounder (SAMS) gridded retrieved temperature data available from the U.S. National Space Science Data Center. In order to characterize variations in solar spectral irradiance at wavelengths where photodissociation of molecular oxygen is important, the flux at 205 nm as measured with the SBUV instrument is chosen to be consistent with earlier studies. The flux at this wavelength has been found from analyses of SBUV solar flux data to be representative of short-term variations throughout the 170–260 nm range that is of importance for ozone photochemistry [DONNELLY et al., 1987].

Figure 1 compares the 205 nm solar irradiance time series with zonally averaged SBUV ozone mixing ratios and SAMS temperatures for the equator at 1.5 mbar (approximately 45 km altitude). This altitude is chosen because it is intermediate between the locations of the ozone response maximum (about 40 km) and the temperature response maximum (about 50 km). A low latitude is selected because of the increasing seasonal and planetary wave amplitudes with increasing latitude which increase the difficulty of detecting changes caused by solar ultraviolet variations. Day-to-day variations and short gaps between daily zonal mean temperature, ozone, and solar ultraviolet time series were minimized using a 7-day running mean and linear interpolation algorithm.

The 205 nm flux time series is characterized by a broad maximum corresponding to the solar activity maximum of 1980–1981 and short-term variations associated with active

region development and solar rotation. The originally measured 205 nm flux data set also contains a long-term trend ascribable to instrument drift. We have therefore employed the Mg II core ratio of HEATH and SCHLESINGER (1986) to represent changes in the 205 nm flux on time scales greater than 35 days. The resulting scaled 205 nm flux time series (normalized to a value of 10.22 W cm^{-3} as measured on November 7, 1978) decreases by approximately 6% between solar maximum in 1980–1981 and late 1984. For comparison, the Solar Mesosphere Explorer satellite has measured a change in monthly mean 200-205 nm flux of approximately 5.5% between early 1982 and early 1985 although instrument error sources are still being evaluated (G. ROTTMAN, private communication).

The 1.5 mbar equatorial SAMS temperature time series (bottom panel) is characterized by semiannual and annual components with superposed shorter-term fluctuations. Because of the strong temperature dependences of the reaction rates that determine the ozone concentration, these semiannual and annual temperature variations produce negatively correlated ozone variations as shown in the center panel. This characteristic emphasizes the need to consider simultaneous temperature measurements when interpreting ozone temporal behavior at altitudes and latitudes where photochemical equilibrium is a reasonable first approximation. Finally, it should be noted that small interannual trends present in both the SBUV and SAMS measurements could be due in part to instrument drift and are not necessarily real.

From the amplitudes of seasonal ozone and temperature variations as well as the possibility of instrument related long-term drifts, it is clear from Figure 1 that detection of solar ultraviolet induced ozone or temperature responses on seasonal and longer time scales from the currently available Nimbus 7 data sets would be very difficult. On the other hand, as can be seen in the top panel, 27-day 205 nm flux variations are as large as 6–7% (peak-to-peak) and are therefore comparable to the probable change in the monthly-mean flux over a solar cycle. Consequently, most recent efforts to detect and characterize middle atmospheric ozone and temperature responses to solar ultraviolet variations have concentrated on the solar rotation time scale.

In order to isolate temporal variations on time scales comparable to the solar rotation period, all time series may be detrended by subtracting the 35-day running mean in each case. In order to allow a direct visual comparison of the resulting short-term 205 nm flux deviations with the ozone and temperature deviations, Figure 2 superposes the UV time series onto the atmospheric time series. Positive correlations between equatorial 1.5 mbar ozone variations on this time scale and solar 205 nm flux variations are evident; this is particularly true during intervals of relatively strong and continuous 27-day solar UV variations such as those occurring in October 1979–February 1980, May–August 1980, and June–August 1982. It is apparent from the lower panel of Figure 2 that 1.5 mbar temperature deviations are not positively correlated with UV deviations at zero lag. However, a tendency for temperature maxima to occur after UV maxima by 5–10 days can be discerned visually in some time intervals, particularly October 1979–February 1980 and June–August 1982.

In order to derive the average low-latitude ozone or temperature response sensitivity to observed changes in the 205 nm solar flux, cross-correlation and linear regression methods have been applied. This sensitivity is defined as the percent change in either ozone mixing ratio or temperature for a 1% change in the 205 nm flux. Also determined is the phase lag in days of either ozone or temperature relative to the 205 nm flux. In order to test the reproducibility of the previous results of HOOD [1986], HOOD and CANTRELL (1988) analyzed separately the two independent time intervals 'A' and 'B' of Figure 2. Figures 3

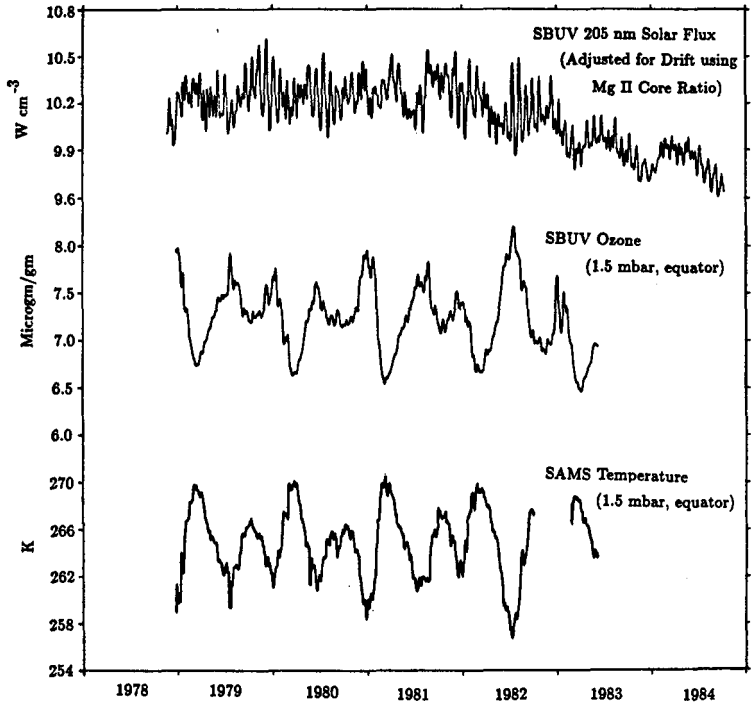

Figure 1. Comparison between the SBUV 205 nm solar flux (adjusted for long-term trends using the Mg II core ratio of HEATH and SCHLESINGER, 1986) and zonal mean equatorial ozone mixing ratio and temperature at the 1.5 mbar level.

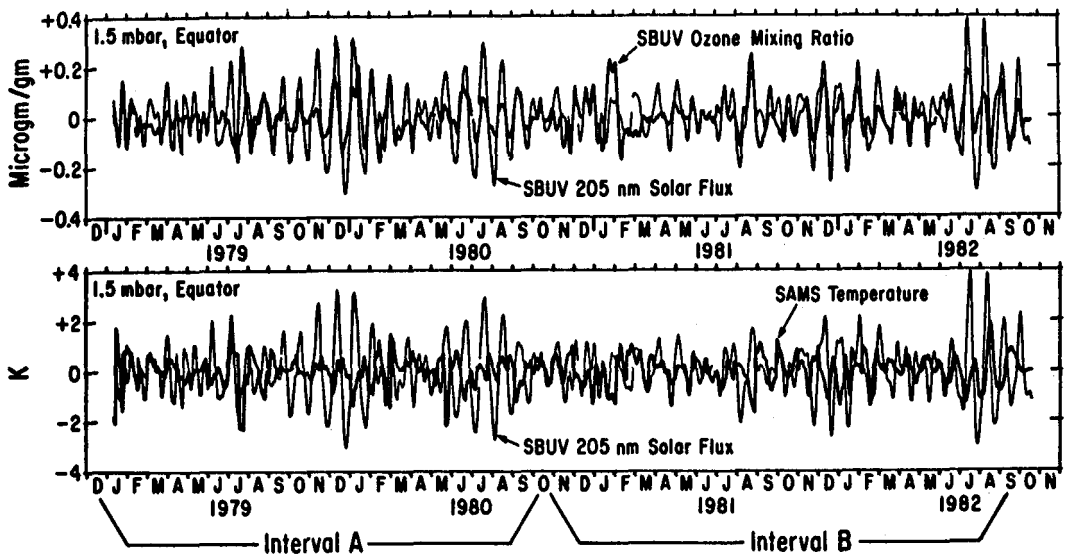

Figure 2. Superposition of the detrended (35-day running mean removed) solar 205 nm flux onto the detrended equatorial ozone and temperature time series at the 1.5 mbar level (from HOOD and CANTRELL, 1988).

and 4 summarize their results. The ozone response is seen to reach a maximum of about 0.5% near the 2 mbar level for a 1% change in the 205 nm flux. Actual peak-to-peak ozone mixing ratio changes were as large as 3% corresponding to maximum 205 nm flux changes of 6–7% on the 27-day time scale. The temperature response maximizes near the stratopause and amounts to 0.06% (about 0.17 K) for a 1% change in the 205 nm flux. Actual peak-to-peak temperature changes were as large as 1 K. Formal error limits for each time interval represent standard deviations from the mean of separate estimates for the five 10° latitude zones between 25°S and 25°N. As shown in Figure 3, ozone response amplitudes and phase lags derived in these separate analyses are generally in agreement. Formal error limits overlap in all cases except for the response amplitude at 2 mbar which is somewhat larger during interval 'B' than during interval 'A'. As shown in Figure 4, temperature response amplitudes and phase lags are also in approximate agreement although formal error limits are significantly larger for the response amplitudes. Temperature phase lags below 2 mbar also appear to be somewhat larger during interval 'B' than during interval 'A'. These response measurements agree well with an independent analysis by KEATING et al. (1987) of the same 4-year time interval.

The ozone response measurements of Figure 3 are compared to two simulations of the expected response calculated using radiative-photochemical models. The solid lines show the response amplitude and phase lag calculated by BRASSEUR et al. (1987) using a one-dimensional time dependent radiative photochemical code. This simulation is in qualitative agreement with the measurements but the amplitude of the calculated ozone response is noticeably less than the observed response above about 5 mbar. It has been suggested that a part of the difference between the model result and the observed ozone response is due to the use of diurnally averaged photodissociation rates in the model calculations. HOOD and DOUGLASS (1989) have reported calculations using a parameterized perturbation-order radiative photochemical model but using a variable solar zenith range in the photodissociation calculations that is more appropriate for comparison with the SBUV measurements. The resulting ozone response amplitude and phase lag are shown in Figure 3 as dashed lines. The increased photodissociation rate changes result in a higher amplitude for the ozone response that is more nearly in agreement with the observed amplitude at levels below about 3 mbar.

As noted earlier, the monthly mean solar 205 nm flux (scaled using the Mg II core ratio) decreases by approximately 6% between solar maximum in 1980–1981 and late 1984 (Figure 1). Adopting this flux variation, the same radiative photochemical code used to produce the dashed line model of Figure 3 for the 27-day time scale may be applied in order to estimate the expected solar cycle variation of ozone mixing ratio at levels between 3 and 10 mbar and at equatorial latitudes. Results show predicted mean ozone mixing ratio decreases of 2.0% at 3 mbar, 2.3% at 4.5 mbar, and 0.8% at 10 mbar for the interval between solar maximum in 1980 and solar minimum in 1985. Such decreases would be small in comparison to seasonal variations and would be difficult to detect relative to other natural sources of variability such as the El Chichon volcanic eruption. The net change in the ozone column at low latitudes resulting directly from these upper stratospheric mixing ratio decreases would be less than 1%.

Although radiative-photochemical models can yield an approximate agreement with the observed ozone responses and phase lags below 3 mbar, it is unlikely that the large discrepancy between observed and theoretically calculated temperature phase lags (Figure 6) can be simulated by such models. As previously argued by HOOD (1986; 1987) and by BRASSEUR et al. (1987), the shortfall of the calculated temperature phase lags results

Figure 3. SBUV ozone response amplitudes (sensitivities) and phase lags determined by linear regression for the indicated time intervals. Error bars are standard deviations from the mean for separate regression estimates for five 10° latitude bands centered on the equator. Also shown for comparison are two theoretical profiles (see the text). (after HOOD and DOUGLASS, 1989)

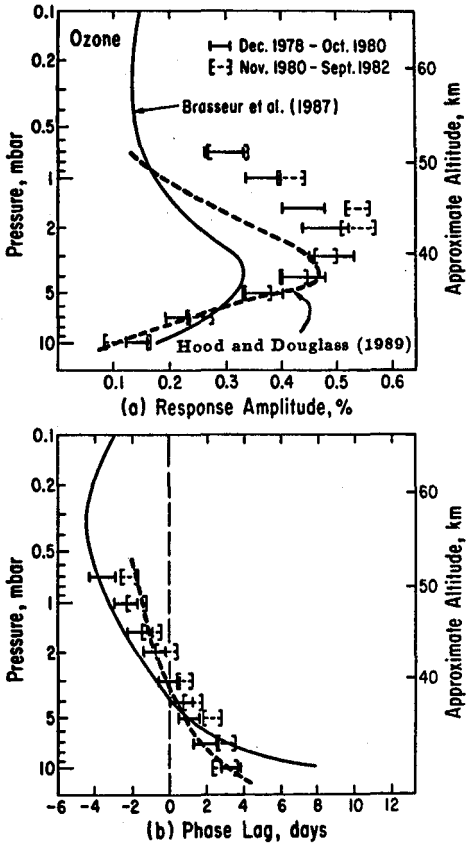

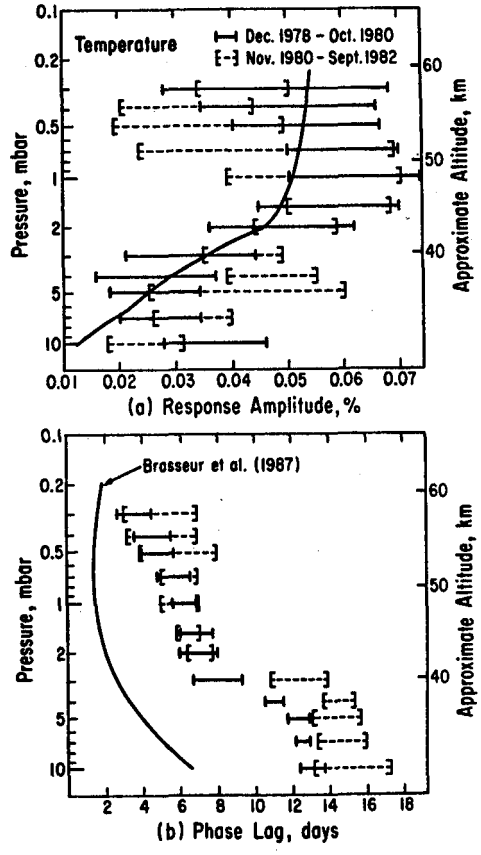

Figure 4. Same as Figure 3 but for SAMS temperature.

from the fact that Newtonian cooling lifetimes in the upper stratosphere are relatively short (e.g. about 5 days near 1.5 mbar; SCHOEBERL and STROBEL, 1978). Consequently, calculated temperature phase lags for 27-day solar ultraviolet forcing are no more than 3-4 days when only radiative heating is considered. It therefore appears that more than a one-dimensional model that considers only photochemistry and radiative heating is needed to provide a complete description of the observed responses. At a minimum, a two-dimensional model with coupled dynamics may be required.

References

Aikin, A.C. and H. J. P. Smith, Mesospheric ozone changes associated with 27-day solar ultraviolet flux variations, *Geophys. Res. Lett., 13*, 427–430, 1986.

Brasseur, G., A. De Rudder, G.M. Keating, and M.C. Pitts, Response of middle atmosphere to short-term solar ultraviolet variations: 2. Theory, *J. Geophys. Res., 92*, 903–914, 1987.

Chandra, S., The solar and dynamically induced oscillations in the stratosphere, *J. Geophys. Res., 91*, 2719–2734, 1986.

Donnelly, R.F., D. E. Stevens, J. Barrett, and K. Pfendt, Short-term temporal variations of Nimbus 7 measurements of the solar UV spectral irradiance, NOAA Tech. Mem. ERL ARL-154, Air Resources Laboratory, Silver Spring, MD, 1987.

Eckman, R.S., The response of ozone to short-term variations in the solar ultraviolet irradiance 2. Observations and interpretation, *J. Geophys. Res., 91*, 6705–6721, 1986.

Gille, J.C., C.M. Smythe, and D.F. Heath, Observed ozone response to variations in solar ultraviolet radiation, *Science, 225*, 315–317, 1984.

Heath, D.F. and Schlesinger, B.M., The global response of stratospheric ozone to ultraviolet solar flux variations, in *Atmospheric Ozone*, C.S. Zerefos and A. Ghazi, eds., D. Reidel Publ. Co., Dordrecht, p. 666–670, 1985.

Heath, D.F. and Schlesinger, B.M., The Mg 280-nm doublet as a monitor of changes in solar ultraviolet irradiance, *J. Geophys. Res., 91*, 8672–8682, 1986.

Hood, L. L., The temporal behavior of upper stratospheric ozone at low latitudes: Evidence from Nimbus 4 BUV data for short-term responses to solar ultraviolet variability, *J. Geophys. Res., 89*, 9557–9568, 1984.

Hood, L. L., Coupled stratospheric ozone and temperature responses to short-term changes in solar ultraviolet flux: An analysis of Nimbus 7 SBUV and SAMS data, *J. Geophys. Res., 91*, 5264–5276, 1986.

Hood, L. L. and A. Douglass, Stratospheric responses to solar ultraviolet variations: Comparisons with radiative-photochemical models, *Proc. Quad. Ozone Symp.*, to appear, 1989.

Hood, L. L. and S. Cantrell, Stratospheric ozone and temperature responses to short-term solar ultraviolet variations: Reproducibility of low-latitude response measurements, *Ann. Geophys., 6*, 525-530, 1988.

Keating, G.M., G.P. Brasseur, J.Y. Nicholson III, and A. De Rudder, Detection of the response of ozone in the middle atmosphere to short-term solar ultraviolet variations, *Geophys. Res. Lett., 12*, 449–452, 1985.

Keating, G. M., J. Y. Nicholson III, D. F. Young, G. Brasseur, and A. De Rudder, Response of middle atmosphere to short-term solar ultraviolet variations: 1. Observations, *J. Geophys. Res., 92*, 889-902, 1987.

Schoeberl, M. R. and D. F. Strobel, The zonally averaged circulation of the middle atmosphere, *J. Atmos. Sci., 35*, 577-591, 1978.

16

N90-28177

GASES OF THE MIDDLE ATMOSPHERE AND SHORT-TERM SOLAR RADIATION VARIATIONS

611642

4B

DANILIN M.Yu., KOUZNETSOV G.I.

119899 Dept.Atmospheric Physics,Faculty of Physics,Moscow State University,Moscow,USSR

Now there is no good agreement between theoretical and experimental data of ozone (O3) response to 27(13)-day solar ultraviolet irradiance variations (SUVIV)(Brasseur et al,1987;Hood,1987,1988 a,b;Keating et al,1987). But a few days duration SUVIV (accompinied ,for example,solar flares (SF)) has not been studied yet. So the main purpose of our research is to investigate amplitudinal,duirnal,seasonal,latitudinal and phase parameters of ozone and other trace gases of atmosphere to such short-term SUVIV.

First,our method for revealing O3 response to SUVIV,caused by fast flare processes is discribed(Danilin et al,1987).We using SF as an indicator of solar activity(Gibson,1973). 3B(N) and 2B(N) SF with time interval of more than 6 days between them were chosen from (Solar-Geophysical Data,1971-1984). Given such SF we selected ozone profiles O_{3i}(The Ozone Data for the World,1971-1984) (simultaneously with W and F10.7 data for the same day) in time interval of ± 2 days from SF occurence. Ozone response ε_i was defined as

$$\varepsilon_i=\frac{O_{3i}-\bar{O}_{3i}}{\bar{O}_{3i}}\cdot 100\%, \qquad (1)$$

where $\bar{O}_{3i}$ -month-averaged ozone concentration at i-level(i=9 (height z>42km), 8(37.5km<z<42.6km), 7(32.7km<z<37.5km), 6(28.2km<z<32.7km),TO-total ozone). In this way we analysed 1939 individual measurements for Jan.1971 - Sept.1984 (see Fig.1). It is important to stress statistically represantative ozone profile response (1-1.8%) and TO response time delay deep into the atmosphere.

We used one-dimensional radiative-photochemical model for study trace gas responses to 27(13)-day SUVIV (Danilin,1989). This solar irradiance perturbations were taken in sinusoidal form with spectral profile $\delta(\lambda)$ according to (Hood et al,1988a;Fig.1b) and $\delta(205nm)=2.57\%$. The value of $\delta(\lambda)$ was decreased by factor of 0.9 for 13-day SUVIV. Temperature response for 27-day SUVIV was adopted according to (Brasseur et al,1987;Fig.3,line 1).

For 27(13)-day SUVIV j-th gas photodissociation rate at height z takes form (2):

$$J_j(z,\chi)=\int_0^\infty I_0(\lambda)\times(1+\delta(\lambda)\times\sin\frac{2\pi t}{27(13)})\times\sigma_j(\lambda)\times\phi_j(\lambda)\times\tau(\lambda,z,\chi)d\lambda \qquad (2)$$

here $I_0(\lambda)$-the solar flux at the top of the atmosphere,

$\sigma_j(\lambda)$-cross-section of j-th molecula,

$\phi_j(\lambda)$-quantum yield,

$\tau(\lambda,z,\chi)$-atmosphere transmission function.

Ozone response was defined both in therms of "sensitivity" (i.e.

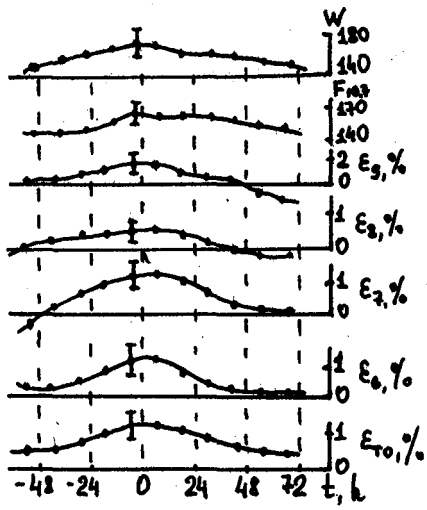

FIG.1. Time dependences of ozone responses ε_i (%) in 6th, 7th, 8th and 9th layers, in TO and corresponding 12 hours-averaged values of W and F10.7 relatively time of flare occurence (t=0).

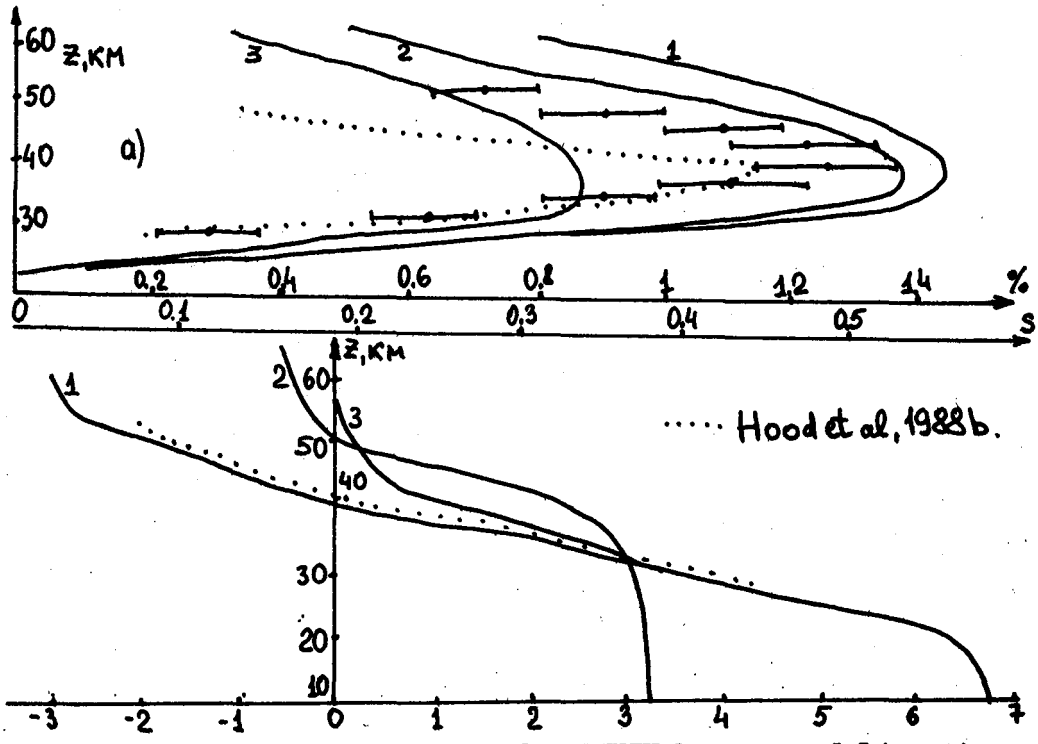

FIG.2. a) Ozone responses to 27 day SUVIV by our model (equator, June): 1-midday, 2- 24-hours-averaged, 3- 13-day-averaged values - and the same by (Hood et al, 1988b, point line) and Nimbus-7 data (Keating et al, 1987);
b) Lag of O3 response (days) for the following scenario: 1 & 3- 27-day SUVIV with and without temperature feedback; 2- 13-day SUVIV with temperature feedback.

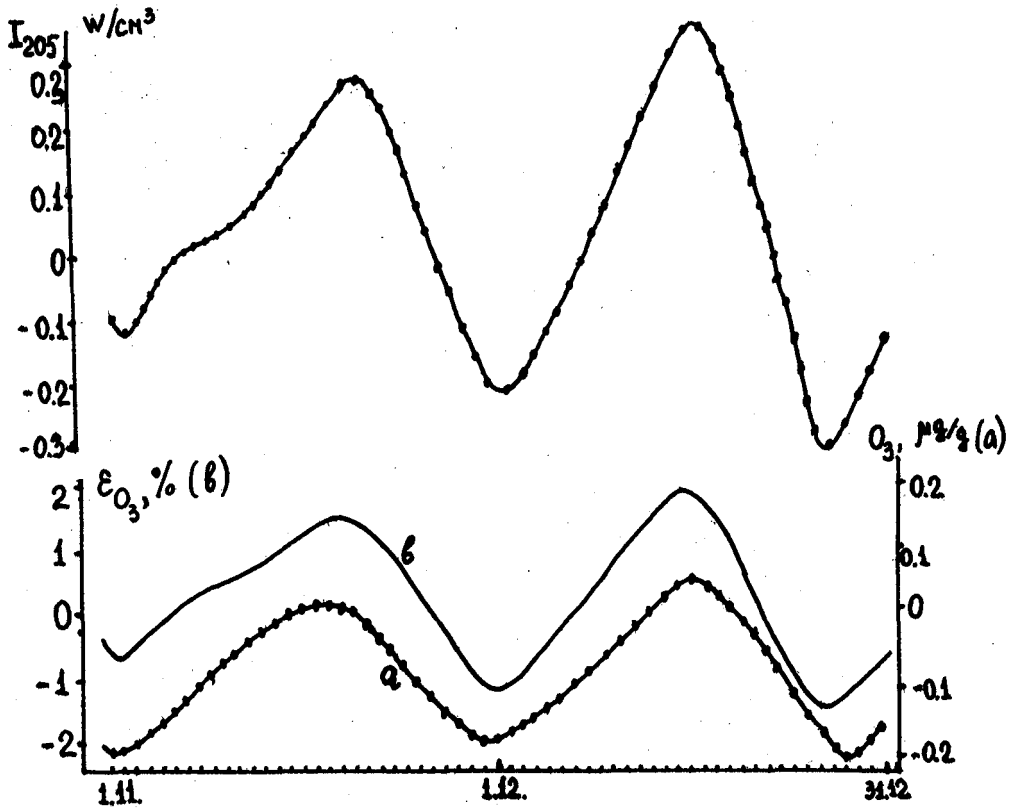

FIG.3.Detrended solar flux I205 (top) and ozone responses (bottom) accordingly to (Hood,1987)(a) and our model calculations(b) during November-December 1979.

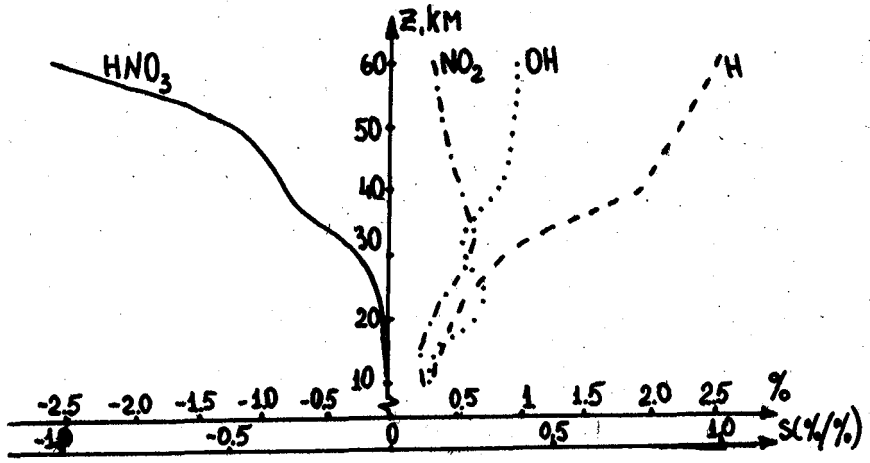

FIG.4.Responses of HNO3,NO2,OH and H to 27 day SUVIV (equator, June,model midday).

%O3/1% at λ=205nm) and in per cent deviation from undisturbed concentration. It was established that duirnal modulation of O3 response was very important. Actually lines 1 and 2 in Fig.2a correspond to ozone responses at model midday and 24 hour-averaged value for the day of 27-day SUVIV sinusoid maximum accordingly. Line 3 in Fig.2a shows the half-period averaged ozone response. Comparisons of our results with "Nimbus-7" data (Keating et al,1987) demonstrate closer agreement in the upper stratosphere,than similar results (Brasseur et al,1987;Hood et al, 1988b). These discrepances are due to different duirnal photodissociation rates model discriptions. Phase characteristics of ozone response are shown in Fig.2b for the mentioned scenario.

Fig.3 illustrates ozone responses at equator at 1.5 mbar (a)by (Hood,1987)and by our model results (b) at 44km (24 hour-averaged) to real profile I205 during November-December 1979. Good agreement between lines a) and b) confirms correctness of our theoretical calculations.

Studying seasonal and latitudinal dependence of O3 response we used the same temperature response dependence by(Chandra,1986). It was established that O3 response became maximum at equator in summer and minimum - in winter polar and midlatitude regions.

Responses of HNO3,OH,NO2 and H to 27-day SUVIV for model midday (equator,June) are shown in Fig.4. Strong HNO3 content decrease (especially in the mesosphere) was caused by increase of both HNO3 photodissociation rates and HNO3+OH -->NO3+H2O reaction rate. NO2 and OH responses were experimentally undetectable due to small values of their sensitivities.

We think that the development of more accurate satellite devices and consideration of dynamical regime change during 27(13)-day SUVIV and other geophysical effects (that mask styding effects)should constitute the main directions of further research.

REFERENCES

Brasseur G.,A.DeRudder,G.M.Keating & M.C.Pitts(1987)//JGR,92,903.

Chandra S.(1986)//JGR,91,2719.

Danilin M.Yu.,G.I.Kouznetsov(1987)//Izv.AN USSR.Phys.Atmosph.Ocean ,23,830.

Danilin M.Yu.,T.M.Matveeva,G.I.Kouznetsov(1988)//Proc.Quandr.Ozone Symp.(Gottingen,FRG,1988),in press.

Danilin M.Yu.(1989) Short-term middle atmosphere trace gas variations.-Thesis-Moscow.

Gibson E.G.(1973) The Quiet Sun.-NASA,Washington.

Hood L.L.(1987)//JGR,92,876.

Hood L.L. & A.R.Douglass(1988a)//JGR,93,3905.

Hood L.L. & A.R.Douglass(1988b)//Quadrn.Ozone.Symp.(Gottingen,FRG) Abstracts,p.179.

Keating G.M.,M.C.Pitts,G.Brasseur & A.DeRudder(1987)//JGR,92,889.

Solar-Geophysical Data(1971-1984),Bould.,Colorado,NOAA,No.317-384.

The Ozone Data for the World(1971-1984),WMO,Toronto,Canada.

17

N90-28178

611643

6 pgs

ATMOSPHERIC PLANETARY WAVES INDUCED BY SOLAR ROTATION

A.A. Krivolutsky

Central Aerological Observatory, The USSR State Committee for Hydrometeorology, 123376 Moscow, USSR

It is known that there are variations in the atmospheric processes with a period close to that of the rotation of the Sun (27 days). The variations are discovered in tropospheric processes (WASSERFAL, 1935), rainfalls (ROSENBERG, 1974), geopotential (KING et al., 1977) and in stratosphere (EBEL and BATZ, 1977; EBEL, 1981; KRIVOLUTSKY, 1982; KRIVOLUTSKY et al., 1987).

The main theoretical problem is the identification of the physical process by which these heterogeneous solar and meteorological phenomena are connected. VOLLAND (1979) using the astronomical observations found a 27-day harmonic of the solar constant with amplitude of about 0.1% and considering the process of heat transfer from surface of the Earth due to its periodic heating as a forcing effect and using methods accepted in the theory of tides obtained that the induced wave corresponding to a selected Rossby--Haurwitz mode (2,-6) should have an amplitude of almost an order of magnituder smaller than that obtained by King. IVANOVSKY and KRIVOLUTSKY (1979) proposed that the periodic heating of the ozone layer by the short wave radiation would be the reason of excitation the 27-day oscillations. It was also assumed that excitement takes place in condition of resonance with an excited mode (1,-5) corresponding to the conditions present in the stratospheric circulations. Now we shall discuss the possibility of the resonant excitation and make the presentation of the data analysis results which support this idea.

THE STRUCTURE OF RESONANCE WAVES

Linear tidal theory may be used to study the generation and the structure of the planetary waves generated by a heat ozone source. With the boundary conditions that the vertical wind should disappear at the ground and that the radiation condition is at infinite, it is found (IVANOVSKY and KRIVOLUTSKY, 1979) that for isothermal atmosphere the height structure becomes:

$$\frac{P_n^s(z)}{P_0(z)} \approx \frac{i(\gamma-1)K_2\cdot(K_1-\frac{\gamma-1}{\gamma})\,e^{\frac{K_2 z}{H}}}{\delta'\cdot(K_2-K_1)\cdot(K_2-\frac{\gamma-1}{\gamma})\cdot P_{00}} \times \int_0^\infty e^{K_2\xi} q_n^s(\xi)\,d\xi \qquad (1)$$

where $\gamma = C_p/C_v$, $K_1 = 1/\gamma$, $K_2 = (1/4 - \gamma - 1/\gamma \cdot \times H/h_n^s)^{-1/2}$, h_n^s - equivalent depth, $\sigma' = \sigma + \alpha S$, α - index of zonal circulation, $\alpha = u/a\cos\Theta$, u - zonal wind, a - radius of the Earth, σ - the frequency of 27-day rotation, $P_0(Z) = P_{00}\exp(-Z/H)$.

It is known that near ${}^{o}h_n^s \approx \gamma H$ the atmospheric waveguide behaves like a resonance cavity, so near this region:

$$h_n^s - H\gamma \approx \frac{\sigma - \sigma_n^s + i\nu_z/\bar{H}^2}{2\Omega} \cdot \frac{\partial h_n^s}{\partial f}$$

where $f = \sigma/2\Omega$, Ω - the angular frequency of the Earth's rotation.

We can use the expression for eigenfrequencies (DIIKY, 1969):

$$\sigma_n^s \approx \alpha \cdot S - \frac{2\Omega S}{n(n+1) + \frac{4a^2\Omega^2}{g h_n^s} B_n^s} \qquad (2)$$

where:

$$B_n^s = \frac{(n-s)(n+s)(n+1)}{(2n-1)(2n+1)n^2} + \frac{(n-s+1)(n+s+1)n^2}{(2n+1)(2n+3)(n+1)^2}$$

Using the expression (2) we find a value:

$$\frac{\partial h_n^s}{\partial f} = \frac{4a^2\Omega^2}{f^2 \cdot g} \cdot \frac{s}{B_n^s}$$

So that one can rewrite the expression (1) in the form:

$$\frac{P_n^s}{P_0(z)} = \frac{i(2-\gamma)\gamma H}{\frac{\partial h_n^s}{\partial f} \cdot P_{00} \cdot \sigma'} \cdot \frac{\Omega\, e^{(K_2 z)/H}}{(\sigma - \sigma_n^s + i\nu_z/\bar{H}^2} \int_0^\infty e^{K_2 \xi} q_n^s(\xi)\, d\xi \qquad (3)$$

where ν_z is eddy viscosity coefficent, $H = \gamma H/\gamma - 1$. For example, the amplitude of the resonant wave ($\sigma \approx \sigma_n^s$) near the surface is:

$$\frac{P_h^s}{P_0(0)} \approx \frac{(2-\gamma)\gamma H}{\frac{\partial h_n^s}{\partial f} \cdot P_{00}} \cdot \frac{\Omega}{\sigma} \cdot \frac{\bar{H}^2}{\nu_z} \int_0^\infty e^{\frac{\gamma-1}{\gamma}\xi} q_n^s(\xi)\, d\xi$$

The 27-day variability of the UV radiation (HEATH, 1973; ROTTMAN, 1983) and the existence of "ozone waves" - global longitudinal inhomogeneity - helps to calculate the value of P_n^s/P (Z) corresponding to ozone heating function:

$$q^s_{n,\sigma}(z) = \frac{1}{2\pi}\int_{-1}^{1}\int_{0}^{2\pi} Q(z,\varphi,\mu)\, e^{-i(s\varphi+\sigma t)}\, \Theta_n^s(\mu)\, d\varphi\, d\mu,$$

$$\mu = \cos\theta$$

$$Q(z,\varphi,\mu) = \sum I_{\lambda\infty}\,\sigma_\lambda \cdot n_{O_3}\cdot e^{-\frac{\tau_{\lambda,O_3}}{\cos z}}$$

$$300\,nm < \lambda < 360\,nm$$

where $I_{\lambda\infty}$ - solar irradiance, σ_λ - crossection of absorption, n_{O3} - concentration of ozone, z - zenit angle, Θ_n^s - function of Hough. With using the values of variability such as:

$$\Delta I_{\lambda\infty}/I_{\lambda\infty} \approx 0.005\ (0.5\%)$$

$$\Delta M_{O_3}/M_{O_3} \approx 0.1\ (10\%)$$

and:

$$\nu_z \approx 5\times10^4\,cm/c^2$$

we get the estimation of the 27-day wave amplitude:

$$P^1_{-5}/P_{oo} \approx 0.005\ (5\ mb)$$

We have used n = -5 and s = 1 because these values of wave-numbers give the eigenperiod near 27 days. The value of the wave disturbance according to our estimation and the expression (3) is near to 100 gpm or more if the resonance conditions exist (on 30 mb).

RESULTS OF DATA ANALYSIS

Now we shall make the presentation of some improvements for the existence of the resonant mechanism.

Figure 2 borrowed from KRIVOLUTSKY et al. (1987) presents evolution of amplitudes of the 27-day harmonic in series of H and W (solar spots number). It could be seen that the curves for H_{30} and W are rather well synchronised and periods exist when the amplitudes of the oscillations with the period close to 27 days are significant (more than 100 gpm).

Figure 3 showes the evolution of the phase difference in 27-day oscillations of H_{30} and W. The relative invariance of the difference should testify to the coherency of the solar and atmospheric oscillations of this period. It could be seen that the

curves for H_{30} and W are rather well synchronised when the amplitudes are significant.

Figure 4 allows to see the longitudinal behaviour of the phase for the period when the amplitude is large. It is clear that the wave is westward with the wave-number s = 1.

CONCLUSIONS

Theoretical calculations with the use of the tidal theory reveal the possibility of resonance in the atmospheric system to the 27-day oscillations (mode n = -5, s - 1) with amplitude of the wave more than 100 gpm on 30 mb surface due to the absorption in Huggins bands which changes by about 1% and to the existence of longitudinal inhomogeneity of total ozone. The data analysis reveals such waves in the atmospheric processes and the correlation with the solar activity.

REFERENCES

Diiky, L.A., The Earth's oscillatins theory, Leningrad, Hydrometeopress, 1969 (in Russian).

Ebel, A., Oscillations of stratospheric circulation with periods near 27 and 13.6 days, MAP Handbook, 2, 468, 1981.

Ebel, A., and W. Batz, Response of stratospheric circulation at 10 mb to solar activity oscillations resulting from the sun's rotation, Tellus, 29, 41-47, 1977.

Heath, D., Space observations of the variability of solar irradiance in the near and far ultraviolet, J.Geoph.Res., 78, 16, 1973.

Ivanovsky, A.I., and A.A. Krivolutsky, About the possibility of resonant exitation of planetary waves, Meteorol. Gidrolog., 6, 97, 1979 (in Russian).

King, J.W., A.J. Slater, A.D. Stevens, P.A. Smith, and D.M. Wilis, Large-amplitude standing planetary waves induced in troposphere by sun. J.Atmos.Terr.Phys., 39, 1357, 1977.

Krivolutsky, A.A., Atmospheric waves of a long period induced by periodic source, Meteorol. Gidrolog. 11, 38, 1982 (in Russian).

Krivolutsky, A.A., V.N. Kuznetsova, and D.A. Tarasenko, Wave motions in the middle atmosphere and relation to the solar activity. Physica Scripta, 36, 382-384, 1987.

Rosenberg, R.L., and J. Cobman, 27-day cycle in the rainfall at Los Angeles, Nature, 250, 481-484, 1974.

Rottman, G.J., 27-day variations observed in solar ultraviolet (120-300 nm), Planet.Space Sci., 31, 1001, 1983.

Volland, H., Periodic variations of solar radiation - a possible source of solar activity-weather effects. J.Atmos.Terr.Phys., 41, 89-94, 1979.

Wasserfall, K.F., The 27-day period in temperature data, Amer. Geoph.Univ.Trans., 16, 1, 1935.

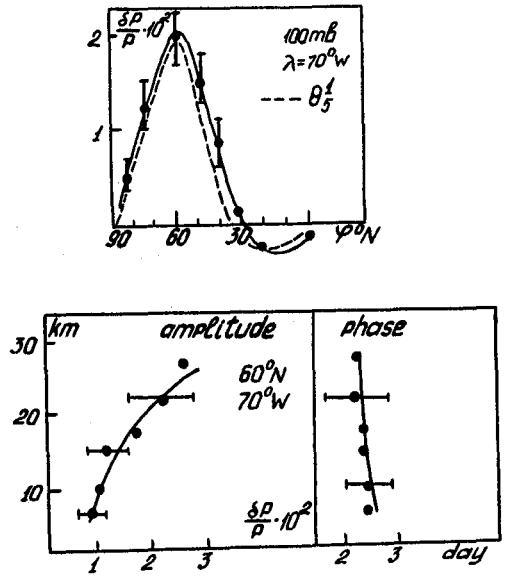

Fig.I.Spatial structure of a transient wave with the27-day period(I972/I973,70 w,60 N)

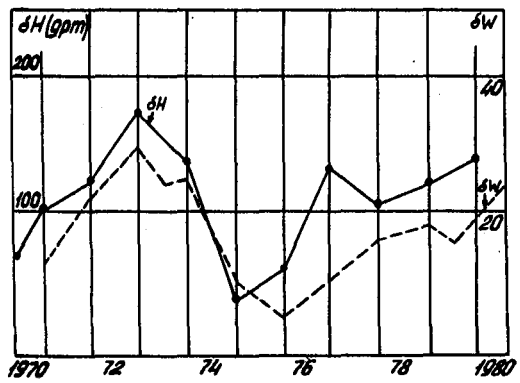

Fig.2.Evolution of amplitudes of the 27-day harmonic in series of H_{30} (i.60.N,70 W) and W(solar spots number)

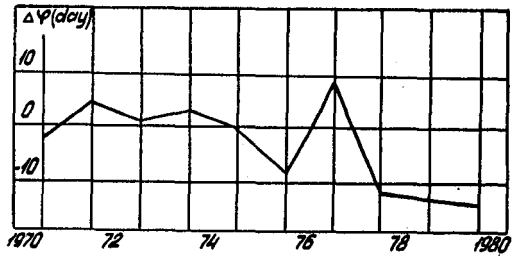

Fig.3. Evolution of the phase difference in the 27-day oscillations of H_{30} (60 N,70 W) and W(solar spots)

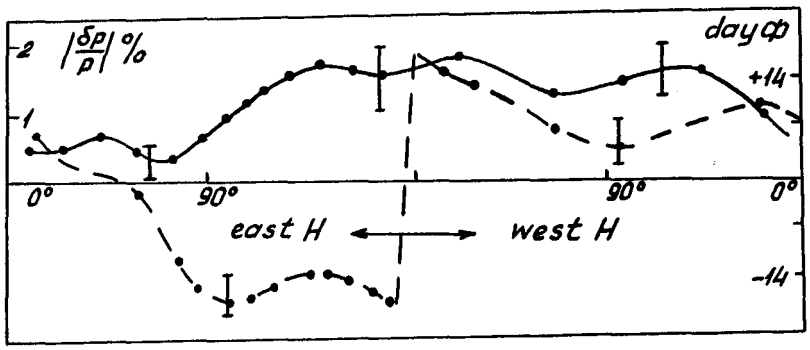

Fig.4. The longitudial structure of the 27-day harmonic in series H_{100}(60 N,1972/1973 ,phase-dashed line)

RESONANT ROSSBY WAVES AND SOLAR ACTIVITY

A.A. Krivolutsky, O.A. Loshkova

Central Aerological Observatory, The USSR State Committee for Hydrometeorology, 123376 Moscow, USSR

Large-scale transient waves are essential part of atmospheric dynamics. Some of these waves (like 27-day waves, KRIVOLUTSKY, 1982; EBEL, 1981; KING, 1977) would have a solar nature. In this paper we want to investigate the contribution of the 27-day planetary waves to a total long-period spectrum of the atmospheric processes during one solar cycle.

DIIKY (1969) showed that the eigenfrequencies of Rossby waves are

$$\sigma_n^s = \alpha s - \frac{2\Omega s}{n(n+1) + (4a^2\Omega^2/gh_n^s) \times B_n^s}$$

where $\sigma^s = 2\pi/T_n^s$, T_n^s - periods of the waves, α - zonal circulation index, a - radius of the Earth, (n,s) - wavenumbers, Ω - frequency of the Earth's rotation, h_n^s - equivalent depth and

$$B_n^s = \frac{(n-s)(n+s)(n+1)}{(2n-1)(2n+1)\ n^2} + \frac{(n-s+1)(n+s+1)\ n^2}{(2n+1)(2n+3)(n+1)^2}$$

IVANOVSKY and KRIVOLUTSKY (1979) proposed that the 27-day wave has a resonant nature ($h_n^s \approx \gamma H$). We shall try to investigate the real atmospheric processes. The method of two-dimensional wave analysis which we can use is described by KRIVOLUTSKY (1981). In this method of analysis a two-dimensional meteorological field is writen in the form

$$Y(t,\lambda) = \sum_{n}^{\infty} \sum_{s=0}^{\infty} \left\{ R_n^s \cdot \cos(\omega_n t + s\lambda + \gamma_n^s) + S_n^s \cdot \cos(\omega_n t + \eta_n^s) \cdot \cos(s\lambda) \right\}$$

where λ - longitude, $\omega_n = 2\pi n/T$, T - time scale, s - zonal wave number, R_n^s, S_n^s - amplitudes of transient and standing waves. The sign of the R_n^s determines the direction of the wave propagation.

Using the following trigonometrical identicals

$$\int_0^T \int_0^{2\pi} \left\{ \begin{array}{l} \cos(\omega_n t \pm s\lambda) \sin(\omega_n t \pm m\lambda)\, dt\, d\lambda \\ \cos(\omega_n t - s\lambda) \cos(\omega_n t + m\lambda)\, dt\, d\lambda \\ \sin(\omega_n t - s\lambda) \sin(\omega_n t + m\lambda)\, dt\, d\lambda \end{array} \right\} = 0$$

$$\int_0^T \int_0^{2\pi} \left\{ \begin{array}{l} \cos(\omega_n t + s\lambda)\cos(\omega_n t + m\lambda) \\ \cos(\omega_n t + s\lambda)\cos(\omega_n t - m\lambda) \\ \sin(\omega_n t - s\lambda)\sin(\omega_n t - m\lambda) \end{array} \right\} dt\,d\lambda =$$

$$= \left\{ \begin{array}{l} \pi T, \; s = m \\ 0, \; s \neq m \end{array} \right.$$

we can the next system

$$\Psi_1^{n,s} = \frac{1}{\pi T} \int_0^T \int_0^{2\pi} Y(t,\lambda) \cos(\omega_n t + s\lambda)\, dt\, d\lambda =$$

$$= R_n^s \cos(\gamma_n^s) + \frac{S_n^s}{2} \cos(\gamma_n^s)$$

$$\Psi_2^{n,s} = \frac{1}{\pi T} \int_0^T \int_0^{2\pi} Y(t,\lambda) \sin(\omega_n t + s\lambda)\, dt\, d\lambda =$$

$$= -R_n^s \sin(\gamma_n^s) - \frac{S_n^s}{2} \sin(\gamma_n^s)$$

$$\Psi_3^{n,s} = \frac{1}{\pi T} \int_0^T \int_0^{2\pi} Y(t,\lambda) \cos(\omega_n t - s\lambda)\, dt\, d\lambda =$$

$$= \frac{S_n^s}{2} \cos(\gamma_n^s)$$

$$\Psi_4^{n,s} = \frac{1}{\pi T} \int_0^T \int_0^{2\pi} Y(t,\lambda) \sin(\omega_n t - s\lambda)\, dt\, d\lambda =$$

$$= -\frac{S_n^s}{2} \sin(\gamma_n^s)$$

So we can find the amplitudes of transient waves

$$|R_n^s| = \left| \frac{\psi_1^{n,s} - \psi_3^{n,s}}{\cos \gamma_n^s} \right| \equiv \sqrt{(\psi_1^{n,s} - \psi_3^{n,s})^2 + (\psi_2^{n,s} - \psi_4^{n,s})^2}$$

$$|S_n^s| = \left| \frac{2\psi_3^{n,s}}{\cos \gamma_n^s} \right| \equiv 2\sqrt{(\psi_3^{n,s})^2 + (\psi_4^{n,s})^2}$$

$$\gamma_n^s = \operatorname{arctg}\left(\frac{\psi_4^{n,s} - \psi_2^{n,s}}{\psi_1^{n,s} - \psi_3^{n,s}}\right); \quad \eta_n^s = \operatorname{arctg}\left(-\frac{\psi_4^{n,s}}{\psi_3^{n,s}}\right)$$

Figure 1, shows the results of two-dimensional analysis for the period 1971-1981. The main result is that the periods of large-scale transient waves are close to the resonant situation ($h \approx \gamma H$). The amplitudes of the waves attain the value of about 100 gpm. Figure 2 shows the vertical structure of the 27-day wave and the role of the wave motions with s = 1,2,3. It could be seen that there is a dominant scale in transient stratospheric waves (s = 1).

So we may conclude that the resonant nature of the 27-day wave is not unicum. There are long-periods waves (50-day wave) in stratosphere which belong to the resonant waves, too. It is a very interesting fact for the solar activity-weather problem.

REFERENCES

Diiky, L.A., The earth's oscillations theory. Leningrad, Hydrometeopress, 1969 (in Russian).

Ebel, A., Oscillations of stratospheric circulation with periods near 27 and 13.6 days, MAP Handbook, 2, 468, 1981.

King, J.L., A.J. Slater, A.D. Stevens, P.A. Smith, and D.M. Willis, Large-amplitude standing planetary waves induced in the troposphere by sun, J.Atmos.Terr.Phys., 39, 1357, 1977.

Krivolutsky, A.A., Atmospheric waves of a long period induced by peridic source, Meteorol. Gidrolog., 11, 38, 1982 (in Russian).

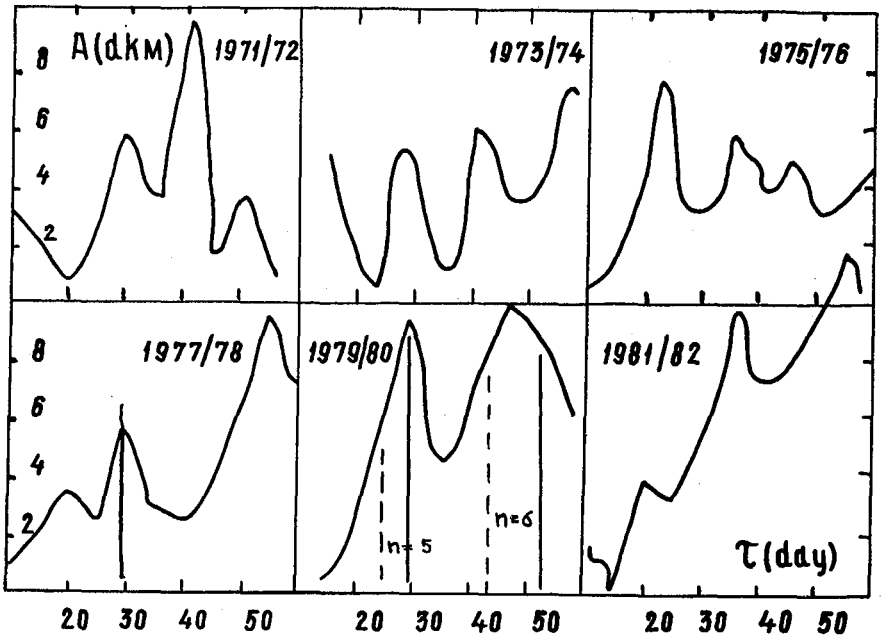

Fig.I. Results of two-dimensional analysis for daily values of the 30 mb heights (60N, transient waves only , S=1, ---- h=∞ , ——— h=10 km)

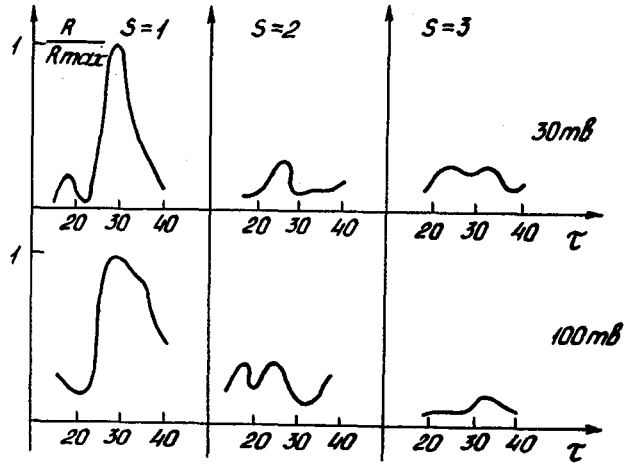

Fig.2. Vertical structure of the transient waves for different zonal wave-numberes(I972/I973)

ON THE RELATIONSHIP BETWEEN THE PHASES OF 27-DAY TOTAL OZONE AND SOLAR ACTIVITY INDICES IN DIFFERENT LATITUDINAL ZONES

I.N. Ivanova, A.A. Krivolutsky, V.N. Kuznetsova

Central Aerological Observatory, The USSR State Committee for Hydrometeorology, 123376 Moscow, USSR

The purpose of this paper is to analyse the dynamics of 27-day total ozone variations during an 11-year solar activity cycle at high and low latitudes.

The stations Churchill (58°45'N; 94°04'W), Goose-Bay (53° 19'N; 60°25'W), and Kodaikanal (10°14'N; 77°28'E) were selected for this analysis, firstly, because of the longest observation rows at these stations, covering the period from 1968 through 1985 and, secondly, due to the fact that, according to earlier sample calculations, the amplitudes of 27-day total ozone variations at high-latitude stations are the largest.

The calculations were made using a specially worked out program permitting, besides the determination of the amplitudes and phases, the observation of the coherence of phases in any time interval. To characterize solar activity, solar radio-flux at 10.7 cm was used, which according to KEATING (1978) and HEATH et al. (1971) correlated well with both the radiation at λ = 210 nm and the global ozone variations.

The results of the calculation of total ozone phases difference and those of the index $F_{10.7}$, as well as the amplitudes of the 27-day variations of these parameters are presented in Figures 1 and 2, respectively. As can be seen in Figure 1, in the periods of maximum solar activity (1968/1972 and 1978-1982), the difference between the phases varies within 5 to 6 days, while in the years of the minima it appears to have a negative value of 6 to 7 days (which corresponds to the total ozone maximum occurrence in about 20 days after the $F_{10.7}$ maximum). At Goose-Bay a somewhat lesser mean difference of phases in the years of maximum solar activity is connected with the sharp change of the phase difference in 1981, and particularly in 1969, which needs an extra detailed analysis. As can be seen in Figure 1 (c,d), the above regularities in total ozone behaviour are not observed in summer, which results also in the unchanged amplitudes of 27-day total ozone variations (Figure 2) during the transition from the minimum to the maximum of solar activity.

In winter, both at the Churchill and Goose-Bay stations we observe the growth of the amplitudes of 27-day total ozone variations in the years of active Sun, which are most pronounced in the ascending branch of 11-year solar cycle. The latitudinal change of the phases of 27-day total ozone variations in winter is shown in Figure 3 (a and b), where the 27-day variations are determined for 5-month rows of daily ozone values, separately for the winters (November through March) of 1975-1976 and 1980-1981. The shaded bands in each of the figures show the phase of the 27-day variation of $F_{10.7}$, which coincides well with the actual occurrence of the maxima in Novembers 1975 and 1980, respectively. As can be seen from Figure 3b, at mid latitudes the maximum of

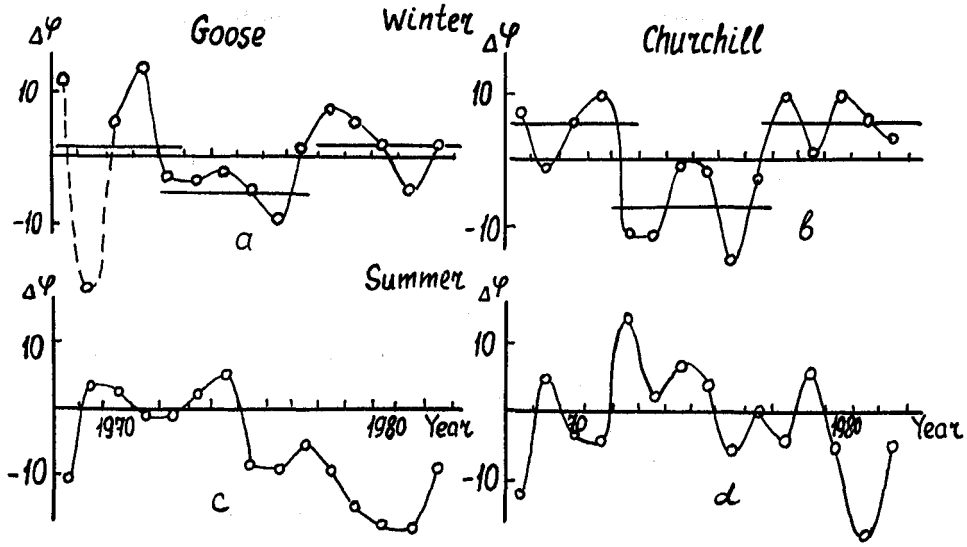

Fig.1. The differences of total ozone and $F_{10.7}$ phases in winter (a,b) and summer (c,d).

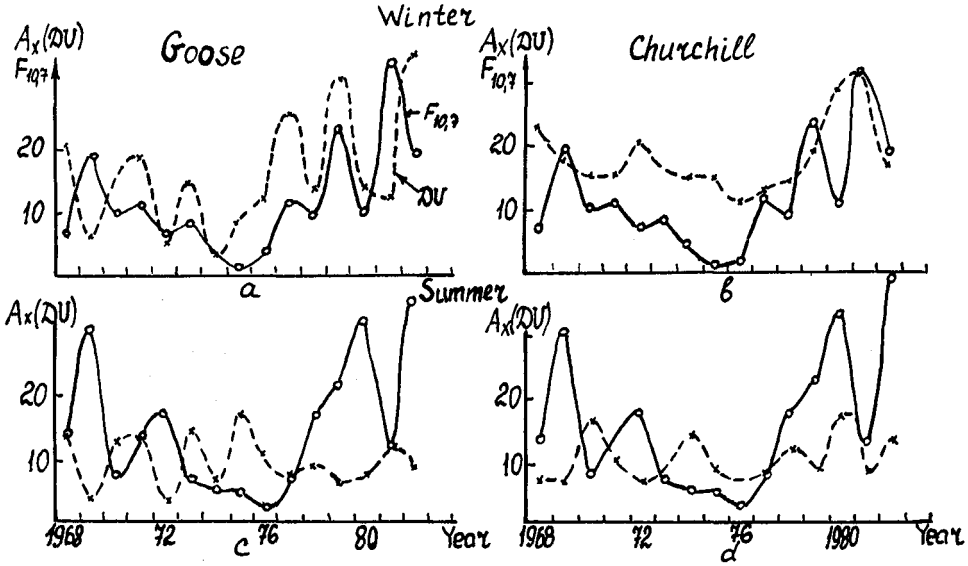

Fig.2. The amplitudes of 27-day total ozone variations in winter (a,b) and summer (c,d).

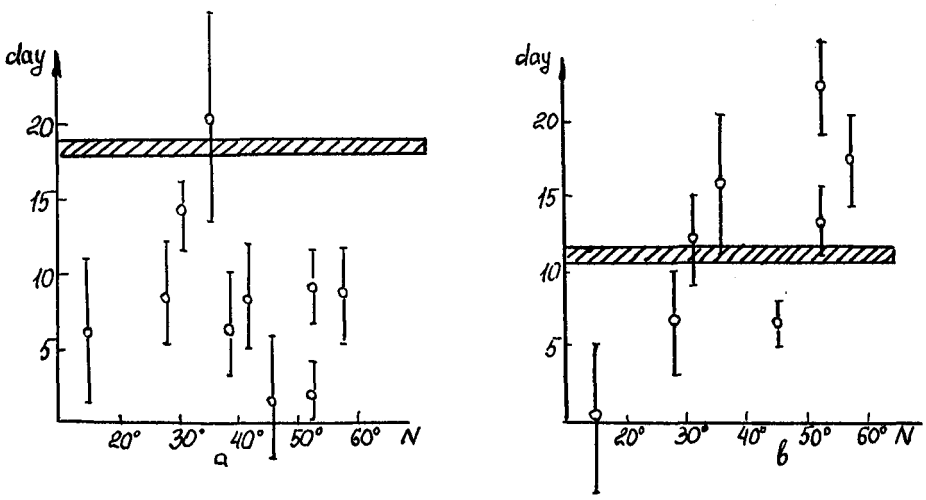

Fig.3. The latitudinal change of the phases of 27-day total ozone variations.

27-day total ozone variations immediately follows the $F_{10.7}$ maximum gradually spreading towards high and low latitudes.

In the years of minimum solar activity one fails to observe a similar relationship.

The spectral analysis of total ozone data and index $F_{10.7}$ for each of the years has shown that from year to year change not only the amplitudes of the variations observed, but also do the periods. Thus, every 4 years a sharp increase occures of the period of $F_{10.7}$ variations up to 30 days, with the following decrease down to 24-25 days. However, total ozone does not show such a periodicity. At Kodaikanal the occurrence of total ozone variations with nearly a 27-day period has an episodic character. Thus, the investigation conducted indicates the necessity of a more detailed analysis of the phenomena considered above.

REFERENCES

Heath D.R., E. Hilsenrath, A.J. Krueger, W. Nordberg, C. Prabhakara, and J.S. Theon, Observations of the global structure of the stratosphere and mesosphere with sounding rockets, International school of atmospheric physics, Erice (Italy), 1971.

Keating G.M., Relation between monthly variation of global ozone and solar activity, Nature, 274, 873-874, 1978.

TOTAL OZONE TIME VARIATIONS DURING THE SPRING REVERSALS IN THE HIGH LATITUDINAL STRATOSPHERE OF THE NORTHERN HEMISPHERE DURING THE 20th AND 21st SOLAR CYCLES

V.G. Kidiyarova

Central Aerological Observatory, 141700 Dolgoprudny, USSR

The principal features of the thermodynamic regime of the stratosphere are governed by the development of the winter stratospheric low and the Aleutian and Atlantic heights. These are fed by the influx of the eddy energy transported into the stratosphere by the planetary waves. The intensity and variability of planetary waves and vortices associated with the waves determine the conditions of low-to-high latitudes ozone transport in the winter hemisphere. Note that the ozone distributions are zonally inhomogeneous.

Figure 1 shows the March 1984 and 1985 course of total ozone (TO) for the stations of Leningrad (Voeikovo, 60°N 30°E) and Markovo (60°N 170°E) and data of spring reversals (D) in Julian dates. Time variations of TO are out of phase at these stations. Voeikovo lies within the area affected by the stratospheric polar cyclonic vortex which blocks the inflow of ozone from low latitudes. Markovo lies within the area affected by the Aleutian high, which usually centres in temperate or subtropical latitudes; the circulation within this vortex stimulates latitudinal exchange. These two thermobaric systems form, as a rule, planetary waves with zonal wave number n = 1. Connections between TO and planetary waves variations are shown in Figure 2. Figure 2 presents the day-to-day course of TO as observed at Voeikovo during February-March 1985, besides the amplitudes of the planetary waves at 30 hPa 60°N are given. Variations of TO are practically in counterphase with planetary wave amplitude variations (KIDIAROVA and TARASENKO, 1987; KIDIAROVA and SCHERBA, 1986).

The planetary wave dynamics is affected by solar activity variations during solar cycles. The 20th solar cycle maximum was accompanied by decreases of stratospheric planetary wave amplitudes, the 21st cycle was accompanied by increases of amplitudes.

Tab. 1. January mean total ozone values for maxima of the 20th and 21st solar cycle (1968 and 1979, respectively).

Station	1968	1979
Churchill	459	364
Resolute	483	325
Lervick	403	322

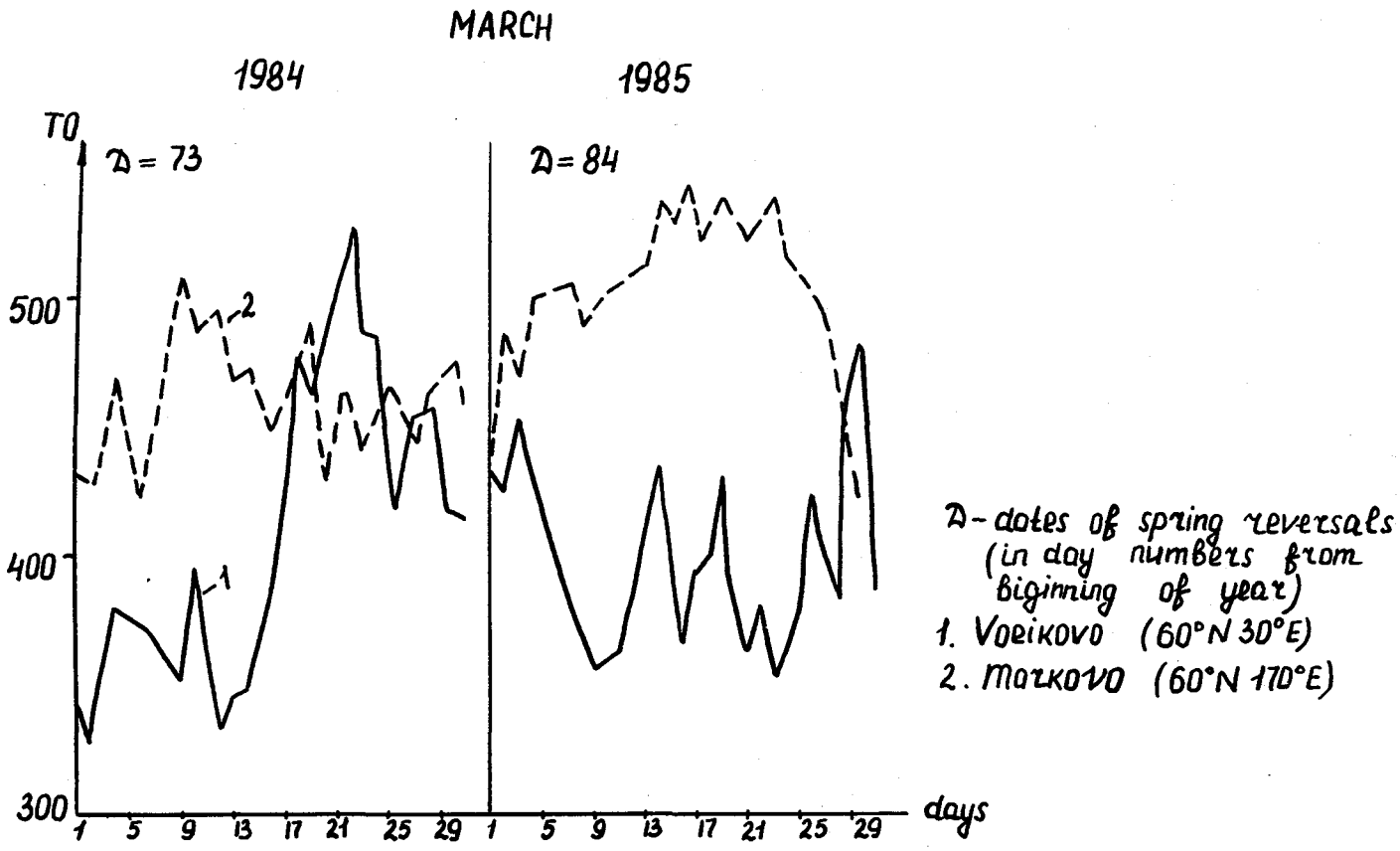

Fig. 1 Day-to-day course of total ozone (TO) at different longitudes

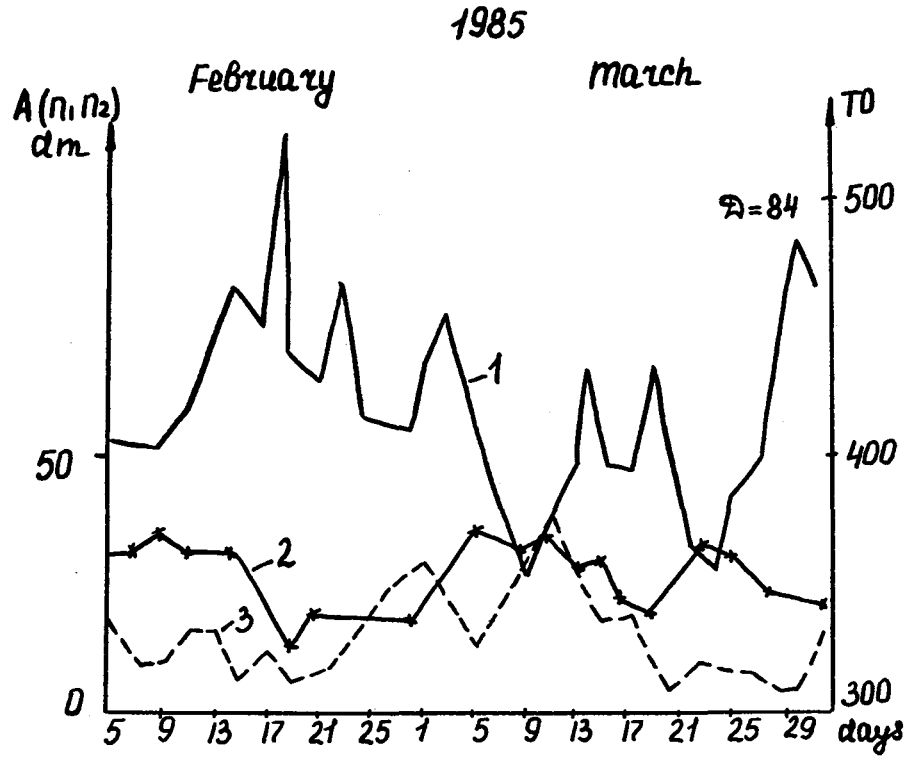

1. total ozone (TO)
2. n=1 amplitudes
3. n=2 amplitudes

Fig. 2 Day-to-day course of total ozone (TO) at Voeikovo and amplitudes of planetary waves with n=1 and n=2 at 30 hPa 60° N for February and March 1985.

Tab. 2. Julian dates of spring reversals (D) and TO in Marches for the eastern (E) and western (W) phases of QBO during the 20th and 21st solar cycles.

	cycle 20		cycle 21	
QBO phase	E	W	E	W
Julian date	88	98	97	89
		TO		
Churchill	468	455	468	466
Volikovo	419	412	416	411
Markovo	474	432	472	452

REFERENCES

Kidiyarova V.G., and D.A. Tarasenko, On the seasonal features of the interconnections between the long-period oscillations in TO and the thermodynamic regime of the extratropical stratomesosphere, In: Atmospheric ozone, Leningrad, Gidrometeoizdat, 278-281, 1987 (in Russian).

Kidiyarova V.G., and I.A. Scherba, Interannual variations of the planetary waves intensity and of the total ozone, Second All-Union Sym. on the Results and Middle Atmospheric Studies, Abstracts, 32, 1986 (in Russian).

THE VERTICAL OZONE DISTRIBUTION DURING MAXIMUM AND MINIMUM SOLAR ACTIVITY

G.A. Kokin, N.I. Brezgin, I.N. Ivanova, V.N. Kuznetsova, E.M. Larin, V.V. Sazonov, A.F. Chizhov, O.V. Shtirkov

Central Aerological Observatory, The USSR State Committe for Hydrometeorology, 123276 Moscow, USSR

To study the latitude variation of ozone vertical distribution the complex experiment was carried out in February-July 1985 between 40°N - 70°S at the Pacific and the Indian Oceans. The great bulk of their data network were taken by the optical rocket ozonometers at the Southern hemisphere.

The results were compared with reference models (KEATING and YOUNG, 1985) containing the most extensive set of ozone observations from VS satellites between 1978 and 1982. To analyse latitude-season ozone variability at fixed altitude levels the experimental ozone concentration data were confirmed with model equatorial data by the equation:

$$K_e(\varphi) = \frac{N_e(\varphi) - N_m(0^\circ)}{N_m(0^\circ)}$$

where N - ozone concentration at a fixed altitude level, φ - latitude, e - index for experimental data, m - index for reference model data.

To compare the experimental data with reference model data, analogous model values $K_m(\varphi)$ were calculated by the equation:

$$K_m(\varphi) = \frac{N_m(\varphi) - N_m(0^\circ)}{N_m(0^\circ)}$$

The results of calculation (Figure 1) indicated a good agreement between experimental and reference model data of relative latitude-season variations of ozone concentration. Maximum variability is observed at 50 km in the equator ($\sim$ 20%) and not exceeded 15% in the other regions at all altitude levels.

The latitude gradient agreement between K_e and K_m is good in April-June, especially at latitudes 50°S-70°S, where ^mK_e is equal to 0.014 deg^{-1} at all altitude levels. The minimum difference between K_e and K_m is located at 40 km in 0°-40°S, and $K_e(\varphi) \simeq 0.005$ deg^{-1} (it is a region of equilibrium state).

Similar experiments were carried out in different regions. The geographical location of first measurements during 1965 were at 47°S, 52°S and 58°S along 78°W (KRUEGER, 1973) and of second measurements during 1979 were along 6°30'N at 55°-88°E (BREZGIN et al., 1984). To compare the measurements in 1965 with 1979, correlation value K'(φ) has been used:

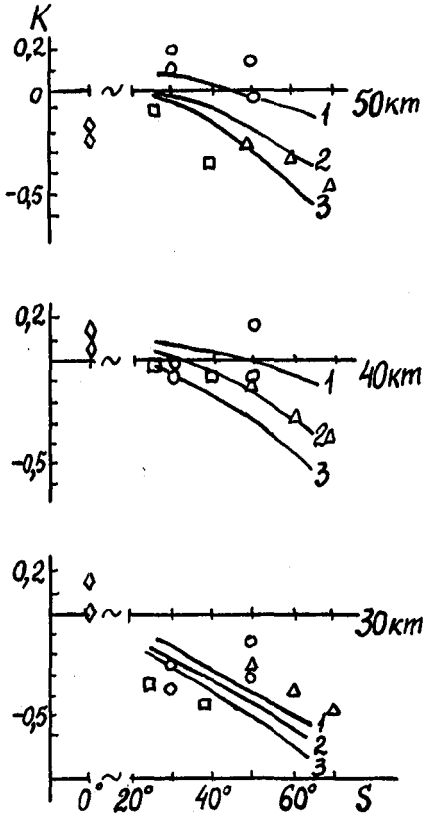

Fig.1. The relative declination of experimental and reference model data at 30, 40 and 50 km levels
for reference model data
1- March; 2- April; 3 - June
for experimental data
o - March, Δ - April, □ - june, ◊ - July

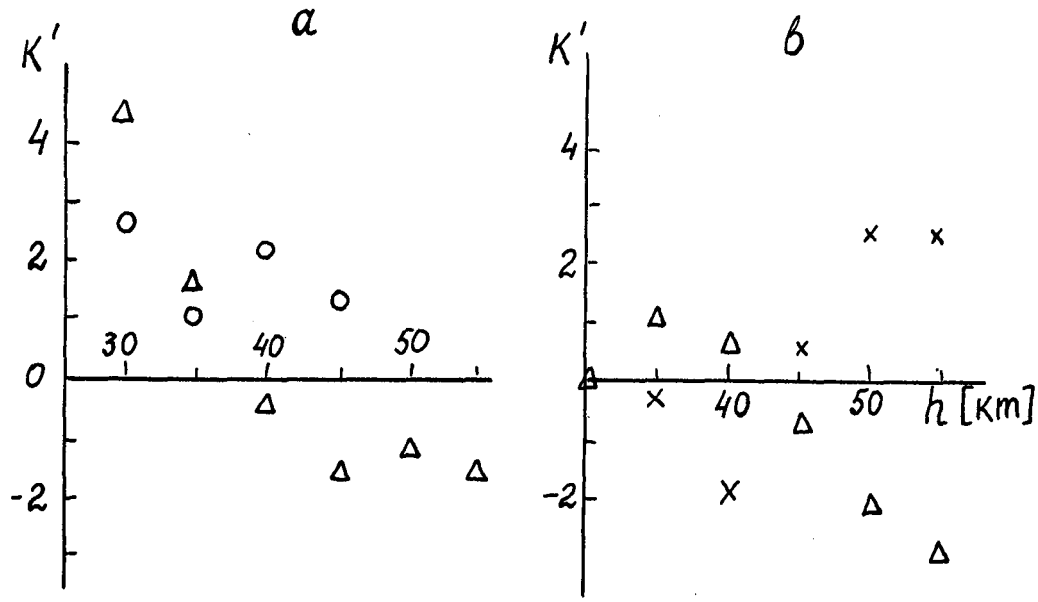

Fig.2. The declination of experimental data from reference model data
a - at 50°S - 60°S
b - at equator
Δ - 1985 data
O - data from /3/
x - 1979 data

$$K'(\varphi) = \frac{N_e(\varphi) - N_M(\varphi)}{N_m(\varphi)}$$

This value represents the relative declination of experimental data $N_e(\varphi)$ (IVANOVA and KOKIN, 1986) from reference model data $N_m(\varphi)$ (KEATING and YOUNG, 1985) at the same latitude φ. Figure 2a shows the value $K'(\varphi)$ at 50°-60°S in 1965 and 1985. The type of declination is in a good agreement in both cases: this declination has a negative value above 40-45 km and has a positive value below this altitude level.

The declination of experimental data from reference model data in 1985 at equatorial region is such as at middle latitudes, but in 1979 the value $K'(\varphi)$ sign is changed. It must be noted a minimum solar activity in 1965 and 1985, but maximum solar activity in 1979. So the increase of ozone concentration can be explained by increase of solar activity. This conclusion is confirmed by IVANOVA and KOKIN (1986).

REFERENCES

Brezgin N.I., A.F. Chizhov, et al., Rocket measurements of ozone and optical aerosol characteristic by USSR and GDR photometers in middle latitudes and tropics, Proc. 3rd Int. Symp. on Cosmic Meteorology, Gidrometeoizdat, Moscow, 1984 (in Russian).
Keating G.M., and D.F. Young, Proposed ozone reference models for the middle atmosphere, Adv. Space Res., 5, No.7, 1985.
Krueger A.I., Mean ozone distribution from several series of rocket soundings to 52 km at latitudes from 50° to 64°S, Pure Appl. Geophys., 106-108, No.5-7, 1973.
Ivanova I.N., and G.A. Kokin, Annual cycle in ozone content at latitudes of 40-50 km, Meteorol. Gidrolog. No.10, 36-43, 1986.

VARIATION OF D-REGION NITRIC-OXIDE DENSITY WITH SOLAR ACTIVITY AND SEASON AT THE DIP EQUATOR

D. K. Chakrabarty[1], S. V. Pakhomov[2] and G. Beig[1]

1 Physical Research Laboratory, Ahmedabad 380 009, India

2 Central Aerological Observatory, USSR State Committee for Hydrometeorology & Control of Natural Environment, SU-123376, Moscow, USSR.

To study the solar control on electron-density(N_e) in the equatorial D-region, a program was initiated with Soviet collaboration in 1979. Total 31 rockets were launched during the high solar activity period, 1979-80 and 47 rockets during the low solar activity period, 1984-86 from Thumba(8°N) to measure the N_e profiles. Analysis of the data shows that the average values of N_e for the high solar activity period are higher by a factor of about 2-3 compared to the low solar activity values. It has been found that a single nitric oxide density, [NO], profile cannot reproduce all the observed N_e profiles. An attempt has been made to reproduce theoretically the observed N_e profiles by introducing variation in [NO] for the different solar activity periods and seasons.

INTRODUCTION

To study the solar activity variation in electron density at the equatorial region an Indo-Soviet collaborative program was initiated in 1979. Under this program total 47 rockets of type M-100 were launched during the low solar activity period(1984-86) and 31 during high solar activity period(1979-80) from Thumba (8.5°N, 76.8°E), India to measure the electron density of the D-region. All the observations were made for solar zenith angle (χ) = 70-80°. To measure N_e a d.c. probe method was used for all the above flights. This avoided any variability due to the different measuring techniques. The details of the technique can be obtained from SINELNIKOV et al (1980). Using these profiles, firstly the empirical models of N_e for low solar activity (LSA) and high solar activity(HSA) periods have been made. An attempt has been made to reproduce them theoretically. Analysis was also done for different months and seasons. To reproduce all the observed profiles it has been found that the nitric oxide density has to be varied both with solar activity and season.

ELECTRON DENSITY MODELS

All the profiles obtained during LSA period(1984-86) and HSA period (1979-80) have been averaged separately. Averaged profiles thus obtained for LSA and HSA periods are plotted in Figure 1. These electron density data were averaged in block of 5 km for the whole altitude range from 65-90 km. The values of standard error in mean have been calculated. These are shown at some altitudes(profile 1 and 2). For the sake of comparison, the N_e profiles obtained by MECHTLY et al(1972) from a mid latitude station for low and high solar activity conditions (χ = 60°) are also shown (profiles 3 and 4). Profile 5 was obtained by Langmuir probe experiment carried out from Thumba, India for LSA- period(SUBBARAYA et al., 1983). It is clear from Figuare 1 that the averaged values of N_e for the HSA period are higher by a factor of about 2 compared to the LSA values. The present HSA values are in agreement with the values of MECHTLY et al.(1972) below 75 km, but above this altitude the present values are higher. The N_e values (LSA) of SUBBARAYA et al(1983) agree well with the present LSA values below about 75 km.

Figure 2 show the electron density profiles obtained for the month of

April during LSA and HSA periods. It is interesting to note here that like in Figure 1, N_e values in April do not show any significant variation. A plot of N_e values for a fixed height does not show any systematic variation. It indicates that the factors other that solar zenith angle also control the electron density.

RESULTS AND DISCUSSIONS

A theoretical attempt has been made to reproduce the observed average electron density profiles of Figure 1 by introducing the variation in nitric oxide density for different solar activity periods and seasons. It has been found that a single nitric oxide density profile can not reproduce the observed N_e profiles of Figure 1. The nitric oxide density profiles which reproduce the observed N_e profiles are shown in Figure 3(profiles 1 and 2). In this figure, two measurements of [NO] at Thumba, one at HSA condition (TORKAR et al, 1985) and other at LSA condition (TOHMATSU and IWAGAMI, 1976) are shown (profile 3 and 4 respectively). The mid latitude profiles of BAKER et al (1977) and MEIRA (1971) are also shown in the same figure. It is clear from this figure that the nitric oxide density values (profile 2) needed to reproduce the high solar activity profile of N_e are higher by a factor of about 5 compared to the low solar activity values (profile 1). It is also to be noticed that, in general, the present [NO] values are higher compared to the observed profiles obtained from the same location. The derived [NO] values for LSA are greater than the measured values(profile 3) by a factor of about ten. The present HSA values of [NO] are greater than the measured HSA values of TORKAR et al(1985) by a factor of about five. One can also see from this figure that the present values are much higher compared to the mid latitude values of profiles 5 and 6.

It appears from Figure 2 and 3 that besides solar activity variation there could be a seasonal variation of [NO] also. To study these aspects, N_e data were analyzed for different seasons(winter, summer, autumn, and spring) for both LSA and HSA conditions. The nitric oxide density profiles required to reproduce these electron density profiles have been derived. These are shown in Figure 4 for LSA and HSA conditions. Lower scale represents the LSA values of [NO] whereas the upper scale represents the HSA values of nitric oxide density. From Figure 4, the following interesting points emerge:-(1) [NO] values show a seasonal variation during both LSA and HSA conditions. (2) for LSA period, [NO] values are minimum in winter and maximum in spring and autumn seasons. The spring value of [NO] at 75 km are higher compared to winter value by a factor of four. (3) For HSA period, trend of nitric oxide variation is almost in opposite phase compared to LSA period below about 77 km. The [NO] value for winter season is higher by a factor of three at 75 km compared to spring value of [NO]. Above 78 km, however, the spring values of [NO] became slightly higher compared to winter and summer values. (4) Both summer and winter values of [NO] show a minimum around 80 km for HSA period. Whereas the autumn and spring values show a constant value of [NO] above about 75 km. It should be mentioned here that the autumn values are based on one month observations only. (5) The LSA values of [NO] show a broad minimum ranging from 75 to 80 km for winter. It is also clear that the minimum in winter season is at 75 km which shifts to 80 km for spring season.

CONCLUSION

Analysis of electron density data obtained by 78 rocket experiments carried out at Thumba, India during the period 1979-86 have been done. In conclusion following points are made:-

(1) The average value of N_e for HSA is found to be higher by a factor

of 2-3 compared to the LSA values. When data were analyzed for a particular month (April), the N_e variation with solar activity was found to be insignificant.

(2) The above variation in N_e has been attributed to the variation in nitric oxide density. A theoretical analysis shows that the HSA value of [NO] is higher by a factor of about five compared to LSA value.

(3) To reproduce the N_e values of different seasons, a seasonal variation in [NO] density is needed.

REFERENCES

Baker, K. D., A. F. Nagy, R. O. Olsen, E. S. Oran, J. Randhawa, D. F. Strobel and T. Tohmatsu, Measurement of the nitric oxide altitude distribution in the mid latitude mesosphere, J. Geophys. Res., 82, 3281-3286, 1977.

Mechtly, E. A., C. F. Sechrist(Jr), and L. G. Smith, Electron loss coefficients for the D-region of the ionosphere from rocket measurements during the eclipses of March 1970 and November 1966, J. Atmos. Terr. Phys., 34, 641-646, 1972

Meira, L. G., Rocket measurements of upper atmospheric nitric oxide and their consequences to the lower ionosphere, J. Geophys. Res., 76, 202-212, 1971.

Sinelnikov, V. M., G. P. Lvova, T. L. Gulyaeva, S. V. Pakhomov and A. P. Glotov, A rocket radiobeacon experiment on the electron concentration profile measurement in the bottom side of the ionosphere, Proc. satellite Beacon Symp., Warszawa, Poland, 1980.

Subbaraya, B. H., S. Prakash, S. P. Gupta, Electron Densities in the equatorial lower ionosphere from the Langmuir probe experiments conducted at Thumba during the year 1966-78, Indian Space Research Organisation, Sci. Rep. SR-15-83, 1983.

Tohmatsu, T. and N. Iwagami, Measurement of nitric oxide abundance in equatorial upper atmosphere, J. Geomag. Geoelectr., 28, 343-358, 1976.

Torkar, K. M., D. Beran, M. Friedrich and S. Lal, Measurement of nitric oxide and related parameters in the equatorial mesosphere and lower thermosphere, Planet. Space. Sci., 33, 1169-1178, 1985.

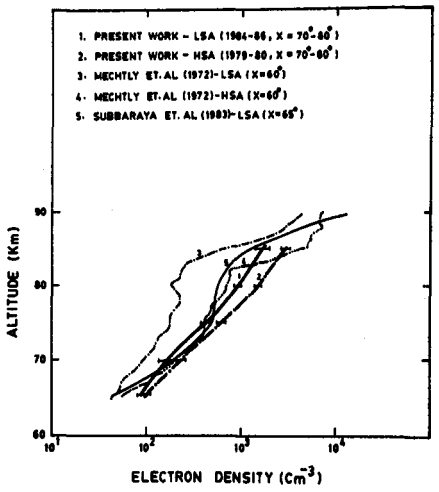

Fig.1. Empirical models of average electron density for LSA and HSA conditions obtained in the present work alongwith the profiles given by other workers.

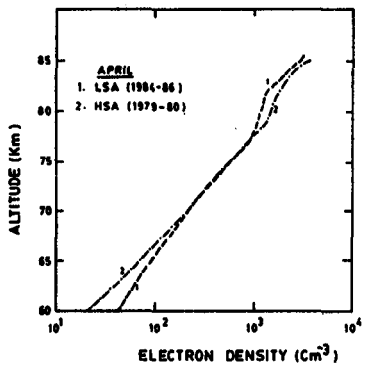

Fig.2. Empirical averaged electron density profiles for the month of April for LSA and HSA conditions.

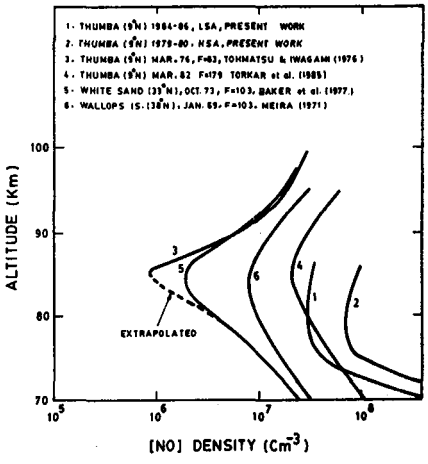

Fig.3. The nitric oxide density models obtained in the present work for LSA and HSA periods alongwith the profiles given by other workers.

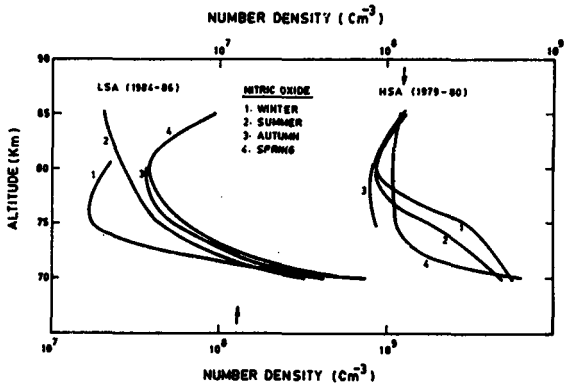

Fig.4. The nitric oxide density models derived for different seasons and solar activity periods.

DIURNAL AND TEMPORAL VARIATION OF UV-FLUX AND ITS DEPENDENCE ON STRATOSPHERIC OZONE

B. S. N. Prasad, H. B. Gayathri and B. Narasimhamurthy

Department of Studies in Physics, University of Mysore
Manasagangotri, Mysore-570 006, INDIA.

ABSTRACT

As part of Indian Middle Atmospheric Programme, global UV-B flux is measured regularly at Mysore (12°N, 76°E). The results of a preliminary analysis on the variation of UV-B flux with atmospheric ozone for the period April-May 1987 are presented in this paper.

EXPERIMENTAL SETUP

The UV-B Photometer radiometer is designed to measure the global (sum of direct and diffuse radiations) UV-B flux at four wavelengths 280, 290, 300 and 310 nm. The photometer system was designed and fabricated at the National Physical Laboratory, New Delhi. The system is made up of three units:

1. Radiometer unit consisting of an integrating sphere, filter wheel and photomultiplier (PM) tube.

2. A high voltage power supply to provide highly regulated 0-1200 VDC for operating the PM tube.

3. Data logger with printer for recording the output signal from the PM tube.

The system was calibrated using the UV-spectroradiometer model 742 of Optronics Laboratories, USA to convert the photometer output(mV) into absolute flux ($W/cm^2/nm$). Photometer filters were found to have the maximum transmission at 283, 295, 303 and 319 nm.

RESULTS

The results reported here are based on the analysis of the UV-B data collected at Mysore during the months April-May 1987. Clear sky conditions generally prevail during this period of the year. Figure 1 shows a typical diurnal variation of global UV-flux at 280 and 300 nm. The ground reaching UV-flux is maximum at local noon (approx. 1220 hrs IST). The noon solar zenith distance reaches overhead position on 23 April and changes to about 11° on 12 June. Five day running average of the noon UV-flux shows a trend which follows closely the solar altitude and exhibits a periodic behaviour (Fig. 2). Power spectral analysis of this noon UV-B shows a periodicity of 12 days. Similar periodicity seen in the trace gas mixing ratios during MAP/GLOBUS 1983 campaign has

been interpreted in terms of horizontal and vertical transport of trace gases (OFFERMAN et al. 1987).

Ozone values (DU) are measured regularly at Kodaikanal (10°N, 77°E) by the India Meteorology Department from Dobson spectrophotometer. Figure 3 shows the temporal variations of ozone and UV-B flux at 290 nm at $\chi = 60^{\circ}$. Similar trend is seen with the ozone and UV-flux at other times of the day. An examination of Fig.3 shows the well known trend in UV-B flux decrease with increase in stratospheric ozone. It is observed that a 3 percent increase in ozone results in a 35 percent decrease in the UV-B flux (global) measured at Mysore. This is much larger than the values computed theoretically (DAVE and HALPERN, 1976). Similar results have been found in the UV-B flux measurements at Delhi (SRIVASTAVA et al. 1984).

Table 1 gives the UV-B flux for April 15 and May 15 at different solar zenith angles.

Table 1: UV-B flux ($W/cm^2/nm$)

		Solar zenith angle			
λnm	Date	noon	20°	40°	60°
280	April 15	3.4(-10)	2.7(-10)	1.65(-10)	0.7(-10)
	May 15	2.3(-10)	2.15(-10)	1.2(-10)	0.52(-10)
290	April 15	1.9(-10)	9.8(-9)	5.2(-9)	2.4(-9)
	May 15	9.2(-9)	8.2(-9)	4.5(-9)	1.85(-9)
300	April 15	5.8(-7)	5(-7)	2.5(-7)	1.1(-7)
	May 15	4.6(-7)	3.9(-7)	2.0(-7)	0.84(-7)
310	April 15	5.6(-6)	4.3(-6)	2.2(-6)	1.0(-6)
	May 15	4.7(-6)	4(-6)	2.05(-6)	0.88(-6)

Read $1(-10) = 1 \times 10^{-10}$

REFERENCES

Dave, J.V. and P. Halpern, Effect of changes in ozone amount on the ultraviolet radiation received at sea level of a model atmosphere, Atmos. Environ. 10, 547-555, 1976.

Offermann, D. and H. Rippel, Disturbance of stratospheric trace gas mixing ratios during the MAP/GLOBUS 1983 Campaign, Planet, Space Sci., 35, 673-684, 1987.

Srivastava, B.N., M.C. Sharma and R.S. Tanwar, Measurement of solar ultraviolet at ground, Indian J. Radio Space Phys., 13, 103-105, 1984.

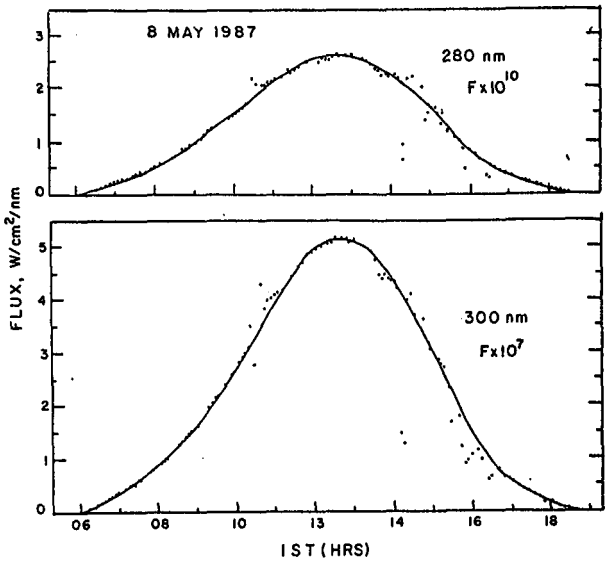

Figure 1. Diurnal variation of UV - B flux at 280 and 290 nm.

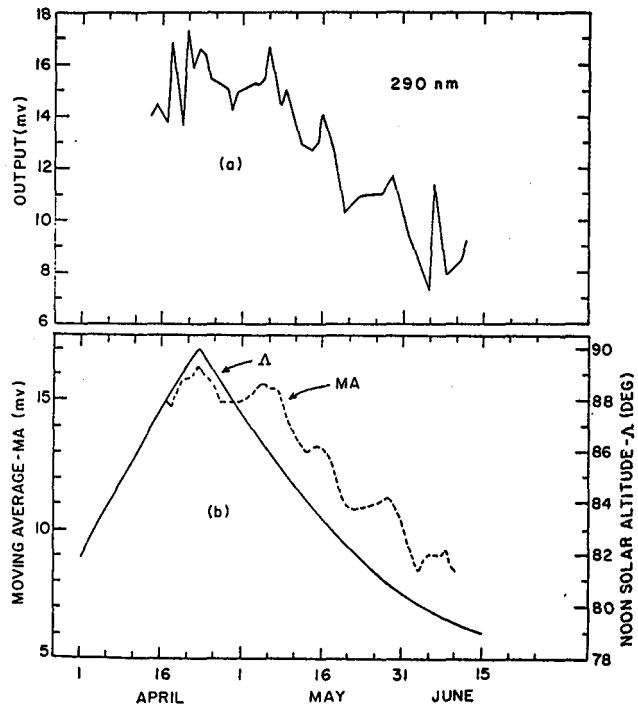

Figure 2 (a). Time series of noon UV - B flux data at 290nm.
(b). 5 day moving average (MA) of the UV - B flux and the noon solar altitude for May - June 1987.

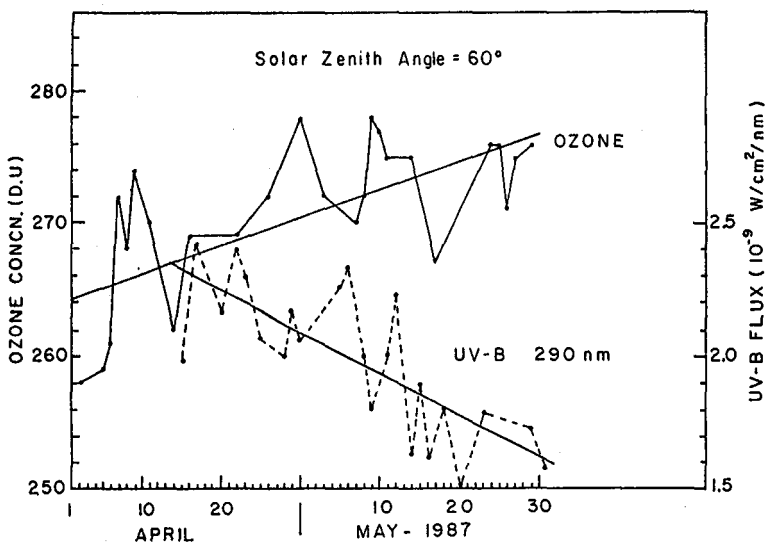

Figure 3. Temporal variation of ozone concentration and UV - B flux at 290 nm for $\chi = 60^{\circ}$.

Physical mechanisms of solar activity effects in the middle atmosphere

A. Ebel,
Institute for Geophysics and Meteorology
University of Cologne, D-5000 Cologne 41, FRG

A great variety of physical mechanisms of possibly solar-induced variations in the middle atmosphere has been discussed in the literature during the last decades. The views which have been put forward are often controversial in their physical consequences. The reason may be the complexity and non-linearity of the atmospheric response to comparatively weak forcing resulting from solar activity. Therefore this review will focus on aspects which seem to indicate non-linear processes in the development of solar-induced variations. Results from observations and numerical simulations will be discussed.

NUMERICAL SIMULATION OF THE MIDDLE ATMOSPHERE CHEMICAL COMPOSITION AND TEMPERATURE UNDER CHANGING SOLAR CONDITIONS

A.M.Zadorozhny, I.G.Dyominov, G.A.Tuchkov

Novosibirsk State University, USSR

There are given results of the numerical experiments on modelling the influence of solar activity on chemical composition and temperature of the middle atmosphere. The consideration is made for peculiarities of solar activity impact under different values of antropogenic pollution of the atmosphere with chlorofluorocarbons and other stuff.

AN INFLUENCE OF SOLAR ACTIVITY ON LATITUDINAL DISTRIBUTION OF ATMOSPHERIC OZONE AND TEMPERATURE IN 2-D RADIATIVE-PHOTOCHEMICAL MODEL

I.G.Dyominov

Novosibirsk State University, USSR

On the base of the two-dimensional radiative-photochemical model of the ozone layer at heights 0-60 km in the Northern Hemisphere there are revealed and analyzed in detail the characteristic features of the season-altitude-latitude variations of ozone and temperature due to changes of the solar flux during the 11-year cycle, electron and proton precipitations.

SOLAR WIND AND HIGH ENERGY PARTICLE EFFECTS IN THE MIDDLE ATMOSPHERE

Jan Laštovička

Geophysical Institute, Czechosl. Acad. Sci., Boční II, 141 31 Prague 4, Czechoslovakia

INTRODUCTION

The solar wind is very variable. There are many different solar wind and high-energy particle phenomena (often mutually related) and their variability, which may affect the Earth and its middle atmosphere: variability of v_{sw}; variability of the interplanetary magnetic field (IMF) B and of its components B_x (radial), B_y (azimuthal), B_z (north-south) - southward turning of B_z appears to be very geoactive; crossing the IMF sector boundary (current sheet in interplanetary space); modulation of galactic cosmic rays by solar wind and its IMF (especially Forbush decreases); relativistic electron events (REP); solar cosmic ray bursts (mainly protons with energies 100 keV - 10 GeV); highly relativistic electron events; high speed streams and shock fronts; interaction regions in solar wind; etc. The mechanisms of their effects often overlap each other.

Disturbances caused by solar wind and high energy particles have high preference to winter higher latitudes since most of the energy is focused into the auroral oval and its vicinity (higher latitudes) and because of the lack of solar UV energy (winter).

GEOMAGNETIC ACTIVITY EFFECTS

The high speed streams, shock fronts and changes in solar wind parameters (v_{sw}, B) enhance geomagnetic activity and generate magnetospheric substorms or geomagnetic storms depending on the magnitude of the solar wind energy input.

The penetration (= precipitation) of energetic particles appears to be the main factor responsible for the middle atmosphere response to geomagnetic storms. These particles consist almost exclusively of electrons (E > 20 keV) at middle latitudes. A local middle atmospheric reponse may be affected by transport from high latitudes.

The energy of the penetrating high-energy particles is lost under impact (collisions) or by X-ray bremsstrahlung production. The bremsstrahlung deposits energy at lower levels in the middle atmosphere than the impact does.

The lower ionosphere responds very dramatically to geomagnetic storms. The energy of the penetrating particles is lost, however, not only through ionization, but also through excitation, heating and dissociation processes. They result in effects of various intensities in the neutral middle atmosphere.

Excitation processes result in airglow. Auroral optical phenomena depend very much on the geomagnetic activity, of course. SHEFOV (1973) and RAPOPORT and SHEFOV (1976) found an aftereffect of the geomagnetic storm to exist in the mid- and low-latitude OH emission (night, h $\sim$ 90 km). The effect in midlatitudes begins a few days after the geomagnetic storm and may last as long as 3-4 weeks. It is an effect of transport from the auroral zone, not of local particle precipitation

(especially at low latitudes).

Any energy deposition reflects itself in temperature. Therefore, a response of the middle atmosphere temperature to geomagnetic activity is expected to exist. The results of the "Sun-Atmosphere 1969, 1971, 1976" experiments performed at Volgograd and the Heiss Island, of some soundings at the Wallops Island and of some other experiments (KOKIN and MIKHNEVICH, 1974; BUTKO et al., 1974; IVANOVA et al., 1981; RAMAKRISHNA and HEATH, 1977; TULINOV et al., 1975) show that the strongest influence of geomagnetic activity on temperature is observed at high latitudes and make it possible to suggest the following scheme of geomagnetic activity (storms) influence on temperature:

- lower thermosphere and upper mesosphere - heating;
- middle mesosphere (70 km) - opposite variation, cooling;
- lower mesosphere (60 km) - moderate heating;
- upper stratosphere - positive but not much significant correlation.

Figure 1 shows the opposite course of temperature and geomagnetic activity-related corpuscular flux as measured in October 1971 over Volgograd (BUTKO et al., 1976). Results of the same rocket flights for 60 km provide a positive correlation of temperature with geomagnetic activity-related corpuscular flux.

The geomagnetic activity also affects both boundaries of the middle atmosphere, the turbopause and the tropopause. ZIMMERMANN et al. (1982) found a strong correlation of A_p with deviations of the turbopause height h_T from the mean diurnal variation (but not with h_T itself). BROWN and GRAVELLE (1985) reported a significant increase of the tropopause temperature and a decrease of the tropopause height two days after a flare-associated high speed stream incidence on the Earth, but not after recurrent streams.

Winds in the middle atmosphere are expected to respond to geomagnetic activity. Since this topic is treated in more detail by KAZIMIROVSKY (1989), we only mention the existence of an apparent difference between North American (weaker effect) and European (stronger effect) results (LAŠTOVIČKA, 1988a).

Turbulence is another important dynamical parameter in the middle atmosphere. It is not possible to determine whether or not there is a direct relation between the energy input during geomagnetic disturbances and the turbulent state of the high latitude mesosphere (THRANE et al., 1985).

Geomagnetic activity influences the chemical composition of the middle atmosphere, particularly that of minor constituents. The most important minor constituents are O_3 (heat balance) and NO (ionization of the lower ionosphere).

Energetic particles are able to produce NO through dissociative recombination of N_2 and reaction: $N + O_2 \rightarrow NO + O$. Due to the quasi-continuous particle penetration in the auroral zone as a result of magnetospheric substorm activity, the NO concentration in the auroral lower thermosphere is 2-3 times higher than in midlatitudes, and decreases towards low latitudes. The NO concentration at higher latitudes is organized according to geomagnetic rather than geographic coordinates. Similar trends also exist in mesospheric nitric oxide. All these characteristics are confirmed by rocket and satellite observations (e.g. references summarized by RUSCH and CLANCY (1987) and LAŠTOVIČKA (1988a).

Figure 2 gives an example of latitudinal dependence of NO

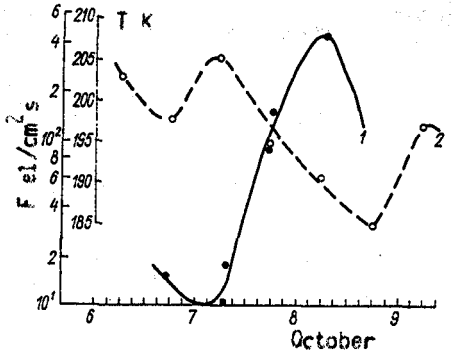

Fig. 1. The opposite course of corpuscular flux (1 - full line - electrons/cm^{2}s) and temperature (2 - dashed line - absolute temperature) on 6-9 October 1971 (BUTKO et al., 1974).

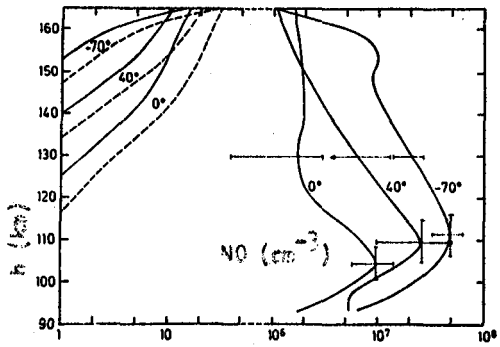

Fig. 2. Three NO-profiles averaged over 5° of latitude (GERARD and NOËL, 1986).

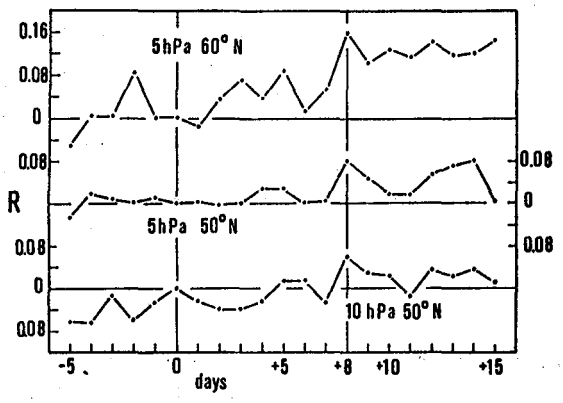

Fig. 3. Changes of stratospheric ozone mixing ratio (R -µg/g) during major geomagnetic storms (61 events, 1979-1983). 0 - day of storm maximum.

concentration in the lower thermosphere based on AE-D measurements. The NO concentration at 70°S is systematically higher than that at 40°N and the NO concentration at equator is again considerably lower.

Some results indicate an increase of NO concentration during post-storm events in middle latitudes, (MÄRCZ, 1983; SINGER et al., 1987). SINGER et al. (1987) suggest that the excess midlatitude NO is created dominantly in situ by local particle bombardment and not by transport.

Another important constituent is ozone. BEKORYUKOV et al. (1976) studied the response of total ozone to geomagnetic storms ($K_p \geq 4$, 1960-70). They found a deep narrow depression in the total ozone in the auroral zone 1 day after the onset of a geomagnetic storm. A considerably weaker but still detectable effect was observed for subauroral zone stations. BEKORYUKOV et al. (1976) try to explain the observed effects in terms of redistribution of stratospheric baric fields. On the other hand, DUHAU and FAVETTO (1989) found a positive correlation between the total ozone concetration observed at the Antarctic Syowa station (1969-85) and the geomagnetic index A_p.

Figure 3 shows our results of investigation of stratospheric ozone response to isolated and major geomagnetic storms (1979-1983). We use the SBUV Nimbus 7 ozone data at 5 and 10 hPa levels and at 40°, 50° and 60°N. Even if we use a "tolerant" criterion of statistical significance - the difference between extreme data points is statistically significant at the 0.05 confidence level - we obtained no statistically significant results for isolated storms and for major storms, 40°N 5 and 10 hPa, 60°N 10 hPa. All "statistically significant" results are given in Figure 4. The maximum is observed on the +8 day, minimum on the -5 day (-4 at 10 hPa). However, in general, we do not observe any well-pronounced effect of geomagnetic storms in the stratospheric ozone.

HIGH-ENERGY PARTICLES

We deal here with 3 types of events: variability of galactic cosmic rays, solar proton events (= solar cosmic rays = solar particle events) and relativistic electron precipitation events. They represent the high-energy part of the spectrum of energetic particles influencing the middle atmosphere. Their effects in the middle atmosphere were reviewed by THORNE (1980).

Galactic cosmic rays are responsible for the ionization of the lowest part of the lower ionosphere and of the stratosphere. They also affect the chemical composition of the middle atmosphere belonging among others to sources of odd nitrogen in the lower stratosphere (THORNE, 1980). The strongest effect in the galactic cosmic ray flux is its Forbush decrease. Some Forbush decrease effects in the mesosphere are treated by SATORI (1989).

The solar proton events (SPE) cause the polar cap absorption (PCA) events in the lower ionosphere, they produce odd nitrogen and odd hydrogen at high latitudes and, consequently, they cause some increase of the nitric oxide concentration above about 50 km and the well-known ozone depletion. The SPE effects in the middle atmosphere are treated in more detail by JACKMAN et al. (1989).

The relativistic electron precipitation (REP) events occur in auroral and subauroral latitudes. Their duration is typically

1-3 h. REP events are associated with magnetospheric substorms. They contribute to the effects of geomagnetic activity in the auroral and subauroral lower ionosphere. The REP events are considered to be the dominant in situ source of nitric oxide in subauroral latitudes in the mesosphere, being important also in the upper stratosphere (THORNE, 1980).

HIGHLY RELATIVISTIC ELECTRONS

BAKER et al. (1987) found an important role of highly relativistic electrons (2-15 MeV) in the middle atmosphere at L-shells about 3-8. Such electrons are largely absent near solar cycle maximum, while they are prominent during the approach to solar minimum. They closely parallel the presence of high-speed solar wind streams (electrons occur on their declining edges), which result from solar coronal hole structures during the approach to solar minimum. Typical rise time of events is 2-3 days with similar decay time (BAKER et al., 1987).

The energy deposition profile of these electrons is shown in Figure 4. The upper part of the "electron" curve represents impact energy deposition, the lower part the bremsstrahlung effect. The highly relativistic electrons dominate during the peak of electron precipitation event between 40-80 (35-85) km with a maximum energy deposition rate between 50-60 km.

The highly relativistic electrons produce odd nitrogen and odd hydrogen. CALLIS et al. (1988) found the production of high levels of odd nitrogen just above the stratosphere and a significant wintertime transport of this odd nitrogen to the stratosphere. This increase of odd nitrogen is expected to decrease ozone concentration. Thus highly relativistic electrons can significantly influence the strato-mesospheric chemistry.

SHELDON (1988) suggested the following chain of phenomena, which leads to the influence of highly relativistic electrons on Antarctic ozone hole formation: enhanced ionization bremstrahlung) in the stratosphere stimulates droplet formation in supersaturated air → formation of polar stratospheric clouds → low stratospheric temperature and ozone depletion.

EFFECTS OF INTERPLANETARY MAGNETIC FIELD

Another factor of solar origin is the interplanetary magnetic field (IMF). There are several possible effects of IMF: those of its components B_z, B_y and B_x, and those of the crossing of the IMF sector boundary. The effects of the changes of IMF components in the lower ionosphere (and probably in the neutral middle atmosphere, if there are any) are essentially a response to the IMF-generated changes in geomagnetic activity. The situation is not so simple, however, when the IMF sector boundary crossing (SBC) effects are considered.

There are two basic types of responses to the IMF SBC, called geomagnetic and tropospheric, both of which are observed in the lower ionosphere. They differ in morphology as well as mechanism (LAŠTOVIČKA, 1979, 1988a).

There are several factors, which make the geoactivity of IMF SBCs variable:

a) The considerable seasonal variability of the ionospheric and atmospheric responses to IMF SBCs.
b) The dependence of the amplitude of effects on the degree of disturbance before the IMF SBC.

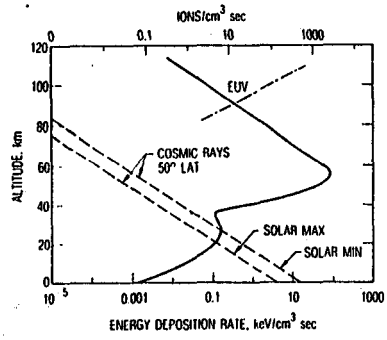

Fig. 4. Energy deposition rate profiles for highly relativistic electrons (full line - peak of an event), galactic cosmic rays and solar EUV radiation (BAKER et al., 1987).

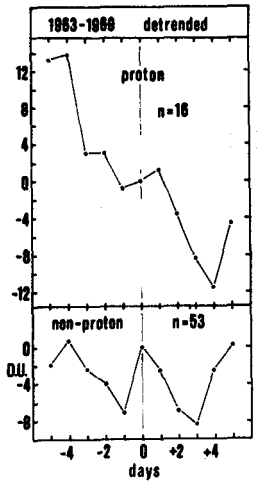

Fig. 5. The IMF SBC effect in the seasonally-detrended midlatitudinal European total ozone, winters 1963-69, for proton and non-proton sector boundaries (BREMER and LAŠTOVIČKA, 1989). Total ozone values in Dobson Units (D.U.) are expressed as a difference from the IMF SBC day value; n - number of IMF SBCs.

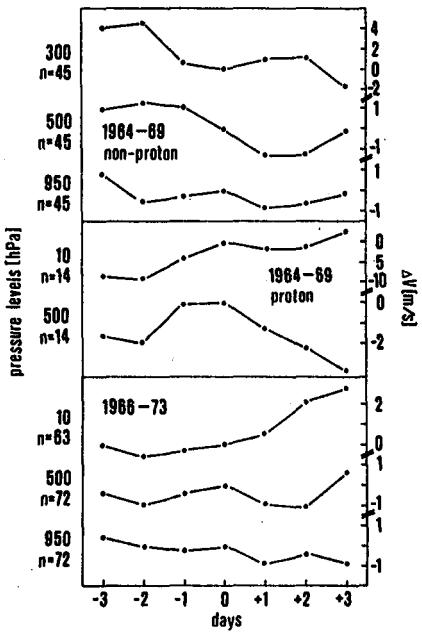

Fig. 6. The IMF SBC effect in wind speed for various pressure levels separately for proton and non-proton boundaries in 1964-69 and for all boundaries in 1966-73. $\Delta V = V - V_o$; n - number of IMF SBCs (LAŠTOVIČKA, 1988b).

c) A different effect of "pro-" and "anti-" sectors, which is important for the geomagnetic type effect.
d) Crossings of proton sector boundaries (the boundaries followed by enhanced streams of low-energy solar protons) evoke considerably stronger effects than crossings of non-proton sector boundaries.

The IMF SBC could influence the ozone concentration. The contradiction between the results of various authors concerning the IMF SBC effect in the total ozone (LAŠTOVIČKA, 1988b) was shown to be rather apparent by BREMER and LAŠTOVIČKA (1989) who found for midlatitude European stations the existence of a statistically significant effect only for proton sector boundaries while the effect of common sector boundaries was quite negligible (Figure 5).

With the use of winter data (December 1979 - December 1982) on the ozone mass mixing ratio between 40°-60°N form the SBUV experiment onboard Nimbus-7, it was found that there was no IMF SBC effect at 0.4, 1, 3 and 10 hPa levels (LAŠTOVIČKA, 1988b; LAŠTOVIČKA and GILL, 1988).

Data on temperature, wind speed and direction, and height of 7 isobaric levels between 1000-10 hPa (10, 30, 50, 100, 300, 500, 1000 or 950 hPa) above Berlin were analysed for winters 1964-73 by LAŠTOVIČKA (1988c). Figure 6 shows for wind speed all the curves, where the difference between mean maximum and mean minimum data points is statistically significant at the 0.1 level (very tolerant criterion). There is no effect in the lower stratosphere (50 and 100 hPa) and only a questionable effect in the middle stratosphere. Similar results were obtained for other parameters.

The observed IMF SBC effects are small. They are in no way a dominant channel of solar activity influence, but they are not negligible in some altitudinal regions.

We may outline the following pattern of the IMF SBC effects in winter at middle latitudes at heights of about 0-100 km (LAŠTOVIČKA, 1988b):

Lower ionosphere - two different effects, the day-time effect of the tropospheric type (quietening) and the night-time effect of the geomagnetic type (disturbance).
Lower mesosphere - no effect in ozone.
Upper stratosphere - no effect in ozone.
Middle stratosphere - no effect in ozone, wind direction and temperature; questionable (if any) effect in isobaric heights and wind speed.
Lower stratosphere - no effect in VAI, isobaric heights, temperature, wind speed and direction.
Troposphere - relatively well-developed effect in VAI and an effect in wind direction, both of the tropospheric type; questionable (if any) effects in isobaric heights, temperature and wind speed.

ENERGY BUDGET

Probably the best attempt to study the energy budget of the middle atmosphere at high latitudes was made in the Energy Budget Campaign (EBC) in Northern Europe in autumn 1980.

Table 1 shows the energy budget at 90 km for two salvoes of the EBC - salvo C (quiet conditions) and salvo A2 (fairly strong geomagnetic disturbance). Even though all the figures given in Table 1 are very rough estimates, there is no doubt that during

salvo C the atmosphere at 90 km was strongly out of balance due to the peculiar turbulent structure of that day (OFFERMANN, 1985). As to the role of energetic particles in the energy budget, Table 1 shows that it increases with increasing magnetic activity, but dynamical, photochemical and radiative mechanisms together appear to play a more important role than the particle energy deposition. Nevertheless, the variability and uncertainty of various energy sources/sinks at high latitudes is high and the question of the role of energetic particle and geomagnetic activity influence in the high-latitude middle atmosphere has not been definitely solved yet.

Table 1
Energy budget at 90 km (heating and cooling per one day) for two salvoes of the Energy Budget Campaign after OFFERMANN (1985).

Energy source/sink	salvo C (quiet)	salvo A2 (disturbed)
Particle precipitation	≤ 1 K	≤ 2.5 K
Solar irradiation	5 K	5 K
IR cooling (15 μm)	- 4 K	- 7.5 K
Wave dissipation	< 1 K	1 K
Atomic oxygen recombination	16 K	5 K
Turbulent cooling	0 K	-10 K
Sum	+ 19 K	- 4 K

BE CAREFUL

Solar wind and high energy particle effects in the middle atmosphere are not usually dominant effects and may be often overlapped and masked by other effects. One must be very careful in selecting input data for studying statistical relations between various factors. It is necessary either to eliminate other influences, or to compensate for them, or to take their effects into account when the results are interpreted. The above presented factors, which make the geoactivity of the IMF sector boundaries variable, may serve as an example.

Some corelations or effects may be considerably modulated by quite unexpected factors, as e.g. the phase of the quasi-biennial oscillation, or the role of planetary waves in the middle atmosphere response to periodic solar UV forcing. Similar factors may influence also the middle atmosphere response to solar wind and high energy particle flux variability.

CONCLUSION

The solar wind variability and high-energy particle effects in the neutral middle atmosphere are not much known. These factors are important in the high-latitude upper mesosphere-lower thermosphere energy budget. They influence temperature, composition (minor constituents - nitric oxide, ozone), circulation (wind system) and airglow. The vertical and latitudinal structures of such effects, mechanisms of downward penetration of energy and questions of energy abundance (trigger mechanisms?) are largely to be solved.

The most important recent finding seems to be the discovery of the role of highly relativistic electrons in the middle

atmosphere at L = 3 - 8 (BAKER et al., 1987).

The solar wind and high-energy particle flux variability appear to form a part of the chain of possible Sun-weather (climate) relationships. The importance of such studies in the nineties is emphasized by their role in big international programmes STEP and IGBP - Global Change.

REFERENCES

Baker, D.N., J.B. Blake, D.J. Gorney, P.R. Higbie, R.W. Klebesadel, and J.H. King, Highly relativistic magnetospheric electrons: a role in coupling to the middle atmosphere?, Geophys. Res. Lett., 10, 1027, 1987.

Bekoryukov, V.I., I.V. Bugaeva, V.S. Purgansky, A.A. Ryazanova, and V.A. Staro-dubcev, On the relation between upper atmospheric processes and solar activity. Proc. All-Union Meeting on Investigation of Dynamical Processes in the Upper Atmosphere, pp. 5-18, Gidrometeoizdat, Moscow, 1976.

Bremer J., and J. Laštovička, The IMF sector structure effects in total ozone in Central Europe, Studia Geophys. Geod., 33, 1989, (in press).

Brown, G.M., and C.A. Gravelle, Short period solar activity events and the tropopause, Paper 11.10.07, 5th Sci. Ass. IAGA/IAMAP, Prague, 1985.

Butko, A.S., I.N. Ivanova, and G.A. Kokin, Some features of thermal and circu-lation regime of the atmosphere, pp. 125-131, Solnechno-atmosfernye svyazi, Gidrometeorizdat, Leningrad (in Russian), 1974.

Callis, L.B., D.N. Baker, J.B. Blake, M. Natarajan, J.D. Lambeth, R.W. Klebe-sadel, and D.J. Gorney, Middle atmospheric production of odd nitrogen by precipitating relativistic electrons, Trans. AGU, 69, 1354, 1988.

Duhau, S., and A. Favetto, Dependence of total ozone concentration with the geo-magnetic activity, Symp. 2.8, 6th Sci. Ass. IAGA, Exeter, 1989.

Gérard, J.C., and C.E. Noël, AE-D measurements of the $_{\mp}^{5}NO$ geomagnetic latitudinal distribution and contamination by $N^{+}(^{5}S)$ emission, J. Geophys. Res., 91, 10136, 1986.

Ivanova, I.N., G.A. Kokin, Yu.N. Rybin, and K.E. Speransky, Measurements of thermodynamic and dynamic parameters of the atmosphere at quiet and disturbed periods within 27-day solar cycle, Problema solnechno-atmosfernyh svyazei, pp. 10-15, Gidrometeoizdat, Moscow (in Russian), 1981.

Jackman, C.H., A.R. Douglass, and P.E. Meade, The effects of solar particle events on the middle atmosphere, Handbook for MAP (this issue), 1989.

Kazimirovsky, E.S., Lower thermosphere (80-100 km) dynamics response to solar and geomagnetic activity, Handbook for MAP (this issue), 1989.

Kokin, G.A., and V.V. Mikhnevich, Some results of the complex experiment "Sun-Atmosphere 1971", Solnechno-atmosfernye svyazi, pp. 3-9, Gidrometeoizdat, Lenin-grad (in Russian), 1974.

Laštovička, J., Lower ionosphere, lower atmosphere and IMF sector structure in winter, J. Atmos. Terr. Phys., 41, 995, 1979.

Laštovička, J., A review of solar wind and high energy particle influence on the middle atmosphere, Ann. Geophysicae, 6, 401, 1988a.

Laštovička, J., The IMF sector boundary effects in the middle

atmosphere, Adv. Space Res., 8, No. 7, 201, 1988b.
Laštovička, J., The sector boundary of the interplanetary magnetic field and the troposphere and stratosphere above Berlin, Z. Meteorol., 38, 114, 1988c.
Laštovička, J., and M. Gil, Stratospheric ozone variability near the IMF sector boundary, Studia Geophys. Geod., 32, 313, 1988.
Märcz, F., Increased NO concentration contributing to the enhancement of radio wave absorption following geomagnetic storms, J. Geophys., 54, 68, 1983.
Offermann, D., The Energy Budget Campaign 1980: Introductory review, J. Atmos. Terr. Phys., 47, 1985.
Ramakrishna, S., and D.F. Heath, Temperature changes associated with geomagnetic activity at Wallops Island, Trans. AGU, 58, 696, 1977.
Rapoport, Z.C., and N.N. Shefov, Comparison of disturbed variations of OH emission and radio wave absorption, Issl. izlucheniya verhnei atmosfery, pp. 12-16, Ylym, Ashkhabad (in Russian), 1976.
Rusch, D.W., and R.T. Clancy, Minor constituents in the upper stratosphere and mesosphere, Rev. Geophys., 25, 479, 1987.
Sátori, G., Electron density profiles in the background of LF absorption during Forbush-decrease and PSE, Handbook for MAP (this issue), 1989.
Shefov, N.N., Behaviour of OH emission during solar cycle, seasons and geomagne-tic disturbances, Polyarnye siyaniya i svechenie nochnogo neba, 20, 23, Nauka, Moscow (in Russian), 1973.
Sheldon, W.R., Electron precipitation, polar stratospheric clouds, and the Antarctic ozone, Trans. AGU, 69, 1389, 1988.
Singer, W., J. Bremer, P. Hoffmann, and J. Taubenheim, Variability of lower ionosphere electron density profiles measured by partial-reflection sounding at midlatitude, Gerl. Beitr. Geophys., 96, 352, 1987.
Thorne, R.M., The importance of energetic particle precipitation on the chemical composition of the middle atmosphere, Pure Appl. Geophys., 118, 128, 1980.
Thrane, E.V., O. Andreassen, T. Blix, B. Grandal, A. Brekke, C.R. Philbrick, F.J. Schmidlin, H.U. Widdel, U. von Zahn, and F.J. Lübken, Neutral air turbulence in the upper atmosphere observed during the Energy Budget Campaign, J. Atmos. Terr. Phys., 47, 243, 1985.
Tulinov, V.F., L.S. Novikov, and V.V. Tulyakov, Corpuscular radiation in the upper atmosphere at altitudes up to 100 km above the Heiss Island, Kosm. Issled., 13, 937 (in Russian), 1975.
Zimmermann, S.P., T.J. Keneshea, and C.R. Philbrick, Diurnal solar cycle and magnetic index relations to turbopause height, Paper STP.IV.1.1, 5th Int. Symp. on Solar-Terrestrial Physics, Ottawa, 1982.

THE EFFECTS OF SOLAR PARTICLE EVENTS ON THE MIDDLE ATMOSPHERE

Charles H. Jackman and Anne R. Douglass[1]

Laboratory for Atmospheres
Code 616
NASA/Goddard Space Flight Center
Greenbelt, MD 20771
U. S. A.

Paul E. Meade

Department of Astrophysical, Planetary, and Atmospheric Sciences
University of Colorado
Boulder, CO 80309
U. S. A.

INTRODUCTION

Solar particle events (SPEs) have been investigated since the late 1960's for possible effects on the middle atmosphere. Solar protons from SPEs produce ionizations, dissociations, dissociative ionizations, and excitations in the middle atmosphere. Either directly or through a photochemical sequence both HO_x (H, OH, HO_2) and NO_x (N, NO, NO_2) are produced as well. These HO_x and NO_x constituents are important because they can lead to the destruction of ozone. Most of these investigations have been primarily focused on the effects of SPEs on ozone, however, a few have been related to the effects of SPEs on odd nitrogen (N, NO, NO_2, NO_3, N_2O_5, HNO_3, HO_2NO_2, and $ClONO_2$) constituents.

The SPEs are good tests for model validation because the large perturbations to the atmosphere associated with SPEs are confined to high latitudes, last only for days to months, and are easily distinguished in satellite data. This allows the comparison of measurements with a wide variety of models, ranging from simple point models to two-dimensional models.

Ozone depletions have been observed during and after nine separate SPEs over the past two solar cycles (HEATH et al. 1977; MCPETERS et al. 1981; THOMAS et al. 1983; SOLOMON et al. 1983; MCPETERS and JACKMAN, 1985). SPEs have also been observed to increase NO during one SPE (MCPETERS, 1986).

The production of HO_x and NO_x and their subsequent effects on ozone can also be computed using energy deposition and photochemical models. We discuss the effects of SPE-produced NO_x species on the odd nitrogen (NO_y) abundance of the middle atmosphere as well as the SPE-produced long-term effects on ozone. The influence of HO_x species on ozone has been discussed in other papers (e.g., SOLOMON et al. 1981; JACKMAN and MCPETERS, 1985) and will not be repeated here.

ODD NITROGEN (NO_y) VARIANCE DUE TO SPEs

The production of NO_y species by SPEs has been predicted since the mid 1970's (CRUTZEN et al. 1975). Recently, a satellite measurement (MCPETERS, 1986) was made of the NO increase after a major SPE (July 1982). This measured NO increase was in good agreement with our predicted NO increase, computed

[1]Universities Space Research Association Resident Associate

assuming 1.25 nitrogen (N) atoms produced per ion pair (PORTER et al. 1976). The agreement between the predicted and measured NO increase has given us confidence in the reliability of the computations for NO_y species' increase caused by SPEs.

A dataset of proton fluxes has become available from Thomas Armstrong and colleagues (University of Kansas) which allows for a daily computation of ion pair production and, subsequently, NO_y production due to SPEs. The proton fluxes are given in integral form for energies greater than 10 MeV, 30 MeV, and 60 MeV. The data are available for the time period 1963 through 1985. We have used those data in a manner similar to that discussed in JACKMAN and MEADE (1988) and compute a daily ion pair production over the 23 year time period in a form suitable for inclusion in our model.

The ion pair production computed with the use of the daily average proton flux data of T. Armstrong compares favorably with the ion pair production computed using the hourly average proton flux data found in the Solar Geophysical Data publication for most SPEs. However for the August 1972 SPE, the ratio of the hourly computed ion pair production to the daily computed ion pair production ranges from about 3.7 in the stratosphere to near 1.0 in the mesosphere. We have normalized the daily to the hourly computed ion pair production for this one SPE only for two reasons: 1) the hourly computed ion pair production is believed to be more accurate than the daily computed ion pair production and 2) the August 1972 SPE is the most important SPE in the last two solar cycles for its effects on the middle atmosphere.

The ion pair production was input into our two-dimensional photochemical model (DOUGLASS et al. 1989) whose vertical range has been extended to be from the ground to about 90 km with about a 2 km grid spacing and from -85°S to 85°N with a 10° grid spacing. It was assumed that 1.25 N atoms are produced per ion pair in this model computation. The SPE production of N atoms was only input at geomagnetic latitudes above 60° (see JACKMAN and MEADE, 1988, for an explanation).

The two-dimensional model was run to an annual equilibrium condition in which the seasonal values of constituents repeat yearly. The model was then run for 23 years from 1963 through 1985 and investigated for changes. For all model runs in this investigation the ultraviolet flux was not allowed to vary with the solar cycle.

Figure 1a illustrates the variability of NO_y at 1.7 mb (44 km) and 75°N over the 23 year period. Note that NO_y can vary dramatically after an SPE, especially after the August 1972 SPE, but the NO_y values generally return to their ambient levels 2 to 6 months after the event. The NO_y seems to be affected only by those SPEs which have an ion pair production over about 100 ion pairs (cm^{-3} sec^{-1}). This is not a strict rule as the time of year and, therefore, the ambient NO_y amount help determine the magnitude of the NO_y change at a certain level (see JACKMAN and MEADE 1988 for further discussion). Some downflux of NO_y from the SPE's mesospheric production of NO_y is also associated with the SPEs and is important during certain seasons (late fall, winter, and early spring). This downflux can also influence the amount of NO_y in the upper stratosphere.

Figure 1a, as well as our analysis of NO_y at other altitudes and latitudes, indicate that the NO_y produced by SPEs over solar cycle time periods does not build up, but can be important at high latitudes on seasonal time-scales. This result is not surprizing given the small fraction of the annual odd nitrogen budget that was computed by JACKMAN et al. (1980) to result from SPEs. The majority of the annual production of odd nitrogen is a result of nitrous oxide oxidation and was recently computed (JACKMAN et al. 1987) to be 2.7×10^{34} NO molecules per year. The largest production of NO molecules from SPEs was in the

year 1972 at the level of 6.4 X 10^{33} NO molecules per year, only 24% of the nitrous oxide source. The production of NO molecules from SPEs in other major SPE-active years is typically half or less than that computed for 1972.

LONG-TERM OZONE VARIANCE DUE TO SPEs

Figure 1b illustrates the variability of ozone at 1.7 mb (44 km) and 75°N over the 23 year period. The ozone decreases are directly correlated with the NO_y increases presented in Figure 1a.

The percentage change in modeled ozone as a result of the August 1972 SPE is given in Figure 2 at two latitudes. The latitudes in the Northern Hemisphere (N.H) at 75°N (Figure 2a) and 55°N (Figure 2b) indicate a larger ozone depletion at 75°N than at 55°N. Other latitudes investigated from our model results show a similar behavior with the larger ozone depletions being associated with the higher latitudes. This behavior was also observed in the BUV ozone data (JACKMAN and MCPETERS, 1987). The magnitude of the depletion observed in the BUV dataset was similar to that predicted by the model computation. For example, about a 15-25% maximum ozone depletion was observed between 70° and 80°N and about a 5-15% maximum ozone depletion was observed between 50° and 60°N.

Our model results at 55°S (not shown) indicates over a 20% ozone depletion, but the model at 55°N indicates a 5-10% depletion in the time period 20 to 60 days after the SPE, implying a large hemispheric difference in the level of ozone depletion. MAEDA and HEATH (1980/81) showed that the S.H. did experience a larger ozone loss than did the N.H. SPE-produced NO_y in winter has a far greater effect on ambient NO_y amounts and, therefore, on ozone levels than does SPE-produced NO_y in summer (see JACKMAN and MEADE, 1988, for more discussion on SPE effects on NO_y amounts).

DISCUSSION AND CONCLUSIONS

Model computations indicate fairly good agreement with ozone data for the SPE-induced ozone depletion caused by NO_y species connected with the August 1972 SPE. Future studies should include a more detailed intercomparison of the ozone behavior with altitude, latitude, and time. It would also be useful to compare these detailed studies with another large SPE, perhaps one that occurs during the current solar active period. Since NO_y constituents are responsible for over 70% of the ozone loss in the stratosphere (JACKMAN et al. 1986), it is useful to validate the NO_y photochemistry which is used in atmospheric models to predict ozone amounts.

Our model computations indicate that NO_y will not be substantially changed over a solar cycle by SPEs. The changes are mainly at high latitudes and are on time scales of several months, after which the NO_y drifts back to its ambient levels.

ACKNOWLEDGEMENTS

The authors would like to thank Thomas R. Armstrong (University of Kansas) for sending solar proton data that was used in the ion pair production computations for this paper. We would also like to acknowledge Sushil Chandra of NASA Goddard Space Flight Center for useful comments on an earlier version of this manuscript.

REFERENCES

Crutzen, P. J., I. S. A. Isaksen, and G. C. Reid, Solar proton events: Stratospheric sources of nitric oxide, Science, 189, 457-458, 1975.

Douglass, A. R., C. H. Jackman, and R. S. Stolarski, Comparison of model results transporting the odd nitrogen family with results transporting separate odd nitrogen species, in press, J. Geophys. Res., 1989.

Heath, D. F., A. J. Krueger, and P. J. Crutzen, Solar proton event: Influence on stratospheric ozone, Science, 197, 886-889, 1977.

Jackman, C. H., and R. D. McPeters, The response of ozone to solar proton events during solar cycle 21: A theoretical interpretation, J. Geophys. Res., 90, 7955-7966, 1985.

Jackman, C. H., and R. D. McPeters, Solar proton events as tests for the fidelity of middle atmosphere models, Physica Scripta, T18, 309-316, 1987.

Jackman, C. H., and P. E. Meade, Effect of solar proton events in 1978 and 1979 on the odd nitrogen abundance in the middle atmosphere, J. Geophys. Res., 93, 7084-7090, 1988.

Jackman, C. H., J. E. Frederick, and R. S. Stolarski, Production of odd nitrogen in the stratosphere and mesosphere: An intercomparison of source strengths, J. Geophys. Res., 85, 7495-7505, 1980.

Jackman, C. H., R. S. Stolarski, and J. A. Kaye, Two-dimensional monthly average ozone balance from limb infrared monitor of the stratosphere and stratospheric and mesospheric sounder data, J. Geophys. Res., 91, 1103-1116, 1986.

Jackman, C. H., P. D. Guthrie, and J. A. Kaye, An intercomparison of nitrogen-containing species in Nimbus 7 LIMS and SAMS data, J. Geophys. Res., 92, 995-1008, 1987.

Maeda, K., and D. F. Heath, Stratospheric ozone response to a solar proton event: Hemispheric asymmetries, Pageoph., 119, 1-8, 1980/81.

McPeters, R. D., A nitric oxide increase observed following the July 1982 solar proton event, Geophys. Res. Lett., 13, 667-670, 1986.

McPeters, R. D., and C. H. Jackman, The response of ozone to solar proton events during solar cycle 21: The observations, J. Geophys. Res., 90, 7945-7954, 1985.

McPeters, R. D., C. H. Jackman, and E. G. Stassinopoulos, Observations of ozone depletion associated with solar proton events, J. Geophys. Res., 86, 12,071-12,081, 1981.

Porter, H. S., C. H. Jackman, and A. E. S. Green, Efficiencies for production of atomic nitrogen and oxygen by relativistic proton impact in air, J. Chem. Phys., 65, 154-167, 1976.

Solomon, S., D. W. Rusch, J.-C. Gerard, G. C. Reid, and P. J. Crutzen, The effect of particle precipitation events on the neutral and ion chemistry of the middle atmosphere, 2, Odd hydrogen, Planet. Space Sci., 29, 885-892, 1981.

Solomon, S., G. C. Reid, D. W. Rusch, and R. J. Thomas, Mesospheric ozone depletion during solar proton events, paper presented at the Sixth ESA-PAC Meeting, Eur. Space Agency, Interlaken, Switzerland, April 12-19, 1983.

Thomas, R. J., C. A. Barth, G. J. Rottman, D. W. Rusch, G. H. Mount, G. M. Lawrence, R. W. Sanders, G. E. Thomas, and L. E. Clemens, Mesospheric ozone depletion during the solar proton event of July 13, 1982, 1, Measurement, Geophys. Res. Lett., 10, 253-255, 1983.

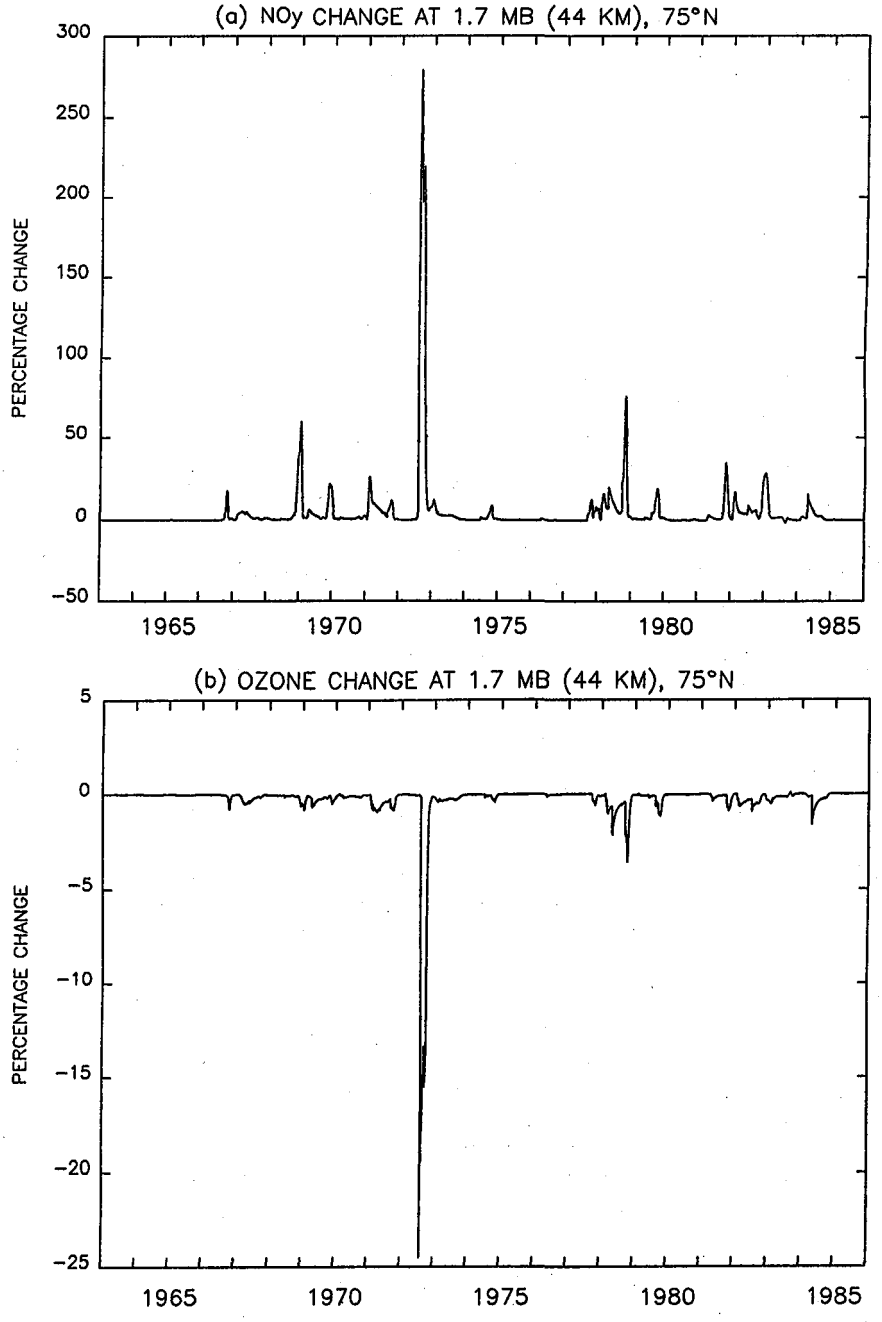

Figure 1. (a) Model predicted NO_y percentage change at 1.7 mb (44 km) and 75°N. (b) Model predicted ozone percentage change at 1.7 mb (44 km) and 75°N.

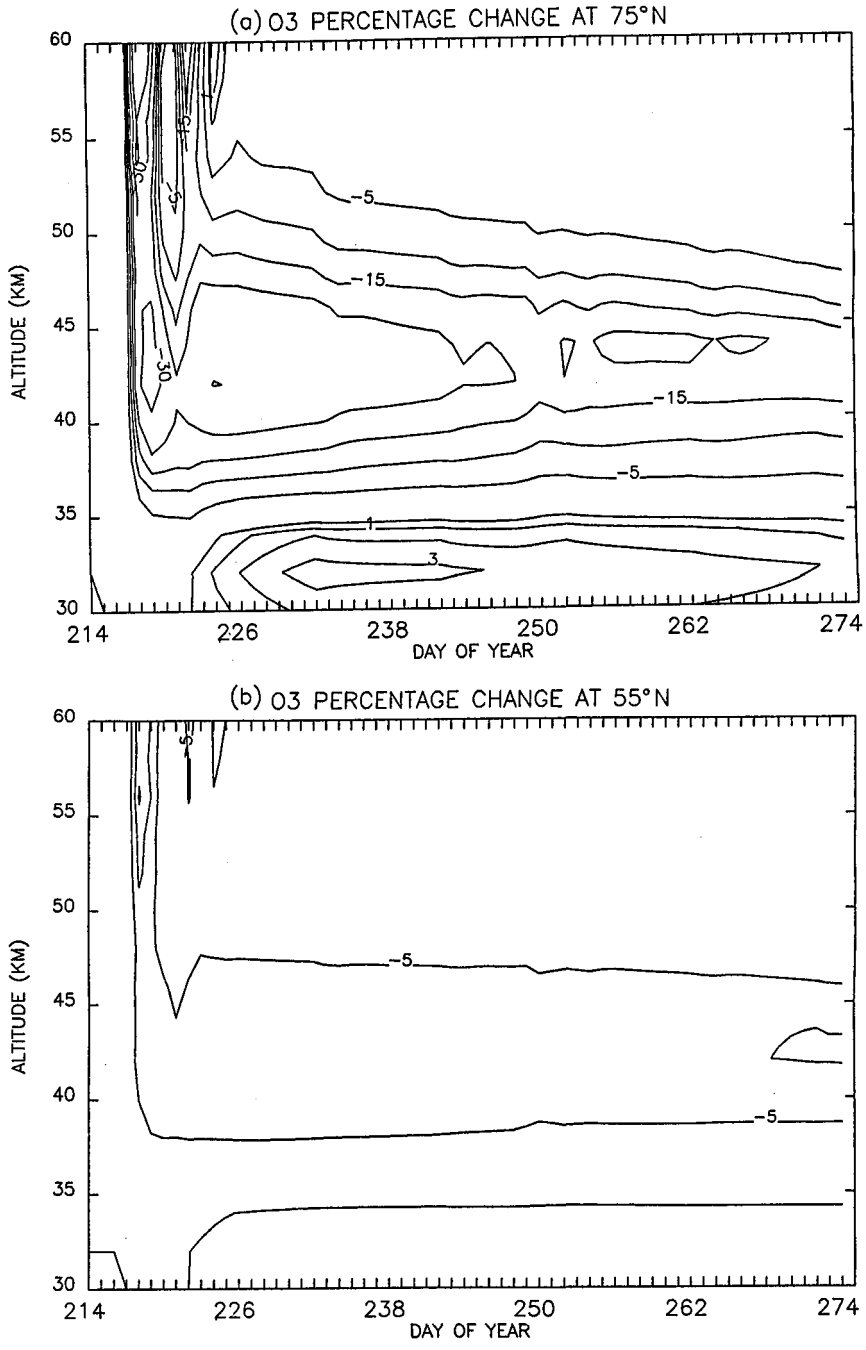

Figure 2. Model predicted ozone percentage change as a function of day of year in 1972 for (a) 75°N and (b) 55°N. The ozone change is a result of the August 1972 SPE and is given at the contour levels of -40, -30, -20, -15, -10, -5, 0, +1, +2, and +3%.

ENERGY DEPOSITION OF CORPUSCULAR RADIATION IN THE MIDDLE ATMOSPHERE

K. Kudela

Inst. Exp. Physics, Slovak Acad. Sci., Košice, Czechoslovakia

INTRODUCTION

Main components of corpuscular radiation contributing to energy deposition (ED in eV $cm^{-3}s^{-1}$) in the atmosphere (10-100 km) are cosmic ray nuclei (CR - galactic and solar) and high energy electrons (HEE), mainly of magnetospheric origin.

COSMIC RAY INTERACTION IN ATMOSPHERE

Two types of interactions with nuclei of air constituents are important: inelastic nuclear interactions and Coulomb collisions. Figure 1 shows the energy losses dE/dx, range h (in height scale) and probability of inelastic nuclear interaction for proton in air (nuclear data from JANNI, 1982).

Nuclear interactions lead to the decrease of initial CR flux due to fragmentation of nuclei and to the creation of "new" corpuscular particles and electromagnetic radiation. Above 50 km ($\sim$ 1 g cm^{-2}) less than 0.2 % protons, 5 % He and 20% of Fe nuclei had their first nuclear interaction. This fraction increases with decrease of h, and below $\sim$ 50 km nuclear interactions must be included for ED calculations.

Relations between the parent CR nuclei and their secondary products, which again undergo nuclear interactions, coulomb collisions and decay, are complicated. In DATTA et al. (1987) it is recognized that gamma rays constitute the resultant component from different decay channels. From the knowledge of γ-ray profile and absorption coefficient of γ-rays in atmosphere, the ion production rate (PR = ED/35(eV)) was predicted which for middle latitude gave good agreement with direct PR measurement below 20 km. Figure 2 illustrates profile of PR down to 10 km. For low latitudes the main sources of PR variability are atmospheric density variations (e.g. seasonal).

The coulomb collisions of CR nuclei in atmosphere lead to direct ionization. The mean relative ionization energy loss, dE/dx, is given by Bethe-Bloch formula (BBF). VELINOV et al. (1974) used BBF for PR computations of CR above 50 km where coulomb collisions are dominant. Figure 3 shows profiles of PR. Due to Z^2 dependence in dE/dx, heavy CR nuclei contribute significantly to the total PR by ionization: CR protons being 86% of CR population give 30% of PR while nuclei Z $\geq$6 (only 1.15% of CR) give 51.5% of total production. For estimation of PR by CR Figure 1 may be used.

Three main factors control the ED of CR (not assuming meteorological variations): geomagnetic filter, modulation effects of CR in heliosphere and solar CR impact.

First of them leads to the latitudinal (λ_m) variations of ED profiles. In real magnetic field, according to trajectory calcu-

lation, the approximation $R = 16.237\ L^{-2.0959}$, L being McIlwan's parameter and R_c - rigidity of particle (R = p/Ze), gives realistic estimate of vertical effective cut-off rigidity (SHEA et al., 1987). This approach does not include fine structure of forbidden and allowed trajectories around R_c and non-vertical directions. R_c is changing during geomagnetic storms. The approach to this problem is in (FLUCKIGER et al., 1986). The simplified estimates for D_{st} = 200 nT give for λ_m = 55° variation in PR $\delta q/q \simeq 50\%$ and for λ_m^{st} = 40° $\delta q/q$ = 20-25 %.

Modulation of CR in solar cycle is the cause of ED variations by CR at higher latitudes. Charge state of anomalous CR oxygen (up to 30 MeV/n) is now established to be O^{+1} (McDONALD et al., 1988); BISWAS et al., 1988), thus its rigidity is rather high. At $\lambda_m \simeq 44°$ the PR at h ≥ 50 km may be affected by this CR component being strongly dependent on solar-cycle phase. These ions can be stripped by residual atmosphere and become stably trapped (BLAKE, 1988).

Variety of solar flare particle energy spectra, composition, angular distribution and temporal profile near the Earth may lead to changes in ED of CR at higher latitudes, which could be significant for 40-90 km.

HIGH ENERGY ELECTRON DEPOSITION

For electrons both angular scattering and energy losses should be included in calculation of ED in atmosphere (WALT, 1968). Scattering on orbital electrons is small in comparison with that on the nucleus, however interactions with orbital electrons are important for energy losses. The angular diffusion leads to large straggling of penetration depth reached by individual electrons. Calculation of electron ED is possible only by numerical methods. For estimation Figure 4 show dependence of stopping-power (both collision - ionization S_{col}, and radiative S_{rad}) and range for electrons h (taken from BERGER and SELTZER, 1983). The concept of range for electron is different from that of protons and it can be used only for rough estimates. The relative fraction of radiative losses increases with energy (bremsstrahlung - BS). BS photons deposite the energy by photoeffect and Compton scattering. For spectra $\alpha^{-1}\exp(-E/\alpha)$, the altitude profile of ED in atmosphere is on Figure 5 (taken from BERGER et al.,1974). ED by monoenergetic electrons was examined in (REES, 1963) giving estimate that only E_e > 30 keV are important below 100 km.

BS of electrons, treated theoretically in (WALT et al., 1979; SELTZER and BERGER, 1974), is used for remote sensing of electron precipitation from satellites (IMHOF, 1981, IMHOF et al., 1982a, IMHOF et al, 1982b), local measurements of balloons (MATTHAEUS et al., 1988) and rockets (SHELDON et al., 1988).

VAMPOLA and GORNEY (1983) used spectra of locally precipitating electrons 36-317 keV to calculate ED profiles. Power-law approximation in spectra yields in two maxima: the main at 70-90 km, where ED is comparable with ED by solar Hα on day side while on night side the ionization by electrons is dominating, and secondary peak ∼40 km due to BS. During meagnetospheric substorms the electron precipitation pattern is drastically changing both temporally and in local time (e.g. GOTSELYUK et al., 1986; GOTSELYUK et al., 1988). Global distribution of electrons E > 30 keV at

low altitudes revealed connection of additional precipitation zones with man-made activity (GRIGORYAN et al., 1981). Detailed global distribution of HEE was studied on OHZORA satellite (NAGATA et al., 1987).

Measurements with good energy resolution showed the "finer structure" of electron precipitation. Preferentially on the night side, electrons with hard spectra (α = 500 keV) precipitate in narrow range of L near plasmapause contributing thus significantly to ED at 70-90 km (IMHOF et al.,1986). Electron spectra in inner belt (L = 1.2 - 2.0) exhibit strong peaks at 50-500 keV (DATLOWE et al., 1985). Thus profile of ED in middle atmosphere, especially in south atlantic anomaly (SAA), could have complicated form.

Narrow peaks in precipitating electron spectra 68-1120 keV within drift-loss cone produced by VLF transmitters in inner zone are reported in (IMHOF, 1981b). Similar conclusion in 36-317 keV at outer edge of inner zone is in (VAMPOLA, 1983). Later study (VAMPOLA and ADAMS, 1988) revealed importance of VLF transmitters for HEE precipitation in inner zone, in the slot and outer zone. Theoretical approach assuming gyroresonant pitch-angle scattering of electrons with waves both near equator as well as at low altitudes is well developed now (INAN, 1987; NEUBERT et al., 1987). An attempt to measure stimulated precipitation of HEE by powerful LF wave emitted from satellite is one of the objectives for Aktivny satellite-subsatellite experiment (SCHEVCHENKO, 1988; TŘÍSKA et al, 1988). Resonance conditions of measured electrons (20-600 keV) give for f = 10 kHz the possible precipitation at L < 3 within the drift loss cone near the bounce loss cone boundary (KUDELA, 1989).

Trapped electrons at geostationary orbit up to E > 10 MeV are present and their intensity is associated with solar cycle activity (BAKER et al., 1986). While auroral electron precipitation is located in narrow interval (around λ_m = 70°) and may cause ED increase above 100 km, very HEE can deposite energy at lower heights and in broad latitude range. BAKER et al. (1987) found significant enhancement of PR at 40-80 km, well above both CR and extreme UV ED. This electron population could be important in coupling SW-magnetosphere variability to the middle atmosphere. Compilation of PR in middle atmosphere by different measurements is presented on Figure 6.

In SAA electrons even with higher energies (E > 100 MeV), apparently not connected with above population, have significant flux (GUSEV et al., 1983) and can conttribute to PR below 40 km. Radiative losses are important for them, too. Penetration of electrons from interplanetary space to high latitudes was studied by McDIARMID et al., (1975) and such HEE were used as a sounding tool for magnetospheric boundary changes and their connection with IMF and SW parameters (KUZNETSOV et al, 1987; KUZNETSOV et al, 1988). Their latitudinal extent is in some cases down to λ_m = 62° and their flux (10^5 $cm^{-2}s^{-1}ster^{-1}$ for E > 30 keV) could contribute to enhanced PR at 90 km.

SUMMARY

Galactic CR depending on solar-cycle phase and latitude are dominant source of ED by corpuscular radiation below 50-60 km. Below 20 km secondaries must be assumed. More accurate treatment

need assuming of individual HE solar flare particles, cut-off rigidities in geomagnetic field and their changes during magnetospheric disturbances.

Electrons E_e > 30 keV of magnetospheric origin penetrating to atmosphere contribute to PR below 100 km especially on night side. High temporal variability, local-time dependence and complicated energy spectra lead to complicated structure of electron ED rate. Electrons of MeV energy found at geostationary orbit, pronouncing relation to solar and geomagnetic activity, cause maximum ED at 40-60 km.

Monitoring the global distribution of ED by corpuscular radiation in middle atmosphere need continuing low altitude satellite measurements of both HEE and X-ray BS from atmosphere as well as measurements of energy spectra and charge composition of HE solar flare particles.

REFERENCES

D.N. Baker et al., J.Geophys.Res. 91, A4, 4265 (1986).
D.N. Baker et al, Geophys.Res.Lett. 14, 10, 1027 (1987).
M.J. Berger, S.M. Seltzer, K. Maeda, J.Atmos.Terr.Phys. 36, 591 (1974).
M.J. Berger, S.M. Seltzer, Stopping powers and ranges of electrons and positrons (2nd edition), NBSIR 82-2550-A, February 1983, 173.
S. Biswas et al., Astrophysics and Space Science 149, 357 (1988).
B. Blake, COSPAR XXVII, Espoo, Finland 1988, p.11.4.5, Abstract, p.153.
D.W. Datlowe et al., J.Geophys.Res. 90, A9, 8333 (1985).
J. Datta, S.C. Chakravarty, A.P. Mitra, Indian J.Radio & Space Physics 16, June 1987, p.257.
E.O. Flckiger, D.F. Smart, M.A. Shea, J.Geophys.Res. 91, A7, p.7925 (1986).
Yu.V. Gotselyuk et al., Studia geoph. et geod. 30, 79 (1986).
Yu.V. Gotselyuk et al., Studia geoph. et geod. 32, 187 (1988).
O.R. Grigoriyan et al, Kosm. issled., XIX, 559 (1981).
A.A. Gusev et al, Proc. 18th ICRC, Bangalore, India 1983, MG10-34.
W.L. Imhof, Space Science Reviews 29, 201 (1981a).
W.L. Imhof et al., J.Geophys.Res. 86, A13, 11225 (1981b).
W.L. Imhof et al., J.Geophys.Res. 87, A2, 671 (1982a).
W.L. Imhof et al., J.Geophys.Res. 87, A10, 8149 (1982b).
W.L. Imhof et al., J.Geophys.Res. 91, A3, 3077 (1986).
U.S. Inan, J.Geophys.Res. 92, A1, 127 (1987).
J.F. Janni, Atomic Data and Nuclear Data Tables, vl. 27, No. 2/3, March/May 1982, Academic Press, N.York, part 2.
K. Kudela, abstract on URSI Conf. on Wave Induced Particle Precipitation and Wave Particle Interactions, Dunedin, N.Z. Febr. 1989.
S.N. Kuznecov et al., Bull.Astron.Inst.Czech. 38, 276 (1987).
S.N. Kuznecov et al., Physica scripta 34, 161 (1988).
D.L. Matthews, J.Geophys.Res. 93,A11, 12941 (1988).
I.B. McDiarmid et al., Geophys.Res. 80, 73 (1975).
F.B. McDonald et al, The Astrophys.J. 333, L109, October 1988.
K. Nagata et al., ISAS Report RN 358, Tokyo, Japan, pp. 20 (1987).
T. Neubert et al., J.Geophys.Res. 92, A1, 255 (1987).
M.H. Rees, Planet Space Sci. 11, 1209 (1963).
S.M. Seltzer, M.J. Berger, J.Atmos.Terr.Phys. 36, 1283 (1974).

M.A. Shea, D.F. Smart, L.C. Gentile, Physics of the Earth and Planetary Interiors 48, 200 (1987).
W.R. Sheldon, J.R. Benbrook, E.A. Bering, Rev.Geophys. 26, 519 (1988).
V.I. Shevchenko, COSPAR XXVII, Espoo, Finland 1988, p. D.1.4.1.
P. Tříska et al., COSPAR XXVII, Espoo, Finland 1988, p. D.1.4.2.
A.L. Vampola, D.J. Gorney, J.Geophys.Res. 88, A8, 6267 (1983).
A.L. Vampola, Geophys.Res.Lett. 10, No.8, G19 (1983).
A.L. Vampola, C.D. Adams, J.Geophys.Res. 93, A3, 1849 (1988).
P. Velinov, G. Nestorov, L.Dorman, The effects of cosmic radiation on the ionosphere and on the propagation of radiowaves (in Russian), Sofia, Bulg.Acad.Sci., pp.307 (1974).
M. Walt et al., in Physics of the Magnetosphere, D. Reidel Publ.Co., Dordrecht - Holland, pp. 534, 1968.
M. Walt, L.L. Newkirk, W.E. Francis, J.Geophys.Res. 89, A3, 967 (1979).

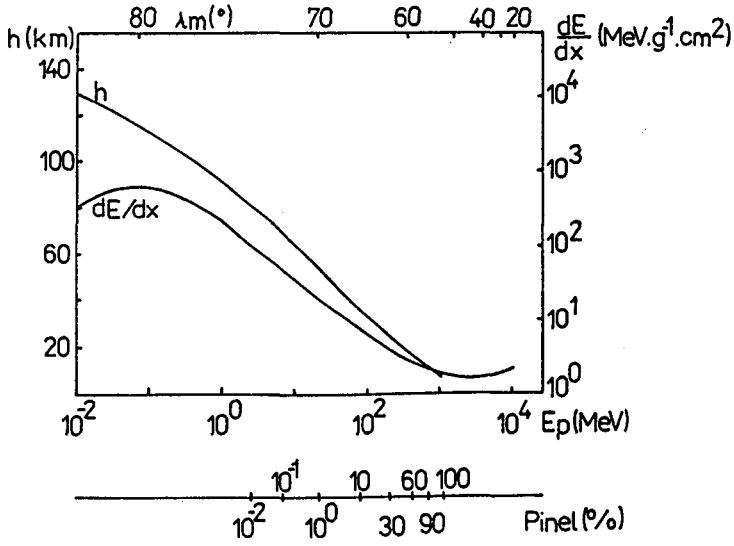

Fig. 1 Energy losses of protons.

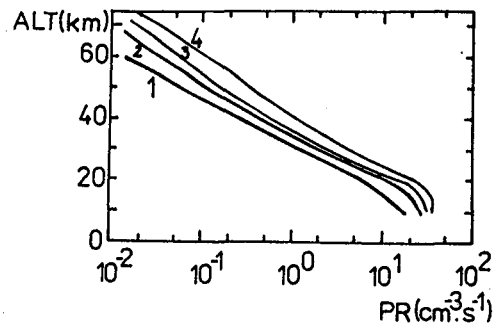

Fig. 2 1, 2 - seasonal variation at 30°; 3, 4 - sol-max, sol-min for 55° (compiled from DATTA et al., 1987).

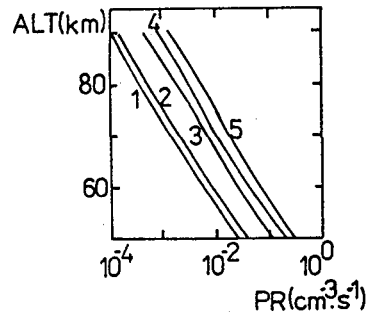

Fig. 3 1, 2 - 0° (sol-max, summer and sol-min winter); 3, 4, 5 - 55° (max summer, max winter, min winter) (from VELINOV et al., 1974).

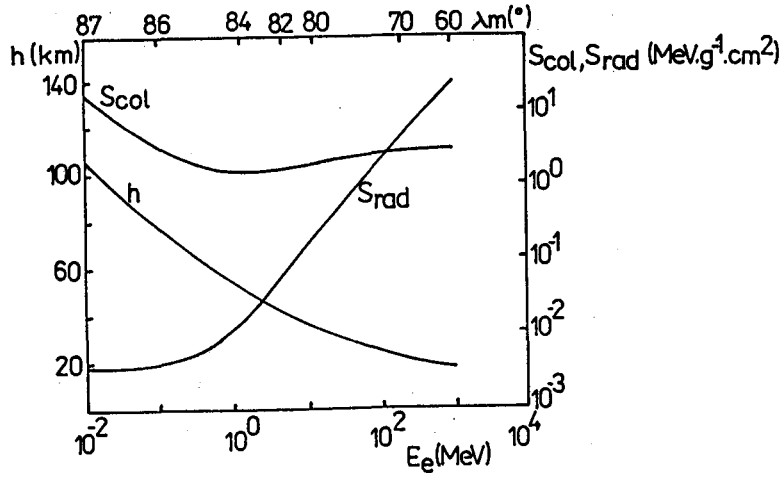

Fig. 4 Losses of energy of electron. Access to different latitudes is given at the top.

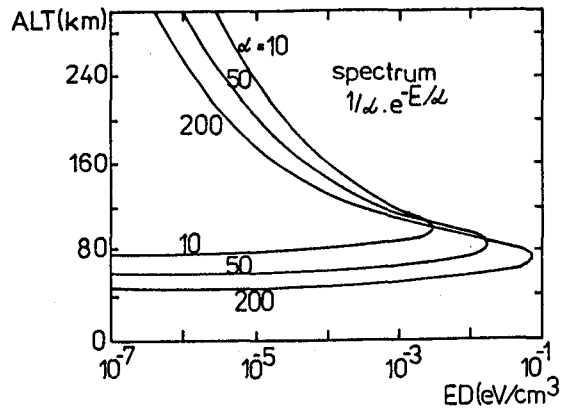

Fig. 5 ED for electron with initial isotropic distribution (for 1 electron/cm^2) (from BERGER et al., 1974).

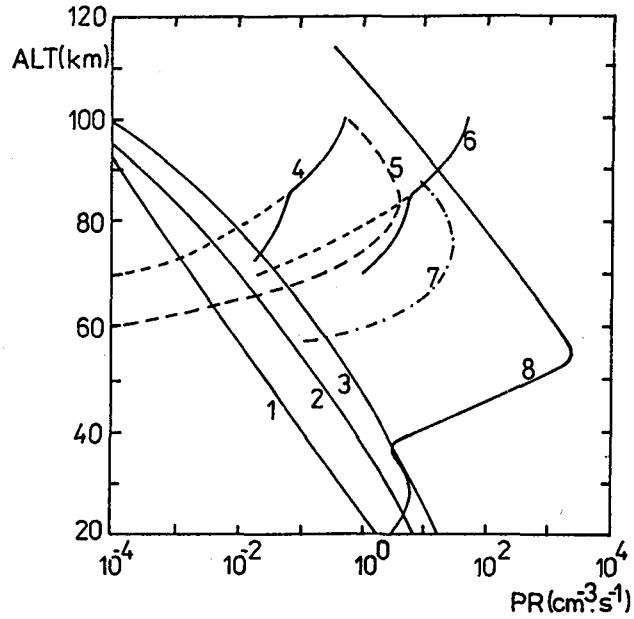

Fig. 6 Comparison of PR by corpuscular radiation. 1, 2, 3 - CR at 0°, 70° max and 70° min. 4, 6 - solar H$_{\alpha}$ scattered and direct. 5, 7 - due to electron precipitation at L = 4 (quiet and K_p = 6). 8 - due to very HEE. Compilation from SHELDON et al., (1988); BAKER et al., (1988) and VAMPOLA and GORNEY (1983).

A CHANGE OF MESOSPHERIC OZONE CONTENT UNDER ELECTRON PRECIPITATION INFLUENCE

I. I. Sosin and N. G. Skryabin

Institute of Cosmophysical Research and Aeronomy
Lenin Avenue 31, 677891 Yakutsk, USSR

The simulation model of a change of O, O_2 and O_3 oxygen component content at the heights 50 - 140 km under electron precipitation influence is presented here. Parameters of the air mass vertical transfer are introduced into the model. Calculation results showed that after the intense precipitation in ~ 3 days the ozone content increased at heights ~ 80 km. These results agree with the experimentally found effects of the content change under precipitation conditions.

Introduction

The experiments during solar proton events (HEATH, 1977; LIPPER, 1985; THOMAS, 1983) show a decrease of ozone content at the flare initial phase. A further behaviour of ozone concentration in the stratosphere and mesosphere differ from each other. For example, a total ozone number at height ~ 37 km after the August 1972 proton flare (HEATH et al., 1977) did not recover for several weeks. In the mesosphere the ozone concentration recovery up to its initial values occurred within a short time and then the further growth of $[O_3]$ in some events was observed. During the solar proton events in July and September 1974 (LIPPER et al., 1985) at 80 km the difference between the proton flux maximum and the ozone density minimum is ~ 36 hours and the maximum ozone content is observed in 4 - 6 days after the flare maximum. For the first time, a possibility of ozone concentration increase at heights between 70 and 85 km was theoretically predicted by CRUTZEN (1980) by an example of the solar flare in August 1972. The ozone content increase after the intensive precipitation of high energy electrons on March 23, 1974 (SKRYABIN et al., 1977) is shown. In this case the electron precipitation with average energy 250 keV occurred as three splashes each of them lasted 15 - 30 min. At this time at 120 - 200 km height there was a transfer intensification downwards of atmospheric masses. A maximum of ozone content increase in the atmosphere column occurred 1 - 3 days after the precipitations and it was ~ 7 - 9% of the initial value of $[O_3]$ (SKRYABIN et al., 1977).

Calculation Method

To find a "pure" contribution of precipitating electrons into the mesospheric ozone content, the polar night conditions are considered, i.e., the time when the short wave radiation of the Sun is absent. It is interesting to determine a maximum increase of ozone content in the mesosphere under the influence of precipitating electrons.

It is known that under precipitation conditions in the mesosphere O atoms are generated. Thus, it is shown (SOCHNEV, 1977) that their formation velocity is determined by the total velocity of ionoformation q(t) and by concentration of the atmosphere components at given height (H):

$$Q(t) = \frac{3.22[N_2] + 4[O_2] + 1.12[O]}{1.15[N_2] + 1.5[O_2] + 0.56[O]}\, q(t). \qquad (1)$$

The electron flux with the exponential energy spectrum is considered here:

$$f(E) = A(t) \cdot \exp(-E/20), \qquad (2)$$

where A(t) is a coefficient which takes into account a temporal change of precipitating electron flux magnitude and reaches 10^9 in maximum, t is time in seconds. It is natural that such huge fluxes cannot exist for a long time but they can occur repeatedly within a day. As a result, such precipitation splashes in the auroral zone can last in total several tens of minutes. Let us assume that

$$A(t) = B \cdot t \cdot \exp\left(-t^2/c\right), \tag{3}$$

where B and C are constants being $5.5 \cdot 10^6$ and 180000, respectively. At these values A(t) reaches its maximum value (10^9 cm^{-2} s^{-1} keV^{-1}) in 5 min. The average precipitation time in this case will be ~ 6 min.

Atomic oxygen disappears in general in the following reactions (McEWAN and PHILLIPS, 1975; CHAMBERLAIN, 1978):

$$O + O + M \rightarrow O_2 + M, \quad \kappa_1 = 3.6 \cdot 10^{-31} \cdot \frac{1}{T} \cdot \exp\left(-\frac{170}{T}\right), \text{cm}^6/\text{s}, \tag{4}$$

$$O + O_2 + M \rightarrow O_3 + M, \quad \kappa_2 = 1.1 \cdot 10^{-34} \cdot \exp\left(\frac{510}{T}\right), \text{cm}^6/\text{s}, \tag{5}$$

$$O + O_3 \rightarrow 2O_2, \quad \kappa_3 = 1.1 \cdot 10^{-11} \exp\left(-\frac{2150}{T}\right), \text{cm}^3/\text{s}, \tag{6}$$

here M is any third particle, K_1, K_2, K_3 are velocity constants of the appropriate reactions.

The reactions (4-6) take place in the atmosphere continuously. Hence, there are the recovery processes of [O], [O_2] and [O_3] which are taken to be constant at the given height and they are equal to the change velocity of these air components obtained from (4-6) under quiet conditions. These velocities are denoted by D(O), D(O_2) and D(O_3).

The equations describing the distribution of oxygen components with the account of the transfer processes are as follows (SOSIN, 1985):

$$\frac{\partial[\Delta O]}{\partial t} = Q(t) + D(O) - 2\kappa_1[O]^2[M] - \kappa_2[O][O_2][M] - \kappa_3[O][O_3] +$$

$$+ \frac{\partial}{\partial z}\left\{(D+K)\frac{\partial[\Delta O]}{\partial z} + \left(\frac{D+K}{T}\cdot\frac{dT}{dz} + \frac{D}{H_O} + \frac{K}{H_{av}} + v\right)[\Delta O]\right\}, \tag{7}$$

$$\frac{\partial[\Delta O_2]}{\partial t} = D(O_2) - \frac{Q(t)}{2} + 2\kappa_3[O][O_3] + \kappa_1[O]^2[M] - \kappa_2[O][O_2][M] +$$

$$+ \frac{\partial}{\partial z}\left\{(D+K)\frac{\partial[\Delta O_2]}{\partial z} + \left(\frac{D+K}{T}\cdot\frac{dT}{dz} + \frac{D}{H_{O_2}} + \frac{K}{H_{av}} + v\right)[\Delta O_2]\right\}, \tag{8}$$

$$\frac{\partial[\Delta O_3]}{\partial t} = D(O_3) + K_2[O][O_2][M] - K_3[O][O_3] +$$

$$+ \frac{\partial}{\partial z}\left\{(D+K)\frac{\partial[\Delta O_3]}{\partial z} + \left(\frac{D+K}{T}\cdot\frac{dT}{dz} + \frac{D}{H_{O_3}} + \frac{K}{H_{av}} + V\right)[\Delta O_3]\right\}, \quad (9)$$

here $[\Delta O]$, $[\Delta O_2]$ and $[\Delta O_3]$ are increments of O, O_2, and O_3 concentrations with respect to their initial contents before the precipitation, T is the temperature by an absolute scale in winter (KASTING, 1981), H_O, H_{O2}, H_{O3}, and H_{av} are the homogeneous atmosphere heights for O, O_2, O_3 and for the component with the average molecular mass, respectively. To find the average molecular mass the atmosphere was considered to consist of N_2, O_2, O_3 and O molecules. The concentration values at heights ≥ 80 km are taken according to (KASTING, 1981). At heights < 80 km the night concentrations of N_2, O_2, and O_3 were used on(McEWAN and PHILLIPS, 1975) and of O on (HUNT, 1973). The transfer coefficients D, K, and V were taken from CHAMBERLAIN (1978); LETTAN (1951); McEWAN and PHILLIPS (1975). The calculations were carried out by the method of probabilistic transitions (SKRYABIN, 1985) for the transfer parameters 0.5 K; 0.5 D; 0.5 V and 2 K, 2 D, 2 V.

Discussion

In Figure 1 the simulation results of $[\Delta O]$, $[\Delta O_2]$ and $[\Delta O_3]$ at various times after the electron precipitation in a form of 6-min splash are presented. From the figure it is seen that when the transfer parameters increase causing the intensification of the air mass displacement downwards, the $[\Delta O]$ decreases and the $[\Delta O_3]$ increases. In Figure 2 the changes of $[\Delta O]$ and $[\Delta O_3]$ in the atmosphere column are presented. With the change of transfer parameters by 0.5, once and twice the maximum values of $[\Delta O_3]$ are $2\cdot10^{15}$, $5\cdot10^{15}$, and $9\cdot10^{15}$ cm^{-2}, respectively. It equals the change of ozone content from a quiet level by 0.3, 0.76, and 1.4%. For 30-min precipitation they will be 1.5, 3.8, and 7%. And the higher is the arrival velocity of the air masses into the lower layer, the earlier is reached the content maximum of $[\Delta O_3]$. As is seen, such changes of ozone content by the order of magnitude correspond to the experimentally obtained effects (SKRYABIN et al., 1977).

References

Chamberlain, J. W., *Theory of Planetary Atmospheres*, Academic Press, New York, 1978.

CIRA-72 *COSPAR International Reference Atmosphere*, Academie-Verlag, Berlin, 1972.

Crutzen, P. J., and S. Solomon, Response of mesospheric ozone to particle precipitation, *Planet Space Sci., 28*, 1147-1153, 1980.

Heath, D. F., A. J. Krueger, and P. J. Crutzen, Solar proton event: Influence on stratosphere ozone, *Science, 197*, 886-889, 1977.

Hunt, B. G., A generalized aeronomic model of the mesosphere and lower thermosphere including ionospheric processes, *J. Atmos. Terr. Phys., 35*, 1755-1798, 1973.

Kasting, J. F., and R. G. Roble, A zonally averaged chemical-dynamical model of the lower thermosphere, *J. Geophys. Res., 86*, 9641-9653, 1981.

Lettan, H., Diffusion in the upper atmosphere, in *Compendium of Meteorology*, ed. T. F.Malone, Am. Meteorol. Soc., Boston, 320-333, 1951.

Lipper, W., D. Felske, and G. Sonneman, Solar particle events in the mesospheric ozone, KAPG Seminar, Hungary 1985.

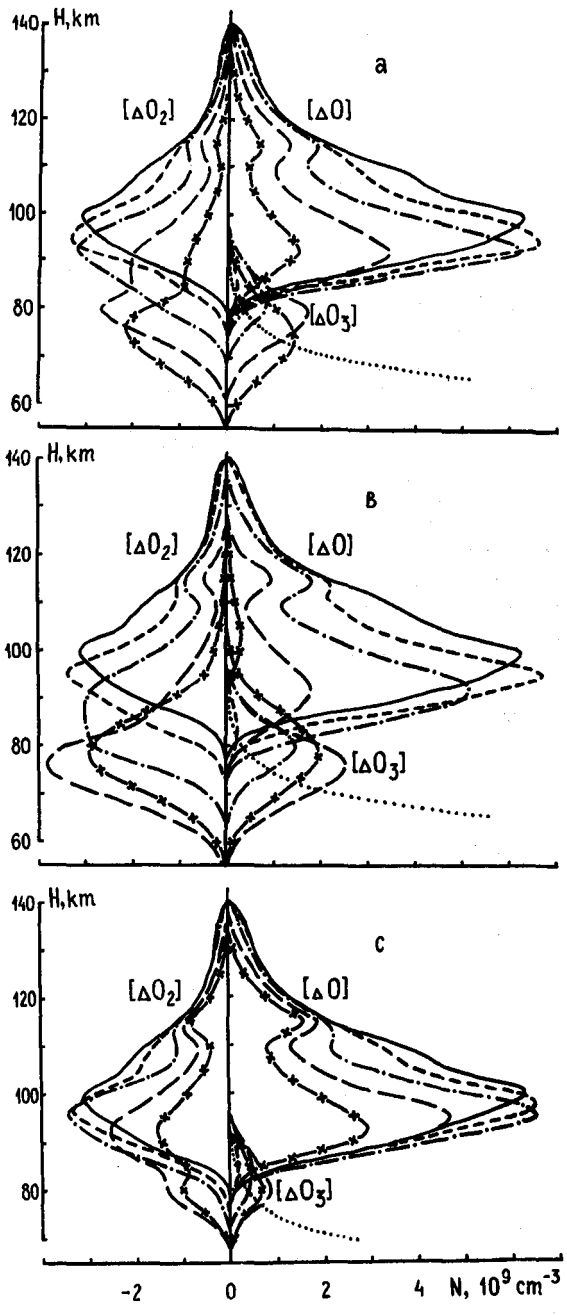

Figure 1 Distributions of $[\Delta O]$, $[\Delta O_2]$ and $[\Delta O_3]$ on heights at various times:

_____ 30 min
- - - - - - - - - - 6 hours
___ · ___ · ___ 1 day
___ ___ ___ 3 days
___ x ___ x ___ 6 days
. . . . . total content of ozone in the upper atmosphere on CIRA 72 model.

a) Coefficients of the turbulent (K), molecular (D) diffusions and the velocity of the averaged vertical wind in winter (V) according to CHAMBERLAIN, 1978; LETTAN, 1951; McEWAN and PHILLIPS, 1975);.
(b) K, D and V are twice increased;
(c) K, D and V are twice decreased.

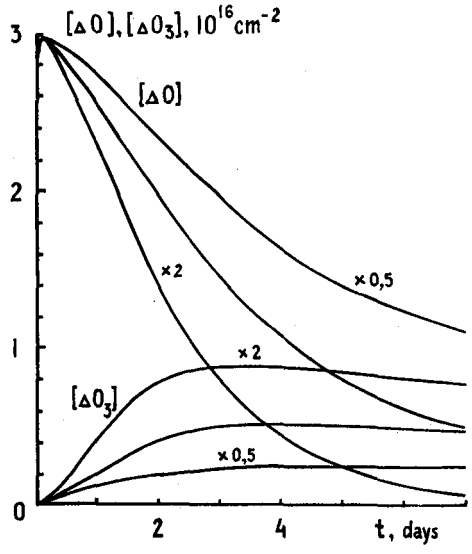

Figure 2. The content of $[\Delta O]$ and $[\Delta O_3]$ in the atmosphere column a single cross section versus time. Figures on curves show K, D and V increase.

McEwan, M. J., and L. F. Phillips, *Chemistry of the Atmosphere*, Edward Arnold, 1975.
Skryabin, N. G., Metod Veroyatnostnykh Perekhodov, Preprint, Yakutsk, YaF SO AN SSSR, 1985.
Skryabin, N. G., V. D. Sokolov, and V. G. Moiseyev, Izmeneniye Soderzhaniya Ozona i Aerozolei na Bolshikh Vysotakh v Svyazi s Elektronnymi Vysypaniyami, Svyaz Fizicheskikh Protsessov v Ionosfere i Magnetosfere Zemli s Parametrami Solnechnogo Vetra, Yakutsk, YaF SO AN SSSR, 63-67, 1977.
Sosin, I. I., Vysotno-Vremennye Profili Atomarnogo Kisloroda i Ozona Obuslovlennoye Vysypaniyami Electronov, Fizicheskiye Protsessy v Subavroralnoi Ionosfere, Yakutsk, YaF SO AN SSSR, 75-93, 1985.
Sochnev, V. G., V. F. Tulinov, and S. G. Yakovlev, Nekotorye Aspekty Vozdeistviya Korpuskulyarnogo Izlucheniya na Atmosferu Zemli v Spokoinykh i Vozmuschennykh Usloviyakh, Effekty Solnechnoi Aktivnosti v Nizhnei Atmosfere, Leningrad, Gidrometoizdat, 47-54, 1977.
Thomas, R. J., C. A. Barth, G. J. Rottman, et al., Mesospheric ozone depletion during the solar proton event of July 13, 1982. Part I. Measurement, *Geophys. Res. Lett., 10*, 253-255, 1983.

SOLAR ACTIVITY INFLUENCE ON COSMIC RAY PENETRATION IN THE MIDDLE ATMOSPHERE

P.I.Vellinov, L.N.Mateev

Space Research Institute, Bulgarian Academy of Sciences
6 Moskovska Str., Sofia 1000, Bulgaria

ABSTRACT

A new improved model for cosmic rays - middle atmosphere interaction is developed. The ionization q(h)-profile dependence on penetrating high energy particles composition (protons, alpha-particles and heavier nuclei) and energy spectra (solar activity modulation included) are investigated. A computer program, realizing the Gaussian algorithm for solving of multidimensional integrals is created. The corresponding electron density profiles N(h) at solar minimum and maximum are obtained, too.

INTRODUCTION

The galactic cosmic rays (GCR) flux is an important factor for the middle and low atmosphere ionization under day and night conditions. GCR form the independent CR- or C-layer at height from 50 to 80 km in the ionosphere, thus forming its base (VELLINOV et al., 1974). Here - at 50-60 km height a region characterized with anomalously high field values up to -4÷-6 V/m (APSEN et al., 1988; KOCHEEV et al., 1976, MAYNARD et al., 1981) is registrated via rocket measurements of the atmospheric electric field E_h-profiles. Thus, GCR ionization proves important for the clarification of a number of problems concerning the middle atmosphere electrodynamics and middle atmosphere - ionosphere interaction. For that purpose, a new model for the GCR - middle atmosphere interaction will be developed that will contribute to the further precision and generalization of previous results (VELLINOV et al., 1974).

GCR IONIZATION IN THE MIDDLE ATMOSPHERE

The electron production rate ($cm^{-3}.s^{-1}$) at height h (km) for the particles type i is

$$q_i(h)=\frac{1}{Q}\int_{E_i}^{\infty}\int_{\varphi=0}^{2\pi}\int_{\theta=0}^{\pi/2+\Delta\theta} D_i(E,h,\theta)\left(\frac{dE}{dh}\right)_i \sin\theta\, d\theta\, d\varphi\, dE \qquad (1)$$

where $Q=35$ eV is the energy necessary for one electron-ion pair formation, (dE/dh) - the particles ionization losses, D(E) - their differential spectra, φ - the azimuth, θ - the angle towards the vertical. As GCR penetrate isotropically from the upper hemisphere from (1) follows:

$$q(h)=\frac{2\pi}{Q}\int_{E_i}^{\infty}\int_{\theta=0}^{\pi/2+\Delta\theta} D_i(E,h,\theta)\left(\frac{dE}{dh}\right)_i \sin\theta\, d\theta\, dE \qquad (2)$$

where E_i is the energy (GeV/nucl) corresponding to the geomagnetic threshold R(GV), $\Delta\theta$ takes into account that at a given altitude the particles can penetrate from spatial angle $(0,90^\circ+\Delta\theta)$ that is greater than the upper hemisphere angle - $(0,90^\circ)$. For $\Delta\theta$ there is the following equation (VELLINOV, 1968):

$$\Delta\theta=90^\circ-\arccos\left(2R_e h+h^2\right)^{1/2}/(R_e+h) \qquad (3)$$

where $R_e=6371$ km is the Earth radius. In the interval 30-100 km

θ changes from 6 to 10°.

For dE/dh we are going to use the dependency (DOBROTIN,1964; VELLINOV et al., 1974, p.202)

$$-\frac{1}{\rho}\frac{dE}{dh} = \begin{cases} 2 \ \text{MeV}\cdot g^{-1}\cdot cm^2 & E = 10^3 \div 0.6\ \text{GeV} \quad \text{region 1} \quad (4) \\ \frac{1.37}{E^{3/4}} \ \text{MeV}\cdot g^{-1}\cdot cm^2 & E = 0.6 \div 10^{-3}\ \text{GeV} \quad \text{region 2} \quad (5) \end{cases}$$

where ρ is the atmosphere density in $g.cm^{-3}$. In fact the particle energy fall law in region 1 (0,6–10 GeV) is

$$E(h)=E - 2.10^{-3}\,\tilde{h}Z^2\,Ch(\theta,h) \qquad (6)$$

where $\tilde{h}=\int\rho(h)dh$ is the depth (g/cm^{-2}), Z is the particle charge, and Ch(θ,h) Chapman function taking into account the spherical form of the atmosphere. During particles penetration in the middle atmosphere their energy decreases while their ionization losses in the region 1 remain constant; in the region 2 they rise drastically according to (5): That effect was not taken into consideration in the previous investigations. After deducting (4,5) in (2) the total equation for the electron production rate is received:

$$q(h)=q_1(h)+q_2(h) \qquad (7)$$

where q_1 from the region 1 practically coincides with the previous calculations (VELLINOV,1968). The ionization in the region 2 will be added to q_1

$$q_2(h) = 1.8\times10^5\,\rho(h)\left[1.37\int_{10^{-3}}^{0.6}\int_{\theta_1}^{\pi/2+\Delta\theta} D(E)\,E^{-3/4}\,f_2(\theta)\sin\theta\,d\theta\,dE + \right. \qquad (8)$$

$$\left. + D(>0.6)\int_{\theta_1}^{\pi/2+\Delta\theta} f_2(\theta)\sin\theta\,d\theta\right]$$

$$f_2(\theta) = \left(\frac{10^{-3}}{E_i+\Delta E}\right)^{3/2} \qquad \Delta E = 2.10^{-3}\left(\tilde{h}-\tilde{h}_2\right) \qquad (9)$$

$$\tilde{h}_2 = \frac{172}{Ch(\theta,h)Z^2/A} + \frac{E_i-0.6}{2.10^{-3}\,Ch(\theta,h)Z^2/A}. \qquad (10)$$

In fact, the function $f_2(\theta)$ normalizes the particles integral spectra in the regions 1 and 2. A is the particles atomic weight. The angle θ_1 is determined with the help of equation (10), when the proportion $\tilde{h}_2(\theta_1,h)=\tilde{h}(h)$ is fulfilled.

COMPUTER REALIZATION OF THE MODEL AND ANALYSIS OF THE RESULTS

The theoretical model thus presented is realized with the help of a computer. The Gaussian method is applied for the solution of multidimensional integrals (PRESS et al., 1987).It is characterized by high precision for the smooth integrant functions, that are well approximated with polinoms. That method is machine run-time efficient – it uses only 10 function values in the integral interval.

Having in mind, that Z/A=1 for the protons and about 0,5 for the heavier nuclei, as well as the actual GCR composition (DORMAN, 1963) q.(h) were calculated for all groups of nuclei: protons (Z=1), alpha-particles (Z=2), light (Z=3÷5), middle (Z=6÷9), heavy (Z=10÷21) and very heavy (Z>22). In consequence the ionizations of the separate groups were summed up and the total ionization q(h) was received.

The calculations were conducted for two GCR spectra - in maximum and minimum solar activity, i.e. the 11-year GCR modulatiion from the solar wind is considered (DORMAN,1963). That modulation is expressed in the reverse solar activity changes and the GCR flux. A part of the results from the program model realization are presented on the Table: q(h) in the upper (80 km) and lower (50 km) part of the C-layer. The results from the previous calculations are given in brackets (VELLINOV et al., 1974). Hence, the contribution of q_2 to the total q can be considerable. From the Table it is seen also that at geomagnetic latitudes over 55° q(h) is growing during the solar minimum period two times, compared to the solar maximum. At middle latitudes the 11-year variation is still considerable, while at low and equatorial latitudes the variation is weak.

C-LAYER ELECTRON DENSITY DURING MAXIMUM AMD MINIMUM SOLAR ACTIVITY

The equilibrium electron density (cm^{-3}) is obtained from equation

$$N(h)=\left[\frac{q(h)}{\alpha_e(h)(1+\lambda)}\right]^{1/2}$$

where $\lambda=N^-/N$ is the negative ions-electrons ratio and α_e is the effective recombination coeficient. Having in mind the α_e values from MITRA (1986)the C-layer electron density was calculated for typical day conditions for middle (41°) and high (55°) geomagnetic latitudes during solar minimum and maximum. The results are given on the Figure and are mean valued in relation to season dependency due to the unsufficient representativeness of the α_e seasonal variations. But, it can be said definitely, that in the C-layer (and below it) maximum in winter N is 30-40% greater than in summer. Over 80 km the season variation changes its sign.

CONCLUSION

The present work consideres new aspects of the C-layer which together with the total GCR ionization in the middle and low atmosphere is of major importance for the global atmospheric-electric circuit in the system of the solar-terrestrial relationships and biorelationships.

The results obtained so far are not final and are an object of further specification. For example under significant θ the particles pass greater quantity of substance connected with the drastic growth of the Ch function. In that case an object of consideration are not only the electromagnetic interactions of GCR (4,5) but the nuclear as well. And those secondary cosmic rays will probably increase still more the obtained herewith electron production rates.

Under high solar activity the importance of the solar cosmic rays in ionization will grow, and hence - in the conductivity, currents, the electric fields and energetic processes in the middle atmosphere (VELLINOV and MATEEV, 1989).

C-Layer Electron Production Rate $q.cm^{-3}\ s^{-1}$ Table

HIGH LATTITUDES - ABOVE 55°, R=1.5 GV

h, km	SOLAR MINIMUM		SOLAR MAXIMUM	
	SUMMER	WINTER	SUMMER	WINTER
80	$7.5\ 10^{-3}$	$3.7\ 10^{-3}$	$4\ 10^{-3}$	$2\ 10^{-3}$
	[$5\ 10^{-3}$	$2.5\ 10^{-3}$	$2.6\ 10^{-3}$	$1.3\ 10^{-3}$]
50	$4.8\ 10^{-1}$	$2.8\ 10^{-1}$	$2.5\ 10^{-1}$	$1.3\ 10^{-1}$
	[$2.5\ 10^{-1}$	$1.5\ 10^{-1}$	$1.3\ 10^{-1}$	$7\ 10^{-1}$]

MIDDLE LATITUDES 41° R=5 GV

80	$3.6\ 10^{-3}$	$1.8\ 10^{-3}$	$2.7.10^{-3}$	$1.5.10^{-3}$
	[$2.4\ 10^{-3}$	$1.2\ 10^{-3}$	$1.8.10^{-3}$	10^{-3}]
50	$2.3\ 10^{-1}$	$1.3\ 10^{-1}$	$1.7.10^{-1}$	10^{-1}
	[$1.2\ 10^{-1}$	$7\ 10^{-1}$	9.10^{-1}	$5.5.10^{-1}$]

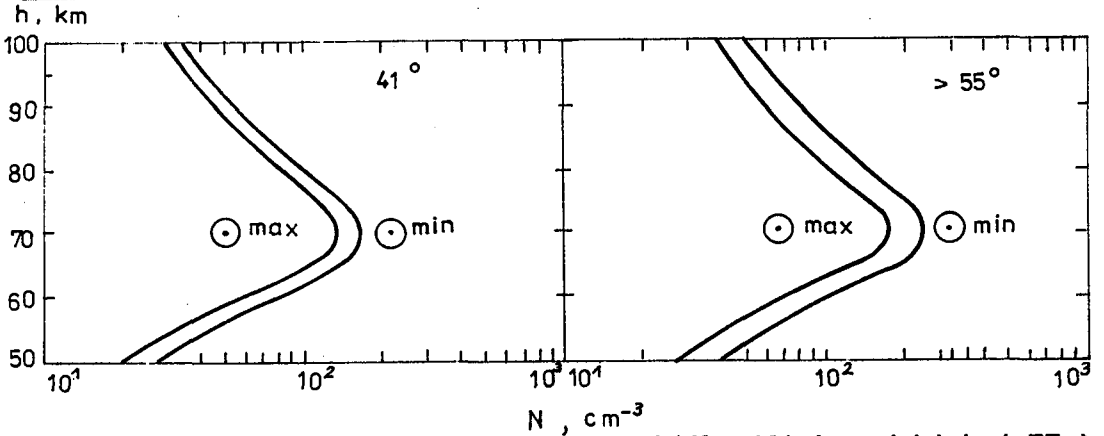

C-layer electron density profiles for middle (41) and high (55) latitudes during maximum and minimum solar activity.

REFERENCES

Apsen,A.G., H.D.Kanonidi, S.P.Chernisheva, D.H.Chetaev and V.M.Sheftel (1988), Magnetospheric Effects in the Atmospheric Electricity, NAUKA Publ.House, Moscow.

Dobrotin N.A. (1964), Cosmic Rays, Gostechteorizdat, Moscow.

Dorman,L.I. (1963), Cosmic Ray Variations and Space Investigation, USSR Acad.Sci., Moscow.

Kocheev,A.A., A.N.Smirnych, A.A.Tutun (1976), Kosmich.Issledvania, 14, 481.

Maynard N.C., C.L.Grockey, J.D.Mitchel and L.C.Hale (1981), Geophys.Res.Lett., 8, 923.

Mitra, A.P. (1986), Indian J.Radio a. Space Phys., 15, 235.

Press,W.H., B.P.Flannery, S.A.Teukolsky and W.T.Vetterling (1987), Numerical Recipes. The Art of Scientific Computing, Cambridge Univ.Press, Cambridge.

Vellinov P.I. (1968), J.Atmosph.Terr.Phys., 30, 1981.

Vellinov, P.I., G.Nestorov and L.I.Dorman (1974), Cosmic Ray Effects on the Ionosphere and the Radiowave Propagation, Bulgarian Acad.Sci.Publishing House, Sofia.

Vellinov,P.I.and L.N.Mateev (1989),Adv.in Space Res.,9 (in press).

INTENSIVE MHD-STRUCTURES PENETRATION IN THE MIDDLE ATMOSPHERE INITIATED IN THE IONOSPHERIC CUSP UNDER QUIET GEOMAGNETIC CONDITIONS

L.N.Mateev, P.I.Nenovski, P.I.Vellinov

Space Research Institute, Bulgarian Academy of Sciences
6 Moskovska Str., Sofia 1000, Bulgaria

ABSTRACT

In connection with the recently detected quasiperiodical magnetic disturbances in the ionospheric cusp, the penetration of compressional surface MHD-waves through the middle atmosphere is modelled numerically. For the CIRA-72 model the respective energy density flux of the disturbances in the middle atmosphere is determined. On the basis of the developed model certain conclusions are reached about the height distribution of the structures (energy losses, currents, etc.) initiated by intensive magnetic cusp disturbances.

Some of the most intensive small-scale magnetic disturbances (SSMD) recorded in the winter cusp are systematically investigated by SAFLEKOS et al. (1978). Intense small-scale magnetic disturbances and associated variations in the electric field have been recorded at height h=850 km on board the Intercosmos Bulgaria 1300 satellite (ARSHINKOV et al., 1985, NENOVSKI et al., 1987). The periodicity and the specific polarization state in some cases suggest that those disturbances have wavelike pattern. A model of compressional surface MHD-waves ducting in the cusp to the ionosphere has been proposed (NENOVSKI and MOMCHILOV, 1987).

However,the ionosphere and middle atmosphere conductivity cannot be considered infinite. The distribution of the SSMD energy transferred to the lower atmosphere layers is controlled by the conductivity variations and if reaching Earth surface - by induced telluric currents. The purpose of the present work is to demonstrate a quantitative picture of the surface MHD waves energy distribution in height within the low ionosphere and middle atmosphere.

In determining energy losses magnitude δW, evaluation of SSMD electric field components and current density in height is needed. The problem has been discussed in regard to the geomagnetic pulsations by HUGHES and SOUTHWOOD,(1976) and POOLE et al. (1988). Those components and the losses δW are determined numerically by the Maxwell equations and the Ohm's law.We introduce the Pedersen /σ_P/, Hall /σ_H/and the direct /$\sigma_{\parallel}$/ conductivities as a function of height. The parameters, determining the conductivity, collision frequencies, etc. components are density, mean molecular weight and temperature. CIRA-Cospar 1972 International Reference Atmosphere data is used for neutral atmosphere. Electron density profiles N(z) under night winter conditions and high solar activity are taken from rocket measurements /BELROSE (1972), HARRIS and TOMATSU,(1972)/at high latitudes.

As in the ionosphere cusp the precipitating particles energy is lower than 1-2 KeV, their ionizing influence under 300 km is ignored. On the opposite - we have considered the galactic cosmic ray ionizing effect, considerable in middle atmosphere

using the results obtained by VELLINOV and MATEEV (1989). The galactic cosmic rays effect on ionization is dominating in the region under 80 km. At 60-80 km height they form separate electron concentration layer /CR- or C-layer/ and positive and negative ion concentrations at 0-60 km with a maximum at about 20 km height. Herewith, ion densities from ARNOLD and KRANKOVSKY (1977) are used that correspond to the earlier ROSE and WIDDLE (1972) and later BRASSEUR and SOLOMON (1984) and BALACHANDRA SWAMI and SETTY (1984) results.

For the N(z)-profiles calculation /70-90 km/ except galactic cosmic rays we have included the effect of the scattered H_α Lyman-alpha radiation /POTEMRA and ZMUDA, 1972/ and the cosmic X-rays /GX333+25, SCO-XR-1, etc./, /MITRA and RAMANAMYRTY (1972)/. The electron density profiles N_e/h/, the positive ions N+/h/, the negative ions N-/h/ are given in Table 1.

The spatial and temporal variations of localized MHD-disturbancies, type

$$f(k_x, z)\exp(ik_x x - i\omega t)$$

are initiated at the upper ionosphere border. We are investigating the penetration of separate Fourier disturbance components $f(k_x, z)$ in the low ionosphere and the middle atmosphere, considered as horizontally homogenious, i.e. the medium is vertically stratificated.

We are investigating the variations in the electric field of the separate Fourier components in height /NENOVSKI and MATEEV, 1989/. According to the HUGHES AND SOUTHWOOD /1976/ model we are giving the initial values at z=0 /Earth surface/. Supposing that the Earth crust is an ideal conducter the boundary conditions for the transversal electric field components are $E_x, E_y = 0$ the vertical magnetic field component $b_z = 0$. The electric field vertical component /$E_z = 10^{-4}$ V/m/ and the magnetic field transversal component /$b_y = 5.10^{-10}$ G/. The Maxwell equations, including the Ohm law are integrated with adaptive step and boundary values at z=0.

The method applied is Runge -Kutta with precision of fourth order. The choice of integration step is made considering the pre-condition for step error. That is valid for each value obtained for the unknown function. With the experimentally verified factor we obtain further precision compensating the truncation error /PRESS et al., 1987/. The sensitivity towards identical sign error accumulation due to drastic step reduction is considered. Due to the adaptivity a definite precision is reached with computational work economy. Thus, efficiency of algorithm run-time is optimized. The higher algorithm order from 4 to 5 is reached on account of the greater number of calculations of the right part of the system of ordinary differential equations (factor 1.375). The efficiency of the applied method is proved in practice /PRESS et al., 1987/. The results from the numerical analysis are shown on Figures 1 and 2. The electric and magnetic field variations in the 0-100 km interval are shown on Figure 1,2 and the losses distribution - on Figure 3. That figures demonstrate the middle atmosphere influence on the MHD-disturbance long-wave harmonics transition: $k_x = 1000.. km^{-1}$, $k_y = 0$. Figures show that the Earth magnetic disturbance b_y reduces about 5 orders in magnitude towards the value at 100 km height. It is characteristic that while on the Earth the b_x component is 0, at 100 km height it is one order in magnitude greater than b_y. The electric field is characterized basically by two of its components - E_x and E_z. E_x reaches 0,1 V/m at 100 km height, while the E_z component is dr-astically reduced /by three orders at about 20 km

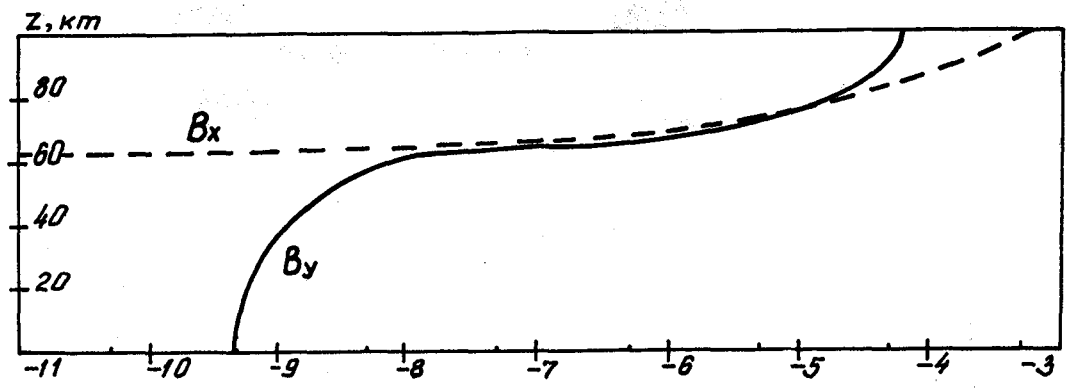

MAGNETIC FIELD e.s.u.

Fig. 1.

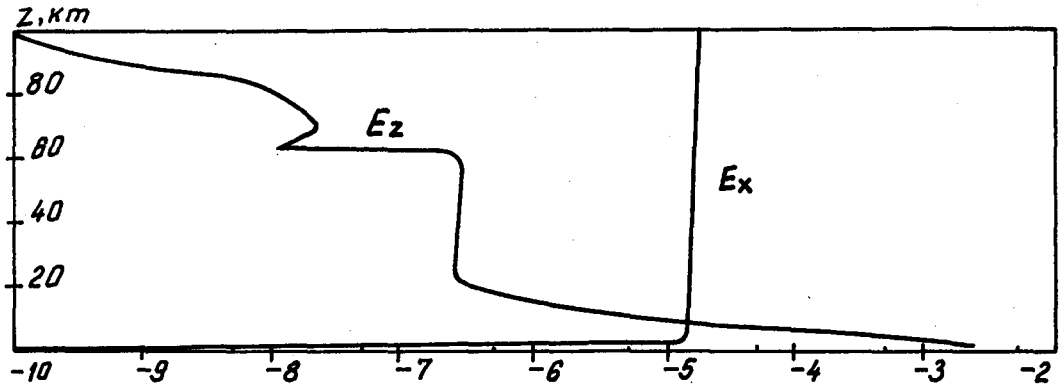

ELECTRIC FIELD e.s.u.

Fig. 2.

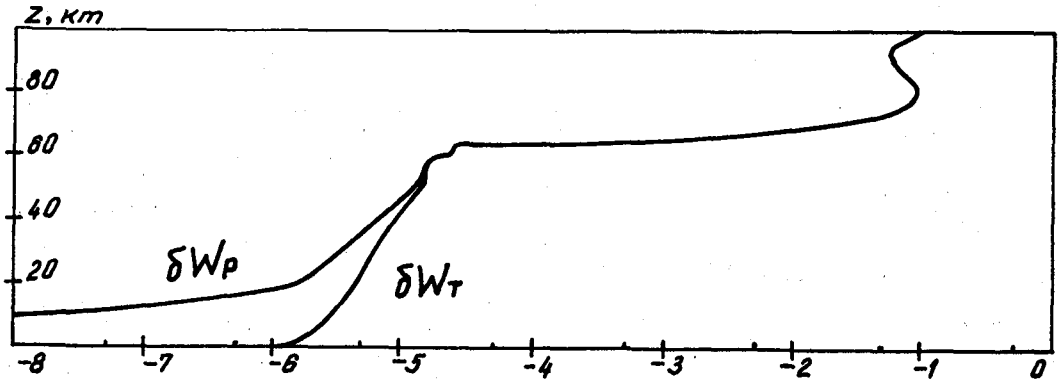

ENERGY LOSSES (ARBITRARY UNITS)

Fig. 3.

height/.

The losses /δW/ from the transition of long-wave MHD disturbances us due, as it can be supposed, to the Pedersen conductivity. That losses prove comparatively high in the middle atmosphere upper region, i.e. - the mesosphere D-region. At about 70 km height the losses are only 20% smaller than in the maximum at 100 km height. Under 70 km the losses reduce drastically. At lower altitudes the MHD-disturbances propagation is not connected with the presence of considerable energy losses. Here the role of the losses caused by the presence of electric field longitudinal component is greater. These results refer to a definite case and consequently are of preliminary character.

The basic conclusion is that the process of MHD-disturbances energy dissipation is not localized only in the E-layer. Under some conditions the middle atmosphere - mesosphere and the D-region participate actively in that process.

Table 1

Height	Density Number		
Z, km	electrons	positive ions	negative ions
100	$3\ 10^{3}$	$3\ 10^{3}$	-
90	$2\ 10^{3}$	$2\ 10^{3}$	-
80	$6\ 10^{2}$	10^{3}	$4\ 10^{2}$
70	$0.5\ 10^{2}$	$5\ 10^{2}$	$4.5\ 10^{2}$
65	-	$3\ 10^{2}$	$3\ 10^{2}$
60	-	$3\ 10^{2}$	$3\ 10^{2}$
55	-	$5\ 10^{2}$	$5\ 10^{2}$
50	-	$7.5\ 10^{2}$	$7.5\ 10^{2}$
45	-	$1.2\ 10^{3}$	$1.2\ 10^{3}$
40	-	$1.8\ 10^{3}$	$1.8\ 10^{3}$
35	-	$2.5\ 10^{3}$	$2.5\ 10^{3}$
30	-	$3\ 10^{3}$	$3\ 10^{3}$
25	-	$5\ 10^{3}$	$5\ 10^{3}$
20	-	$5\ 10^{3}$	$5\ 10^{3}$
15	-	$3\ 10^{3}$	$3\ 10^{3}$
10	-	$2.1\ 10^{2}$	$2.1\ 10^{2}$
5	-	$1.5\ 10^{1}$	$1.5\ 10^{1}$
0	-	$1\ 10^{0}$	$1\ 10^{0}$

REFERENCES

Arnold,F. and D.Krankowsky (1977) in: Dynamical and Chemical Coupling Between the Neutral and Ionized Atmosphere, D.Reidel,Publ. Co., Dordrecht, Boston

Arshinkov,I., A.Bochev, P.Nenovski, P.Marinov and L.Todorieva (1985) Adv.Space Res. 5, 127

Balachandra Swamy, A.C. and C.S.G.K. Setty (1984), Adv.Space Res. 4, 6, 41

Belrose, J.S. (1972), in: Aeronomy Report No48. COSPAR Symp. on D- and E-region ion chemistry. Univ. of Illinois, Urbano, Illinois, p.133

Brasseur,G and S.Solomon (1984) Aeronomy of the Middle Atmosphere, D.Reidel Publ.Co., Dordrecht /Boston/, Lancaster

Hughes, W.J. and D.J.Southwood (1976), J.Geophys.Res. 81, 3234

Mitra, A.P. and Y.V.Ramanamyrty (1972) in: Aeron.Rep. 48,

Univ. of Illinois, p.120.
Nenovski,P., A.Bochev and I.Arshinkov (1987) Planet.Space Sci., 35, 1553.
Nenovski,P. and G.Momchilov (1987) Planet.Space Sci. 35, 1561.
Nenovski P. and L.Mateev (1989) Compt.Rend.Acad. Sci. 42,No2.
Poole, A.W.V., P.R.Sutcliffe and A.D.M. Walker (1988) J.Geophys.Res. 93, A12.
Potemra,T.A. and A.J.Zmuda (1972) in Aeron.Rep. No48, Univ.Illinois, p.116.
Press,W.H., B.F.Flannery, S.A.Teukolsky and W.T.Vetterling (1987) Numerical Recipes - The Art of Scientific Computing, Cambridge Univ.Press, p.555.
Rose,G and H.V.Widdel (1972) in Aeronomy Rep. 48, p.144.
Saflekos,N.A., T.A.Potemra and T.Iijima (1978), J.Geophys.Res. 83, A4.
Vellinov,P.I. and L.N.Mateev (1989) (this issue).

LOWER THERMOSPHERE (80-100 km) DYNAMICS RESPONSE TO SOLAR AND GEOMAGNETIC ACTIVITY (Overview)

E.S.Kazimirovsky

Siberian Institute of Terrestrial Magnetism, Ionosphere and Radio Propagation, 664033, Post Box 4, Irkutsk, USSR

ABSTRACT: The variations of solar and geomagnetic activity may affect the thermosphere circulation via plasma heating and electric fields, especially at high latitudes. The possibility exists that the energy involved in auroral and magnetic storms can produce significant changes of mesosphere and lower thermosphere wind systems. A study of global radar measurements of winds at 80-100 km region has revealed the short-term effects (correlation between wind field and geomagnetic storms) and long-term variations over a solar cycle. It seems likely that the correlation results from a modification of planetary waves and tides propagated from below, thus altering the dynamical regime of the thermosphere. Sometimes the long-term behavior points rather to a climatic variation with the internal atmospheric cause than to a direct solar control.

The variations of solar and geomagnetic activity may affect the thermosphere circulation via plasma heating and electric fields, especially at high latitudes. The 80-100 km layer, occuring at the lower thermosphere, is a transition layer between an upper ionized region where motions are strongly influenced by electromagnetic processes and a lower neutral region where motions are controlled primarily by dynamics resulting from internal atmospheric causes. It is important to determine the maximum depth in the atmosphere to which the direct and indirect effects of solar and geomagnetic activity and variability penetrate. There are two main classes of processes to be considered: those associated with the variability of solar irradiance in various wavelength bands and those associated with the corpuscular radiation of the Sun.

The effects generated by solar wind variability and high-energy particles are well developed and fairly well understood in the lower ionosphere, whereas they are not much known and understood in the lower-lying layers and the neutral middle atmosphere.

The search for a coupling of solar and geomagnetic activity changes with middle atmosphere and lower thermosphere dynamics has been the subject of investigations for decades. Short-duration effects (correlation with geomagnetic storms, current intensity variations in the auroral electrojet, etc.) and long-term variations over a solar cycle were extensively investigated. There are some theoretical and numerical models of the lower thermosphere dynamics response to solar and geomagnetic activity. Nevertheless the results still remain rather ambiguous and controversial.

A zonally averaged chemical-dynamical model of the thermosphere (ROBLE and KASTING, 1984) was used to examine the effect of

high-latitude particle and Joule heating on the lower thermosphere neutral composition, temperature and winds at solstice for solar minimum conditions. It was found that high-latitude heat sources drive mean circulation cells that reinforce the solar-driven circulation in the summer hemisphere and oppose this circulation in the winter hemisphere.

Using a three-dimensional, time-dependent global model the response of the lower thermosphere to an isolated substorm was simulated (FULLER-ROWELL and REES, 1984). It was found that in the lower thermosphere (~120 km) a long-lived vortex phenomenon is generated. Initially two oppositely rotating vortices are generated by the effects of ion drag during the period of enhanced high-latitude energy input centred on the polar cap/auroral oval boundary, one at dusk and the other at dawn. After the end of substorm the dawn cyclonic vortex dissipates rapidly while the dusk anti-cyclonic vortex appears virtually self-sustaining and survives many hours after the substorm input has ceased.

Possible effects of solar variability on the middle atmosphere have been discussed (COLE, 1984; GARCIA et al., 1984) - solar variability in emission in the UV and EUV, variability of cosmic rays and auroral ionization rates, solar proton events, corpuscular heating in auroras, Joule heating by auroral electrojet, auroral NO production and gravity wave emission by the auroral electrojet.

GARCIA et al. (1984) examined the global response of the middle atmosphere (16-116km) to the solar variability between the maximum and minimum of the 11-year cycle of solar activity. In the upper mesosphere and lower thermosphere a temperature increase was found to occur, but for the most part this increase did not bring about any large changes in the zonal winds because the temperature increases are nearly uniform in latitude and do not affect the horizontal temperature gradient.

As for the experimental evidence, a solar-cycle dependence of LF drift wind (90-100 km) was for the first time found by SPRENGER and SCHMINDER (1969). For the years 1957-68 they obtained, for the winter period, a positive correlation of the prevailing wind with solar activity (represented by the 10.7 cm radio emission of the Sun) whereas the amplitude of the semi-diurnal tidal wind showed a negative correlation. This result was emphasized in the COSPAR International Reference Atmosphere 1972 (CIRA 72). It was confirmed by meteor radar wind measurements (PORTNYAGIN et al., 1977; BABAJANOV et al., 1977). Further, GREGORY et al. (1980, 1981, 1983) on the basis of an analysis of partial reflection wind data, 60-110 km, have inferred the 11-year cycle response of seasonal zonal flow which varies with altitude. Saskatoon data have been reviewed to determine whether a solar cycle modulation exists in them. It has been found that all circulation regimes in the mesosphere and lower thermosphere, i.e., both summer and winter, above and below ~95 km, show such a modulation, and that is as large as, if not larger than the effect at Kuhlungsborn, which was described as "considerable". Let us remember that much of data used in the CIRA-72 model for latitudes about 50°N were obtained during a solar minimum. Prevailing winds at Saskatoon increase from solar minimum to solar maximum by factors of up to 2-4. A comparison of trends in mean winds over Canada with those over Central Europe and East Siberia with the difference of about 20° geomagnetic latitude reveals that the effect of

solar and geomagnetic activity is stronger for higher geomagnetic latitudes.

The data collected from experimental ground-based remote measurements of 80-110 km winds were analyzed in terms of seasonal and long-term solar cycle behavior (DARTT et al., 1983). The annual variations depend on solar activity rather weakly, but the occurence of stronger westerlies (at 90 km during winter) in solar maximum than those in solar minimum years was confirmed with independent data at 50°N and 35°S. In addition, it appears that zonal winds are more southerly in spring and early summer in solar maximum years than in solar minimum years in the northern hemisphere. There are enough discrepancies between experimental data and theoretical models, though the stronger winter westerlies and summer easterlies during solar maximum are predicted by theory.

An analysis of long term meteor radar wind measurements for three midlatitude stations (D'YACHENKO et al., 1986) shows the significant solar cycle oscillations with periods of not only the 11 years but also the 22 year cycles. The variations of the prevailing winds with 22 year period are approximately in phase or antiphase with the 22 year solar activity cycle depending on the season. The variations with 22 year period dominate for variations of zonal prevailing wind velocities during the cold periods and meridional winds in autumn months. Meridional prevailing winds in November-February vary mainly with the 11-year cycle. In other months of the year the amplitudes of the 22 and 11 year velocity variations of prevailing winds are commensurable. For amplitudes of a semidiurnal tide the oscillations with the 22-year period prevail for all seasons. The authors noted that solar activity dependence of zonal and meridional component amplitudes of semi-diurnal tide are quite similar, whereas the character of corresponding dependences of zonal and meridional prevailing wind is different.

It may be noted that the results concerning a solar dependence of wind parameters below 100 km are controversial to date. The above-mentioned positive correlation of prevailing wind with solar activity (SPRENGER and SCHMINDER, 1969) may be changed by a negative correlation with an indication of a new change after 1983 (GREISIGER et al., 1987). The negative correlation with solar activity of the semi-diurnal tidal wind in winter remained unchanged (as late as 1984) and proved also to be the same in summer and for annual averages. Nevertheless the authors concluded that long-term behaviour points rather to a climatic variation with an internal atmospheric cause than to a direct solar control. This conclusion was made on the basis of continuous wind observations in the upper mesopause region over more than twenty years.

ZIMMERMAN and MURPHY (1977) plotted yearly averaged occurence rates of turbulence and turbulent diffusivity summed over the altitude region 70 to 90 km and compared them with solar activity indices. These data suggest a correlation with a two year time lag. ZIMMERMAN comments that it is fairly apparent that this occurence is wave induced and that one should look into the lower atmosphere for the source mechanism of these waves to understand more properly the solar relationship.

In addition to solar cycle variations short-term response of lower thermosphere dynamics to geomagnetic storm or current intensity variations in the auroral electrojet were inferred. Several mechanisms through which a short-term response may

develop are provided by ion-neutral frictional coupling. The ion-drag momentum and Joule heat sources may either directly drive motions of the neutral gas or launch atmospheric waves that propagate to lower latitudes. At high latitudes particle precipitation and magnetospheric convection may influence the internal atmospheric waves upward propagation from the lower atmosphere and thereby affect the mesosphere. As altitude increases from the mesosphere to the thermosphere, at some point the additional influence of auroral processes is superposed on this complex collection of interacting waves and turbulent motions. Hence the geomagnetic activity affects both boundaries of the middle atmosphere - the turbopause (upper) and the tropopause (lower).

In order to investigate the response of neutral winds at the lower thermosphere to variations in magnetospheric forcing, it is necessary to have observational techniques with reasonably continuous measurement capability at this altitude.

There are some recent experimental results. The geomagnetic control of ionospheric D-region dynamics was revealed and confirmed on the basis of continuous LF drift measurements (1978-1983) over East Siberia (KAZIMIROVSKY et al., 1986; VERGASOVA, 1988a, 1988b). The monthly mean parameters of the wind system are different for quiet ($Kp \leq 3$) and disturbed ($Kp > 3$) conditions. There is an increase in stability of the meridional wind with increasing level of geomagnetic activity. On the basis of 31 events the influence of geomagnetic storms on the winds was considered, and it became apparent that the variation of zonal and meridional winds during geomagnetically disturbed nights differs from those for undisturbed nights before and after the storm. Calculations made by the superposed epoch method for weak ($Ap < 50$), moderate ($50 \leq Ap < 100$) and strong ($Ap > 100$) storms show that the zonal wind during weak and strong storms decreases but increases for moderate storms. The meridional wind increases during weak and strong storms, while after the storm there is a reverse of meridional wind. We did not find conclusive evidence for geomagnetic effects on semi-diurnal tides, except for a decrease of tidal phase during disturbed nights.

We may compare our results with recent findings of other investigators. SCHMINDER and KURSCHNER (1978, 1982) found the influence of geomagnetic storms on the measured wind in the Central Europe upper mesopause region deduced from ionospheric drift measurements. But they interpreted the disturbances of the wind field as an effect of increasing in the reflection level, so that the measurements during a geomagnetic storm relate to a different altitude with different wind conditions. Nevertheless we may note the increased zonal wind variability including possible reversals. LASTOVICKA and SVOBODA (1987) found some correlation (~ -0.4) of 5-day medians of Collm mean winds and $\sum Kp$ for winter.

At Saskatoon (subauroral zone) MANSON and MEEK (1986) observed small but significant cross correlations between semidiurnal tidal amplitudes from 90 to 105 km and the Ap index. Tidal amplitudes remained reduced from time lags of zero to about 5 days following the interval of increased Ap. Reduced diurnal tidal amplitudes were also found in the lower E-region, at 105 km. It may be noted that small increases in eastward and equatorward mean winds (incoherent scatter, Millstone Hill) as well as reduced semidiurnal tidal amplitudes at 105 km during geomagnetically disturbed conditions were reported by WAND (1983) some years ago.

Some of these effects might be explained by geomagnetic-activity induced changes in lower thermosphere temperature and density, which alter the dissipation of the upward propagating tides. MAZANDIER and BERNARD (1985) also found the effect of geomagnetic storm on the meridional circulation and semidiurnal tide, especially the phase of tide at 90-180 km, revealed by incoherent scatter measurements at midlatitude station Saint-Santin.

The amplitude of gravity waves was found to be positively correlated with intervals of increased Ap near zero time lag at heights from 90-105 km (MANSON and MEEK, 1986). Rocket measurements of turbulent transport in the lower ionosphere collected by ANDREASSEN et al. (1983) confirm the increase of turbulence for high geomagnetic activity. But the vertical turbulent diffusivity in the lower thermosphere above 110 km deduced from ionospheric sporadic E parameters by BENCZE (1983) decreases during geomagnetic storm. This would mean that the height of the turbopause increases. ZIMMERMAN et al. (1982) found a strong correlation of Ap with deviations of the turbopause height from mean diurnal variation (but not with the height itself). THRANE et al. (1985) found that it is not possible to determine whether or not a direct relation exists between the energy input during geomagnetic disturbances and the turbulent state of the high-latitude mesosphere.

Extensive investigations have been made at auroral zone observatories Poker Flat (MST-radar) by BALSLEY et al. (1980, 1982, 1983), JOHNSON et al. (1984), JOHNSON and LUHMAN (1985a, 1985b, 1988) and Chatanika by JOHNSON et al. (1987). The results were controversial. Initially it was found that zonal winds in the 80-90 km altitude region were enhanced toward the west while intensified electrojet currents flowed overhead. It appeared that the enhancement in the zonal wind amounts to some tens of meters per seoond and the wind field variations may lag behind the electrojet variations by between 2 and 4 hours (BALSLEY et al., 1980, 1982, 1983). The incoherent scatter measurements would show enhanced eastward winds above 100 km on disturbed day, as well as reduced semidiurnal and increased diurnal tidal amplitudes (JOHNSON et al., 1987). These results are not in conflict with those of MANSON and MEEK (1986) since a lower altitude range has been addressed in this study. But recently (JOHNSON and LUHMAN, 1988) it was shown that the presence of like frequencies in the available geomagnetic activity indices and in the neutral wind data makes the detection of any small neutral wind response to changes in the level of activity extremely difficult. Examination of all Poker Flat and Chatanika results suggested the conclusion that the 90 to 100 km altitude region constitutes the altitude range in which the effects of magnetospheric forcing begin to be detectable observationally in horizontal neutral winds at high to midlatitudes. Below this altitude significant and consistent responses are not evident. In order to alter the neutral dynamics at lower altitudes drastically more energetic inputs are required.

LASTOVICKA (1988) proposed that the apparent difference between North American (weaker effect) and European (stronger effect) results may be partly explained by the use of winter or late autumn data in Europe versus summer data in North America (Poker Flat and Chatanika) and by the fact that particularly strong events (e.g. geomagnetic storms - mainly studied in Europe) but not short-term weaker fluctuations (mainly studied in North America) can affect wind fields. Sometimes the longi-

tudinal effect (KAZIMIROVSKY et al., 1988) may be significant.

It should be noted in conclusion that the solar and geomagnetic activity variations are important but not dominant in the upper mesosphere-lower thermosphere circulation (wind system). Incorrect application of statistical methods to experimental data sets may lead to artifacts and misunderstanding.

At present we can only speculate about a suitable physical process. The lack of reasonably reliable mechanisms is a problem of vital importance. It may be a common reason for variations of the wind regime at the lower thermosphere and magnetic activity - the dissipation of energy from external sources at high latitudes and its transfer equatorward. A change in the wind system may exert an influence on the density and structure of the middle atmosphere and on conditions of internal waves propagation from below. Hence the variability may be changed. It is quite possible too that the change in the 80-100 km wind system associated with geomagnetic activity variations is caused by enhanced electron concentrations in the ionospheric D-region. Also, magnetic activity induced by disturbances in the wind field of the neutral atmosphere should not be ruled out as a possibility.

The most difficult problem which will limit our progress is that of understanding the cumulative interaction of small- and large-scale dynamics occuring within the lower atmosphere, the coupling between the thermosphere and lower atmosphere from below. Of course, these studies are needed, in order to determine whether all the highly variable middle atmospheric dynamical processes can influence processes within our lower atmosphere and thus affect our immediate environment.

There is a need to organize an effective monitoring system that would be reasonably intensive and extensive. What is desired from future research is a qualitative assessment of all the significant couplings, trigger mechanisms and feedback processes. Many problems are largely to be solved.

REFERENCES

Andreassen, O., T.Blix, B.Grandal, and E.V.Thrane, 6th ESA Symp.Eur. Rocket and Balloon Programmes and Relat.Res., Interlaken, 1983. Paris, 39-40, 1983.

Babajanov, P.B., V.M.Kolmakov, and R.P.Chebotarev, Solar activity and wind energy at the upper atmosphere, Astr. Circ., No. 950, 1977.

Bencze, P., Turbulence in the lower thermosphere during geomagnetic storm deduced from ionospheric sporadic E parameters. Acta Geodaet.Geophys. et Montanist. Hung., 18, 109-117, 1983.

Balsley, B.B., D.A.Carter, and W.L.Ecklund, A note on the short-term relationship between solar activity and the wind field near the mesopause, Report to MADT Symposium, Urbana, USA, 15 pp., 1980.

Balsley, B.B., D.A.Carter, and W.L.Ecklund, On the relationship between auroral electrojet intensity fluctuations and the wind field near the mesopause, Geoph.Res.Lett., 9, No.3, 219-222, 1982.

Balsley, B.B., D.A.Carter, and W.L.Ecklund, On the potential of radar observations for studying coupling processes between the ionosphere and the middle atmosphere. Weather and Climate Responses to Solar Variations, Colo., USA, Univ. Press, 144-160, 1983.

CIRA-1972, COSPAR International Reference Atmosphere, Akademie-Verlag, Berlin, 1972.
Cole, K.D., Possible effects of solar variability on the middle atmosphere, J.Atmos.Terr.Phys., 46, 721-725, 1984.
Dartt, D., G.Nastrom, and A.Belmont, Seasonal and solar cycle wind variations, 80-100 km, J.Atmos.Terr.Phys., 45, 707-718, 1983.
D'yachenko, V.A., L.A.Lysenko, abd Yu.I.Portnyagin, Long term periodicities in lower thermospheric wind variations, J.Atmos. Terr.Phys., 48, 1117-1119, 1986.
Fuller-Rowell, T.J. and D.Rees, Interpretation of an anticipated long-lived vortex in the lower thermosphere following simulation of an isolated substorm, Planet. Space Sci., 32, 69-85, 1984.
Garcia, R.R., S.Solomon, R.G.Roble, and D.Rusch, A numerical response of the middle atmosphere to the 11-year solar cycle, Planet. Space Sci., 32, 411-423, 1984.
Gregory, J.B., A.H.Manson, and C.E.Meek, Response of middle atmosphere circulation to solar activity, Report to MADT Symposium, Urbana, USA, 12 pp., 1980.
Gregory, J.B., C.E.Meek, and A.H.Manson, Mean zonal and meridional wind profiles for the mesosphere and lower thermosphere at 52°N, L=4.4, during solar maximum, Atmosphere-Ocean, 19, 24-34, 1981.
Gregory, J.B., C.H.Meek, and A.H.Manson, Solar cycle variation of mesospheric winds at 52°N, Weather and Climate Responses to Solar Variations. Colo, USA, Univ.Press, 161-167, 1983.
Greisiger, K.M., R.Schminder, and D.Kürschner, Long-period variations of wind parameters in the mesopause region and the solar cycle dependence, J.Atmos.Terr.Phys., 49, 281-285, 1987.
Johnson, R.M., J.G.Luhmann, C.T.Russell, B.B.Balsley, and A.C. Riddle, A comparison of auroral zone mesopause wind power spectra with geomagnetic activity indicators, Abstr. XXV COSPAR, Graz, paper 5.6.4., 1984.
Johnson, R.M. and J.G.Luhmann, Neutral wind spectra at the auroral zone mesopause: geomagnetic effect?, J.Geophys.Res., 90, 1735-1743, 1985a.
Johnson, R.M. and J.G.Luhmann, High-latitude mesopause neutral winds and geomagnetic activity: A cross-correlation analysis, J.Geophys.Res., 90, 8501-8506, 1985b.
Johnson, R.M., R.G.Wickwar, R.G.Roble, and J.G.Luhmann, Lower thermospheric winds at high latitude: Chatanika radar observations, Ann.Geophysicae, 5, 383-404, 1987.
Johnson, R.M. and J.G.Luhmann, Cross-correlation of high-latitude upper mesospheric neutral winds with AE and Kp, J. Geophys.Res., 93, 8625-8632, 1988.
Kazimirovsky, E.S., E.I.Zhovty, and M.A.Chernigovskaya, Dynamical regime of the ionospheric D-region over East Siberia during quiet and disturbed conditions, J.Atmos.Terr.Phys., 48, 1255-1258, 1986.
Kazimirovsky, E., A.H.Manson, and C.E.Meek, Winds and waves in the middle atmosphere at Saskatoon (52°N, 105°E), J.Atmos. Terr.Phys., 50, 243-250, 1988.
Lastovicka, J. and K.Svoboda, On the correlation of the midlatitude lower ionosphere with solar and meteorological parameters during MAP/WINE winter of 1983/1984, Physica Scripta, 35, 906-909, 1987.

Lastovička, J., A review of solar wind and high energy particle influence on the middle atmosphere, Ann.Geophysicae, 6, 401-408, 1988.

Manson, A.H. and C.E.Meek, Comparisons between neutral winds near 100 km at Saskatoon (52°N, 107°N, L=4.4) and variations in the geomagnetic field (1979-1989), Ann.Geophysicae, 4A, 281-286, 1986.

Mazandier, C. and R.Bernard, Saint-Santin radar observations of lower thermospheric storms, J.Geophys.Res., 1985, 90, 2885-2895, 1985.

Roble, R.G. and J.F.Kasting, The zonally averaged circulation, temperature and compositional structure of the lower thermosphere and variations with geomagnetic activity, J.Geophys. Res., 89, 1711-1724, 1984.

Schminder, R. and D.Kürschner, The influence of geomagnetic storms on the measured wind in the upper mesopause region deduced from ionospheric drift measurements, J.Atmos.Terr. Phys., 41, 85-88, 1978.

Schminder, R. and D.Kürschner, The influence of geomagnetic storms on the results of l.f. drift measurements in the mid-latitude upper mesopause region, Z.Meteorol., 32, 328-329, 1982.

Sprenger, K. and R.Schminder, Solar cycle dependence of winds in the lower ionosphere, J.Atmos.Terr.Phys., 31, 217-221, 1969.

Thrane, E.V., O.Andreassen, T.Blix, B.Grandal, A.Brekke, C.R. Philbrick, F.J.Schmidlin, H.U.Widdel, U. von Zahn, and F.J. Lübken, Neutral air turbulence in the upper atmosphere observed during the Energy Budget Campaign, J.Atmos.Terr.Phys., 47, 243-264, 1985.

Vergasova, G.V., Geomagnetic storm effects on the lower-ionosphere dynamics over East Siberia, Issled.geomagn.,aeron. fiz. Solntsa, 80, 20-28, 1988a (in Russian).

Vergasova, G.V., The correlation of prevailing winds in the midlatitude thermosphere with helio- and geomagnetic activity, Issled.geomagn.,aeron.fiz. Solntsa, 81, 161-172, 1988b (in Russian).

Wand, R.H., Geomagnetic activity effects on semidiurnal winds in the lower thermosphere, J.Geophys.Res., 88, 9243-9248, 1983.

Zimmerman, S.P. and E.A.Murphy, Stratospheric and mesospheric turbulence. Dyn. and Chem. Coupling Between Neutral and Ionized Atmos., NATO Adv. Study Inst. Series, 35-47, 1977.

Zimmerman, S.P., T.J.Keneshea, and C.R.Philbrick, Diurnal, solar cycle and magnetic index relations to turbopause heights, Paper STP.IV.1.1., Ottawa, 1982.

EFFECTS OF SOLAR ACTIVITY IN THE MIDDLE ATMOSPHERE DYNAMICAL REGIME OVER EASTERN SIBERIA, USSR

V.A.Gaidukov, E.S.Kazimirovsky, E.I.Zhovty, and M.A.Chernigovskaya

Siberian Institute of Terrestrial Magnetism, Ionosphere and Radio Propagation, 664033, Post Box 4, Irkutsk, USSR

ABSTRACT: Lower thermospheric (90-120 km) wind data has been acquired by ground-based spaced-receiver method (HF, LF) near Irkutsk (52°N, 104°E). There is interrelated solar and meteorological control of lower thermosphere dynamics. Some features of solar control effects on the wind parameters are discussed.

The region 90-120 km is a part of the middle atmosphere. The response of wind regime of that region to solar and geomagnetic activity was revealed by numerous authors (KAZIMIROVSKY, 1985; LASTOVICKA, 1987). Our data of LF D1 wind measurements from 1975 to 1985 at D region of the ionosphere (frequency 200 kHz) and HF D1 wind measurements from 1972 to 1976 at E-region (vertical sounding, 2.2 MHz) gave the possibility for further investigations.

Statistical analysis of data for D-region (78 months) allowed us to conclude that there is a distinct relationship between monthly averaged prevailing winds (zonal and meridional) and solar activity. But we did not find such relationships for tidal components. The variations of zonal (V_{ox}) and meridional (V_{oy}) prevailing winds may be approximated in the following way:

$$V_{ox}(M,F) = 17.1 + 3.9\sin(\pi M/6) - 7.3\cos(\pi M/6) + 4.4\sin(\pi M/3) + 5.7\cos(\pi M/3) + 5.4\,F_{10.7}/100, \ m\,s^{-1};$$

$$V_{oy}(M,F) = 5.4 - 1.8\sin(\pi M/6) + 3.0\cos(\pi M/6) - 1.6\sin(\pi M/3) + 3.7\cos(\pi M/3) + 4.7\,F_{10.7}/100, \ m\,s^{-1}. \quad (1)$$

Here M is month number (for instance, January has number 1), $F_{10.7}$ - index of solar activity, the flux of solar radioemission (10^{-22}Wm^{-2}Hz^{-1}). This approximation is valid for $60 < F_{10.7} < 240$. As shown in Fig. 1, the correlation between prevailing winds and solar activity is rather positive. This result is in agreement with some recently published papers (ZHOVTY, 1984; KAZIMIROVSKY, 1985).

Some years ago we investigated the seasonal variations of the absolute differences between geomagnetically quiet and disturbed conditions for the parameters of D-region winds (KAZIMIROVSKY et al., 1986). Now we have done the same for E-region winds during 1972-1976. The solar activity decreased from $F_{10.7} \simeq 100$-150 for 1972 to $F_{10.7} \simeq 70$-80 for 1976.

Data obtained during periods with $K_p \leq 3$ were classed as quiet conditions, and those for $K_p > 3$ as disturbed conditions.

The seasonally averaged diurnal variations of wind velocity were approximated thus:

$$V_k(t) = V_{ok} + \sum_{n=1}^{3} V_{nk}\cos\left[\frac{\pi n}{12}(t - t_{nk})\right], \quad (2)$$

$k = x, y$; t_{nk} - the phase of n-harmonics for the k-component of velocity. For each season we calculated the averaged differences:

$$\Delta V_{ok} = | V_{ok}^{q} - V_{ok}^{d} |,$$
$$\Delta V_{nk} = | V_{nk}^{q} - V_{nk}^{d} |, \qquad (3)$$

between quiet (q) and disturbed (d) conditions.

In most cases ΔV_{ok} and ΔV_{nk} increase with solar activity decreasing; therefore the stability of wind system increases with increasing solar activity. We know that the thermospheric neutral density correlates positively with solar activity. Possibly, this process affects the circulation and the influence of geomagnetic activity diminishes. At present we can only speculate about the suitable physical mechanism. But the lack of the definitive conclusions stresses the necessity of continuation of experimental researches of ionospheric motions.

REFERENCES

Kazimirovsky, E.S., Solar-terrestrial relations in the dynamics of the lower ionosphere. Issled. Geomagn., Aeron., Fiz. Solntsa, 71, 215-224 (in Russian), 1985.

Kazimirovsky, E.S., E.I.Zhovty, and M.A.Chernigovskaya, Dynamical regime of the ionospheric D-region over East Siberia during quiet and disturbed conditions, J.Atmos.Terr.Phys., 48, 1255-1258, 1986.

Laštovička, J., A review of solar wind and high energy particle influence on the middle atmosphere, Annales Geophysicae, 6, (4), 401-408, 1987.

Zhovty, E.I., The response of lower ionosphere dynamics to solar activity. "Disturbances of extraterrestrial origin in the lower ionosphere". Extended Abstracts, Symposium KAPG, Praha, 1984.

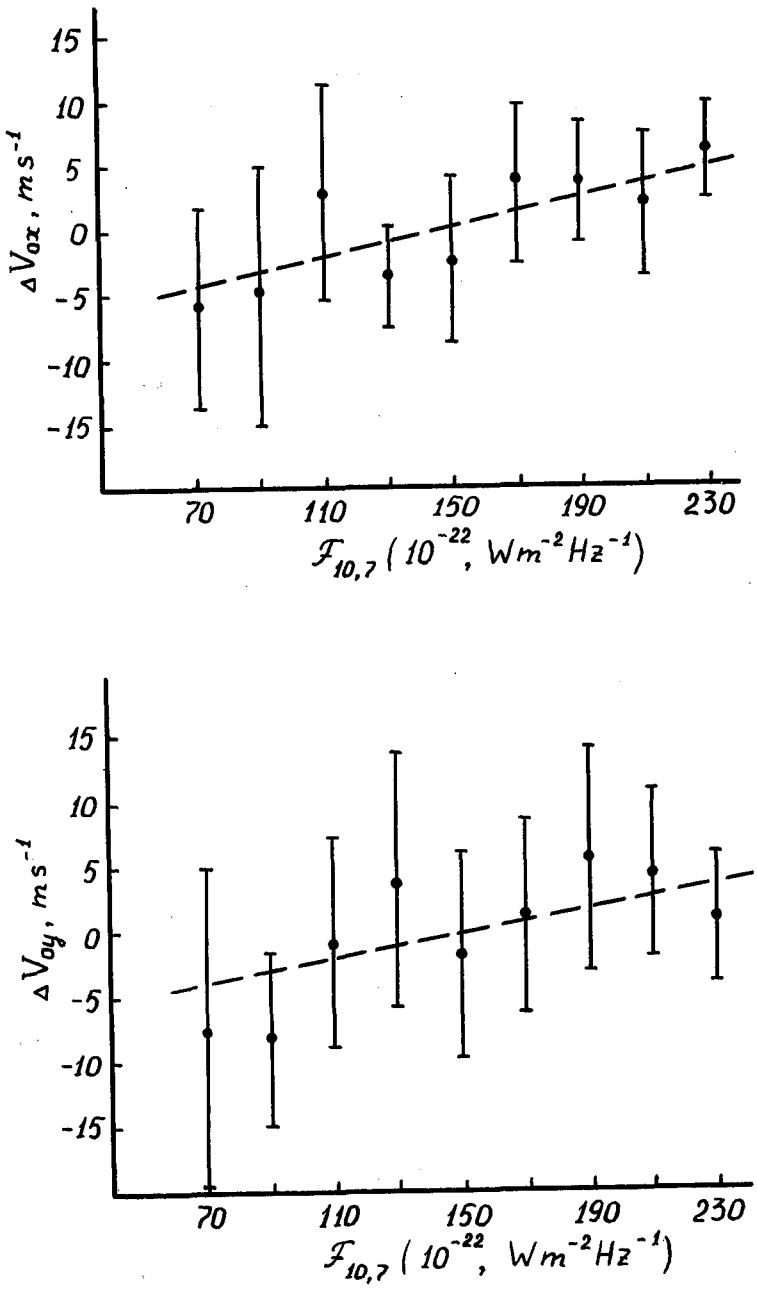

Figure I. Dependence on solar activity (I0,7 cm radio flux) of the zonal (V_{ox}) and meridional (V_{oy}) prevailing winds at D-region over East Siberia for I975-I985.

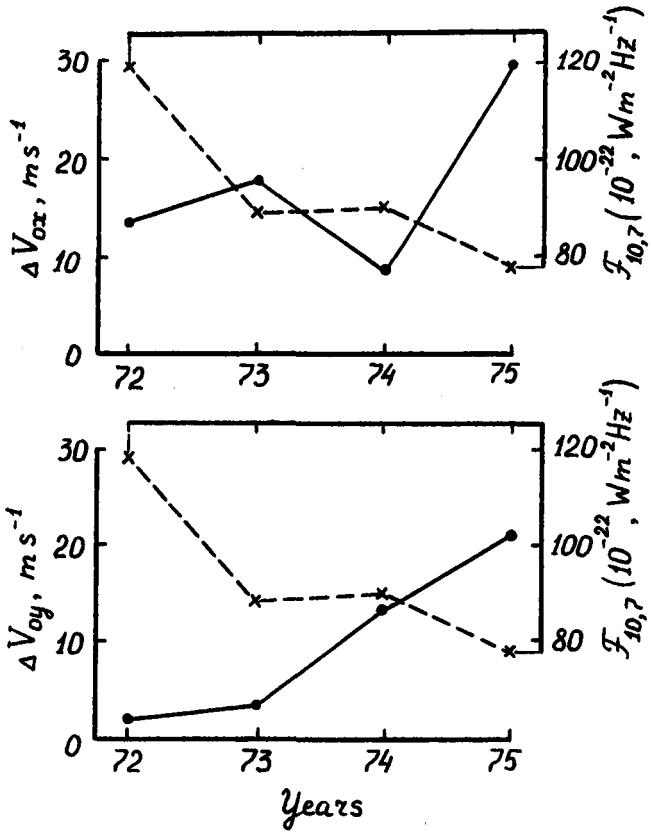

Figure 2. Seasonal averaged variation of ΔV_{ox} and ΔV_{oy} versus variation of $\mathcal{F}_{10.7}$. (Autumn).

SOLAR ACTIVITY INFLUENCES ON ATMOSPHERIC ELECTRICITY AND ON SOME STRUCTURES IN THE MIDDLE ATMOSPHERE

Reinhold Reiter

Former Director of the Fraunhofer Institute for Atmospheric Environmental Research
D-8100 Garmisch-Partenkirchen

INTRODUCTION

This paper is restricted on processes in the troposphere and the lower stratosphere (higher atmosph. see MATSUHITA, 1983). *General aspects of global atmospheric electricity* are summarized in Chapter III of NCR (1986), VOLLAND (1984) has outlined the overall problems of atmospheric electrodynamics, and ROBLE and HAYS (1982) published a summary of solar effects on the global circuit. The solar variability and its atmospheric effects (overview by DONELLY et al, 1987) and the solar-planetary relationships (survey by JAMES et al. 1983) are so extremely complex that only particular results and selected papers of direct relevance or historical importance can be compiled in this article.

A LOOK BACK AT THE HISTORY

BAUER (1925) first suggested a correlation between the electric field (E) recorded from 1902-1922 at 5 stations and the sun spot number. Also GISH and SHERMAN (1936) reported on solar effects in atmospheric electric data. However, ISRAEL (1961/1973) stated that solar influences on atmospheric electricity are unlikely. Of course, sunspot numbers are not the best for such an investigation and long term observations also raise problems. Hence Reiter used solar flares (SF) as ***well defined short term*** solar events. He showed that after flares E and the air earth current (I) increase significantly by 20-60% (REITER 1960, 1964/85, 1969, 1971) when they are recorded on mountain peaks during fair weather and above the mixing layer. These findings have been confirmed by COBB (1967) and SARTOR (1969). Then MARKSON (1971) considered in great detail solar and other extraterrestrial influences on atmospheric electricity and thunderstorms by including also Forbush decreases (FD) in the galactic cosmic rays (GCR) and the sector structure boundary passages (SBP) of the solar magnetic field (based on WILCOX 1965 et al.,1968). MÜHLEISEN (1974) executed an extensive work by applying radiosondes in order to study the long term variation of the electric ionospheric potential (EIP) which was shown to be correlated directly with the relative sunspot number 1963 - 1970.

In conclusion the following viewpoints particularly appeared as to be regarded in further investigations (of course, some more could be drawn):

a) For relevant studies the use of ***short term events*** being well defined by time and intensity and which are clearly linked with the solar activity seem to be most useful: e.g. SF, SBP of the interplanetary magnetic field, solar proton events, behavior of the solar wind and of the corona hole the importance of which has been recognized recently.

b) When studying short term events it is important to consider the respective ***phase of the solar cycle*** at the same time which can strongly modify the feature of the result (see REITER 1979).

c) For investigating solar-atmospheric electrical relations the parameters should be recorded or measured exclusively during ***fair weather*** conditions and ***above the mixing layer*** either on high mountain tops (REITER, COBB, see above) or at very remote islands or polar regions, or by airplane (MARKSON 1976), by balloons (MÜHLEISEN 1974, OGAWA et al. 1967, 1969) and other carriers.

SEVERE CRITIQUE

Critique has been claimed concerning the seriousness of sun-atmosphere investigations. And since atmospheric electricity cannot be separated from the behavior of specific parameters of aeronomy and meteorology all of those have

been lumped together by this concern (e.g. see SHAPIRO 1979 who doubts the work of MARKSON 1971 and of WILCOX et al. 1974, 1976 on the SBP-vorticity index relation). A harsh refusal has been published by GREEN (1979) concerning misconceptions and misinterpretations in the investigations of sun-weather relationships. His reproach has been rather often repeated: lack of physical mechanisms connected with an overvalue of pure statistical associations. Another serious critique has been compiled recently in an extended article by TAYLOR (1986) who reviewed also some work in atmospheric electricity. He mainly points out the controversy and the lack in the work based on SBP and the suggestions of a link between cosmic ray induced changes in the stratospheric ionization rate and thunderstorm activity (MARKSON 1978a, LETHBRIDGE 1981). However, Taylor accepts the results on connections between FD (therefore also SF) and the behavior of atmospheric electrical parameters as well as trigger of stratospheric intrusions (REITER 1977b,1979). He points out that -if successively isolated and explained- external forcing *of short term variations in the dynamics* of the lower atmosphere would be of major accomplishment.
Another review of results of sun-atmosphere investigations has been given by EDDY (1983) which is still worth mentioning also today: no equivocal connection between solar variations and meteorological processes has yet been established. It must be made clear that studies of solar perturbations and their influences on the lower atmosphere are undeniably a proper part of *atmospheric physics in general*. Eddy concludes with three general ***recommendations*** the importance of which is still unchanged: (a shortened version)
a) The question of possible solar influence on special atmospheric phenomena must be treated within the general framework of solar-terrestrial physics and atmospheric science. Facts of adjoining disciplines must be fully regarded.
b) More effort should be devoted to the development of physical models and mechanisms.
c) The data base on which all the studies rest should be expanded and strengthned. This needs apart of an enhanced and improved monitoring of all important parameters describing the solar activity also measurements of solar-induced perturbations in the upper, middle and lower atmosphere. Electric and magnetic fields and their changes by the incidence of solar particles should be included.
Here, obviously, the overall criticism turns over in valuable recommendations which should be accepted and applied without reserve.

SOME OF THE RECENT INVESTIGATIONS OF IMPORTANCE

HOLZWORTH and MOZER (1979) found a direct evidence of solar flare modification of stratospheric electric fields. FISCHER and MÜHLEISEN (1980) reanalyzed their data on the EIP and found an influence of the SBP. TAKAGI et al. (1984) also found an effect of SBP (only for -/+) on the fair weather electric field on the earth's surface. He furthermore discussed the influence of cosmic ray variations on the EIP, the currents from thunderstorms and on I. However, he erroneously explained the SF effect by enhanced solar protons and attributed the variation of the GCR to the solar activity in general. It is a matter of fact that the SF effect is mainly based on the FD in the GCR and that energetic solar protons which reach the lower atmosphere are extremely rare and do normally not appear in connection with a flare except of very rare cases. Also OLSON (1983) tried to interpret the solar influence on the atmospheric electrical parameters. MEYEROTT et al. (1983) analyzed long term measurements (10 years) of the EIP but found no correlation with variations of the GCR intensity. However, the EIP seems to be better correlated with the stratospheric aerosol burden caused by volcanic eruptions (REITER 1986 et al., OLSEN 1983). This again is a hint showing that long term investigations are not a reasonable basis for solar-terrestrial studies.
Here some remarks on suggestions by MARKSON (1974, 1978b, 1981, 1983) are required. He claimed that a direct influence of solar events on the current between the ionosphere and the earths surface exists. Those, so MARKSON argues,

liberate cosmic rays which reduce also the columnar resistance above each thunderstorm. By this way the upward electric current of positive charges being accumulated on top of the thundercloud by the charge separation processes is enhanced and the generators put more charge onto the ionosphere. However, only in very rare cases (f.e. see the event in August 1972) solar protons have such a high energy that they can penetrate down to the lower stratosphere. After SF normally the FD occurs and the ionization rate in the lower stratosphere and upper troposphere drops. But this is the inverse effect compared with MARKSON's model. Finally it may be pointed out that some competent ***reviews on solar-terrestrial relationships*** have been published recently: ROBLE and HAYS (1982), NEWELL (1984), and ROBLE and TZUR (1986). These reviewers agree with the claim of solar effects on E and I and on stratospheric intrusions published by the author.

THEORETICAL CALCULATIONS AND MODELING

A new era appeared with the theoretical treatment of atmospheric electrical data. ROBLE and HAYS (1979), TZUR et al. (1983), TZUR and ROBLE (1985), ROBLE (1985) and ROBLE and TZUR (1986) were successful in a mathematical modeling of the global atmospheric electric circuit and they could show that their results are in concordance with experimental results by REITER, COBB, and others. MAKINO and OGAWA (1983, 1984) also calculated the pattern of the global circuit based on assumptions of the global thunderstorm distribution. They confirmed the effect of solar flares on E and I (found by REITER 1960, 1964 and COBB 1967) quantitatively by incorporating the influence of the FD in 57.5°N on the stratospheric ionization rate (Fig.1d).

RESULTS RECENTLY OBTAINED

Fig.1 shows the departures of E and I from the mean fair weather values (in %) some days before, during and after SF events. Fig.1a recalls the finding by COBB (1967). Figs.1b, 1c show the result by Reiter as it appears when a new series of data (1977-1981) is added to the former (REITER 1971) of 1967-1971. There is no doubt that this extension over now 2 solar cycles (No.20, 21) sufficiently confirms the previous results. The departures of E and I from the mean fair weather values during solar quiet are more than 3σ and consequently significant. Fig.1d shows the theoretical result by MAKINO and OGAWA (1984) for 3 km altitude (=Zugspitze station). They calculated the departures of E and I after SF based on the FD in the GCR for 57.5°N as expected in the mean. MAKINO and OGAWA state: *these results are consistent with the features of Reiter's observation.* By this way the recommendations b) and c) by EDDY (1983) are realized: the amount of data was increased and the primary result could be confirmed. A reasonable physical mechanism has been established by independent investigators.

Although the applicability of SBP in solar-terrestrial investigations has yet not been finally accepted, the results of two independent studies based on SBP dates (by SVALGAARD 1976) are shown in Fig.2a. In the case of a passage of the typ -/+, E and I measured on Zugspitze Peak in 3 km a.s.l. significantly depart (REITER 1976, 1977a) from the fair weather mean by +15 to +20% showing a maximum in the +2 day. In the same figure the E and I values are overlaid by the daily mean concentration of the isotope Be7 (halflife time 53 days) in the air at the same station. Be7 is constantly produced in the lower stratosphere in 20-27 km by nuclear reaction of cosmic rays with air molecules and its concentration in the upper troposphere is normally rather low. However, by each intrusions of stratospheric air through the tropopause near a folding, Be7 significantly increases also in 3 km altitude and indicates an intrusion confidently (REITER et al. 1971, REITER 1977b, 1979). Fig.2a consequently shows that the increase in E and I after SBP is coupled with an enhancement of stratospheric intrusions. Fig. 2b confirms that this is significantly linked with the solar activity: at the same time when the FD is initiated (drop in the neutron density, upper panel of 2b) the concentrations of Be7 strongly increa-

ses (the weak drop of the GCR intensity during a FD has no direct influence on the Be7 generation). This coupling of E,I effects with stratospheric dynamics is in accordance with recommendation a) by EDDY (1983). The trigger by solar events of dynamic processes in the lower stratosphere also appears by considering the day by day variations of the stratospheric O_3 pattern. Fig.3 shows one example (for more see REITER 1983). From March 10 to March 19 (Fig. 3b) a FD lasted and during the same sequence the initially normal and rather smoothed stratospheric O_3 profile became totally scattered (3a): a complex overlay of stratospheric and tropospheric air strata above the tropopause occurred (for more details see REITER 1983).

Using the values of 480 O_3 radiosonde flights during 37 sequences with 8 - 30 day by day ascents along the solar cycle No. 21 and the 35 cases of well established FD, the scatter (σ^2) of the stratospheric O_3 values before, during and after the FD has been calculated (Fig. 4a). From the -2 day to the key day the value of scatter increases significantly and then it consistently drops. The increase of the O_3 scatter on the key day amounts more then 2 times of its standard deviation (sigma in Fig. 4a).

By using the same key days, also a significant (compare sigma values) change in the tropopause height on and after the FD is shown (4b): it drops in the average by 40 hPa. Also these results confirm the importance of the GCR for solar-terrestrial studies of the stratospheric dynamics in accordance with TAYLOR (1986). In this case the GCR may have the character of an indicator of important short term solar events. Here also the work of NEUBAUER (1983) should be mentioned. He demonstrated solar impacts on dynamic processes in the lower stratosphere which corroborate the findings shown in Figs. 3 and 4.

Last but not least a recent result of recordings (E, I, air conductivity, all meteorological parameters) executed at a new private mountain station in 1780 m a.s.l. should be mentioned (Fig. 5). During an exceptional and long lasting fine weather period in January 1989 three strong and one heavy solar flares (imp.3b) occurred during which the station was constantly above the mixing layer. Fig. 5b shows the behavior of the 10 cm flux, of the GCR intensity and the flare calendar. A FD occurred on 16 January and the 10 cm flux showed a peak at the same day. A magnetic storm was reported for January 20. From January 17 to 18, E and I increased remarkably and remained until 21 January by 30 - 70 % higher than the fair weather mean. This is a single event being consistent with the results obtained statistically and demonstrated in Fig.1.

REFERENCES

BAUER, L.A., Correlations between solar activity and atmospheric electricity. Terr. Magn. and Atmosph. Electr. 30, 17, 1925.

COBB, W.E., Evidence of a solar influence on the atmospheric electric elements at Mauna Loa observatory. Monthly Weather Rev. 95, 12, 1967.

DONELLY, R.F. et.al., Solar variability and its stratospheric, mesospheric, and thermospheric effects. J. Geophys. Res. 92, 795-914, 1987.

EDDY, J.A. An historical review of solar variability, weather and climate. In: B.M.McCormac, Weather and climate responses to solar variations, Colorado Associated University Press, 1983.

FISCHER, H.J. and R. MÜHLEISEN, The ionospheric potential and the solar magnetic sector boundary crossings. Rept. Astron. Inst. Univ. Tübingen FRG, 1980.

GISH, O.H. and K.L. SHERMAN, Electrical conductivity of the air up to an altitude of 22 km. Nat. Geogr. Soc. Stratosphere Ser., 2, 94-116, 1936.

GREEN, J.S.A., Possible mechanisms for sun-weather relationships. J. Atmos. Terrest. Phys., 41, 765-770, 1979.

HOLZWORTH, R.H. and F.S.MOZER, Direct evidence of solar flare modification of stratospheric electric fields. J. Geophys. Res. 84, 363-367, 1979.

ISRAEL, H. Atmosphärische Elektrizität, Akadem. Verlagsges. K.G., Leipzig 1961; engl. version: Atmospheric Electricity, Israel Progr. Sc. Transl. 1973

JAMES, D.E. (Edit.), Solar-Planetary Relationships: Aeronomy. Reviews Geophys. and Space Phys., 21, 215-520, 1983.

LETHBRIDGE, M.D., Cosmic rays and thunderstorm frequency. Geophys. Res. Lett. 8, 521-522, 1981.
MAKINO, M. and T. OGAWA, Interpretat. of the solar flare modificat. of atmospheric electr. field and air-earth curr. In: Weather and climate responses to solar variations, Colorado Associated University Press 1983.
MAKINO, M. and R. OGAWA Responses of atmosph. field and air-earth current to variat. of conduct. profiles. J.Atmos. and Terrest. Phys. 46, 431-445, 1984
MÜHLEISEN, R., The global circuit and its parameters. In: H. Dolezalek and R.Reiter (Edit.) Electrical proc.in atmospheres, Steinkopff, Darmstadt, 1974
MARKSON, R., Considerations regarding solar modulat. of geophys. parameters, atmospheric electricity and thunderstorms. PAGEOPH, 84, 161-202, 1971.
MARKSON, R., Solar modulat. of atmospheric electrificat. through variat.of the conductivity over thunderst. In: Proc. NASA Sympos. on Possible relationships betw. solar act. and meteorol. phenomena, W.R.Bandeen (Edit.) 1974.
MARKSON, R., Ionosph. potential variations obtained from aircraft measurem. of potential gradient. J. Geophys. Res. 81, 1980-1990, 1976.
MARKSON, R., Solar modulations of atmospheric electrification and possible implications of sun-weather relationship. Nature, 273, 103-109, 1978.
MARKSON, R., The role of atmospheric electricity in sun-weather relationships. Proc. ONR workshop on solar-terr. weather relations, Minneapolis, MI, 1981.
MARKSON, R., Solar modulation of fair-weather and thunderstorm electrification In: Weather and climate responses to solar variat., Colorado Ass.Press 1983.
MATSUSHITA, S. Electric currents and potent.in the upper atmosph. produced by solar variat. In: Weather and clim. respons...Colorado Ass. Univ. Press 1983
MEYEROTT, R.E. et al. On the correlation between ionosph. potential and the intensity of cosm. rays. In: Weather and climate resp....Colorado Press 1983
NCR, Nat.Res.Council, Studies in geophysics, Nat. Acad. Press Washington, 1986
NEUBAUER, L., Sudden strat. warmings correlat. with sudden commencements. Weather and Climate response to solar variat. Colorado Ass. Press 1983.
NEWELL, R.E., Implications of sun-weather relationships for atmos. electricity In: Proc. VII Int. Conf. on Atmosph. Electricity, AMS, Boston, MA, 1984.
OLSON, D.E., Interpret. of the solar influence on the atmos. electrical parameters. In: Weather and climate resp.to solar variat. Colorado Press 1983.
OGAWA, T. and Y. TANAKA, Balloon measurements of atmosph. electr. potential gradient, J. Geomag. and Geoelectr. 19, 307-315 (1967).
OGAWA, T. et al., Measurements of atmosph. electr. field, current and conductivity in the stratosph. Inst. Space Aeronomy Sci. Univ. Tokyo 1969
REITER, R., Relationships between atmos. electric phenomena and simultaneous meteorological conditions. Final Rep, USAF Contract AF 61 (052)-55 1960.
REITER, R., Fields currents and aerosols in the lower troposphere. German ed. Steinkopff Darmstadt 1964, english edit. Amerind Co. New Delhi 1985
REITER, R., Solar flares and their impact on pot. gradient and air-earth current at high mountains. PAGEOPH, 72, 259, 1969.
REITER, R., Further evidence for impact of solar flares on potential gradient and air-earth current at high mountains. PAGEOPH, 86, 142-158, 1971.
REITER, R., The electric potential of the ionosphere as controlled by the solar magnetic sector structure. Naturwissenschaften, 63, 192, 1976.
REITER, R. The electr.potential of the ionosph.as controlled by the sol.magn. sect.struct.studies over one solar cycle. J.Atm.Terr.Phys. 39, 95-99, 1977a.
REITER, R., Stratospheric-tropospheric exchange influenced by solar activity. Results of a 5 year study. Arch. Met.Geophys.A. 26, 127-154, 1977b.
REITER, R., New results regarding the influence of solar activity on the stratospheric-tropospheric exch. Arch.Met.Geoph.Biokl. A, 28, 309-339, 1979.
REITER, R., Modification of the stratospheric ozone profile after acute solar events. In: Weather and climate responses.. Colorado Ass. Univ. Press 1983
REITER, R., et al. Results of 8-year measurements of aerosol profiles in the stratosph., effects on global climate. Meteor. Atmos.Phys. 35, 19-48, 1986
ROBLE, R.G., On solar-terrestrial relationships in atmospheric electricity, J. Geophys. Res., 90, 6000-6o12, 1985.

ROBLE, R.G. and P.B. HAYS, Electrical coupling between the upper and lower Atmosphere. In: Solar-Terr.Influences on Weather + Climate, D.Reidel, 1979.
ROBLE, R.G. and P.B.HAYS, Solar-terrestrial effects on the global circuit In: Studies in Geophysics, Nat. Res. Council, Washington D.C. 1982.
ROBLE, R.G. and I. TZUR, The global atmospheric-electrical circuit In: Studies in Geophysics, Nat. Res. Council, Washington D.C.,1986.
SARTOR, J.D., Solar flares and high-altitude electric fields and conductivity, AGU National Fall Meeting, San Francisco, 1969.
SHAPIRO, R., An examination of certain proposed sun-weather connections J. Atmosph. Sciences, 36, 1105-1116, 1979.
SVALGAARD, L., Interplanetary Sector Structure 1947-1975, SUIPR Rept.648,1976
TAKAGI, M. and A. IWATA, Solar influence on the earth's electric field. Proc. VII International Conference on Atm. Electr. AMS, Boston, 1984.
TAYLOR, H.A., Selective factors in sun-weather research, Rev. Geophys. 24, 329-348, 1986.
TZUR, I. and R.G. ROBLE, The interaction of a dipolar thunderstorm with its Global electrical environment. J. Geophys. Res., 90, 5989-5999, 1985.
TZUR, I. et al., The response of the earth's global electrical circuit to a solar proton event. In: Weather and Climate response.. Colorado Press 1983.
VOLLAND, H., Atmospheric electrodynamics. Springer-Verlag, Berlin, 1984.
WILCOX, J.M., The interplanetary magnetic field, solar origin and terrestr. effects. Space Sci. Rev., 8, 258-328, 1968.
WILCOX, J.M. and N.F. NESS, Quasi-stationary corotating structure in the interplanetary medium. J. Geophys. Res., 70, 5793-5805, 1965.
WILCOX, J.M. et al., Influence of solar mag. sector structure on terrestrial atmosph. vorticity. J Atmos. Sci. 31 581-588, 1974.
WILCOX, j.M. et al., On the reality of a sun-weather effect. J. Atmos.Sci. 33, 1113-1116, 1976.

FIGURE 1

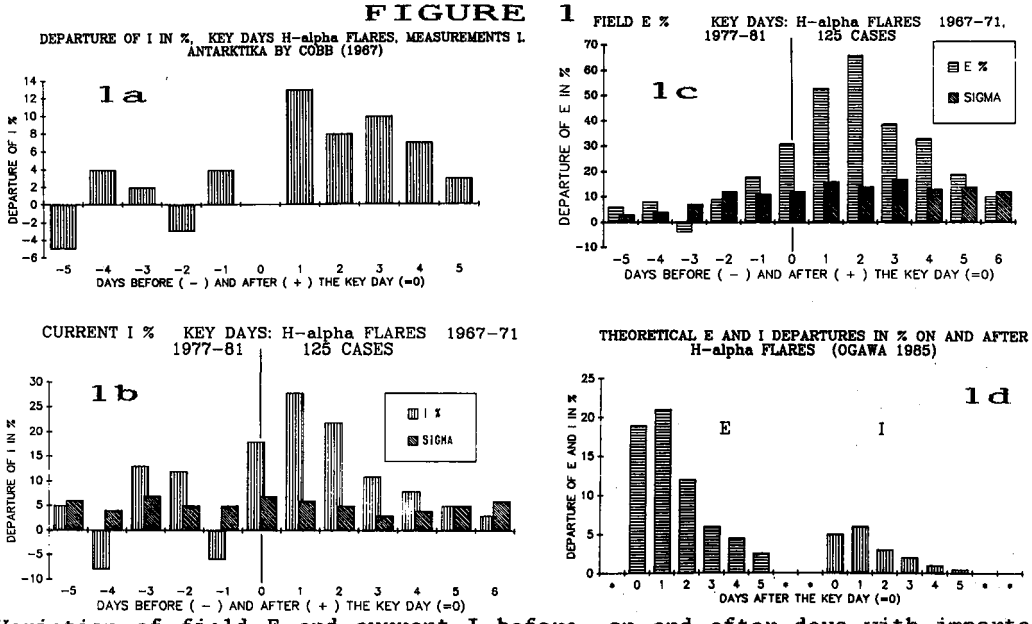

Variation of field E and current I before, on and after days with important and isolated solar flares (= key day 0).
a) The result by COBB (1967) based on I measurements at Mt. Mauna Loa.
b) and c) Recordings by REITER on Zugspitze Peak (2964 m a.s.l.) during fair weather. Data of 1967-1971 (REITER 1971) have been updated by new ones of 1977-1981. Departure of E and I in % from mean fair weather level = 0%. Number of key days = 125. Sigma = standard deviation.
d) Theoretical result by MAKINO and OGAWA (1984) confirming a), b) and c).

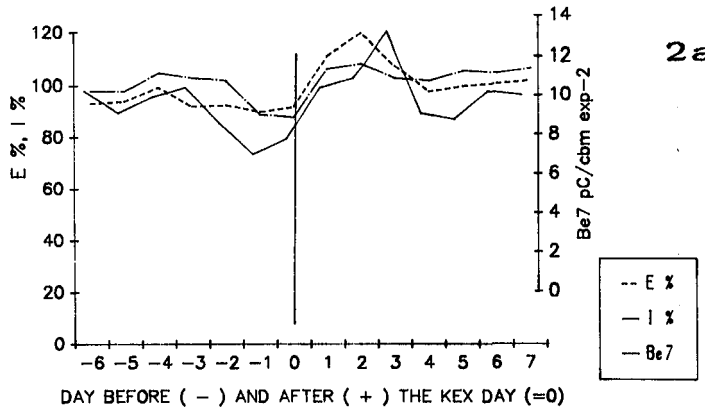

2a

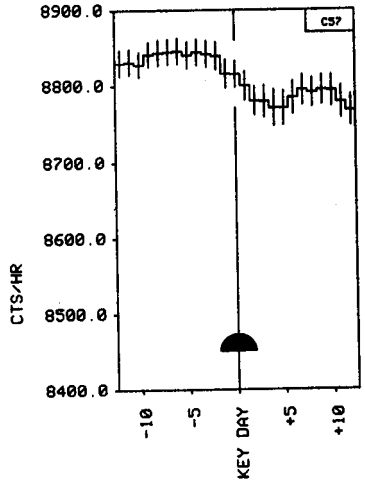

2b

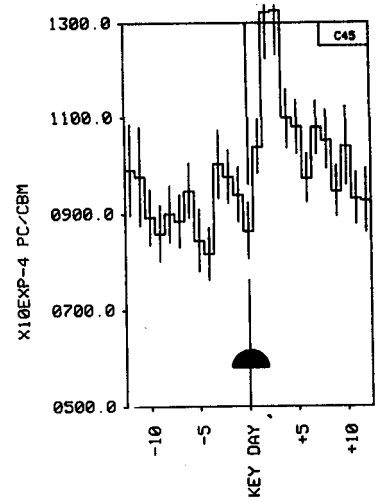

KEY DAY: ↑ H_α FLARES

FIGURE 2

a) Behavior of E, I, and Be7 concentration (all measured on Zugspitze in 2964 m a.s.l.) before and after days (in total 80) with sector structure boundary passages of type: > −/+ >

b) Variation of the galactic cosmic ray intensity (counts/hr) and of the Be7 concentration before, during and after solar flares (total: 60 key days)

FIGURE 3

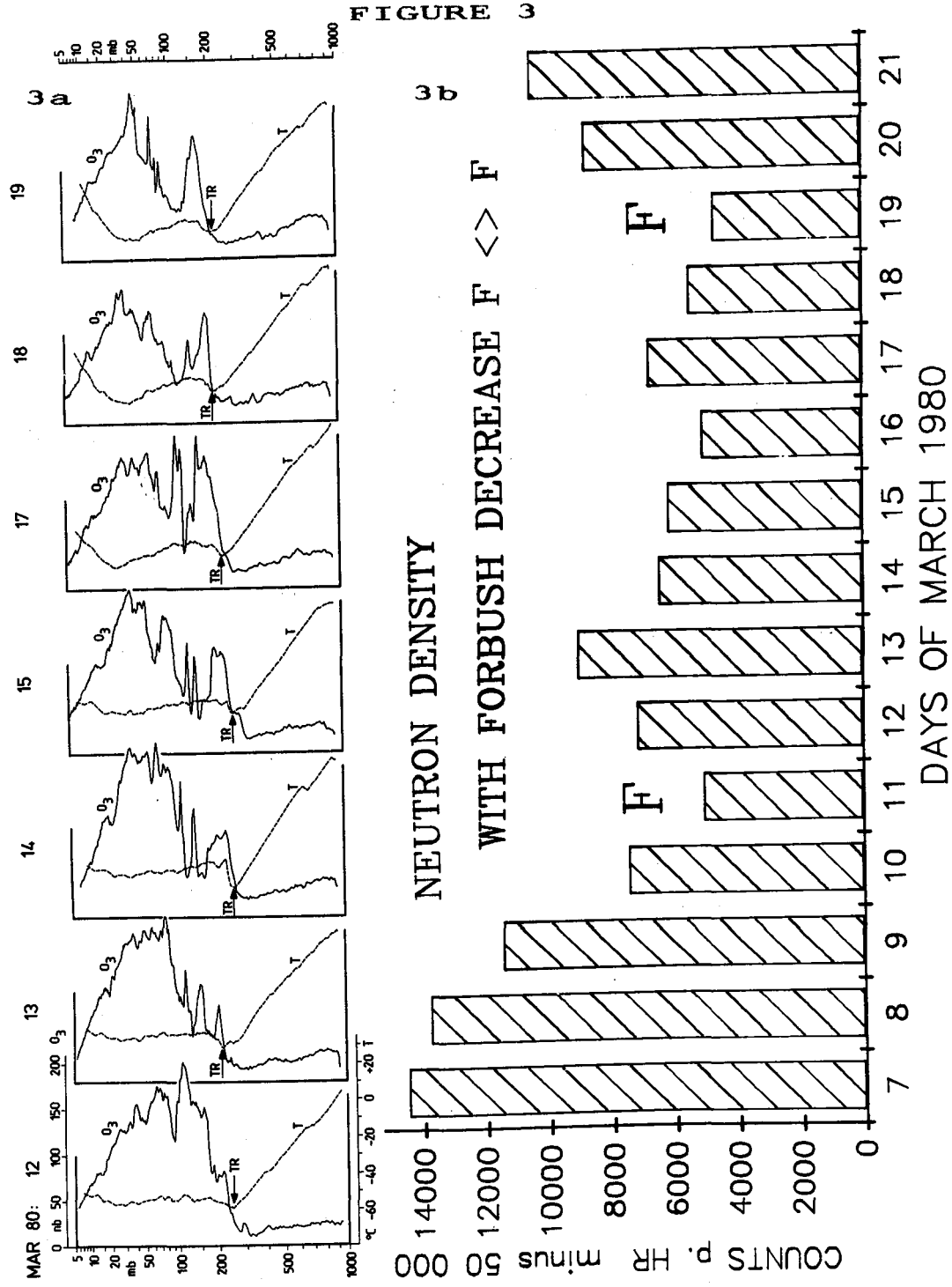

a) Daily stratospheric O_3 and temperature (T) profiles obtained by radiosonde during a sequence of 7 days.
b) mean daily neutron densities from March 7 until March 21, 1980. A strong Forbush decrease was reported from March 10 to March 19.

FIGURE 4

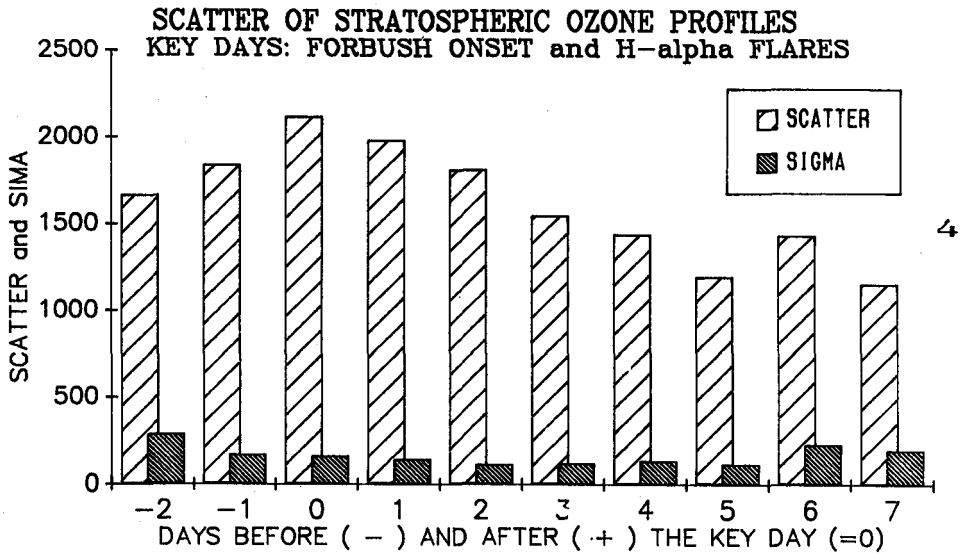

4a

4b

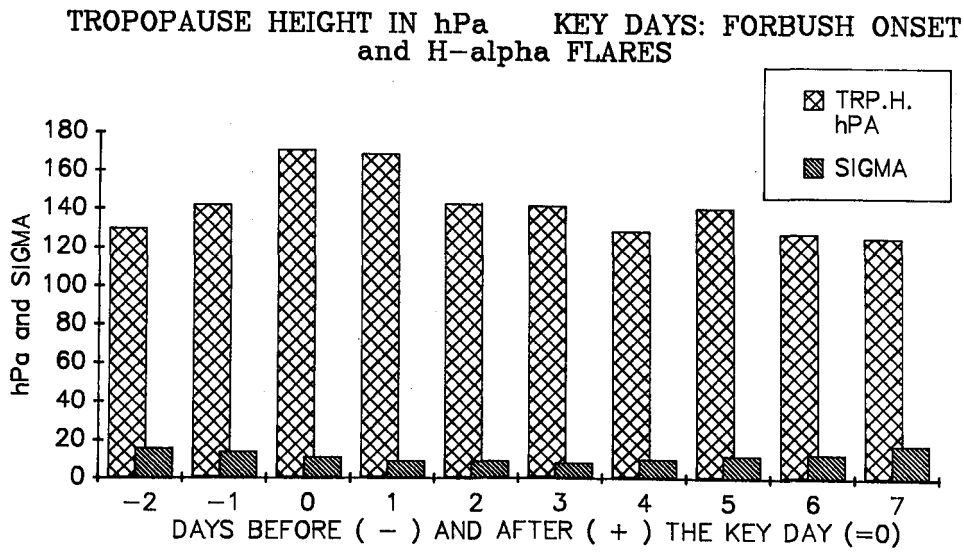

a) The scatter (σ^2) in the stratospheric O_3 profiles of 35 sequences of day by day radiosonde ascents superimposed before, on, and after key days with a significant Forbush decrease. Sigma is the standard deviation of the scatter value.

b) Departure of the tropopause height expressed in hPa, data based on the same radiosonde ascents and key days as in a).

FIGURE 5

FIELD AND AIR EARTH CURRENT, 100 % = FAIRE WEATHER MEAN

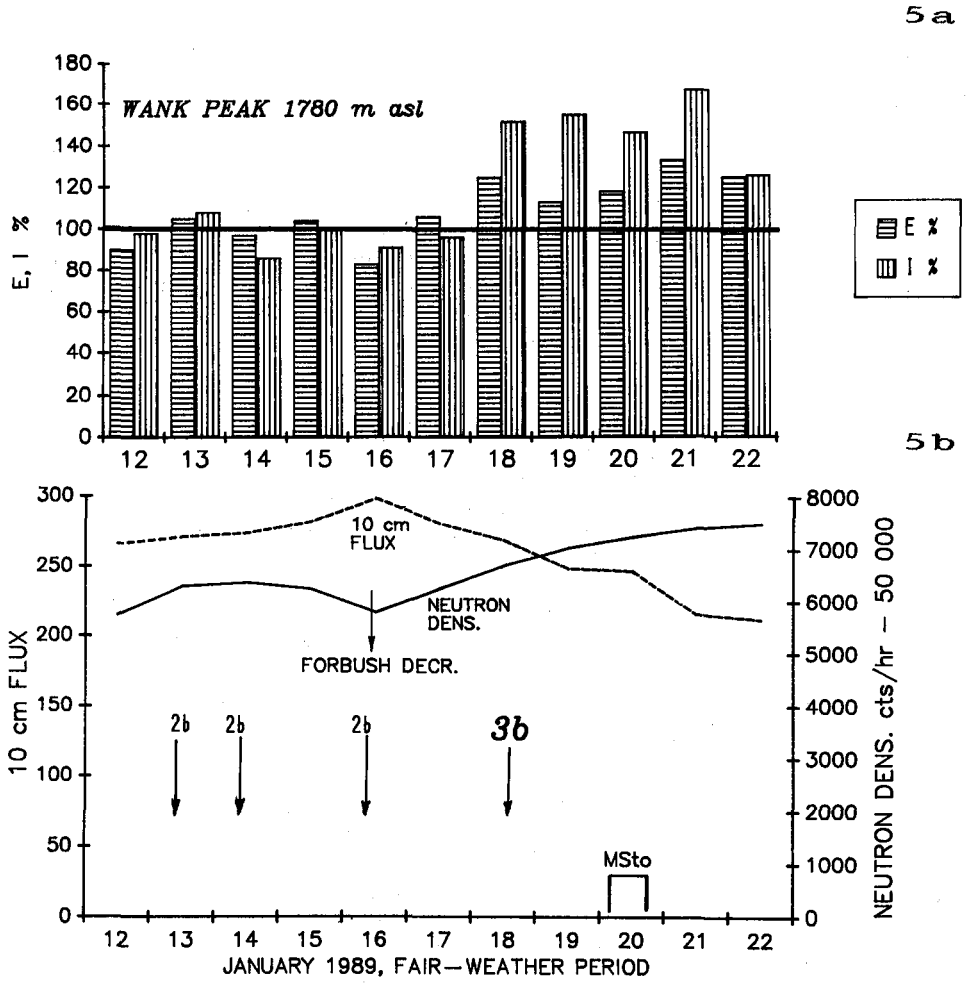

a) Daily mean values of E and I recorded on a mountain top in 1780 m a.s.l. in January 1989. The values are expressed in % of the mean fine weather data without solar events (set = 100%, heavy line).
b) Daily mean values of the 10 cm flux and the galactic cosmic ray intensity on the same days. Solar flares of importance 2b and 3b are inserted.
MSto = magnetic storm.

MEASUREMENTS OF MESOSPHERIC ELECTRIC FIELD UNDER VARIOUS GEOMAGNETIC CONDITIONS

A.A.Tyutin, A.M.Zadorozhny

Novosibirsk State University, USSR

The results of measurements of electric field strength in the mesosphere are given for high and middle latitudes. At high latitudes, there is observed a distinct dependence of the height profile of electric field on the geomagnetic disturbance level.

RELATIONSHIP BETWEEN SOLAR ACTIVITIES AND THUNDERSTORM ACTIVITIES IN THE BEIJING AREA AND THE NORTHEAST REGION OF CHINA

Hong C. Zhuang and Xi C. Lu

Institute of Space Physics, Academia Sinica
P. O. Box 8701, Beijing, China

ABSTRACT

An analysis of the relationship between the IMF section boundary crossing, solar flares, the sunspot eleven-year cycle variation and the thunderstorm index is given, using the superposition epoch method, for data from more than 13,000 thunderstorms from 10 meteorological stations in the Beijing area and the Northeast region during 1957 to 1978. The results show that for some years a correlation exists between the thunderstorm index and the positive IMF section boundary crossing. The thunderstorm index increases obviously within three days near the crossing and on the seventh day after the crossing. The influence of the crossing on thunderstorms is stronger in the first half year than the latter half year. For different classes of solar flares, the influences are not equally obvious. The solar flares which appeared on the west side, especially in the western region (from 0° to 30°) have the most obvious influence. There is no discernible correlation between the thunderstorm index and the sunspot eleven-year cycle.

INTRODUCTION

As early as AD 187 there was a written record of the correlation between solar activities and meteorology in an ancient Chinese book: " there is a black color as large as a melon within the Sun. When the Sun becomes black, the water on the ground will be flooding. " It indicates a correlation between the peak of the sunspot and floods. Recently there is a number of statistical data analyses in China on floods and droughts, precipitation, characteristics of rains, water flow of rivers and water levels of rivers and lakes and so on, which reveal certain correlations with solar activities. As usually realized, annual precipitation is, to a certain extent, linked with thunderstorm activities. Thunderstorms are phenomena of atmospheric electricity. In order to understand the physical mechanism of the correlation between solar activities and meteorological phenomena such as precipitation, several ways have been proposed through which the effects of solar activities can transport into the lower atmosphere and give some impact upon meteorological phenomena. Atmospheric electricity is one of the most possible ways. The possible picture seems like this. Solar activities may influence the environment of atmospheric electricity. Atmospheric electrical properties may influence the formation of thunderstorms, and then influence the annual precipitation and other related meteorological phenomena.

In China we have systematic collections of thunderstorm data for the whole country covering more than a million square km over the last 20 years. These data are very unique for analyzing the correlation with solar activities. The work shown here was done in 1986, based on data of 10 basic meteorological stations in Beijing and the Northeast regions. These areas are not the most frequent thunderstorm regions, but there were still about 13,000 thunderstorms during the 19 years from 1957 to 1978.

CALCULATION

The superposition epoch analysis is used to analyze the correlation between the Interplanetary Magnetic Field (IMF) section boundary crossing, solar flares and the index of thunderstorms. The definition of the index of thunderstorm τ is: $\tau = (f - \bar{f}) / s$, where f is the number of thunders per day; $\bar{f}$ is the average value of f of the same epoch days included in the superposition analysis; s is the standard mean deviation of the fluctuation of f for each epoch day.

During the analysis, different classes of data were divided according to different situations, such as: for different years, i.e., the first half year (from April to June), the latter half year (from

July to October), and the whole year; for different solar activity levels, i.e., high activity years (57-59, 68-70), low activity years (63-65, 57-77), ascending years (65-67) and descending years (59-63, 70-75); for different polarities of the section boundary, i.e., positive boundary (the direction of IMF being away from the Sun turns toward the Sun), and negative boundary (IMF toward the Sun turns away from the Sun); for different locations of solar flares on the solar disk, i.e., six regions as E1 (0° - 30° east of the central meridian of the solar disk), E2 (30° - 60° east), E3 (60° - 90° east), W1 (0° -30° west of the central meridian of the solar disk), W2 (30° - 60° west), and W3 (60° - 90° west); for different durations of the solar flares, i.e., shorter than 1.5 hours and longer than 1.5 hours; for different brightness of the solar flare, i.e., bright flare and non-bright flare, and so on.

RESULTS

(A) IMF Section Boundary Crossing

For whole year data, about one third of the thunderstorm index shows a discernible correlation with the boundary crossing, being much more obvious for positive boundary than negative boundary.

Figure 1 shows some examples of the superposition epoch which shows the correlation between the index of thunderstorm frequency and the positive boundary crossing of interplanetary magnetic field sections. The upper two panels are Northeast data from 4 stations in 1968 and 1976. N is the number of total cases. Dotted lines are confidence level of 1%. Figure 2 is for negative boundary crossing. The lower two panels are the Northeast region. The upper three panels are the Beijing region.

(B) Solar Flares

Figure 3 shows an example of the superposition epoch curve of the thunderstorm index with respect to solar flares. The key days are solar flare burst days. For all cases of the east region solar flare, both the northeast region and the Beijing region the correlation exists only for a bright flare whose duration t is less than 1.5 hours and appears in the east region 2 of the solar disk. For the west region solar flare, region W1 is the most obvious region in which the solar flare will seemingly influence thunderstorm frequency.

CONCLUDING REMARKS

Having conducted all the superposition analyses for the different classes of data, we will summarize our impression about the correlation between thunderstorms and solar activity, including the IMF boundary crossing as follows:

1. The influence of magnetic boundary crossings on thunderstorm frequency is rather weak. Only a few years' data show an increase of thunderstorm frequency within 3 days or 7 days after the positive boundary crossing. Almost no influence after a negative crossing.
2. The influence of solar flares on thunderstorms is rather obvious. The thunderstorm frequency experiences a discernible enhancement after the flare burst, especially for the flare which appears in the west and especially in region W1 of the solar disk.
3. Statistics for the first half and the latter half year data show that the influence of the latter half year solar flare is stronger than the first half year flare.
4. The correlation between sunspot number and thunderstorm frequency is not discernible.
5. The results of the correlation statistics for different cases are different; for the Northeast and Beijing regions are also different. The results from our data are not identical with other authors. These facts show that the influence of solar activities on thunderstorms may be affected by local meteorological conditions.

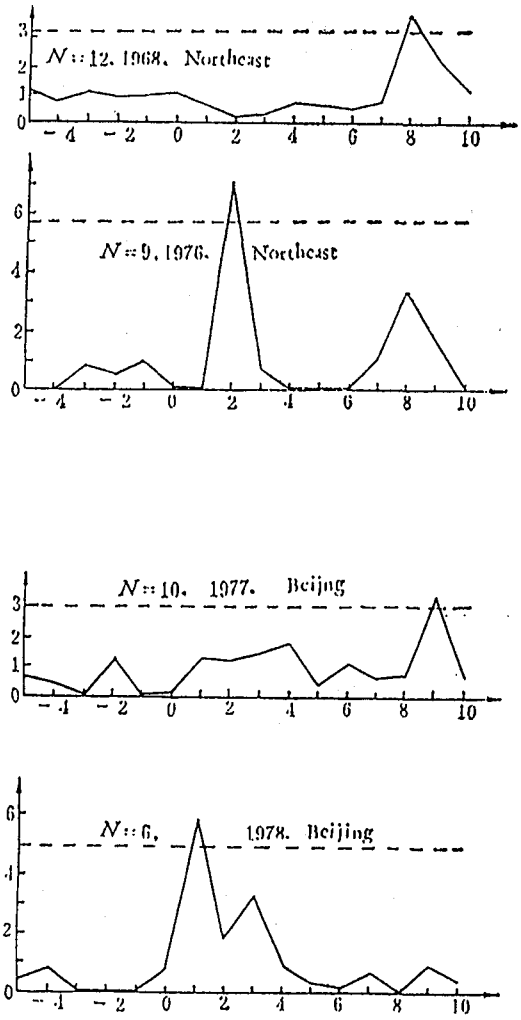

Figure 1. Superposition epoch analysis of thunderstorm index to positive IMF section boundary crossing.

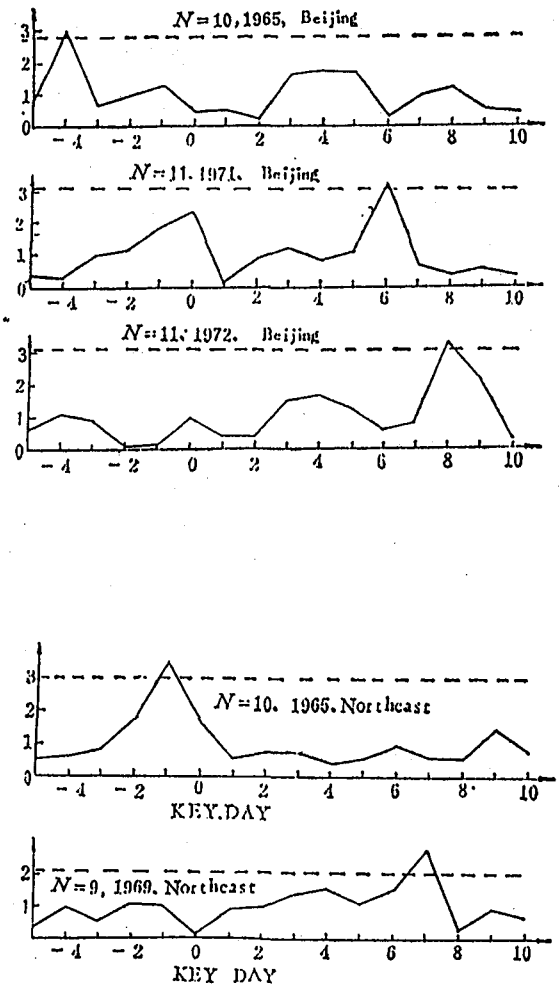

Figure 2. Superposition epoch analysis of thunderstorm index to negative IMF section boundary crossing.

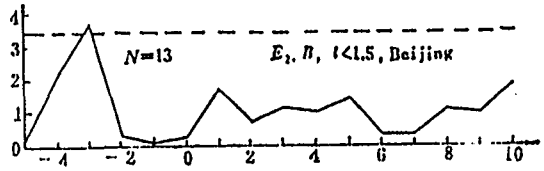

(a)

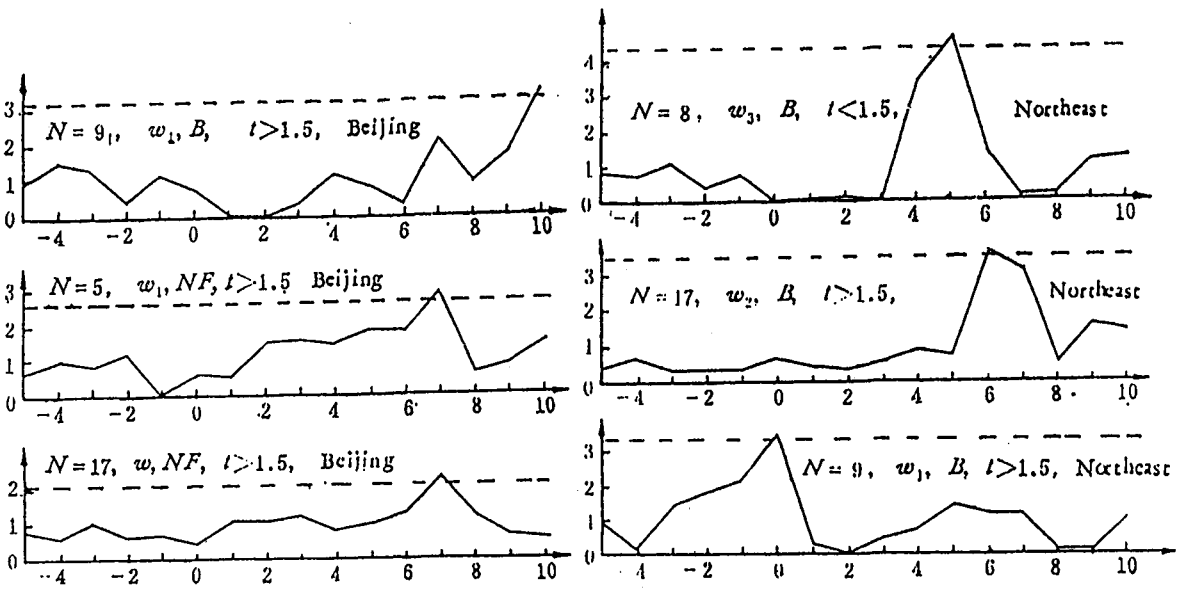

(b)

Figure 3. Superposition epoch curves of thunderstorm index to solar flare burst day. (a) appeared on the east side; (b) appeared on the west side.

GENERAL OVERVIEW OF THE SOLAR ACTIVITY EFFECTS ON THE LOWER IONOSPHERE

A.D.Danilov

Institute of Applied Geophysics,
Glebovskaya, 20-b, Moscow, I07258, USSR

Abstract

Solar activity influences the ionospheric D - region. That influence manifests both in the form of various solar induced disturbances and in the form of the D - region dependence on solar activity parameters (UV-flux, interplanetary magnetic field, solar wind ets) in quiet conditions. Relation between solar activity and meteorological control of the D region behaviour is considered in detail and examples of strong variations of aeronomical parameters due to solar or meteorological events are given.

The question of solar activity (SA) influence on the ionospheric D-region is not as simple as it might look at the first approach. The matter is, that D-region as well as the whole ionosphere occurs as a result of the ionization process in the terrestrial neutral atmosphere which in its turn is completely controlled by the sun. Thus, considering solar activity influence on the D-region one has to distinguish direct effects, when this influence comes through variations of ionizing agents (electromagnetic, or corpuscular), and indirect ones, when solar activity alters the state of neutral medium, which leads to corresponding changes in the state of the ionized component.

The direct effects are more obvious and easy to understand. They come from the fact that the electron concentration $[e]$ which we consider as the most important characteristic of the D-region is defined (in quazi-equilibrium conditions) by

$$q = [e] \cdot \alpha_{eff} \qquad (I)$$

q being the ionization rate and α_{eff} - effective recombination coefficient. All the direct effects of SA on the D-region are contained in q even though α_{eff} may vary and be dependent on SA through indirect effects.

Thus, it is worth briefly considering the ionization sources in the D-region and discussing their variations with SA. It is well known that most part of the D-region ionization is due to solar Layman-α emission interacting with nitric oxide molecules. Layman is considered as a stable enough emission. Its variations during the whole solar cycle lie between $3 \cdot 10^{11}$ and $6 \cdot 10^{11}$ photons cm^{-2} s^{-1} (SIMON, 1982). According to review (NUSINOV, 1987) various authors accept for $L\alpha$ - variations from minimum to maximum SA values of 30-100%. These variations are much smaller, than uncertainities (and probably - variations)of NO-concentrations at the D-region heights. Thus, one should not expect well pronounced variations of the D-region behaviour with SA due to Ly-α variations. The other sources of the D-region

ionization are X-rays ($\lambda \leq 3.0$ nm), galactic cosmic rays and solar emission with λ = I02.7-III.8 nm (the latter ionizing only excited O_2 ($^1\Delta_g$) molecules). Variations of I02.7-III.8 nm emission do not essentially exceed that of Ly-α (see Table I) so we hardly have here a source of strong D-region variations during SA-sycle. Variations of the galactic cosmic rays with solar activity are well known. Ionization rate q due to cosmic rays in the D-region during solar minimum is nearly twice that during solar maximum.

Table I

Amplitude of maximum to minimum SA (M/m) variations of various ionization sources

Source	Ly-α	I02.7-III.8nm	X-rays	Cosmic rays
M/m	I.3-2	2-2.5	5-I0	0.6
Ref.	(NUSINOV,I987)	(HINTEREGGER, I98I)	(BANKS and KOCKARTS, I974)	(BRASSEUR and SOLOMON,I984)

The most changeable ionizing agent in the D-region is X-rays. Variations of its intensity during solar cycle depends on wavelength and generally are strong enough. The values of X-ray flux for λ = 4.I - 3.I nm and levels of SA (very quiet, quiet, moderate, high) according to BANKS and KOCKARTS (I973) are 7.5 $I0^6$, I.5 $I0^7$, 3.0 $I0^7$ and 4.5 $I0^7$ $cm^{-2}s^{-1}$.

Fig. I shows q - values in the D-region due to various ionization sources and their possible variations from minumum SA(m) to maximum SA(M). It is seen that even during high SA the imput of X-rays in the ionization rate q is small in the most part of the D-region. That means that we should hardly expect regular changes of the D-region ionization rate during SA cycle stronger than variations of Ly-α intensity.

Looking at formula (I) we see that the latter means that we should expect $[e]$ variations with the amplitude of I.I5-I.4 if there is a quadratic recombination law (α_{eff} is constant at fixed height) and of I.3-2 if there is a linear law (α_{eff} vary nearly as $[e]^{-1}$).

In fact that is what we see in due experimental data - regular variations of the D-region electron concentration in the solar cycle are rather weak and much less, than that due to various disturbances. To illustrate that, we use the figure showing $[e]$ variation with solar zenith angle χ for summer conditions (DANILOV et al., I982) and mark at each point the value of $F_{I0.7}$ - flux for the day of the experiment (see Fig.2). As one can see from that Figure there seems to be no pronounced dependence on $F_{I0.7}$ - all the experimental points lie on the same curve representing $[e]$ - dependence on χ .

Quite different picture we have for various events, manifesting SA. There we have very strong variations of ionization rate q with consequent changes of all the D-region parameters. Table 2 shows variations of q due to x-rays ionization during solar flares of various intensity (prominent, strong, moderate) according to MITRA (I974).

Table 2.

Ionization rates in the D-region due to solar flares according to MITRA (I974)

h, km	q cm^{-3} s^{-1}		
	Prominent	Strong	Moderate
60	2.10^{1}	1.5	$1.2\ 10^{-1}$
65	6.10^{1}	4	4.10^{-1}
70	$1.5\ 10^{2}$	$1.2\ 10^{1}$	1
75	$5\ 10^{2}$	$4\ 10^{1}$	3.5
80	$1.5\ 10^{3}$	10^{2}	10^{1}
85	$3\ 10^{3}$	$2.5\ 10^{2}$	$2.5\ 10^{1}$

Fig.3 presents variations of q-values during SPE events (SWIDER, I979). Comparing both sets of q with Fig.I one can see, that the ionization rates due to X-rays and energetic particles in disturbed conditions are several magnitude higher than in quiet conditions. It is worth emphasizing that during very strong SPE or REP (relative electron precipitation) events strong ionization may take place even at altitudes much lower than normal D-region down to 30-40 km (see BRASSEUR and SOLOMON, I984). An example of that also give curves 5-7 in Fig.3.

Strong variations of q in the D-region should inevitably lead to essential changes not only of $[e]$ but of the whole recombination cycle as well, including α_{eff}, rate of clustered ions formation B, ion composition parameter f^{+}, negative ions parameter λ and so on. For SPE events we have data on the effective recombination coefficient which show that there in fact is a variation (decrease of α_{eff}) during the events. Fig.4 (DANILOV and SIMONOV, I98I) show values of α_{eff} for summer (I972) and winter (I969) SPE-events. It is well seen that α_{eff} in disturbed conditions ($[e] \geq 10^{4}$ cm^{-3}) is much lower (especially for winter SPE) than for quiet conditions ($[e] \leq 10^{3}$ cm^{-3}). Theory of the ionization cycle in the upper D-region (DANILOV, I986) gives a clear explanation to that fact - the decrease of α_{eff} is due to decrease of the ion composition parameter f^{+} ($f^{+} = [clus^{+}]/[NO^{+}, O_2^{+}]$. That effect has been measured for I969 SPE - event (NARCISI, I972).

Table 3

Values of the ion composition parameter f^{+} for quiet winter conditions and for November, I969 SPE

	Day		Night	
	80 km	85 km	80 km	85 km
Winter (average)	2.0	$5 \cdot 10^{-1}$	$2 \cdot 10^{1}$	$> 10^{-1}$
SPE-I969	$9 \cdot 10^{-3}$	$1.9 \cdot 10^{-4}$	$1.6 \cdot 10^{-2}$	$5.9 \cdot 10^{-4}$

The f^{+}- parameter in its own turn decreases because of the reducing of the effectiveness of clustered ion formation B. In

the SPE conditions the primary ions produced by the process of ionization became O_2^+ instead of NO^+ in quite conditions and that leads to substatution of B (No^+) by B(O_2^+), the latter at fixed height being lower, than the former.

In the lower part of the D-region where there is a saturation of clustered ions ($f^+ >> 10$) and variations of f^+ - parameter does not influence α_{eff}, the latter during disturbances of SPE-type still changes, but due to decrease of the negative ion parameter λ, because

$$\alpha_{eff} = (1 + \lambda)(\alpha^* + \lambda\alpha_i) \qquad (2)$$

where α^* and α_i - averaged constants of dissotiative recombination and mutual recombination process correspondingly.

Principally the same picture should take place during sudden ionospheric disturbances SID, following solar flares. During SID we observe strong enchancement of [e] and reducing of α_{eff} (MITRA 1974) but there is no ion composition measurements to check the effects of f^+ decrease.

Weaker, but nevertheless much pronounced changes of the D-region parameters do take place during other events, produced by the energetic particle fluxes (Auroral Absorption AA, REP). In all those cases we have increase in the electron concentration due to enhanced q-values and decreased α_{eff}.

One more comment should be made concerning Fig.4.There is a well pronounced difference between α_{eff} - values for summer and winter SPE. This difference reflects the fact that there is a strong seasonal variation of α_{eff} (see DANILOV and SIMONOV, 1981) due to seasonal variations of the ion composition, produced by meteorological processes (DANILOV, 1986). That means that effect of solar event (for example SPE) is modulated by the meteorological influence. In our particular case that means that the same SPA-proton fluxes (the same q) produce much stronger disturbances of the electron concentration in winter than in summer.

Summarising the above said one may state that there are two types of influence on the ionospheric D-region - direct solar and meteorological. If we compare the magnetude of the effects due to SA and meteorological control we will find (see Table 4) that regular variations of the meteorological origin are much stronger than that due to SA. For spontaneous disturbances the picture is quite opposite - the amplitudes of variations for the principal parameters are higher for SA-produced events.

Above we have already mentioned the effect of α_{eff} decrease during SPE-events. That decrease strongly depends on the season, and that is a good example of the meteorological control filtering the effects of SA. In fact it happens rather often, because the reaction of the D-region to the external disturbance (in the form of X-rays or corpuscules) depends upon the internal state of the D-region (ion composition, λ - ratio, effective recombination coefficient), determined mainly by the neutral atmosphere and so controlled by the meteorological processes.

Table 4
Amplitudes of SA and meteorological effects in the upper D-region

	$[e]$	α_{eff}	f^+
		Regular	
SA	< 50%	< 50%	< 50%
Seasonal	2	2-3	5-10
		Spontaneous	
SPE	$> 10^2$	≈ 10	10^2-10^3
WA	$\approx 10^2$	3-4	≈ 30

A good example of that statement provides Fig.5 (DANILOV et al., 1983), demonstrating seasonal variation of the sudden phase anomaly (SPA) effects in VLF. Fig.5 shows that the reaction of the D-region on solar flares is different for summer and winter, which manifests the meteorological control of the pure effect of SA.

There is the other side of the medal. Having some ways to influence the middle atmosphere dynamics and/or thermodynamics by SA without direct effect on the D-region we have indirect SA influence on the latter through the alteration of the meteorological situation. The most obvious example is variation of solar UV-emission in 120-200 nm interval. This emission is not able to change q-values in the D-region, but influences the O_2 dissotiation and so by the formation of the ozone should alter dynamical picture in the whole middle atmosphere. The latter, as we understand now, is strictly connected with many aspects of structure and photochemistry (including conditions for propagation of internal gravity ways) and so will influence the D-region through minor constituents, temperature dependence of reaction rates, turbulence ets. That is what we call indirect influence of SA on the lower ionosphere.

That kind of influence is probably the one which provides observed connection of the D-region behaviour with such manifestations of SA as solar wind (see LASTOVICKA 1988) and geomagnetic activity. If we put aside events with strong enough electron precepitation we will find that there is no correlation with geomagnetic activity and no or rather weak correlation with solar activity (LASTOVICKA and SKOBODA, 1987). The latter means that (since we cannot imagine negative influence of SA on the D-region) the direct positive effect of SA is compensated by the indirect one through SA influence on the middle atmosphere as a whole.

Reference

Banks P. and Kockarts G., 1973, Aeronomy, Academic Press, New York.

Brasseur G. and S.Solomon, 1984, Aeronomy of the Middle Atmosphere, D.Reidel Publ. Comp., Dordrecht.

Danilov A.D., 1986, in.: Ionospheric issledovania (in Russian) N39, P.33.

Danilov A.D., A.B.Orlov, L.P.Morosova, V.P.Kishuk, 1983, Geomagnetism i aeronomia (in Russian), V.23, P.311.

Danilov A.D. and A.G.Simonov, I98I, in.: Ionospheric issledovania (in Russian) N34, P.54.
Danilov A.D., A.G.Simonov, N.V.Smirnova, S.U.Le domskaya, I982, in: Prostranstvenno vremennaya structure niznei ionospheri (in Russian), Moscow, IZMIRAN, P.43.
Lastovicka J., I988, Annales geophysical, V.6, P.40I.
Lastovicka J. and K.Svoboda, I987, physicia Scripta, V.35, P.906.
Mitra A.P., I974, Ionospheric effects of solar flares, D. Reidel Publ. Comp., Dordrecht.
Narcisi R.S., I972, Aeronomy Report, University of Illinois, N.48, P.I82.
Nusinov A.A., I987, In: Itogi nauki i techniki (in Russian) Moscow, V.26, P.80.
Simon P., I982, Solar Phys., V.74, P.273.
Swider W., I979, In: Solar-Terrestrial Prediction Proceedings, Boulder, US Dept.Commerce, V.4, P.599.

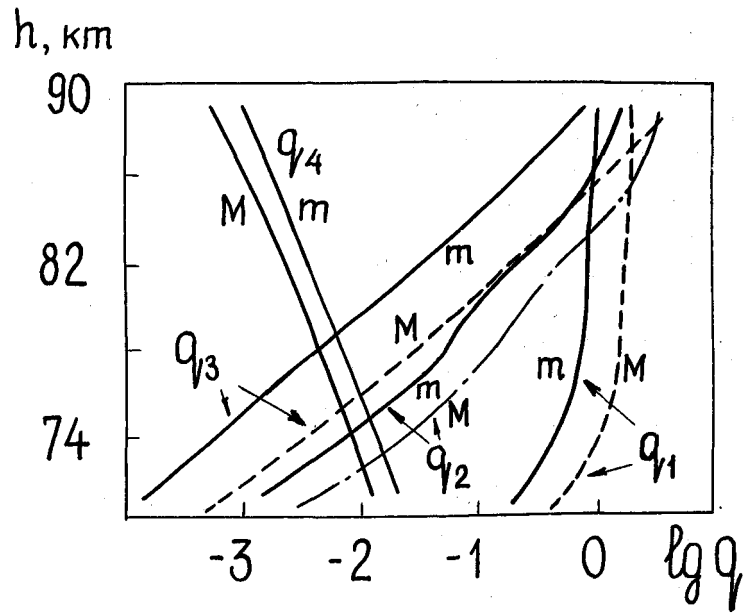

Fig.I. Ionization rates in the D-region for maximum (M) and minimum (m) SA due to various sources: Ly- plus NO - q_I; λ =III.8 - I02.7 nm plus O_2 ($^1\Delta_g$) - q_2; x rays - q_3; cosmic rays - q_4.

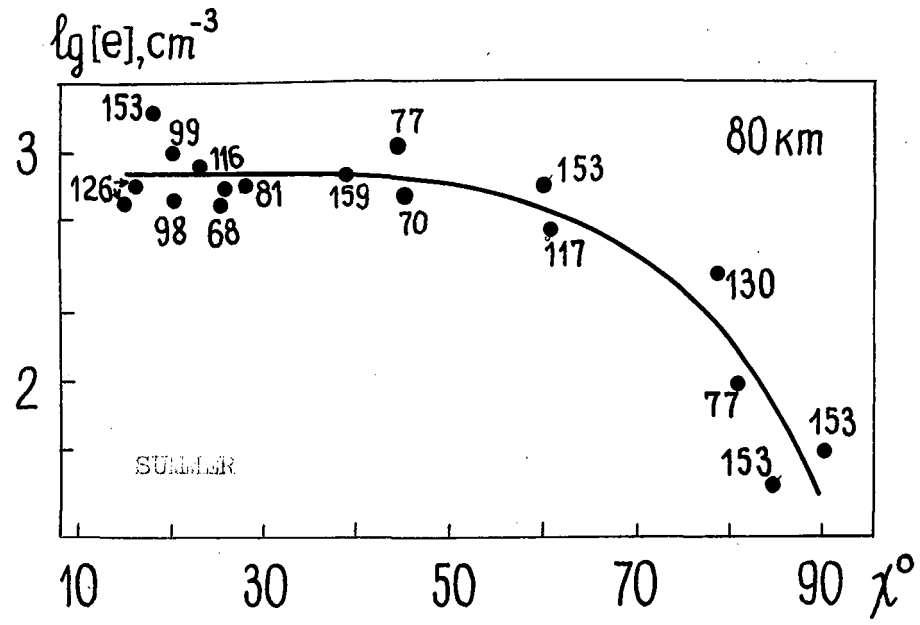

Fig.2. Electron concentration measured on rockets in summer at various solar zenith angles χ . Numbers at the points show solar I0.7 - cm flux at the day of the flight.

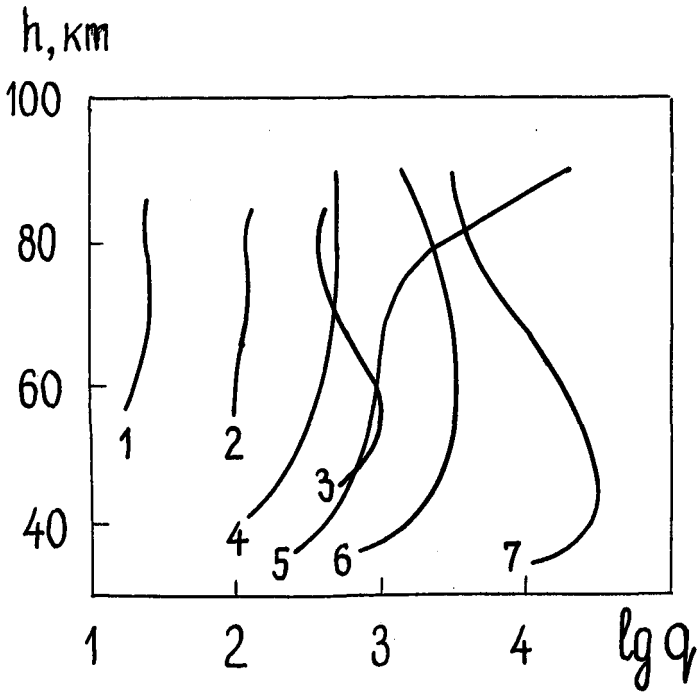

Fig.3. Ionization rates in the D-region during SPE-events according to Swider (1979) (1-3 Nov.1969 event, 4-7 Aug. 1972 event)

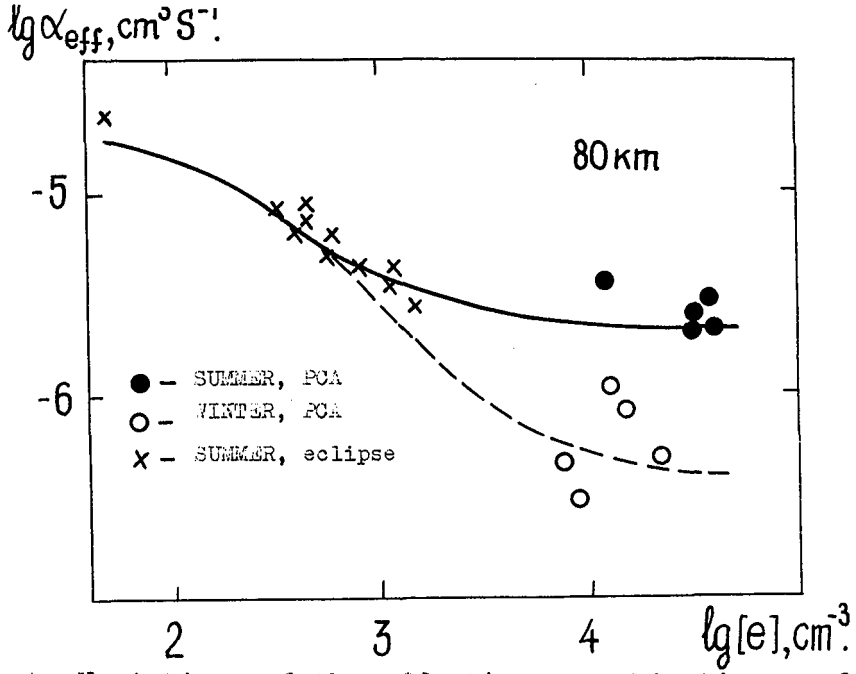

Fig.4. Variations of the effective recombination coefficient α_{eff} in summer (solid line) and winter (broken line) conditions (Danilov and Simonov, 1981).

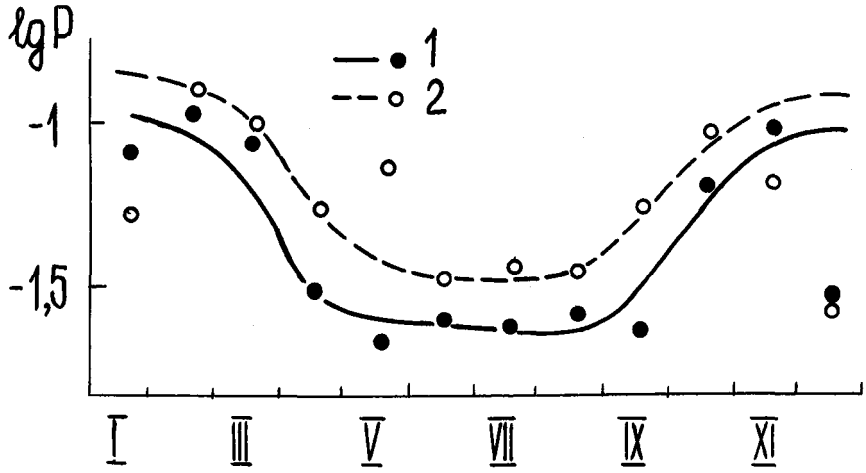

Fig.5. Seasonal variation of P (fraction of illuminated time when SPA effects were observed) in 1979 according to Danilov et al. (1983). (1 - Leningrad, 2 - Kühlungsborn).

ELECTRON DENSITY PROFILES IN THE BACKGROUND OF LF ABSORPTION DURING FORBUSH-DECREASE AND PSE

G. Sátori

Geodetic and Geophysical Research Institute of the Hungarian Academy of Sciences, H-9401 Sopron, POB.5, Hungary

ABSTRACT

Based on the simulation of different Forbush-decrease and particle precipitation effects in the D-region electron density profiles in the mid-latitudes the ionospheric absorption of low-frequency /LF/ radio waves has been determined. The absorption variations at different frequencies are strongly affected by the shape of the electron density profile. A structure appears which sometimes resembles the letter S /in a sloping form/. Both the height /around 70-72 km/ and the depth of the local minimum in the electron density contribute to the computed absorption changes of various degree at different frequencies. In this way several observed special absorption events can be interpreted.

INTRODUCTION

The lowest part of the D-region is formed by galactic cosmic ray ionization. After geoactive solar flares the Forbush-decrease of galactic cosmic rays can cause an ionization deficit in the bottom part of the D-region and the magnetic storm followed by particle precipitation can almost simultaneously result in an extra-ionization in the upper part of the D-region. The electron density during these ionization disturbances determinesthe LF absorption. It is the purpose of the present paper to give a qualitative estimation of the change of LF absorption due to a combined effect of Forbush-decrease and geomagnetic post-storm event /PSE/ by simulating them in a mid-latitude electron density profile. Results are compared with absorption measurements.

CALCULATIONS

Be $a(h)=q_{HEP}(h)/q_R$ the ratio of an ionization profile disturbed by magnetospheric high energy particles /HEP/ during a post-storm event /PSE/ to the reference ionization profile belonging to the reference electron density profile, N_R, determined for mid-latitudes. It is assumed that the lower part of the D-region electron density profile stems from the ionization effect of galactic cosmic rays, namely $q_R=q_{CR}$ and $a(h)=0$. In this case a Forbush-decrease causes a change of the electron density, ΔN_F, due to a change of the ionization, Δq_F. Using the continuity equation under equilibrium condition and neglecting transport processes one gets:

$$\Delta N_F = N_R \left[(1+\Delta q_F / q_{CR})^{1/2} - 1 \right]$$

In the cosmic ray layer the relative variation of the ionization, $\Delta q_F/q_{CR}$ can be computed from the changes of the energy spectrum of cosmic rays [VELINOV, 1971].

For the geomagnetic latitude of Kühlungsborn /Φ=54.4°/ the high energy particles generally intrude into the D-region till a depth 75-80 km. LAUTER et al. [1977] estimated the ratio $a(h)$ in the upper D-region. By computing electron density variations, ΔN_F,

in the lower D-region due to Forbush-decreases and using different ratios, a(h), in the upper D-region, electron density profiles disturbed by a Forbush-decrease and high energy particles /HEP/ have been simulated.

Sometimes high energy particles can intrude into the lowest D-region as shown by electron density measurements using the partial reflection technique simultaneously with satellite observations [MONTBRIAND, BELROSE, 1976] . In this case a(h) = $=q_{HEP}/q_{CR}$ corresponds to the ratio of the two particle ionization sources in the lower D-region apart from the X-ray bremsstrahlung ionization. The electron density changes, ΔN_F, due to a Forbush--decrease are then:

$$\Delta N_F = N_R (1+a)^{1/2}\left[\left(1+\frac{1}{1+a}\ \Delta q_F/q_{CR}\right)^{1/2}-1\right]$$

The left side of Fig.1 shows the simulated electron density profiles. Profile N_1 is perturbed by a Forbush-decrease in the lower D-region and by HEP in the upper D-region. Profile N_2 shows an electron density profile disturbed both by a Forbush-decrease and HEP in the lower D-region. A local minimum appears around the height of 70-72 km in the electron density profile. Profile N_3 is only modified by HEP in the whole D-region. The right side of Fig.1 shows the ratios of disturbed and reference electron density profiles.

Using these electron density profiles, the absorption of radio waves at 245 kHz and 128 kHz have been calculated by full wave solution simulating the A3 /oblique incidence/ method [SÁTORI, BREMER, 1987] . Absorption values calculated in this way can be directly compared to the experimental absorption data measured in Kühlungsborn.

Table 1 shows the absorption differences with respect to the absorption of the reference profile and it is completed by the attenuation values of VLF electromagnetic waves at 27 kHz computed on the basis of the wave-guide mode theory for a wave-guide height of 70 km [SÁTORI, 1978].

Table 1

Absorption in dB	$L_{\parallel\perp}$ (N_R)	$\Delta L_{\parallel\perp}$ (N_1)	$\Delta L_{\parallel\perp}$ (N_2)	$\Delta L_{\parallel\perp}$ (N_3)
245 kHz	67.9	0.8	6.8	14.6
128 kHz	67.1	-5.1	0.1	10.9
Attenuation in dB/1000 km	$\alpha(N_R)$	$\Delta\alpha(N_1)$	$\Delta\alpha(N_2)$	$\Delta\alpha(N_3)$
27 kHz	3.3	-0.9	1.0	1.1

These computed absorption profiles enable us to interprete unusual absorption events when there is no absorption after--effect at 245 kHz in spite of HEP condition, even more when there is an absorption decrease at 128 kHz, both due to the Forbush--decrease effect /Profile N_1/.

Actually the absorption profile computed on the basis of Profile N_2 elucidates the event of July, 1982 with a large magnetic storm and an exceptionally deep Forbush-decrease. Namely at 245 kHz and 27 kHz the PSE is evident, while at 128 kHz prac-

tically there is no change in the absorption [Fig.2]. In this case both a Forbush-decrease and a HEP condition have been assumed in Profile N_2 in the bottom part of D-region. The HEP condition that is the increased electron density was effective on the absorption and the attenuation computed at 245 kHz and 27 kHz, respectively, while the absorption without change calculated at 128 kHz was equally responsive to the HEP condition and to the decrease of the electron density due to the Forbush-decrease with a local minimum just below the reflection level of 128 kHz signals.

CONCLUSION

The ionospheric effect of a Forbush-decrease can cause a decrease of electron density with a maximum intensity about at height of 70-72 km. Occasionally it is able to modify the geomagnetic absorption after-effect of LF waves resulting in an unusual absorption fine structure differing from the PSE phases, mainly at day-time and sunset/sunrise/ conditions.

Acknowledgements. The author gratefully thanks J. Bremer for his assistance in the computer processing of electron density profiles.

REFERENCES

1. Lauter, E.A., Bremer, J., Grafe, A., Deters, I., Evers, K., The post-storm ionization enhancements in the mid-latitude D-region and related electron precipitation from the magnetosphere, HHI-STP-Report, 9, 1977.
2. Montbriand, L.E., Belrose, J.S., Changes in electron precipitation inferred from spectra deduced from D region electron densities during a post-magnetic storm effect, J. Geophys. Res., 81, 2213, 1976.
3. Sátori, G., Interpretation of simultaneous variations of galactic cosmic rays and of the level of atmospheric radio noise, Acta Geod. Geoph. Mont. Hung., 13, 475, 1978.
4. Sátori, G., Bremer, J., Perturbation of electron density profiles in the lowest D-region by Forbush-decreases, Adv. Space. Res., 7(6), 87, 1987.
5. Velinov, P., On variations of the cosmic ray layer in the lower ionosphere, J. Atmos. Terr. Phys. 33, 429, 1971.

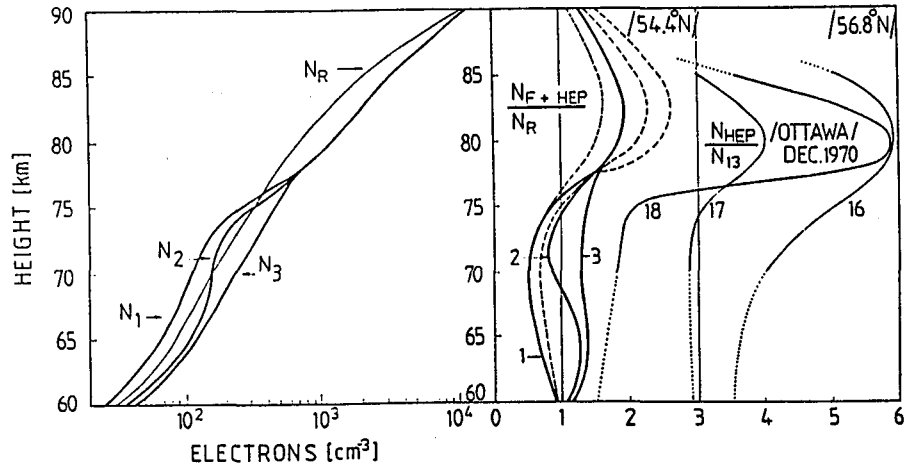

Fig.1 Electron density profiles /N_1, N_2, N_3/ simulated for Forbush-decrease and HEP conditions /left side/. The ratio of disturbed /N_1, N_2, N_3/ and undisturbed /N_R/ electron density profiles for geomagnetic latitude of 54.4° and for the event of December 13-20, 1970 measured in Ottawa /right side/.

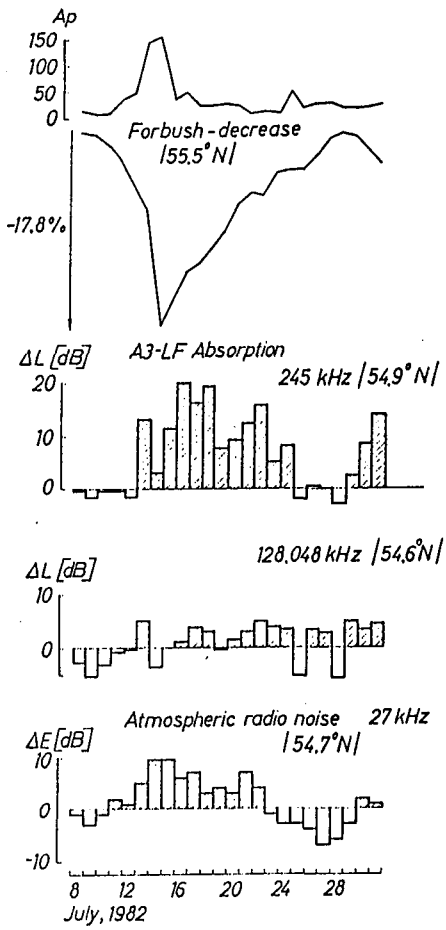

Fig. 2

A_p indices; cosmic ray intensity deviations in percents on the basis of Moscow neutron monitor data; LF absorption measured at 245 kHz and 128.048 kHz in Kühlungsborn /the average of the deviations from the monthly median at cos $\chi = 0^0$ and night/ and four-hourly averages of the radio noise level recorded at 27 kHz also in Kühlungsborn /deviation from the monthly median/ during the geomagnetic storm of July, 1982.

THE INFLUENCE OF IMF ON THE LOWER IONOSPHERE PLASMA IN HIGH AND MIDDLE LATITUDES

J. Bremer
Academy of Sciences of the GDR
Heinrich-Hertz-Institute of Atmospheric Research and Geomagnetism
Observatory of Atmospheric Research
DDR-2565 Kühlungsborn, GDR

Abstract: As shown by ground-based absorption measurements, the lower ionospheric plasma is markedly controlled by the structure of the IMF. Whereas in high auroral and subauroral latitudes this effect is very pronounced, in midlatitudes its influence is less important. A comparison of these results with satellite data of the IMF and the solar wind speed confirms the important role of these components, not only during special events but also for the normal state of the ionospheric D-region plasma.

1. Introduction

As known from DUNGEY (1961) the vertical component B_z of the IMF in the solar-magnetospheric coordinate system markedly controls the energy transfer from the solar wind into the magnetosphere. Whereas negative B_z components should favor this transfer, positive B_z values should inhibit such an input.

Assuming an IMF which is emitted together with the solar wind parallel to the solar equator, the B_z component shows systematic variations due to daily and seasonal changes of the position of the geomagnetic dipole axis of the Earth with respect to the solar rotation axis. In Figure 1 the seasonal (a) as well as diurnal (b) variations of B_z are presented for an IMF with A- (full curves) as well as T- (dashed curves) polarity. After Figure 1a an IMF with A-polarity induces positive B_z values during the spring half-year and negative B_z values during autumn, whereas an IMF with T-polarity causes reverse signs of B_z, respectively. Following a proposal by LAUTER et al. (1978) IMF sectors with negative B_z values are called "pro sectors" and sectors with positive B_z values "anti sectors". The diurnal B_z variation (Figure 1b) having a markedly smaller amplitude than the seasonal component has minima near 11 UT for A- and near 23 UT for T-polarity.

In this paper the influence of the IMF on the plasma of the lower ionosphere shall be investigated mainly during IMF sector boundary crossings (SBC). The dates of these SBC are taken from a special list of WILCOX (1982).

2. Results

As the ionospheric plasma markedly depends on the highly variable solar EUV radiation as well as internal atmospheric processes, it is often difficult or even impossible to separate these phenomena from effects caused by the IMF sector structure. On the other hand, the individual SBC data are sometimes incorrect. Therefore, here mainly the results of statistical investigations are shown using the method of superposed-epoch analysis with the first day of the new IMF sector as the key day (zero).

In Figure 2 the results of such an analysis are shown using noon absorption data at 3 MHz measured at the GDR Antarctic Station "Georg Forster" (70.77°S; 11.83°E) during June 1976 and November 1978. Whereas in the upper part (Figure 2a) all SBC are used independently of the direction of the IMF, in the other parts the total number of SBC are divided into transitions with respect to IMF polarity (T → A transitions: Figure 2b; A → T transitions: Figure 2c) and transitions with respect to the B_z component of the IMF (anti → pro, pro → anti sector transitions:

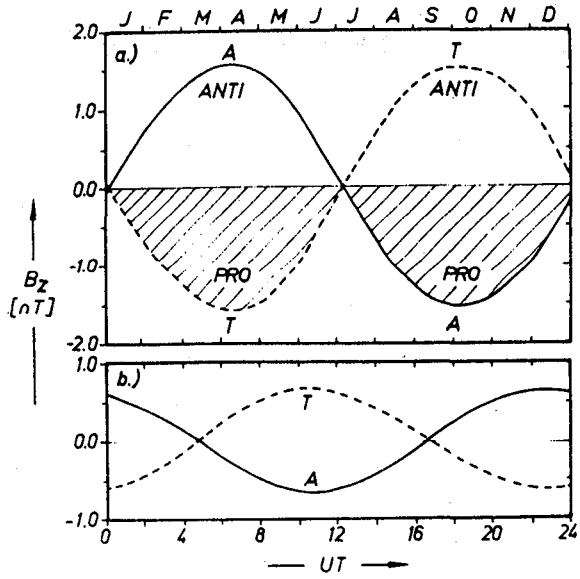

Figure 1. Mean seasonal (a) and diurnal (b) variation of the B_z component of the IMF in the solar-magnetospheric coordinate system for A- (full curves) and %-polarities (dashed curves) with an IMF amplitude B = 5 nT.

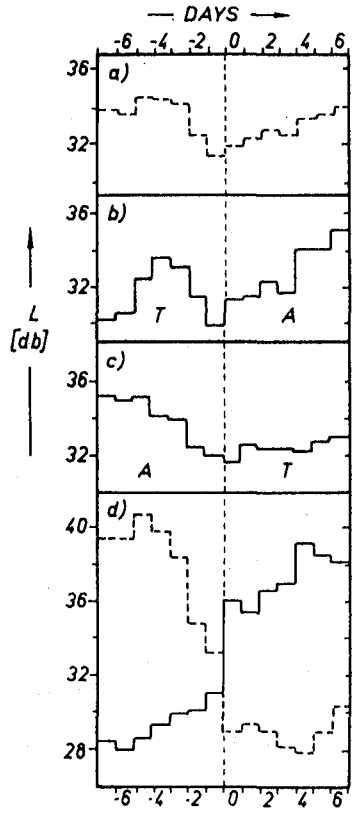

Figure 2. Mean variation of ionospheric noon absorption in Georg Forster station (70.77°S, 11.83°E) at 3 MHz during IMF sector boundary crossings independent of IM direction (a), for crossings from T→ A polarity (b), for crossings from A → T polarity (c) and for crossings from pro → anti (dashed curve) as well as anti → pro sectors (full curve) (d), respectively.

Figure 2d). In Figure 2a-c only small variations of ionospheric absorption are to be seen, only the minimum near day –1 seems to be typical. The slightly enhanced absorption at A polarity (Figure 2b and c) also observed by MANSUROV et al. (1976) seems to be connected with enhanced particle precipitation during noontime because due to the diurnal B_z variation (see Figure 1b) near noon IMF sectors with A-polarity induce lower B_z values than T-sectors. More pronounced variations of ionospheric absorption are observed, however, if IMF sectors are distinguished by their B_z component. In pro sectors the absorption is higher by about 10 - 12 dB than in anti sectors. The transition between both sectors is very steep with absorption changes of about 4 - 5 dB from day –1 to day 0. As can be seen from Figure 2d, but also from similar investigations with other ionospheric absorption data as well as different geomagnetic indices (BREMER and LAUTER, 1984; BREMER, 1986), the transition from anti → pro sectors is more pronounced than the transition from pro → anti sectors. As the B_z component of the IMF plays an essential role in the ionospheric plasma, in the following only pro → anti and anti → pro SBC will be used.

To investigate the IMF influence on the plasma of the lower ionosphere in dependence on latitude we used the results of the Finnish riometer chain. In the left part of Figure 3 daily mean values of the hourly maximum CNA data at 27.6 MHz are shown for the period between February 17 and March 2, 1981. After WILCOX (1982) a sector boundary crossing from A to T sector occurs between February 23 and 24, marked by the dashed line. Whereas before the SBC which is an anti sector the absorption is very small at all stations; during pro sector conditions after February 24 the absorption is markedly enhanced. The excessive absorption is highest in high geomagnetic latitudes (shown in brackets in Figure 3) and is smaller in lower latitudes but nevertheless remarkable also in 57.6°N geom. latitude. The geomagnetic Ap index shown at the top of the right part of Figure 3 is also enhanced after the sector boundary crossing. Beside these ground-based data also interplanetary data are shown (KING, 1986) like solar wind speed and the IMF B_z component as well as the energy coupling function ε introduced by PERREAULT and AKASOFU (1978). Whereas the solar wind speed is characterized by a minimum before the sector boundary crossing the B_z component changes its sign from plus to minus. To demonstrate this change more clearly, on February 24 half-day mean values have been calculated for B_z and ε instead of daily mean values estimated otherwise. In conclusion we can state that during pro sector conditions the energy input from solar wind into the magnetosphere markedly increases, followed by precipitation of high energetic particles into the middle atmosphere and enhanced CNA.

At the top of the left-hand part of Figure 3 also the IMF data derived from ground-based measurements (Solar Geophysical Data, 1981) are shown which in this case do not agree with the SBC data from WILCOX (1982) who took into consideration also satellite data. Such uncertainties in SBC data estimated from ground-based measurements are not so critical if statistical investigations like superposed-epoch analyses are made only, since about 85% of these SBC data should be correct (SVALGAARD, 1976).

In Figure 4 the results of superposed-epoch analyses are shown using again daily mean values calculated from hourly maximum CNA data at 27.6 MHz measured at 7 stations of the Finnish riometer chain. The SBC are characterized by dashed lines. For pro → anti sector transitions as well as anti → pro transitions we always observe higher absorption during pro sector conditions rather than during anti sectors. The differences between both conditions become smaller with decreasing latitude but can also be detected at Nurmijärvi in 57.6° geom. latitude. Generally the increases of absorption with anti → pro transitions are steeper than for pro → anti transitions, mainly to be seen above 60° geom. latitude, a fact already mentioned above.

In order to compare the superposed-epoch analyses of Figures 2 and 4 with interplanetary data in Figure 5, the results of similar analyses are shown using daily mean values of the solar wind speed, the B_z component and the ε function during the period from 1975 to 1979 where a lot

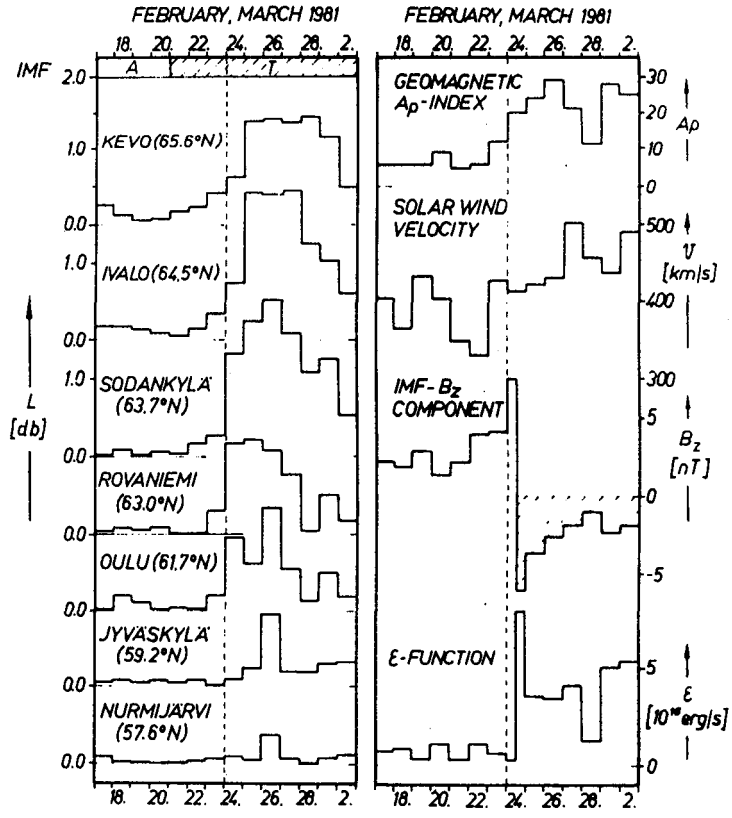

Figure 3. Variation of CNA at different geomagnetic latitudes, geomagnetic Ap index as well as satellite data of solar wind speed, B_Z component of the IMF and energy transfer function ε during the period from February 17 until March 2, 1981. The IMF polarity data (A or T) are from Solar Geophys. Data and the SBC (dashed lines) from WILCOX (1982).

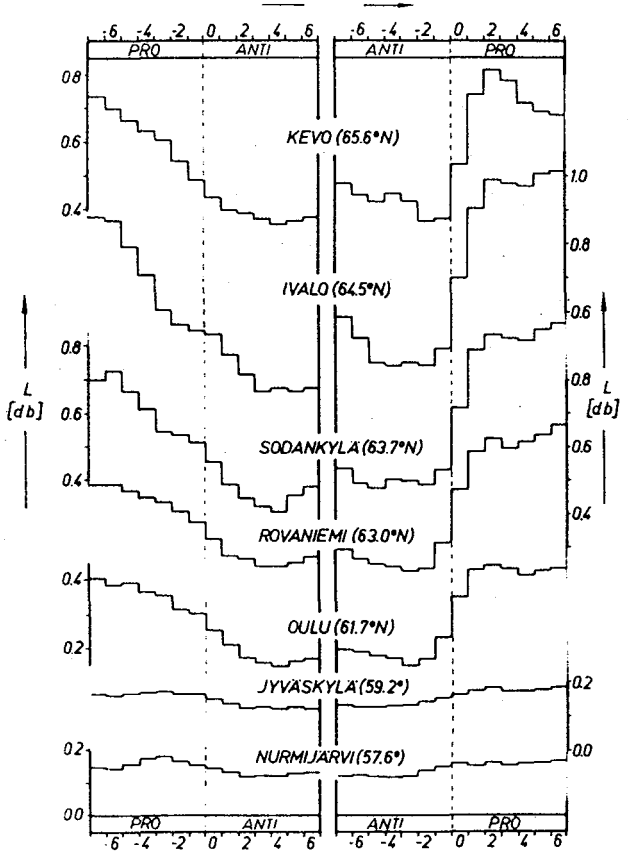

Figure 4. Mean variation of daily mean values derived from hourly maximum CNA data for 1979 until 1982, during IMF sector boundary crossing from pro → anti and anti → pro sector conditions in dependence on geom. latitude. The dashed lines mark the SBC after WILCOX (1982).

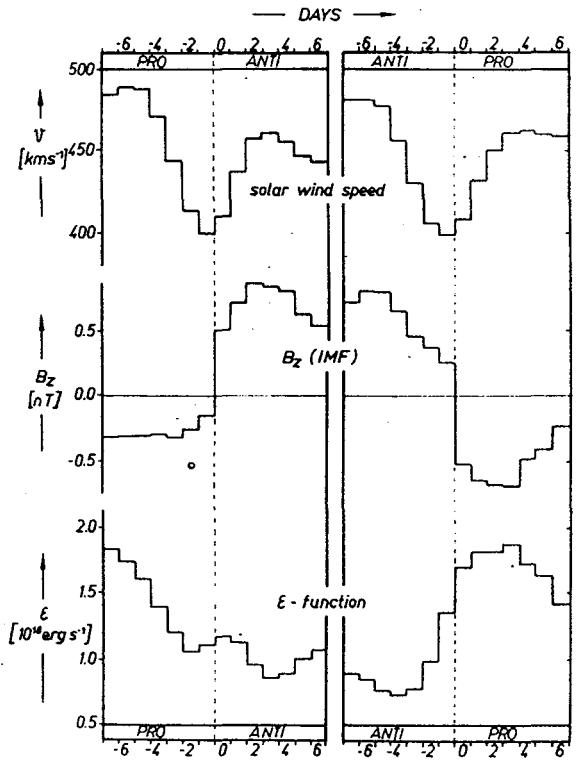

Figure 5. Mean variation of the solar wind speed v, the IMF B_z component and the energy transfer function ε calculated for transitions of IMF pro → anti and anti → pro sector conditions using satellite data 1975-1979.

of such satellite data is available (KING, 1979, 1986). The mean variation of the solar wind speed is very similar for pro → anti and anti → pro sector transitions with a pronounced minimum at day –1 just before the SBC. As to be expected, the B_z component is negative during pro sectors, but positive during anti sectors. The energy coupling function ε is higher during pro sectors than during anti sectors. Whereas ε shows a steep increase during the anti → pro sector transition, the decrease of ε during pro → anti transitions is not so steep and even shows a small secondary maximum just after the SBC on day 0.

3. Discussion and Conclusions

As demonstrated by Figure 5, the energy transfer from solar wind into the magnetosphere connected with a precipitation of high energetic particles into the middle atmosphere mainly depends on the B_z component of the IMF. Thus during times with negative B_z values enhanced fluxes of precipitating particles induce a higher ionization level in the ionospheric D region and therefore higher absorption of radio waves as observed in Figures 2 - 4. Therefore, the proposed classification of IMF sector in pro and anti sectors after their B_z component seems to be well justified.

Whereas the main differences between pro and anti sectors are caused by the B_z component also the solar wind speed v modulates the particle precipitation and, therefore, the ionospheric absorption since ε is proportional to v. Thus the relatively flat variation of absorption during pro → anti sector transitions (Figures 2 and 4), connected with the secondary maximum of the solar coupling function ε (Figure 5), is caused by the steep increase of the solar wind speed at the front of the anti sector. In geomagnetic indices even a secondary maximum can be observed during the transition from pro → anti sector (BREMER, 1986). Also the absorption minimum on day –1 just before the SBC in Figure 2a where all SBC were used irrespective of their polarization, is caused by the minimum of solar wind speed (see Figure 5) as in this case the influence of the B_z component is covered by the averaging process.

As the precipitation of high energetic particles becomes smaller with decreasing geom. latitude also the effect of IMF sector structure becomes less important in midlatitudes (Figures 3 and 4). This fact could be confirmed by investigations using LF absorption data at Central Europe not shown here. Only when using a large amount of data, small effects similar to those discussed here could be detected. At geom. latitudes above about 60°, however, the IMF influence may be essential if the concept of pro and anti sectors is used.

References

Bremer, J., Der Einfluss interplanetarer Strukturparameter auf das ionospherische Plasma in auroralen und sub auroralen Breiten, *Geod. Geoph. Veröff. R.I.H. 13,* 3-14, 1986.

Bremer, J., and E. A. Lauter, Dependence of the high latitude middle atmosphere ionization on structures in interplanetary space, *Handbook for MAP 10*, edited by J. Taubenheim, 200-204, 1984.

Dungey, J. W., Interplanetary magnetic field and the auroral zones, *Phys. Rev. Lett., 6,* 47-48, 1961.

Ionospheric Absorption Data, Geophysical Observatory Sodankylä of the Finnish Academy of Science and Letters, 1979-1982.

King, J. H., Interplanetary medium data book, Rep. NSSDC 7908 and 8604, NASA Goddard Space Flight Center, Greenbelt, MD 1979 and 1986.

Lauter, E. A., J. Lastovicka, and Z. Ts. Rapoport, Midlatitude post-storm events and interplanetary magnetic field, Phys. Solariterr., Potsdam 7, 73-82, 1978.

Mansurov, S. M., L. G. Mansurova, and Z. Ts. Rapoport, Ionospheric radio wave absorption in the auroral zone and the interplanetary magnetic field sector structure, *Planet. Space Sci., 24,* 55-59, 1976.

Perreault, P., and S.-I. Akasofu, Study of geomagnetic storms, *Geophys. J. Roy. Astron. Soc., 54,* 547-573, 1978.

Solar Geophysical Data, National Geophysical and Solar-Terrestrial Data Center, NOAA, Boulder, CO USA, 1981.

Svalgaard,L., Interplanetary sector structure 1947-1975, SUIFR Rep.No. 629, Stanford, CA USA, 1976.

Wilcox, J.M., Tabulation of well-defined boundaries in the interplanetary magnetic field, Private Communication, 1982.

SOLAR COSMIC RAY EFFECTS IN THE LOWER IONOSPHERE

A.V. Shirochkov

Arctic and Antarctic Research Institute, Leningrad, USSR

INTRODUCTION

The polar cap absorption (PCA) events are the most remarkable geophysical phenomena in the high-latitude ionosphere. Their effects are extended on the whole polar region in the both hemispheres. The PCA events are caused by the intense fluxes of the solar cosmic rays (SCR) which are generated by the solar proton flares. Entering into the Earth's magnetosphere and ionosphere the SCR fluxes create excessive anomal ionization at the ionospheric heights of 50-100 km which exceeds usual undisturbed level of ionization in several orders of magnitude. The PCA events can be considered as catastrophe in relation to the polar ionosphere because all radiosystems using ionospheric radiochannel ceased to operate during these events. On the other hand the abnormally high level of ionization in the ionospheric D-region during the PCA events create excellent opportunities to conduct fruitful aeronomical research for the lower ionosphere. Obvious scientific and practical importance of the PCA events leads to publishing of special PCA catalogues. The Soviet scientist have prepared several of such catalogues (LOGACHEV et al., 1983). The ionospheric effects caused by the SCR fluxes were profoundly described in the classical paper (BAILEY, 1964). Nevertheless several aspects of this problem are not studied properly. This paper is an attempt to clarify these questions.

ELECTRON DENSITY PROFILE VARIATIONS DURING THE PCA EVENTS

The D-region ionization level during the PCA events is due to two main factors: SCR flux intensity and Solar luminosity level. Excellent example of this situation is the PCA event of April, 1969, which is shown at Figure 1. Curves 1 and 2 indicate the variations of 30 MHz riometer absorption correspondently at Vostok Station (Antarctica, invariant latitude Φ' = 83.3°S) and at the icedrifting station North-Pole-16 (Φ' = 81°N); curve 3 - the solar protons with $E_o \geq 10$ MeV intensity variation recorded at the "Explorer-10" satellite. The small vertical arrows at the time axis indicate the local noon at Vostok Station. The "North Pole-16" Station was fully illuminated by the Sun during the whole event. One can see day-to-night absorption variations at Vostok Station while the absorption variation at "North Pole-16" Station even in small details repeat the SCR flux variations.

It is interesting to summarize reliable data on the electron density profiles during the PCA events for daytime and nighttime conditions separately. Such data for the daytime PCA events are shown on Figure 2. The rocket measurements data are shown by the solid curves and the ground-based measurements data- by the dotted lines. The numbers on the curves indicate correspondent absorption values. The curves for great values of absorption correspond to greater values of electron density and are located at comparatively low heights (sometimes as low as 43 km). Identical

situation is observed during the nighttime PCA events (see Figure 3). Naturally, the value of absorption (and correspondent N_e values) during nighttime is lower in comparison with the same daytime values. The maximum of electron density is located at 80-85 km. The data of Figures 2 and 3 give additional evidence of average solar proton energy which caused the PCA events. For the daytime events such energy is $E_o \geq 10$ MeV, while for the nighttime events it is $E_o \simeq 5$ MeV.

There is no detailed study of the F-region electron density behaviour during the PCA events. General opinion is that F-region of ionosphere does not change under influence of SCR fluxes. There are experimental evidence of it (HANSUCKER, 1973). The numerical model calculations of the ionization rate during the PCA events confirm such conclusion (BAILEY, 1964). Strictly speaking, there is possibility to have considerable value of ionization rate from SCR with $E_o \simeq 800$ MeV at the heights of 200 km. In this case one must take into account various processes of nuclear interactions of solar protons with atmosphere (such as evaporation, cascade chains etc.). On the other hand, solar protons of such energies do not create any ionization in the D-region.

EFFECT OF MIDDAY RECOVERY OF ABSORPTION

The riometer data from auroral station reveal the effect of a notable decrease of absorption during some PCA events in hours around geomagnetic noon. This phenomenon was called midday absorption recovery effect. Remarkable peculiarity of this effect is that none of existing aeronomical models of PCA-disturbed D-region could reproduce it. Therefore there are strong reasons to believe that this effect is due to the magnetospheric processes. One of it could be anisotropic pitch-angle distribution fo SCR during the solar protons movement toward dayside in the quasi-trapped region. Numerous satellite measurements show that in these situations the solar proton trajectories are located deeply inside in the closed field lines region and a boundary of the SCR penetration moves toward the high-latitude at prenoon MLT hours (BURROWS, 1972). This effects is due to different degree of the ring current asymmetry during the PCA events (WILLIAMS and HEURING, 1973). A natural explanation of the effect could be phenomenon of magnetosphere asymmetry and caused by it diurnal variation of the geomagnetic cut-off threshold with its increasing at daytime. This explanation contradicts with obvious fact that the midday recovery effect is observed not in every PCA event at auroral latitudes. It was found that this effect preferably occurs during PCA events produced by solar flares on the eastern Sun hemisphere (ULYEV, 1988). Besides that, the periods of the midday recovery appearance the satellite data demonstrate notable softening of the SCR energetic spectra. Occurrence of this effect diminishes sharply at invariant latitudes greater than 70° as well as at latitudes less than 62°. The same thing is evident with increasing geomagnetic activity level. This situation is shown on Figure 4, taken from (ULYEV, 1988). So presence/absence of the midday recovery effect gives information about heliolongitude of a flare which produced PCA event as well as about type of the SCR energetic spectra.

CONJUGACY EFFECTS

The early conjugate observations (SAUER, 1968) during PCA events revealed quite different response of the polar ionosphere in opposite hemispheres to the solar protons fluxes. A number of factors can be responsible for such situation. Amongst them are: different solar illumination regime at the observation points; a different heliolongitude of a solar flare which caused PCA event (HAURWITZ et al., 1965); character of the interplanetary magnetic field (IMF) orientation during the PCA events (REID and SAUER, 1967). Up to now there is no full understanding of a role of each of these factors in the lower polar ionosphere behaviour during the PCA events. Recently one more pair of the high-latitude conjugate stations began to operate: Mirny (Antarctica) and Spitzbergen (Arctica). Their invariant latitude is 75°.

Figure 5 shows riometer absorption variations at Mirny (dotted line) and Spitzbergen (solid line) during the June 6-9, 1979 PCA event together with the concurrent IMF parameters. The North Hemisphere lower ionosphere was fully sunlit at this time while it was in complete darkness in the South. One could expect that under the same solar proton fluxes illumination riometer absorption at Spitzbergen would significantly exceed absorption at Mirny. In fact, absorption magnitude at Mirny was even greater sometimes than at Spitzbergen. The solar flare which caused this PCA event occurred on 5 June 1979 on the eastern solar hemisphere (LOGACHEV et al., 1983), i.e. long before the PCA event started to be developed. Therefore, one could not expect any kind of the SCR fluxes anisotropy at this time. We think that the observed North-South asymmetry in the SCR intensity during the 6-9 June 1979 PCA event can be successfully explained in the framework of the magnetotail model proposed by SIBECK et al. (1985). One can see almost exact coincidence of the absorption increase at Spitzbergen with a sharp $+B_Y$ rise. This absorption increase took place at the morning hours (in MLT) what is in a good agreement with the GOSLING et al. (1985) model of a plasma distribution in a distant tail. Low-energy solar protons with Larmor radius equal to 1.5 - 2 R_E responsible for riometer absorption can penetrate into the tail lobes through described by SIBECK et al. (1985) "windows" without any trouble.

Concurrently with a $+B_Y$ increase a similar rise of the $-B_X$ IMF component took place (see Figure 5). This situation is favourable for a plasma penetration to the South Hemisphere from the interplanetary space. Perhaps, a combination of these factors provided conditions for a such unusual North-South absorption distribution which is shown on Figure 5. A conclusion can be made that the results of riometer observations at conjugate points during 6-9 June 1979 PCA event give a strong confirmation of a distant magnetotail model proposed by SIBECK et al. (1985). These riometer observations also support idea of a strong IMF control of a distant magnetotail structure. The solar protons whose Larmor radius is more than 5 R_E ($E_o \geq 30$ MeV) perhaps are not influenced by the IMF orientation during their entering into magnetosphere. Actually these protons give a small contribution to riometer absorption.

RADIOCOMMUNICATION EFFECTS

It is well known that the PCA absorption magnitude stronly depends on frequency. This dependence can be described by equation:

$$A_1/A_2 = (f_2/f_1)^n$$

where A_1 - absorption values at frequency f_1; A_2 - absorption values at frequency f_2; n = 1.5-2. Usually riometers operate at frequency 30 MHz. So, if we have absorption at 30 MHz equal to, say, 10 dB, a correspondent absorption at f = 1 MHz will be ≈ 60 dB; at f = 100 MHz - 1 dB, at f = 150 MHz - 0.4 dB. These evaluations are given for the case of vertical incidence of radiowave on the ionosphere. In the case of oblique incidence absorption value would be increased in accordance with the secant law, i.e. it would be greater in 5-7 times for oblique radiopath of 2000 km lenght. The experimental data show that the greatest influence of the PCA events one can expect at the radiopaths located entirely in the polar latitudes. In this case the lowest usable frequencies (LUF) considerably increase with concurrent diminishing of the maximal usable frequencies (MUF). The final result is a significant decrease of operating frequency range including the cases wof complete disappearence of communication. It is clear that the PCA events influence would be greater at the radiopaths operating at LF and VLF radiowaves. Such navigation systems like Loran-C could not operate properly under PCA conditions. Crude estimations show that the PCA event with maximum absorption equal to 20 dB at 30 MHz could significantly diminish efficiency of all radiosystems operating at frequencies up to 120 MHz. Recent series of the PCA events in March 1989 of very long duration demonstrate a strong necessity to develop a reliable model for prediction of the PCA evenets appearance. Preliminary data on the March, 1989 PCA events intensity are given below (Soviet riometers in Arctica and Antarctica data):

PCA event 1. Start 08.03 at 07-30 UT; Finish 14.03 at 21-00 UT; A_{max} = 10.5 dB at 08-00 UT 13.03.89.

PCA event 2. Start 17.03 at 21-30 UT; Finish 20.03 at 15-00 UT; A_{max} = 6.65 dB at 08-05 UT 18.03.89.

PCA event 3. Start 23.03 at 20-00 UT; Finish 25.03 at 01-00 UT; A_{max} = 2.4 dB.

REFERENCES

Bailey D.K., Polar cap absorption, Planet.Space Sci., 12, 495, 1964.

Burrows J.R., A review of magnetospheric characteristics of solar flare particles, Proc. COSPAR symp. on solar particle event of November 1969, ed. J.C. Ulwick, AFCRL-72-0472, 243, 1972.

Gosling J.T., D.H. Baker, S.I. Bame, W.C. Feldman, R.D. Zwickl, and E.L. Smith, North-south and dawn-dusk asymmetries in the distant tail lobes: ISEE-3, J.Geophys.Res., 90, 6534, 1985.

Hansucker R.D., Overview of solar events and related auroral-zone geophysical observations during the August 1972 storm, WDC-A Rep. UAG-28, Boulder, 11, 1973.
Haurwitz M.W., S. Yoshida, and S.-I. Akasofu, Interplanetary magnetic field asymmetries and their effects on polar cap events and Forbush decreases. J.Geophys.Res., 70, 2977, 1965.
Logachev Y.I. (editor), Catalogue of the solar proton events 1970-1979, Moscow, Nauka, 1983 (in Russian).
Reid G.C., and H.H. Sauer, Evidence for non-uniformity of solar proton precipitation over the polar caps, J.Geophys.Res., 72, 4383, 1967.
Sauer H.H., Nonconjugate aspects of recent polar cap absorption events, J. Geophys. Res., 73, 3058, 1968.
Sibeck D.G., G.L. Siscoe, S.A. Slavin, E.J. Smith, B.T. Tsurutani, and R.P. Lipping, The distant magnetotail response to a strong interplanetary magnetic field B_y : twisting, flattening and field line bending, J.Geophys.Res., 90, 4011, 1985.
Ulyev V.A., Personal communication, 1988.
Williams D.J., and F.T. Heuring, Strong pitch angle diffusion and magnetospheric solar protons, J.Geophys.Res., 78, 37, 1973.

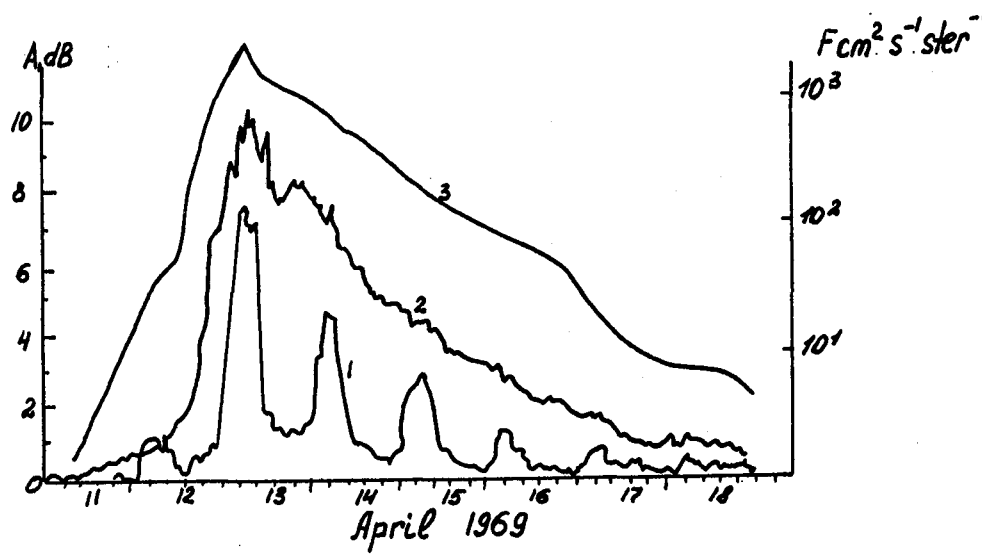

Figure 1. The April 1969 PCA event:
1 - riometer absorption at Vostok Station
2 - riometer absorption at North-Pole-16 Station
3 - Solar proton with $E_0 \geqslant 10$ MeV flux

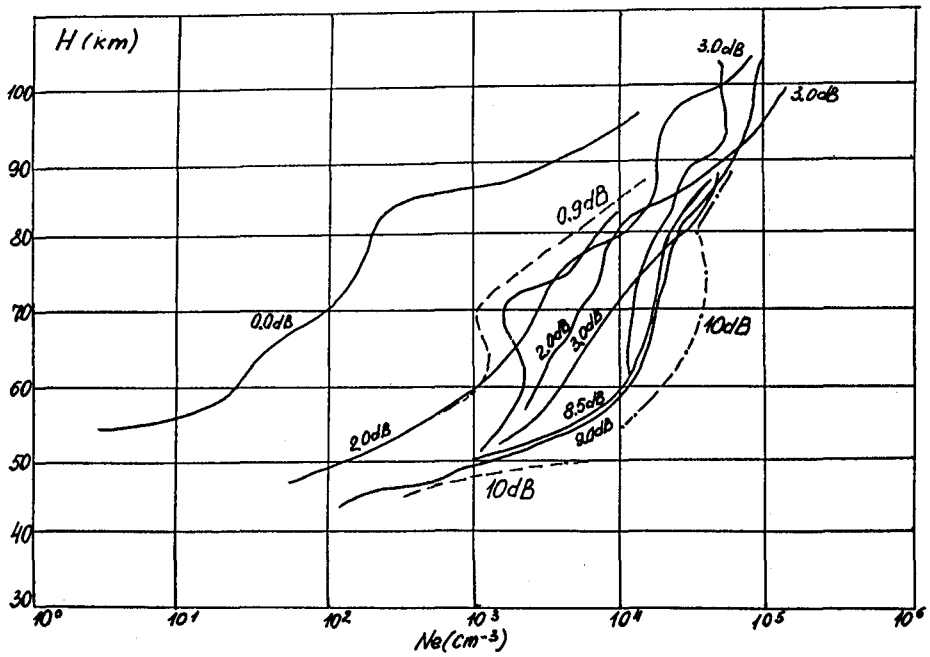

Figure 2. Electron density profiles for daytime PCA events.

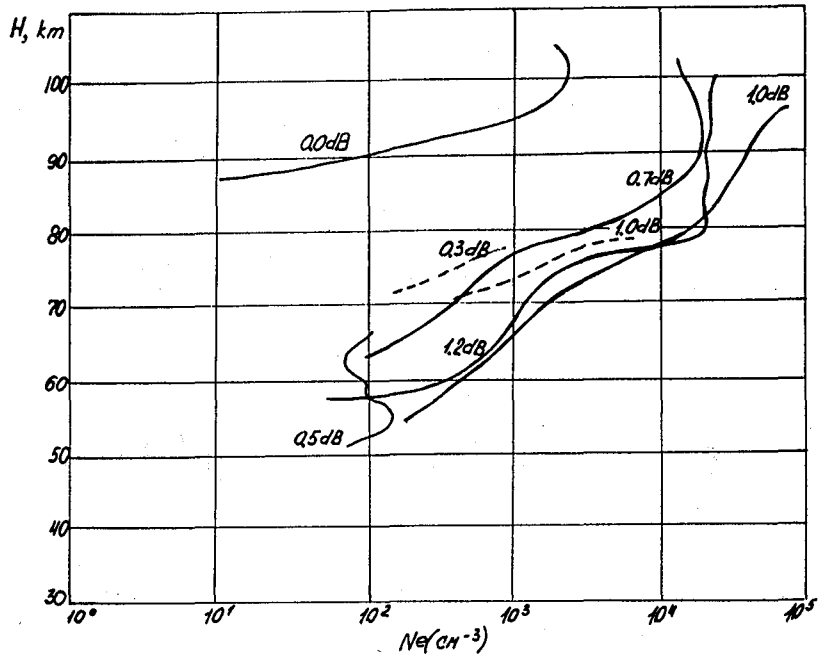

Figure 3. Electron density profiles for nighttime PCA events.

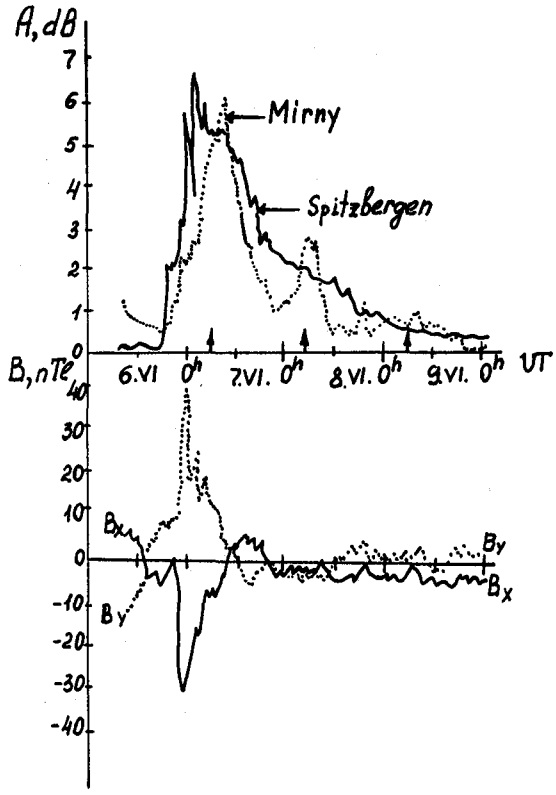

Figure 4. Riometer absorption variations at Mirny and at Sptizbergen during the 6-9 June 1987 PCA event (ypper panel) together with corresponding variations of the IMF components (lower panel).

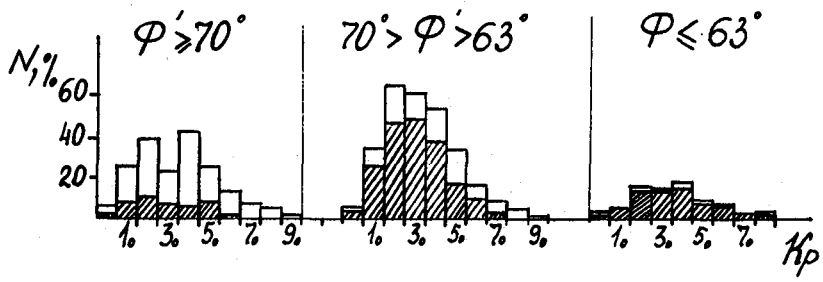

Figure 5. The PCA events occurrence in 1970-79 in various latitudinal belts: hatched parts: events with midday recovery effect.

SOLAR OR METEOROLOGICAL CONTROL OF LOWER IONOSPHERIC FLUCTUATIONS (2-15 AND 27 DAYS) IN MIDDLE LATITUDES

D. Pancheva*, J. Laštovička**

* Geophysical Institute, Bulg.Acad.Sci., "Acad.G.Bonchev", bl.3, 1113 Sofia, Bulgaria

** Geophysical Institute, Czechosl.Acad.Sci., Boční II, 141 31 Prague 4, Czechoslovakia

Several types of short- and long-term effects of solar activity on the lower ionosphere have been discussed in the literature. They are related to solar flares, the sector structure of the interplanetary magnetic field and some periodicities in sunspots or solar radio flux. The most evident periodicities of the Sun are the 11 year cycle of its activity and the differential rotation period near 27 days (25-30 days). The response of the lower ionosphere to the 11 year solar cycle is considered by many authors. Here, the following questions are discussed: which periods between 2 and 15 days and near 27 days occur in ionospheric absorption during the interval July 1980 - July 1985 and are these periods related to similar periods in solar Ly-α flux, geomagnetic activity, or neutral wind near 95 km observed in Collm (GDR).

We use day-time absorption data obtained by the A3 method for the following radio-paths: Allouis-Sofia (164 kHz), Deutschlandfunk-Panská Ves (1539 kHz), Pristina-Sofia (1412 kHz) and Luxemburg-Panská Ves (6090 kHz). With the use of these data the electron density variations in the lower ionosphere can be analyzed. The amplitude spectra of time series are obtained. As a criterion for statistical significance, the confidence level 0.1 is selected. Within the range of periods of 2-15 days, the highest amplitudes are exhibited by the spectral lines at: 2.4-3.2, 4-6, 10.5-12 and about 13.5-14 days. All time series have also well expressed spectral lines between 26 and 28 days. We investigate the development of these fluctuations in time. The data are grouped by seasons. The observed fluctuations display a well expressed seasonal course. Fluctuations with the shortest period (2.4-3.2 days) have their main maximum in summer and a secondary one in winter. The 4-6-day fluctuations are most obvious during the equinox while the long-period 10.5-12 and about 13.5-14 day fluctuations have their basic maxima in winter and the secondary ones in equinox.

An attempt is made to clarify the nature of the observed fluctuations in absorption. The height region responsible for the radiowave absorption studied is ionized by the H-Lyman-alpha flux (121.6 nm - measured by the SME satellite). The statistically signifi- cant spectral lines existing in the Ly-α amplitude spectrum are only those with periods between 25 and 28 days (connected with solar rotation) and near 13.5 days. Consequently, only the 13.5-14- and about 27-day fluctuations in absorption could be generated by the variations of the Ly-α flux. In order to trace the connection between these fluctuations, we use a complex demodulation. This method allows us to obtain the instantaneous characteristics of the fluctuation under consideration. Figure 1

presents the time variations of the instantaneous amplitudes of the 13.5-day fluctuations in the Ly-α flux and in absorption for 164 kHz and 1412 kHz paths. The periods of amplification of this fluctuation in the Ly-α flux are denoted by arrows. It is obvious that a connection between the amplification of fluctuations in Ly-α on the one hand, and in absorption on the other, hardly exists (perhaps with the exception of the period April-May 1982 when an activation of fluctuations in absorption is observed). The 13.5-day fluctuation, existing in the lower ionosphere, has its basic maximum in winter. It seems that in the lower ionosphere the 13.5-day fluctuation is mainly due to meteorological and not to solar activity variations.

The fluxes of high energy particles are an important ionization source of the ionospheric D-region. Their precipitation can play a dominant role not only during geomagnetic storms, but several days after. We analyse the geomagnetic aa(N)-index as an indirect characteristic of particle precipitation in middle latitudes of the Northern Hemisphere. The statistically significant spectral lines are those corresponding to periods of: 4-6, 8, 11.5 and 13.5-15 days. Comparing the statistically significant periods during the seasons for the absorption and the aa(N)-index, we notice a comparatively good coincidence only in the interval of 4-6 days. This is the only fluctuation that could partly stimulate analogous fluctuation in the ionospheric absorption.

Variations of the prevailing wind in the lower thermosphere play a very important role in the meteorological control of the lower ionosphere. Therefore, we use the neutral wind measured at Collm (GDR) by the D1 method as a neutral atmosphere parameter representing the effect of dynamics on the radiowave absorption. For the zonal wind statistically significant spectral lines have periods: 6-7, 10.4-12 and 14-15 days and for the meridional wind periods: 2.4, 4-6, 8.2-9, 10.8-12 and 14-15 days. We investigate the seasonal course of these fluctuations. The long-period (10-12-days) fluctuations have the basic maximum in winter and a secondary one in equinox. The result is analogous to the seasonal course of the long period fluctuations in absorption. The comparison between the seasonal courses of the two fluctuations shows a perfect coincidence. Consequently, we can say that these fluctuations are related. The 4-6-day fluctuations in the neutral wind are best expressed in the equinox. This fact is identical with the seasonal course of the analogous fluctuations in absorption. The comparison between the two fluctuations shows a similarity, but not so well expressed as it was with the 10.5-12 day fluctuation. It is almost beyond doubt that the short-period 2.4-3.2-day fluctuation in absorption is closely connected with the analogous fluctuation in the neutral wind (such a high frequency fluctuation exists neither in the Ly-α flux, nor in the aa(N)-index). The seasonal course of this fluctuation observed in wind coincides with those in absorption, i.e. the main maximum in summer, a secondary one in winter.

The last investigated is the fluctuation with a period of about 27 days. Figure 2 shows the time variations of the instantaneous amplitudes of 27-day fluctuations in the Ly-α flux and in absorption with the use of the complex demodulation method. The following results are obvious:

1) When the Ly-α flux has very well expressed 27-day fluctuations

(as in July-August 1982), there is of course an ionospheric response, but the 27-day fluctuations in absorption are not the strongest ones.
2) There is a very well visible seasonal course of a 27-day fluctuation in absorption with winter maxima.
3) The periods of winter amplifications of 27-day fluctuations in absorption occur when they are almost absent in Ly-α flux (as in winter 1984/85). This last result is rather strange. It provoked us to analyse another time interval. We chose 1970-1980 . For this interval no Ly-α data are available to us, so the solar radio flux $F_{10.7}$ was used. The result was the same: an opposite course between the amplitudes of 27-day fluctuations in absorption and in solar radio flux.

What could be the reason for this opposite relationship between the amplitudes of 27-day fluctuations in absorption and in the solar ionizing flux? It is well known that the vertical propagation of planetary waves through critical levels in the stratosphere can occur only if the mean winds are westerly but less than a critical velocity (predominantly in winter season). The stratospheric circulation depends on the temperature distribution, which reacts to changes of ozone connected with solar UV perturbations. Recent studies of solar UV related changes of ozone have shown that during periods of amplifications of 27-day fluctuations in the solar UV flux (or in $F_{10.7}$, Ly-α flux) ozone in the stratosphere has a measurable response. This reaction could create critical levels in the stratosphere during winter. These levels do not permit the vertical propagation of the planetary waves with a period of about 27 days which are excited in the lower atmosphere. These waves cannot penetrate to mesospheric altitudes and cannot influence the electron density distribution or ionospheric absorption. When 27-day variations are almost absent in solar fluxes, then there are no conditions for creating critical levels in the winter stratosphere. Then the planetary waves with a period of about 27 days excited in the lower atmosphere can propagate vertically upwards and influence the ionospheric absorption.

Summarizing, we may say that the probable meteorological origin of the observed fluctuations in radiowave absorption seems to offer a possibility of monitoring fluctuations in the upper mesosphere and lower thermosphere in the planetary wave period range by means of radiowave absorption measurements.

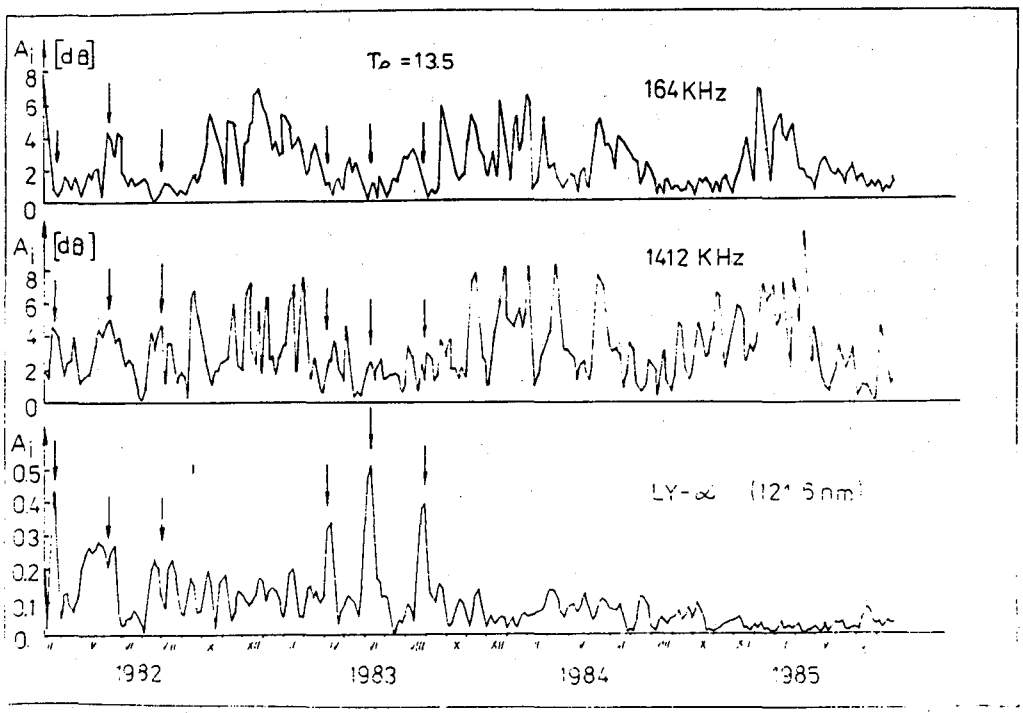

Fig. 1. The time variations of the instantaneous amplitudes of the 13.5-day fluctuation in the Lyman-alpha flux and in the ionospheric absorption for 164 kHz and 1412 kHz radio-paths.

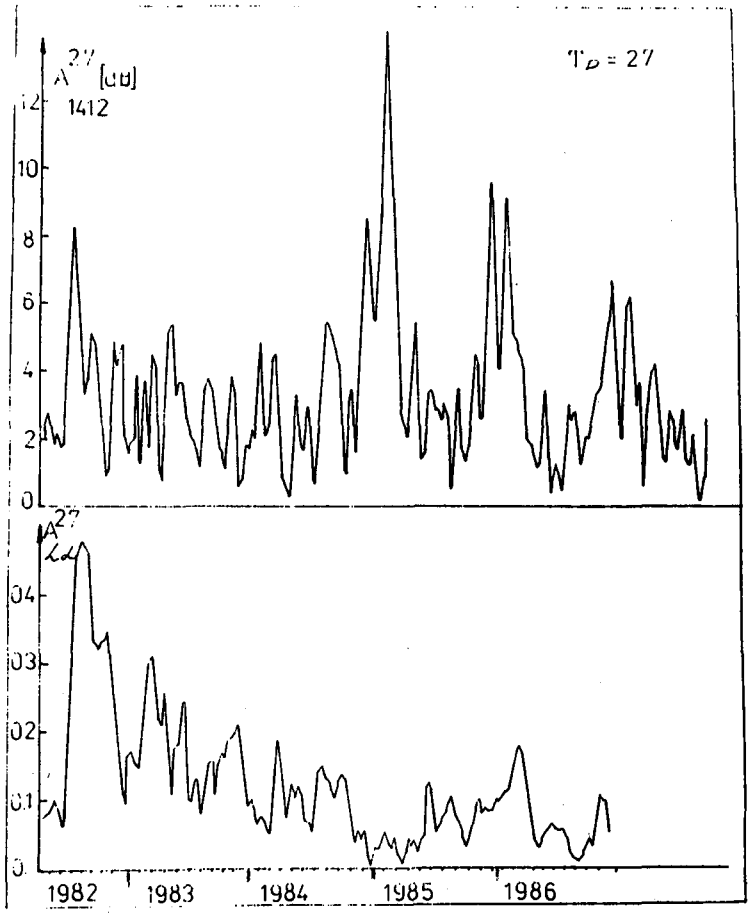

Fig. 2. The time variations of the instantaneous amplitudes of the 27-day fluctuation in the Lyman-alpha flux and in the ionospheric absorption for the 1412 kHz radio-path.

THE 27-DAY VERSUS 13.5-DAY VARIATIONS IN THE SOLAR LYMAN-ALHPA RADIATION AND THE RADIO WAVE ABSORPTION IN THE LOWER IONOSPHERE OVER EUROPE

B.A. de la Morena*, J. Laštovička**, Z.Ts. Rapoport***, L. Alberca****

*Atmospheric Sounding Station "El Arenosillo", 21130 Mazagon (Huelva), Spain
**Geophysical Institute, Czechosl. Acad. Sci., Boční II, 141 31 Praha 4, Czechoslovakia
***IZMIRAN, 142092 Troick, Moscow Region, USSR
****Ebro Observatory, Roquetes (Tarragona), Spain

INTRODUCTION

PANCHEVA et al. (1989) analysed variations of radio wave absorption in the lower ionosphere at 5 LF radio paths (A3 method - oblique incidence on the ionosphere) in Central and Southern Europe. They found several ranges of dominant periods between 2-15 days. However, all are of meteorological origin and the "solar" period T $\simeq$ 13.5 day (half of the solar rotation period) has not been observed with the expected amplitude.

In order to clarify the question of "solar" periods in absorption, we study the pattern of the solar Lyman-alpha radiation (the principal ionizing agent of the lower ionosphere) and of the radio wave absorption at five widely spaced places in Europe. We use the A3 absorption at 1539 kHz (Panská Ves, f_{eq} = 650-700 kHz, reflection point 50.3°N, 11.8°E) and twice at 2830 kHz (El Arenosillo, f_{eq} = 1.2 MHz, reflection point 38.5°N, 5.3°W; Ebro Observatory, f_{eq} = 1.4 MHz, reflection point 40.6°N, 1.6°W), and the f_{min} parameter (an indirect measure of absorption) from Moscow (55.5°N, 37.3°E) and Rostov upon Don (47.2°N, 39.7°E). We investigate two consecutive periods, March-June 1982 and July -October 1982. The former displays a very suppressed 27-day variation in Lyman-alpha. The 13.5-day variation seems to prevail (Figure 1). The latter displays a pure solar rotation variation in Lyman-alpha (Figure 2) with the largest amplitude observed during the whole 21st solar cycle.

RESULTS

The period March-June 1982 (Figure 1) displays rather poor similarity in development of Lyman-alpha and both absorption and f_{min}. Some gaps in data are caused by solar flares (SWF) and by technical problems. The lower frequency cut-off of f_{min} (1.0 MHz Moscow, 1.4 MHz Rostov) is given by the technical characteristics of ionosondes. Some increases of absorption and f_{min} are due to a considerable increase of the background X-ray flux and to the occurrence of weaker X-ray bursts, which enhance the absorption but are not strong enough to create a clear SWF. Such increases are observed e.g. on June 12-13 (1539 kHz), June 11 (El Arenosillo) or June 15-16 (f_{min}).

In order to support "visual" results from Figures 1 and 2, the correloperiodogram analysis (KOPECKÝ and KUKLIN, 1971) of the Lyman-alpha radiation, absorption (1539 kHz) and f_{min} (Moscow) was performed in the period range of 2-32 days for both periods. As to the period March-June 1982, for Lyman-alpha it

yielded two dominant periods 26.5-27 and 13-13.5 days at the confidence level of 0.01 with equal amplitudes of 0.105 (in units of Figure 1), and a less important period of 21 days (confidence level 0.05, amplitude 0.064). The period late March-June was dominated by T = 13.5 day. The f_{min} parameter displayed three periods at the 0.1 confidence level, 10.5, 13 and 19 days with amplitudes 0.044, 0.044 and 0.046, respectively. Owing to the low confidence level and to the step of 0.1 MHz in determining f_{min}, they all appear to be rather insignificant. The absorption exhibits two periods, 32 days (0.01 confidence level, 2.95 dB amplitude) and 17.5 day (0.1 confidence level, 2.2 dB amplitude). Thus both ionospheric parameters display periods different from those observed in Lyman-alpha. This confirms the conclusion drawn from Figure 1 about a poor similarity between the time-development of Lyman-alpha and ionospheric parameters.

Figure 2 shows that during the period of a well-developed solar rotation variation in July-October 1982 there is a remarkable similarity between variations of the solar Lyman-alpha radiation, radio wave absorption (except for Ebro data in late August - early September) and f_{min}. The correlation is again perturbed by the factors discussed in relation to Figure 1, but also by the post-storm effects of three strong magnetic storms (marked by S in Figures 1 and 2) with $K_p max > 8$, particularly by those in September. The effect of the very strong proton flare of July 11 (PF in Figure 2) coincides with the maximum of the Lyman-alpha flux.

The correloperiodogram analysis of the Lyman-alpha radiation, absorption (1539 kHz) and f_{min} (Moscow) for the period July-October 1982 yields in all three parameters the dominant solar rotation period at the confidence level of 0.01 - 25.5 day (amplitude 0.39) in Lyman-alpha, 25.5 day (amplitude 6.4 dB) in absorption and 24.5 day (amplitude 0.15 MHz) in f_{min}. The spacing between the consecutive Lyman-alpha maxima in Figure 2 is 24, 27, 24 and 27 days, i.e. just 25.5 day on average. The amplitude of solar rotation oscillations is in all three parameters much larger than that for any periodicity in the March-June period. Other periods - 13 days in Lyman-alpha (0.05 confidence level, 0.099 amplitude) and 19 days in both absorption (0.05 confidence level, 2.6 dB amplitude) and f_{min} (0.1 confidence level, 0.06 MHz amplitude) - are much weaker than the solar rotation oscillations.

CONCLUSION

When the solar Lyman-alpha flux variability is very well developed (July-October 1982), then it dominates in the lower ionospheric variability. The most pronounced Lyman-alpha variation on time scale day-month is the solar rotation variation (about 27 days). When the Lyman-alpha variability is developed rather poorly, as it is typical for periods dominated by the 13.5 day variability, then the lower ionospheric variability appears to be dominated by variations of meteorological origin. This fact and the considerably varying amplitude of the 13.5 day solar oscillation are probably the reason why T = 13.5 day was not found by PANCHEVA et al. (1989) to be of primary importance in the lower ionospheric variability. The above conclusions hold for all five widely spaced places in Europe. The interesting 19-day variability will

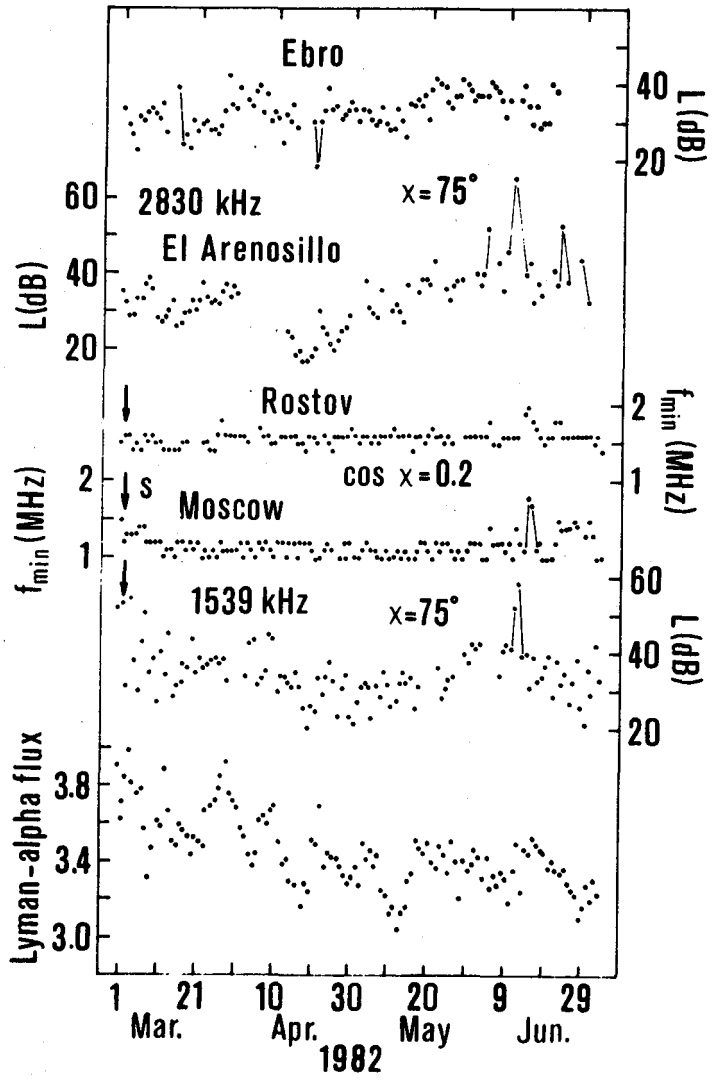

Fig. 1. Lyman-alpha flux, radio wave absorption (three A3 circuits) and f_{min} (Moscow and Rostov upon Don) during the period of suppressed 27-day variation in Lyman-alpha (March-June 1982). The Lyman-alpha flux is in 10^{11} photons/cm^{-2} s^{-1}. S - strong geomagnetic storm ($K_p$max = 8).

be studied in more detail in another paper.

Acknowledgements: We thank W.K. Tobiska for sending us the Lyman-alpha data, G.J. Rottman for permission to use them, E. Apostolov for the correloperiodogram computer code and J. Koráb for help with correloperiodogram computations.

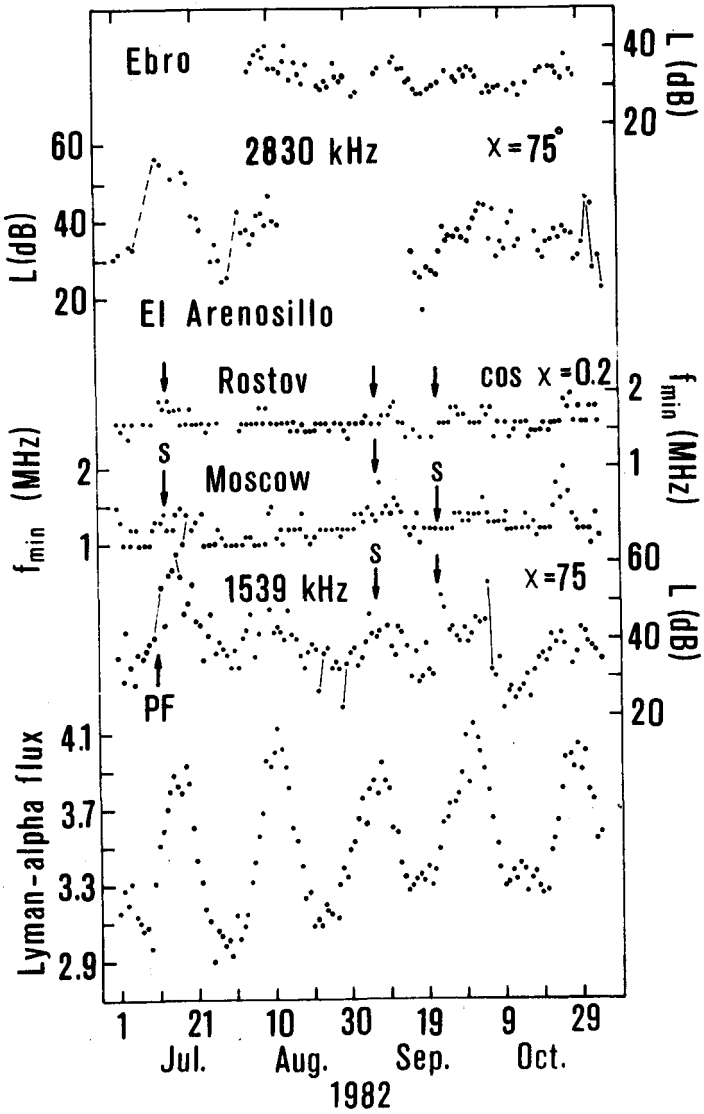

Fig. 2. The same as Figure 1 for the period of the well-developed solar rotation variation in Lyman-alpha (July-October 1982). S - strong geomagnetic storms ($K_p max \geq 8$). PF - strong proton flare.

REFERENCES

Kopecký, M., and G.V. Kuklin, Issl. Geomagn. Aeron. Fiz. Solnca, 2, 167, 1971 (in Russian).
Pancheva, D., and J. Laštovička, Solar and meteorological control of lower ionospheric fluctuations (2-15 days) in middle latitudes, Handbook for MAP (this issue), 1989.

THE PROBABILITY OF SWF OCCURRENCE IN RELATION TO SOLAR ACTIVITY

L.P.Morozova

Institute of Applied Geophysics,
Goscomhydromet, USSR

Solar terrestrial researches have revealed substantial meaning of nonsteady events on the Sun, mainly solar flares, for the processes taking place in ionosphere. Solar flares result in the numerous consequences, account and prediction of which become necessary in our days. It is well known, that ionospheric disturbances following solar flares cause strong disturbances in the ionosphere, which severely violate radio-systems (communication, navigation, etc.). In the given paper we consider possibilities of sudden short wave fadeouts (SWF) prediction.

It was long ago when solar physicists came to the conclusion that solar flares are not the exclusive events of solar activity, but represent a natural phenomenon in the active regions development (RUST, 1976).

Thus, SID effects, evoked by the sudden increase of X-radiation in the range of 1-8 A during the flares, may not be considered as the single phenomena, but as a flow of casual events. So the long-term prediction of SWF effects occurrence probability may be based on the probability characteristics analysis of their occurrence on different phases of solar activity for a particular time interval. At the same time, it is assumed that a slow changing of statistic model parameters in the solar activity cycle takes place.

For solving the problem there were obtained and analyzed hystograms of SWF occurrence frequency distribution for one particular day using data on their registration within the World network of SID monitoring stations for the period of 1974-1985, published in "SOLAR GEOPHYSICAL DATA" (1967-1985).

Observation data were processed separately for various phases of solar activity. Thus, the results of 1974, 1975 and 1985 characterized solar activity minimum, results of 1976 and 1977 - growth phase, results of 1978-1980 - solar activity maximum, results of 1972, 1973 and 1984 characterized falloff phase of solar activity.

Figure 1 gives an example of the experimental data in the form of hystograms of n events probability distribution (n varies from 0 to 10) on a day for solar activity maximum or for solar activity minimum. Hystograms for all solar cycle phases are similar. They have maximum at n=0 with a different maximum value for various cycle phases of solar activity. The greatest number of days without SWF effects (i.e.=0) is typical for solar activity minimum; for this period P(0)=0.81. For the period of solar activity maximum this value is the least P(0)=0.37. Average value of SWF occurrence frequency on a day of solar

activity minimum is n=0.45 but at solar activity maximum n=1.7.

Occurrence of SWF effects may be considered as a rare casual event. So it was quite natural to use Poisson distribution for theoretical description of occurrence frequency. After comparison a great difference between theoretical and experimental distributions was revealed. We may assume than SWF effects are rare casual events but separate effects are not independent. Flare activity on the Sun, leading to SWF occurrence in ionosphere, is a complex multiparametric process, depending upon spatial distribution of active regions on the solar disk, upon magnetic fields of these regions and upon many other parameters. Thus, it is evident that a model of independent occurrence (Poisson model) is not adequate to real conditions of SWF occurrence.

Experimental hystograms analysis allows to suggest that exponential distribution may be chosen as most suitable simplified distribution for their description. Satisfactory approximation with empiric distributions has been obtained with the help of superposition of two exponents.

Approximation expression was obtained for every phase of solar cycle, and besides coefficients were chosen empirically, basing on the experimental hystograms.

Solar activity minimum:

$$P(n) = 0.76*\exp(-2.7n) + 0.1*\exp(-0.54n) \qquad (1)$$

Solar activity maximum:

$$P(n) = 0.14*\exp(-0.26n) + 0.23*\exp(-0.86n) \qquad (2)$$

Increase phase of solar activity:

$$P(n) = 0.67*\exp(-2.6n) + 0.11*\exp(-0.51n) \qquad (3)$$

Falloff phase of solar activity:

$$P(n) = 0.46*\exp(-2.6n) + 0.17*\exp(-0.41n) \qquad (4)$$

Thus, approximate analytical expression for SWF occurrence frequency distribution may be presented in general as follows:

$$P(n) = A1*\exp(-\alpha 1 n) + A2*\exp(-\alpha 2 n) \qquad (5)$$

where coefficients A1, A2, $\alpha 1$ and $\alpha 2$ vary with a change of solar activity. On this base we assume that there may be link between parameters of approximate expression (5) and solar activity index, for example, relative sunspot number R_z or so-called Wolf number.

Fig.2 shows variation of parameters values A1, A2, $\alpha 1$, $\alpha 2$ and R_z during 21-st cycle of solar activity. It should be mentioned that approximate expression parameters are changing in the cycle with periodicity, typical for R_z variations.

So it is possible to express the coefficients of analytical expression (5) as a function of sunspot number:

$$A1 = A10 - \Delta A1(t)*y,$$

$$\alpha 1 = \alpha 10 - \Delta\alpha 1(t)*y,$$

$$A2 = A20 + \Delta A2(t)*y, \qquad (6)$$

$$\alpha 2 = \alpha 20 + \Delta\alpha 2(t)*y$$

where

$$y = R_z - (R_z)min/(R_z)max - (R_z)min \qquad (7)$$

It should be mentioned that in formulae (6) the values of A_{10}, α_{10} and $\Delta A1$, $\Delta\alpha 1$ for fixed phase of solar activity cycle remain constant, being obtained on the base of assembly average for every period.

Link of approximate expression parameters with Wolf numbers is determined by expressions (6). And it is known that nowadays sunspots are the most precisely predictable values, characterizing solar activity (VITINSKIY, 1963).

Using the prediction of R_z values (Solar Geophysical Data, 1976-1985) of expressions (6) we obtain parameters of approximate analytical expression (5) that allow further to calculate n SWF effects occurrence probability on day for a given period beforehand, that is to realize long-term prediction. It is possible as well to give forecasting of expectable average number of SWF effects in the period of interest.

Results of control predictions have shown that statistical model is satisfactory describing empirical distribution of SWF effects occurrence for various phases of solar activity, or gives the assessment of average number of effects for a particular period, for example, a year in advance. The results of long-term prediction by average values are statistically only slightly different from monitoring results.

Thus, our work has shown that the possibility of long-term prediction of SWF effects occurrence frequency is conditioned by slow temporal variations of statistic model parameters and by link of these parameters with sunspot number as well.

REFERENCES

1. Rust D. An active role for magnetic fields in solar flares. Solar Phys., 1976, No.47, p.21.

2. Solar Geophysical Data. Prompt report. 1967-1985.

3. Vitinskiy Yu.I. Solar activity predictions. M.: AS USSR, 1963. 152 p.

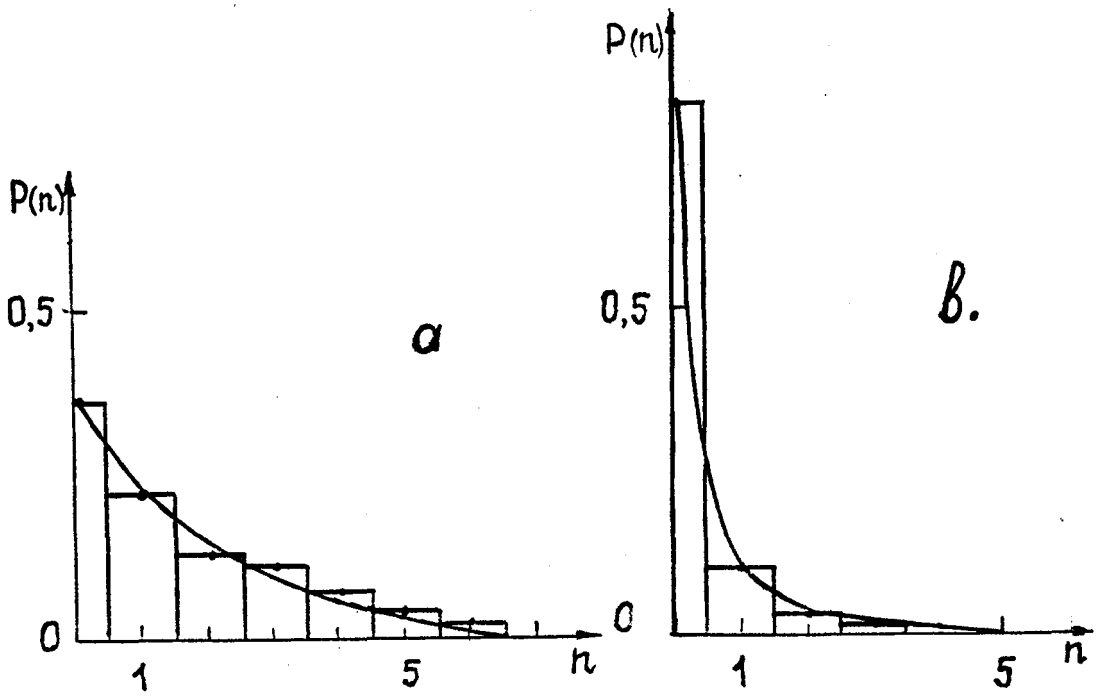

Fig. 1. Distribution hystograms of SWF effects occurrence probability in one day: a) solar activity maximum; b) solar activity minimum.

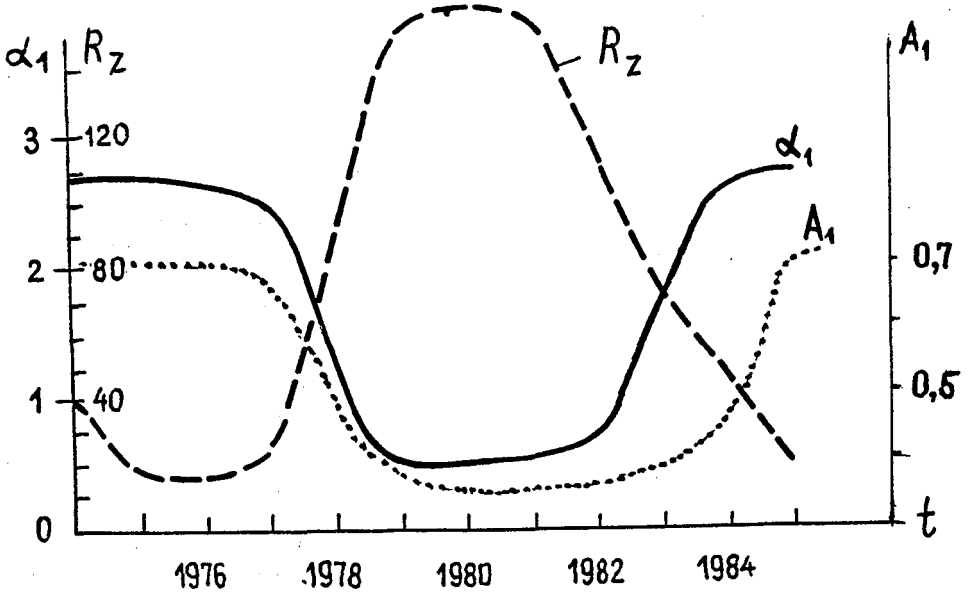

Fig.2.Variation of statistical model coefficients and sunspot number for the period of 1974-1985.

POST-FLARE EFFECTS IN THE LOWER IONOSPHERE OF MIDDLE LATITUDES

L. Křivský

Astronomical Institute, Ondřejov 25165, Czechoslovakia

Beginning in the 1960s, we started to record cosmic radio noise from the region around the Polar Star on 29 MHz (KŘIVSKÝ and TLAMICHA, 1960) at the Ondřejov Observatory near Prague (49°54'N). Since the aerial characteristic was not too narrow, we received radio bursts of solar origin (of flares) at the noise level, SCNA effects (sudden cosmic noise absorption) at the time of intensive flare X-emission and in some rare cases, after large proton flares, small absorption effects of a few hours duration (KŘIVSKÝ, 1969). These post-flare absorption effects in cosmic noise are evidently analogous with PCA effects (polar cap absorption) and are connected with ionospheric absorption of radio cosmic noise, caused by fast particles of subcosmic radiation.

The recording of long-term absorption effects after large particle flares at European midlatitudes was reported in our astronomical papers already at the beginning of the 1960s. It was then usual to record radio cosmic noise with riometers at frequencies of about 18 MHz in the polar or subpolar regions in an effort to record PCA effects of subcosmic radiation (HAKURA, 1968). We attempted to record the complex of emissions mentioned as well as the effects in a new frequency range (30 MHz), which did not agree with the ideas of the contemporaneous representatives of the Ionospheric Department of the Geophysical Institute in Prague.

In recent years radio cosmic noise has been recorded at the Úpice Observatory in NE Bohemia (KLIMEŠ and KŘIVSKÝ, 1988).

We are presenting now a report on these long-term after flare effects of cosmic radio noise absorption (AF-CNA) at middle latitudes to the geophysical and ionospheric community for the first time.

The complex of the mentioned effects is demonstrated on the example of the observations and records of the proton flare of September 26, 1963. Figure 1 shows the development of the proton flare in Hα; the flare was of the usual flare-channel type, i.e. in the shape of two diverting ribbons connected with a rising flare-loop system at altitude. Figure 2a depicts the measurement of the width of the Hα line of this flare, and Figure 2b shows the record of atmospherics on 27 kHz with the X-emission effect which produced an anomalous ionospheric D-region (SEA - sudden enhancement of atmospherics); Figure 2c is a copy of the cosmic noise record on 29 MHz, and Figures 2d-f records of the radio flare bursts made with a radiometer on three individual frequencies; all the records are from the Ondřejov Observatory.

The flare started a few minutes after 07 00 UT and ended 09 10 UT. The CN records (c) clearly show that after the beginning of the flare, a fluctuating radio emission of the flare was recived, the decreasing values indicating a SCNA effect (7.2 dB). At about 09 10 UT the originaly undisturbed level was recovered and later, after 09 40 UT, a gradual long-term small absorption effect is

displayed. The duration of this after flare effect was a few hours.

The arrival of particles of sub-cosmic radiation was indicated by a PCA effect recorded by riometers (HAKURA, 1968), beginning at 11 15 UT on the same day. The commencement of the CNA after end of the flare, at about 09 40 UT (before the beginning of the PCA in the polar region), is probably connected with the arrival of faster particles in the ionosphere of middle latitudes. The geomagnetic storm with SSC began at 19 42 UT on September 27, 1963 (arrival of a particle cloud with a shock wave). The cosmic-ray Forbush decrease observed near the South Pole by Czechoslovak measurements began at 20 00 UT on September 27, 1963 (FISCHER and KŘIVSKÝ, 1965).

REFERENCES

Fischer, S., and L. Křivský, Solar effects on the cosmic radiation at the Vostok station - Sep 1963, Bull. Astr. Inst. Czechosl., 16, 316, 1965.

Hakura, Z., Polar cap absorption and associated solar-terrestrial events troughout the 19th solar cycle, NASA Techn. Note D-4473, 1968.

Klimeš, J., and L. Křivský, Catalogue of Decametre Radio Bursts Recorded at the Upice Observatory during Cycle No 20 (1965-1976), Publ. Astr. Inst. Czechosl. Ac. Sci. Ondrejov, 73, 1988.

Křivský L., Flare of 26.IX.1963 and its emission, Bull. Astr. Inst. Czechosl., 20, 163, 1969.

Křivský L., and A. Tlamicha, Emission of the 1960 May 13 flare and absorption of cosmic noise, Bull. Astr. Inst. Czechosl., 11, 238, 1960.

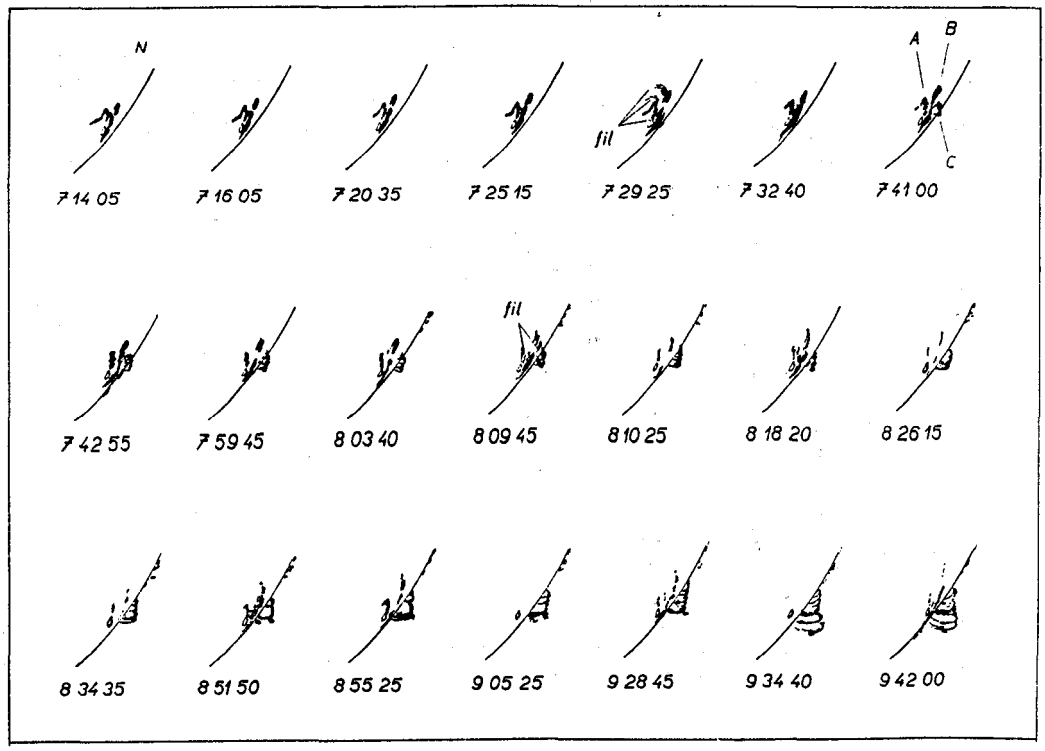

Fig. 1 Drawings of selected stages of evolution of the proton flare of Sep 26, 1963. The drawings were derived from the Hα photographs of various exposures. The empty field is a spot, the flare field is represented by a black surface. Some of the pictures showed flare absorption filaments; these are marked by arrows and shadowing. The lower flare ribbons in the chromosphere are marked A, B, the ascending tops of loops with C.

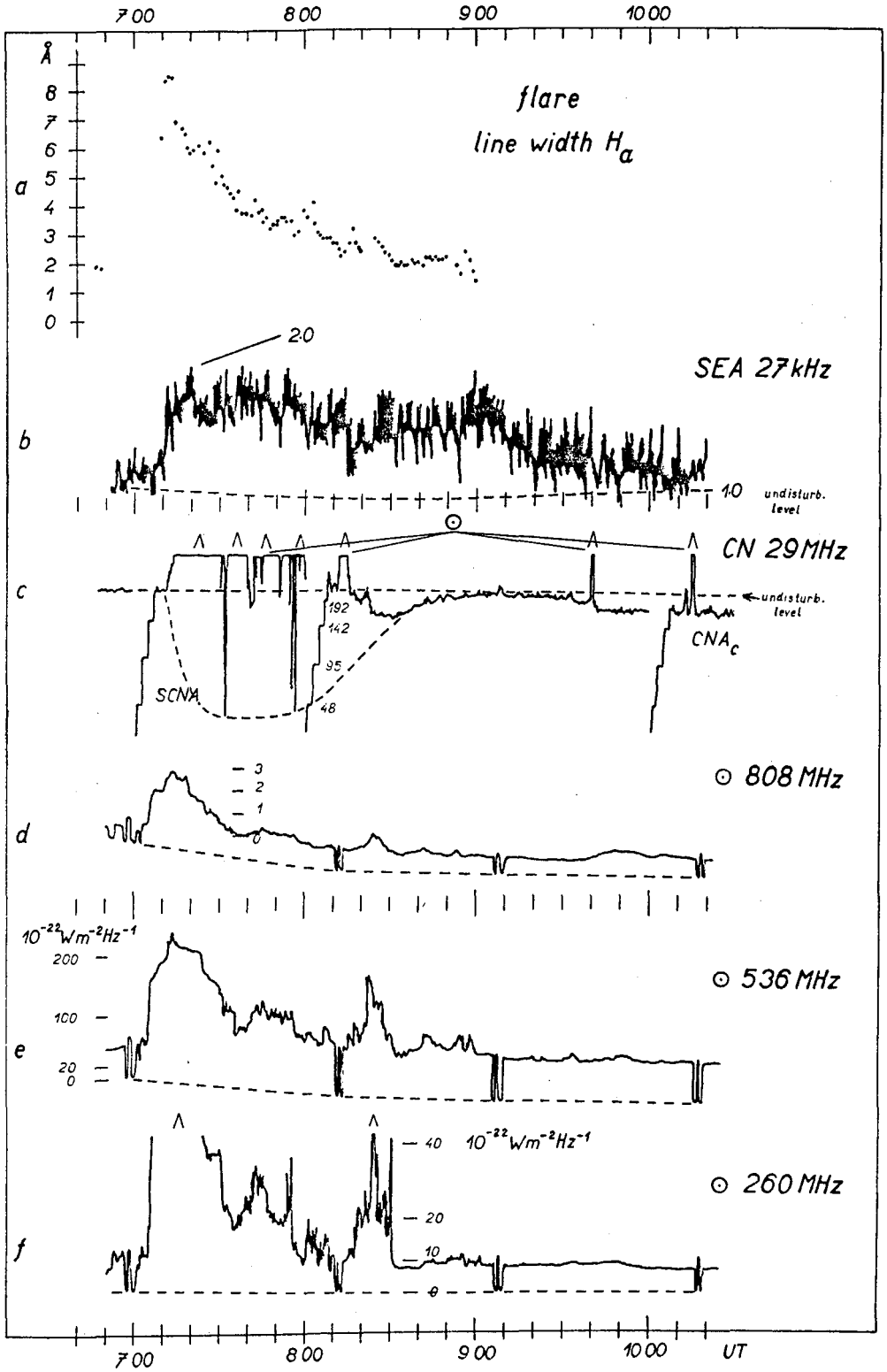
7 00
8 00
9 00
10 00
Å
8
7
6
5
4
3
2
1
0
a
flare
line width H_α
2·0
SEA 27 kHz
b
1·0
undisturb. level
CN 29 MHz
c
192
142
95
48
SCNA
CNA$_c$
undisturb. level
⊙ 808 MHz
d
3
2
1
0
10^{-22} Wm^{-2}Hz^{-1}
200
100
20
0
⊙ 536 MHz
e
40
20
10
0
⊙ 260 MHz
f
UT

Fig.2

THE NATURAL VLF EMISSION AS DIAGNOSTICS AND ESTIMATION MEANS OF THE FLUXES OF SOLAR X-RAY BURSTS

Murzaeva N.N.

Institute of Cosmophysical Research and Aeronomy,
Lenin Ave., 31, 677891 Yakutsk, USSR

Abstract. The possibility to detect the chromospheric flares based on the natural VLF emission intensity data on the Earth's surface is considered. Diagnostics of the change of solar X-ray burst flux at 0.5-4 Å° and its estimation are discussed as possible.

The effect of solar flare short-wave emission on the Earth's ionosphere was considered by A.Mitra (1977) where the determination of solar X-ray fluxes by indirect methods is described. In low-frequency range for this aim are used the signals of transmitters operating at tens-hundreds kilohertz frequencies. The records of the natural emission (atmospherics) are considered to be suitable for the detection of flares but to be hardly used for the investigation of ionosphere physics as the detected noise represents the integral effect of many sources and the sources are of a random character.

Here the possibility is studied of the detection of solar chromospheric flares and the estimation of X-ray flux accompanied by powerful bursts in the range 0.5-4, 1-8 Å based on the change of the regular noise background intensity of the natural low-frequency emission detected on the Earth.

For many years in Yakutsk (φ = 62°N; λ = 129,7°E) the natural ELF-VLF emission at 0.5-10 kHz is being detected continiously. One of the types of continious low-frequency emission is a regular noise background (RNB) determined as a separate class (Vershinin, Ponomarev, 1966). RNB is is available constantly on the records and is characterized by a smooth temporal rounding. A spectral distribution of RNB intensity is two emission bands in ELF-VLF ranges divided by a deep minimum at 2-4 kHz (Murzaeva, 1974).

For the analysis were used the records of ELF-VLF emissions obtained in Yakutsk in 1973-1974 by 8-channel registrator (Druzhin et al., 1976) and from 1978 to now by 13-channel registrator in 0.5-10 kHz range. Besides, satellite data of solar X-ray fluxes were used (SGD, 1973-1985).

A comparison of RNB records with solar X-ray fluxes showed that the change of ELF-VLF emission intensity and its value depend on a value of X-ray burst flux. Almost simultaneously with solar X-ray burst the RNB intensity increases at 0.5-3 kHz and decreases at ~3-10 kHz. The enhancement maximum is at 0.5-0.8 kHz, the highest weakening - at 4-6 kHz (Murzaeva, 1977; 1981). The increase of X-ray flux by an order of 2-4 causes both weakening and an enhancement of ELF-VLF emission RNB intensity from ~2-3 to ~15-20 dB.

A change of RNB intensity spectral distribution during solar flares was considered by Murzaeva, Fligel (1980; 1984).

In Fig.1 is shown RNB intensity averaged on 5 flares in 1973-1974 and in 1981 versus a frequency. On Y-axis is put a ratio of RNB intensity measured at a flare maximum (I_b) to a pre-flare RNB level (I_o) calculated as 10 lg I_b/I_o (Murzaeva, 1977).

In Fig.2 is presented an example of RNB intensity change during a flare at various concrete frequencies of the range under investigation and solar X-ray flux record obtained by the satellite (SGD, 1973). A dynamics of VLF emission intensity at 5.6 kHz and of X-ray flux repeat each other (in counterphase). However, ELF emission intensity increase during a flare is not always observed and a frequency at which occurs a transfer from RNB intensity increase to its decrease is rather variable. Besides, ELF emission intensity enhancement caused by the influence of enhanced solar X-ray flux on the ionosphere is hardly different from ELF emission flare caused by other types of ionospheric and magnetospheric disturbances. At the same time a sharp weakening of RNB intensity at VLF frequencies observed during chromospheric flares is opposite to VLF emission bursts and is of a characteristic for chromospheric flares form. Therefore to study the variations of solar X-ray fluxes were used the experimental data at 5.6 kHz which, besides, appears to be at frequency range where RNB intensity weakening is maximum during a flare and RNB record level is high enough as compared with the instrument noise.

Sometimes during several hours one can observe a number of flares, for instance, on July 21, 1981. The variations of RNB level caused by them are superposed on its regular daily changes. Nevertheless, (see Fig.3) in the behaviour of RNB curve is reflected the dynamics of flare X-ray flux. A picture is being clarified if to subtrack the daily variations of RNB intensity from the total curve course.

We carried out a statistical treatment of the experimental data on a number of chromospheric flares and estimated solar X-ray flux during flares. In the case when X-ray fluxes (F) increase during a flare by an order of ~ 2 or more they are as $F = c(I_b/I_o)^{\kappa}$ where c and κ are determined based on the experimental data. The estimated X-ray flux (in the first approximation) is shown in Fig.3. A comparison with the satellite data (SGD, 1982) evidences its agreement.

Thus, using data of continious ground-based registration of the natural VLF emission one can:

- on characteristic for the period of chromospheric flares form of RNB intensity decrease of VLF emission to detect solar flares accompanied by powerful solar X-rays bursts;
- on the change of VLF emission RNB intensity to carry out a continious diagnostics of changes of solar X-ray burst flux and to estimate its value.

REFERENCES

Mitra A. Ionospheric Effects of Solar Flares. M.: Mir, 1977.

Murzaeva N.N. Regulyarny shumovoi fon ONCh izlucheniya. V kn.: Nizkochastotnye volny i signaly vo vneshnei ionosfere. Apatity. Izd-vo Kolskogo filiala AN SSSR. 1974. S.20-23.

Murzaeva N.N. Regulyarny shumovoi fon ONCh izlucheniya vo vremya solnechnykh vspyshek. V kn.: Svyaz ONCh izluchenii verkhnei atmosfery s drugimi geofizicheskimi yavleniyami. Yakutsk. Izd-vo YaF SO AN SSSR. 1977. s.21-34.

Murzaeva N.N., Fligel D.S. O vliyanii solnechykh vspyshek na spektralnye kharakteristiki nepreryvnogo nizkochastotnogo izlucheniya. V kn.: Issledovaniye struktury i volnovykh svoistv okolozemnoi plazmy. M.: IZMIRAN. 1980. s.24-39.

Murzaeva N.N. O vozmozhnosti registratsii khromosfernykh vspyshek po izmeneniyu intensivnosti regulyarnogo shumovogo fona KNCh-ONCh izlucheniya. Bul.NTI. Problemy kosmofiziki i aeronomii. Yakutsk: YaF SO AN SSSR. 1981, iyul, s.22-23.

Murzaeva N.N., Fligel D.S. Izmeneniye spektrov regulyarnogo shumovogo fona vo vremya solnechykh vspyshek. V kn.: Magnitorfernye issledovaniya. M.: 1986, No.7, s.150-154.

Solar Geophysical Data (Comprehensive Report), No.351, Part 2. 1973.

Solar Geophysical Data (Comprehensive Report), 1973-1985.

Valkov S.P., Druzhin G.I., Shvetsov V.D., Nikitin Yu.P., Petrov V.G. Apparatura dlya registratsii ONCh izlucheniya. V kn.: Nizkochastotnye signaly vo vneshnei ionosfere. Yakutsk. Izd-vo YaF SO AN SSSR, 1976. s.107-117.

Vershinin E.F., Ponomarev E.A. O klassifikatsii nepreryvnogo ultranizkochastotnogo izlucheniya verkhnei atmosfery. V kn.: Zemnoi magnetizm, polyarnye siyaniya i ultranizkochastotnoye izlucheniye. Vyp.I. Irkutsk, SibIZMIR AN SSSR. 1966. s.35-44.

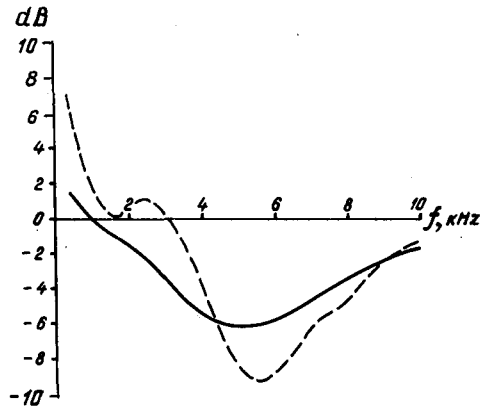

Fig.1. A change of RNB intensity averaged on 5 flares in 1973-1974 (———), in 1981 (– – –)

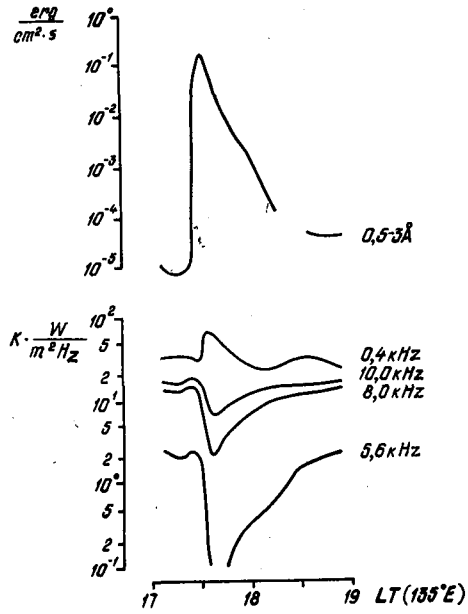

Fig.2. A change of RNB intensity during the May 3, 1973 flare at various frequencies and solar X-ray flux on satellite data (SGD, 1973)

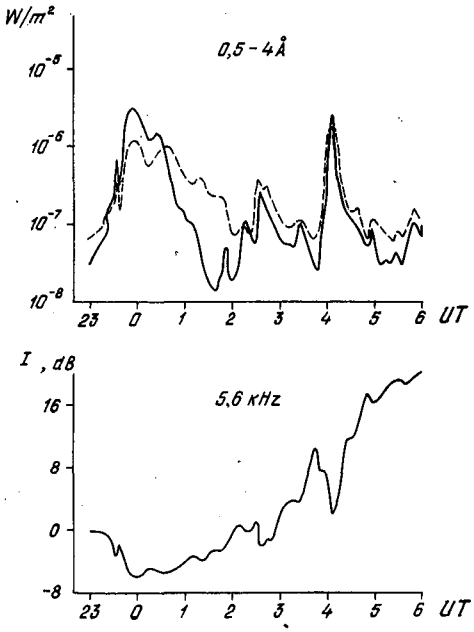

Fig.3. The record of RNB intensity of the natural VLF emission and solar X-ray flux (satellite data - SGD, 1982) during a number of flares on 21.07.81 (——), X-ray flux obtained on VLF emission data (– – –).

IONOSPHERIC EFFECTS OF THE EXTREME SOLAR ACTIVITY OF FEBRUARY 1986

J. Boška*, D. Pancheva**

* Geophysical Institute, Czechosl.Acad.Sci., Boční II, 141 31 Prague 4, Czechoslovakia

** Geophysical Institute, Bulg.Acad.Sci., "Acad. G. Bonchev" 3, Sofia 1113, Bulgaria

During February 1986, near the minimum of the 11-year Solar sunspot cycle, after a long period of totally quiet solar activity (R_Z = 0 on most days in January) a period of a suddenly enhanced solar activity occurred in the minimum between solar cycles 21 and 22. Two proton flares were observed during this period. A few other flares, various phenomena accompanying proton flares, an extremely severe geomagnetic storm and strong disturbances in the Earth's ionosphere were observed in this period of enhanced solar activity.

Two active regions appeared on the solar disc. Region NOAA 4711 occurred on the disc between 31 January - 11 February 1986. Several large flares appeared in this active region. The most important flares, two proton flares, were observed in this region 4 February, 0732 - 0835 UT imp. 3B and 6 February 0618 - 0732 UT, imp. 3B. Another large flare occurred in this region on 7 February 1014 - 1035 UT imp. 3B. The second active region NOAA 4713 occurred on the solar disc between 3 - 15 February. Its most important flare was observed on 4 February 1025 - 1128 UT.

The flares in both active regions were associated with enhancement of solar high energy proton flux which started on 4 February of 0900 UT. The enhancement of the solar proton flux on 6-9 February 1986 with maximum on 7 February 1730 UT and the end on 8 February is depicted in Fig. 1.

Associated with the flares, the magnetic storm with sudden commencement had its onset on 6 February 1312 UT and attained its maximum on 8 February (Kp = 9). Its development in Kp is also shown in Fig. 1.

The sudden enhancement in solar activity in February 1986 was accompanied by strong disturbances in the Earth's ionosphere, SIDs and ionospheric storm. The highest SID event, importance 3+, was observed on 4 February 0735 - 0945 UT. Two proton flares (4,6 February) were folowed by PCA events in the lower ionosphere.

The strong geomagnetic storm culminating on 8 February caused a strong ionospheric storm. The effects of this storm, as observed by the ionosonde at Pruhonice observatory (49°59'N; 14°33'E), are plotted in Fig. 2. Variations of the critical frequency of the F2 layer of the ionosphere from 7 to 11 February are shown in Fig. 2. The positive part of the storm effect began on 7 February forenoon and at about 1600 UT was followed by a sudden decrease of the critical frequency of the F2 layer (from 7.5 MHz to 2.3 MHz) while the virtual heights increased. The negative part of the storm characterized by spread echoes and low critical frequency lasted until 11 February. On 8 February from 1500 quite unusual effects were observed, unusually E layer h'= 155 km; foE = 2.25 MHz (higher virtual height and higher frequency than the normal E layer), which may be interpreted as a particle E layer, which appeared on the ionogram at 1500 UT (Fig. 3). This effect was followed by the appearance of a quite extraordinary layer (in 1615

UT) with virtual height of about 200 km (Fig. 4). This layer existed 1 hour and then droped down and became an Es layer type of a (auroral) which existed until 2200 UT.

These effects and type Es are quite unusual in our middle latitudes and were probably connected with strongly increased auroral activity.

The effect of the geomagnetic storm on the lower ionosphere consisted of two different types. The first type, observed at high latitudes, consisted in a large increase of electron density coincident with the geomagnetic storm. At midlatitudes we observed the post-storm effect (PSE), which consisted of the first phase (PSE I) coincident with the geomagnetic storm and the second phase, observed after the geomagnetic storm (PSE II). For the detection of post-storm effects, caused by the geomagnetic storm on February 1986 we used A3 absorption measurement given in table. 1.

TABLE 1

frequency	observ.	geomagn. lat. of refl.point
245 kHz	KUHLUNGSBORN	55°
1539 kHz	PANSKA VES	50°
164 kHz	SOFIA	45°
747 kHz	SOFIA	42°
1412 kHz	SOFIA	43°

The first phase (PSE I) of the post storm effect started on 6 February, the maximum of the geomagnetic storm was on 8 February (Ap = 202, ΣKp 62) and the end of the first phase had PSE on 10 February. PSE II started on 11 February. The results for night time absortpion data in given measuring paths (Fig. 4) indicated that the first phase of the PSE was well developed only for the northern most measuring path (p = 245 kHz, ø = 55°). The second phase of PSE II absorption enhancement on that path decreased very quickly (up to day +3 after PSE I end). This result indicates a direct effect in high latitudes rather than midlatitudes. On the other band, the results for 164 kHz and 747 kHz represent a typical midlatitude case with missing phase I and very well developed phase II. The case of 1539 kHz is very like the behaviour of the transitional type, normally observed in the subauroral zone, with the transition of the time of the commencement of the first phase with latitude. The effect on 1412 kHz is developed very weakly. The existence of the third phase PSE III after 15 February is not quite clear, either. This latitude boundary is in accord with the hypothesis on equatorward expansion of the auroral zone during geomagnetic storm in early February 1986.

REFERENCES

Solar Geophysical Data: 1986, No. 499; No. 500, No. 501, Part I, No. 504, Part II. Boulder.
E.A. LAUTER ET AL.: HHI-STP-REPORT No. 9 (1977), BERLIN

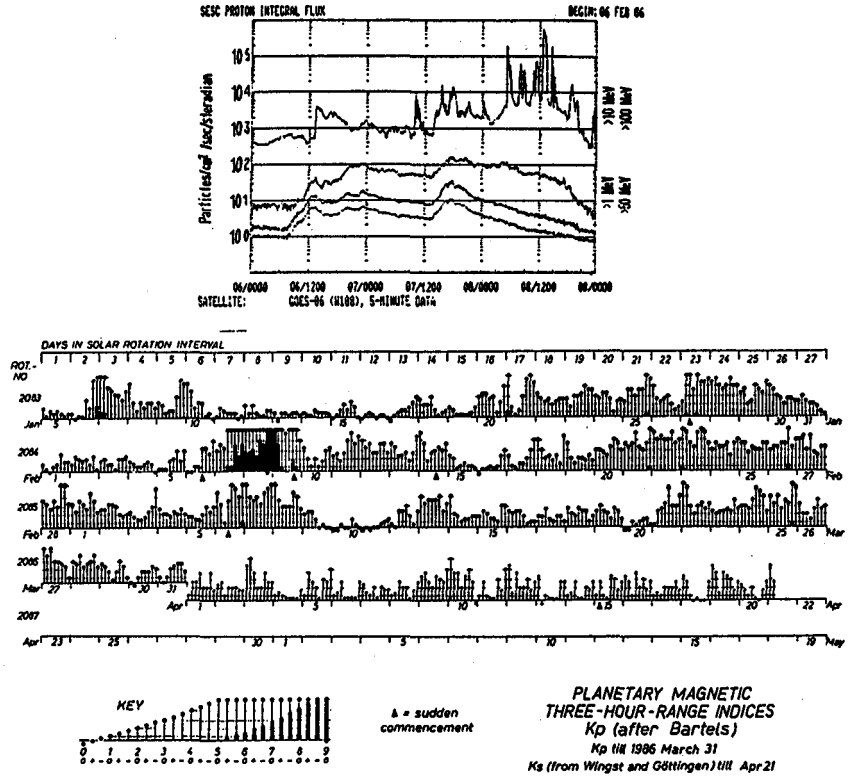

Fig. 1: The enhancement of the high energy proton flux as observed on 6-9 February 1986 Below: Planetary magnetic three-hour range indices Kp.

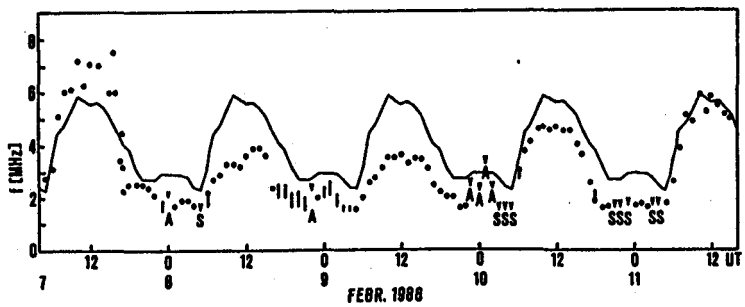

Fig. 2: Critical frequencies of F2 layer, Pruhonice. full line - median of foF2 in FEBRUARY, v - foF2 less than given value; A - blanketing Es layer; S - interference.

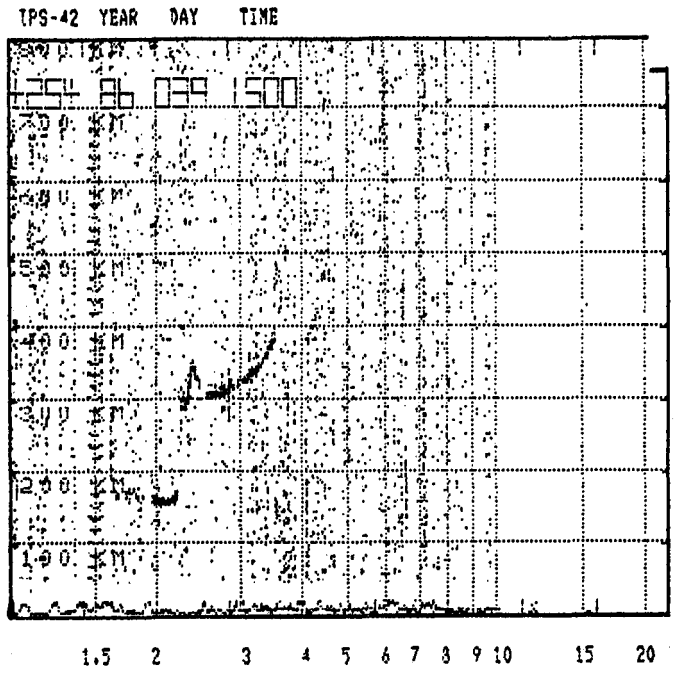

Fig. 3: Ionogram with particle E layer; Pruhonice; 08.2.1986 - 1500 UT

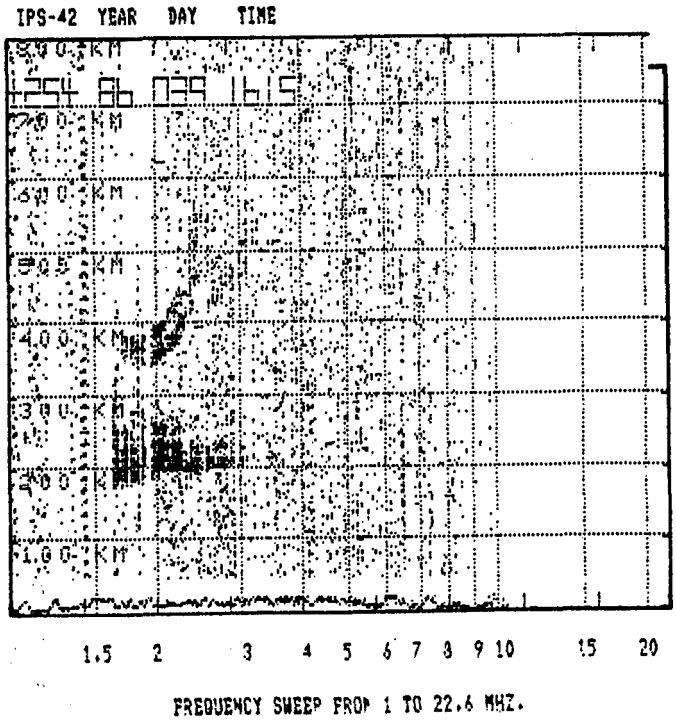

Fig. 4: Ionogram with extraordinary layer. Pruhonice, 8.2.1986 - 1615 UT.

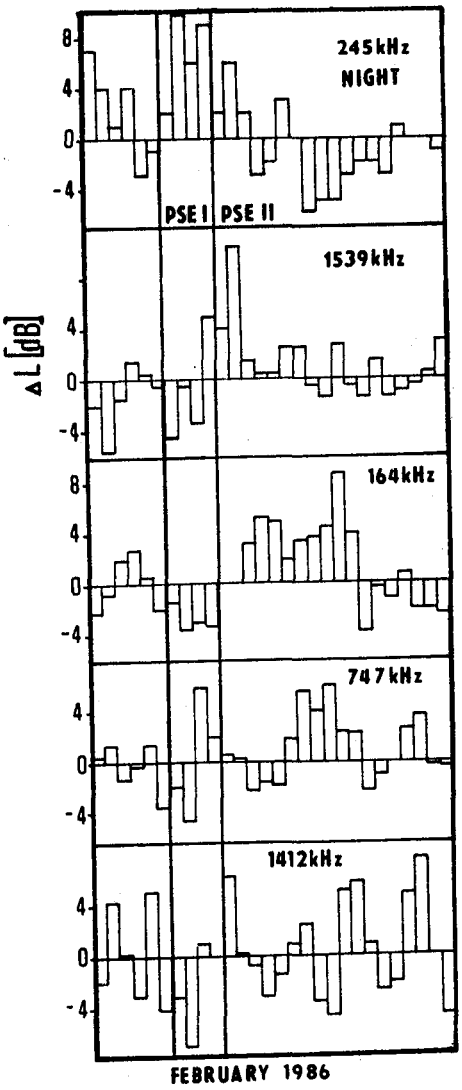

Fig. 5: The effect of the geomagnetic storm of February 1986 in the lower ionosphere. Δ L - changes in ionospheric A3 absorption on several measuring paths.

C4

ON THE RELATION BETWEEN THE ELECTRON CONTENT OF THE IONOSPHERIC D-REGION, VARIATIONS OF THE RIOMETER ABSORPTION, AND THE H-COMPONENT OF THE GEOMAGNETIC FIELD

L.V.Zelenkova, V.A.Soldatov, J.V.Arkhipov, V.F.Laikova

Research Institute of Physics, Leningrad State University,
Stary Petergof, 198904, Leningrad, USSR.

The correlation between lower ionosphere disturbances, geomagnetic variations and radiowave absorption is one of the most actual problems of geophysics.

In this work we investigate the correlation between the electron density profile structure and riometer absorption, and between the absorption and the H-component magnetic field, in order to determine the relation between the [e]-profile parameters and the geomagnetic field variations.

1. To calculate theoretically the electron density behaviour during disturbed conditions from riometer absorption data, one can use the well-known formula: $[e]=\sqrt{q/\Psi}$, where q ($cm^{-3}s^{-1}$) is the ion production rate and Ψ (cm^3s^{-1}) is the effective loss rate.

PARTHASARATHY [1966] presents the relations between riometer absorption and the integral precipitating electron flux with E>40keV in the following form: $A(dB)=3.3\ 10^{-3}\sqrt{J(>40keV)}$.

ZELENKOVA [1988] showed that provided the integral precipitating electron flux has the power form as $J(>E)=k\cdot E^{-\gamma}$ we can find the flux parameters k and γ. For $\gamma=2$: $k=3{,}3^{-2}\ 10^{6}\ 40^{2}\ A^2$. Thus, for each value of riometer absorption, it is possible to obtain the differential precipitating electron flux responsible for it.

Then we obtain the ion production rate using the formula from paper by KHVOROSTOVSKIY [1987].

2. To determine the height profile of [e], the investigations of effective loss rate variations were made using the published data referenced in the paper by GLEDHILL [1986]. All the height profiles were separated into 4 groups:

1) Ψ_1 height profiles for the day-time quiet conditions (12 profiles),
2) Ψ_2 height profiles for the night-time quiet conditions (7 profiles),
3) Ψ_3 height profiles for the day-time disturbed conditions (13 profiles),
4) Ψ_4 height profiles for the night-time disturbed conditions (5 profiles).

Mean profiles for 4 types of conditions are shown in Fig.1. The value of the disturbed (both day-time and night-time) effective loss rate is less than the quiet one as seen from Fig.1 even taking into account the considerable error (shown). The fact of dependence of the effective loss rate on ionospheric disturbance level was established in the paper by ZELENKOVA [1981]. Using a 3-ion D-region model for the height range of $\lambda=[M^-]/[e]>1$, the analytical dependence was derived also in that paper.

Because the formula from paper by ZELENKOVA [1981] is correct when $\lambda>1$, we used also a combined profile of Ψ, where effective loss rate was calculated for the heights from 50km to the height where Ψ becomes equal to $2\ 10^{-7}\ cm^3s^{-1}$, and such a value of Ψ was assumed up to h=95km. In the height range 95-120km Ψ varied uniformly from $2\cdot10^{-7}$ to $2\cdot10^{-8}$ cm^3s^{-1} [ADAMS,1965].

3. The experimental rocket profiles of the electron density were taken from the work of MIYAZAKI [1978] in form of a catalogue [NESTEROVA,1985]. To compare the calculated and the experimental profiles, we chose the parameter

$$\Delta\omega=([e]_c-[e]_m)/[e]_c \qquad (1)$$

where $[e]_c$ is the calculated electron concentration and $[e]_m$ is that measured during the rocket ascent.

Moreover, the availability of both ascent and descent rocket electron

density profile data allowed us to estimate a similar parameter:

$$\Delta\omega = ([e]_a - [e]_d)/[e]_a \qquad (2)$$

where $[e]_a$ is the electron density corresponding to the fixed height during the rocket ascent, $[e]_d$ being that obtained during the rocket descent.

Tab.1 shows the absolute values of parameters $|\overline{\Delta\omega}|$ and $|\overline{\Delta\omega_i}|$.

The estimation of $\Delta\omega$ was performed with Ψ_4 (mean night-time disturbed conditions profile, abbreviated as NGN in Tab.1) using combined Ψ profile (abbreviated as NGT in Tab.1) for the riometer absorption between 0.3 and 5dB.

4. Experimental profiles of [e] from the paper by MIYASAKI [1978], complemented with those from PFISTER [1967] and DERBLOM [1973] were analysed by ZELENKOVA [1982] by using four parameters which characterise the [e]-profile structure of the disturbed D-region. These are h_1 - height of 10^2 cm^{-3} electron appearance, h_2 - height of strong enhancement of [e]-gradient and N_2 - concentration of the "step" bottom, N_3- concentration of electrons at h=95km. Tab.2 shows the variation of the above mentioned parameters versus riometer absorption between 0.3 and 5 dB.

5. Generally accepted parameter that reflects magnetic field variation during geomagnetic disturbances is the AE-index.

We attempt to connect the electron density profile parameters with the AE-index.

Profiles were compiled from the catalogue of MCNAMARA [1978] and also from the catalogue of NESTEROVA [1985], where they are given in a digital form. Only the auroral zone profiles during disturbances were selected, which corresponds to the indexes 9-13 [NESTEROVA,1985; MCNAMARA,1978].

Thus, 44 profiles for night-time conditions were chosen.

All the profiles were selected into different groups according to the AE-index value in the following manner: $0 < AE < 100$(6), $100 < AE < 200$(9), $200 \leqslant AE < 300$(8), $300 \leqslant AE < 400$(8), $400 \leqslant AE < 500$(7), $500 \leqslant AE < 600$(2), $AE \geqslant 600$(4).

Attention was paid to geographic location of stations: Andoya(69.3°N, 16°E)(25), Syowa(69.5°S,39°E)(11), College(64.9°N,212°E), Churchill(58.8°N, 265.8°E)(2) (the number of profiles is in the brackets).

Parameters that characterise the electron density distribution in the D-region are the heights of appearance of the electron density equal to 10^2 cm^{-3}, 10^3 cm^{-3}, 10^4 cm^{-3}, respectively.

Mean profile of the electron density distribution was calculated (Tab.3).

6. To compare the electron density variations obtained using AE-index with 4-parameter model (see part 4), we study the relations between the riometer absorption and AE-index. We got the ionospheric data from Finnish Academy of sciences and compared them with AE-index. We explore the data from 1978-1979 years. Two intervals were chosen: $19\text{-}22^h$ LT and $23\text{-}01^h$ LT. Such dependences are shown in Fig.2 for the stations Kevo and Sodankyla. One can conclude from the Fig.2:

1)the absorption for the night-time ($23\text{-}01^h$ LT) is greater for farther to the south station (for the same AE-index);

2)both for Kevo and Sodankyla the riometer absorption is greater at $23\text{-}01^h$ LT than $19\text{-}22^h$ LT.

Using Fig.2, it is easy to obtain the riometer absorption for each value of AE-index.

Tab.3 summarises the results from Fig.2 and from the catalogue. The designations are: AE is the AE-index in γ, N is the number of profiles, A,dB is the magnitude of the riometer absorption; $h(N_{10^2})$, $h(N_{10^3})$, $h(N_{10^4})$, are the heights of appearance of the appropriate electron density.

Conclusions from the data of Tab.1, 2 and 3 :

1. Theoretical investigations allow us to determine the height distribution of [e] with relative error less than 100%. At the same time, the experimental measurements are subject to relative error (ascent and descent) as large as 50%. That reflects a wide variability of auroral ionosphere, rather then imprecision of the experiment.

2. Both experimental and theoretical investigations shows the enhancement of riometer absorption due to:

a) the appearance of equilibrium electron density about 10^2 cm^{-3} at heights h<50km (lower part of D-region),

b) the increase of [e] by more than an order of magnitude in the upper part of the D-region (h>90km).

Parameter h_1 characterize the hardness of electron flux spectrum, while the parameters N_2 and N_3 characterize the intensity of the flux.

As seen from Tab.2,3 the best accordance between the experimental and calculated (restored) parameters of [e]-profile appears. The discrepancy between the h_{1m} and h_1 (19-22), h_1 (23-01) is explained by the fact that the station becomes situated northward of the precipitation zone during the large values of AE-index.

REFERENCES

Adams G.W., Masley A.J. Production rates and electron densities in the lower ionosphere due to Solar cosmic rays. J.Atm.Terr.Phys.,27,289,1965.

Derblom U., Ladell L. D-region parameters at high latitudes obtained from rocket experiments. J.Atm.Terr.Phys.,35,2123,1973.

Gledhill J.A. The effective recombination coefficient of electrons in the ionosphere between 50 and 150 km. Radio Sci.21,399,1986.

Khvorostovskiy S.N., Zelenkova L.V. Geomagn.and aeron.,27,599,1987(in Russian).

McNamara L.F. Ionospheric D-region profile data base. Report UAG-67,1978.

Mechtly E.A., Bowhill S.A., Smith L.G. Changes of lower ionosphere electron concentrations with solar activity. J.Atmosph.Terr.Phys.34,1899,1972.

Miyazaki S. Ionospheric plasma probe studies and ionospheric structure studied by space vehicle observations. J.Radio Res.Lab.25,153,1978.

Nesterova I.I., Ginsburg E.I. Catalog of D-region electron density profiles of the ionosphere. Novosibirsk,1985(in Russian).

Parthasarathy R., Berkey F.T., Venkatesan D. Auroral zone electron flux and its relation to broadbeam radiowave absorption. Planet.Space Sci.14,65,1966.

Pfister W. Auroral investigations by means of rockets. Space Sci.Rev. 7,642,1967.

Zelenkova L.V. Dissertation,1981(in Russian).

Zelenkova L.V. D-region electron density distribution. Geomagn.Res. N 14,101,1976.

Zelenkova L.V. Structure of the electron density profile during auroral disturbances. Magnetosph.res.N 1,187,1982(in Russian).

Zelenkova L.V., Soldatov V.A. Restoration of the impinging electron differential fluxes from riometric absorption. Magnetosph.res.N 11,133,1988 (in Russian).

TABLE 1

h, km	$\overline{\lvert\Delta\omega\rvert}$ (NGT)	$\overline{\lvert\Delta\omega\rvert}$ (NGN)	$\lvert\overline{\Delta\omega_i}\rvert$
70	0.47	0.62	0.59
75	0.47	0.70	0.45
80	0.44	0.34	0.50
85	0.68	0.76	0.60
90	0.53	0.75	0.47
95	0.85	0.98	0.36
100	1.12	0.99	0.40

TABLE 2

A, dB	h_{1m}, km	h_{1c}, km	h_2, km	N_2, cm^{-3}	N_{3m}, cm^{-3}	N_{3c}, cm^{-3}
0.3	68	65	78	3 10	3 10	4 10
0.5	60	56	80	10	7 10	6 10
1.2	58	55	83	2.5 10	8 10	10
1.3	57	-	82	2 10	10	-
1.5	58	55	83	10	3 10	2 10
2.6	55	52	75	8 10	4 10	3 10
5.0	55	50	-	-	5 10	6 10

TABLE 3

$\leqslant$ AE, γ $<$	N	A, dB (19-22)	A, dB (23-01)	h_{10^2}, km	h_{10^3}, km	h_{10^4}, km
0 - 100	6	0.2	0.4	64±9	74±4	83±4
100 - 200	9	0.5	0.7	62±2.2	72±5	82±5
200 - 300	8	0.9	1.2	50±8	67±6	80±2
300 - 400	8	1.3	1.7	63±5.5	73±3.5	80±3
400 - 500	7	1.5	2.5	79±8	79±8	87±8
500 - 600	2	2.0	3.0	83±3	89±1	96±4
> 600	4	2.3	4.0	67±5	65±5	75±5

Fig. 1

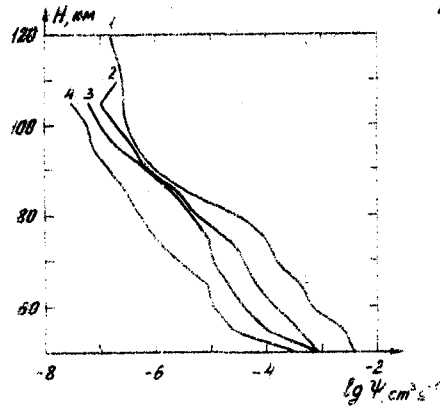

Fig. 2

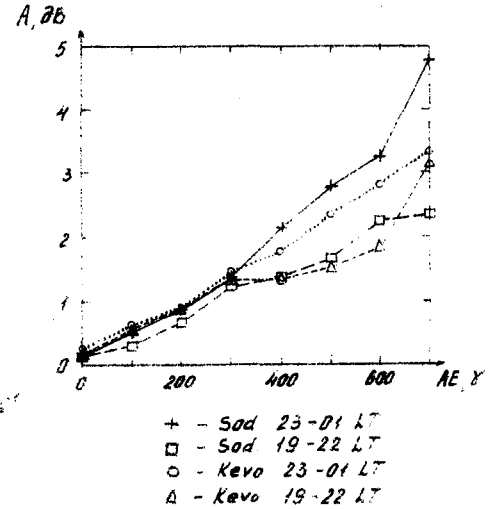

INFLUENCE OF NON-STATIONARY FIELD OF MAGNETOSPHERIC CONVECTION ON THE D-REGION

A.Yu.Eliseyev, Yu.V.Kashpar, A.A.Nikitin

Research Institute of Physics,Ulyanovskaya ul.1,198904 Leningrad,USSR.

INTRODUCTION. Perturbations of F-region electron density caused by the extension of magnetospheric convection electric field to middle latitudes are already well known (TANAKA and HIRAO,1973). For the D-region the first observations are believed to be reported by ELISEYEV,KASHPAR and NIKITIN (1988). On several occasions, following the southward turning of the Bz-component of interplanetary magnetic field (IMF) small disturbances of the D-region electron density were detected at night by steep-incidence VLF sounding in Gelendzhik on the Black Sea (ELISEYEV et.al,1988) which may be attributed to the influence of the penetrated convection electric field (CEF). In this paper some evidence is given of a local-time dependence of the CEF effect in the D-region and a rather good correlation is demonstrated at the initial stage of disturbance between high-latitude magnetic field variations and simultaneous perturbation of the midlatitude ionospheric reflection height.

OBSERVATIONAL TECHNIQUE AND RESULTS. The abnormal component of the sky-wave VLF field was picked up by a transversal loop aerial at a site in Gelendzhik, about 100 km southward from transmitting station. Midpath invariant latitude is 40 degrees. The VLF-monitoring technique was most similar to that of HOPKINS and REYNOLDS (1954). The CEF search and identification was based on the following selection criteria. Firstly, night-time periods only were considered for there was little hope to detect the CEF-effect at heights as low as 70-75 km by day. Secondly, the wanted disturbance should immediately follow a sudden change of IMF Bz-component preceded by a period of positive Bz, the situation most favourable for CEF penetration into the midlatitude ionosphere. Because of the lack of more detailed information on Bz we had to use its hourly values (COUZENS and KING,1986). In order to fix more precisely the time of CEF onset, H-magnetograms were used from the high-latitude observatory Abisko (Sweden, Φ=66°). It is believed that variations in high-latitude current system which cause the observed magnetic disturbance at Abisko, are mainly due to changes in the magnetospheric convection (or polar cap) electric field. And finally, it was natural to anticipate simultaneous perturbations both in VLF reflected signal at Gelendzhik and in H-magnetogram at Abisko, at least at the beginning of the disturbance.

The VLF data available for 1976-1980 allowed to select several CEF-events which had occured after the turning of Bz-component to the south. An example is shown in Fig. 1, where the relative phase Φ_Δ and amplitude A_Δ of the abnormal component of the 14.9 KHz signal as received at Gelendzhik are compared to disturbance in H-component of geomagnetic field at Abisko on February 15,1980. Unfortunately there was a two-hour gap in Bz-data, so it is only possible to say that the polarity change occured between 1900 UT and 2100 UT, but the H-magnetogram from Abisko implies that the convection electric field started to rise approximately at 2000 UT. This was followed at 2015 UT by a rather abrupt fall of the reflected VLF signal strength and a minor general increase of signal phase lag with superimposed stronger short-period phase oscillations. A burst of phase oscillations at about 2140 UT was accompanied by a similar burst in amplitude variations. The mean quasi-period of phase oscillations between 2020 and 2200 UT appeared to be 13.6 minutes which was lower than the short-period fluctuation quasi-periods before and after the disturbance. Then, 2200 to 2300 UT, relatively small but strikingly synchronous oscillations with a 13.3-minute mean quasi-period could be noticed in VLF phase and geomagnetic field records (Fig.1 a,b). The maximum peak-to-peak variation of VLF phase reached 38 centicycles (it is equivalent to the 4.8 kilometre range of reflection height variation). The slow component of reflection height rise (in

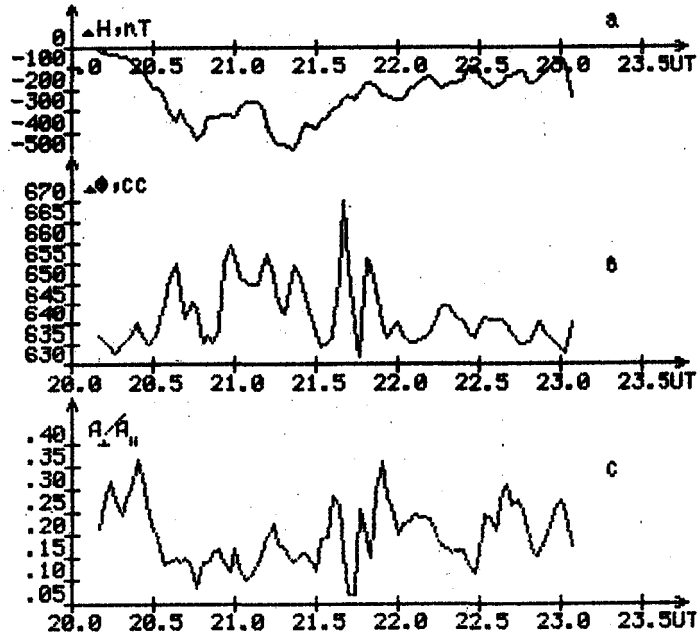

Fig.1
The disturbance of February 15, 1980: a) deviation of the horizontal component of geomagnetic field H at Abisko, Sweden; b) VLF skywave phase disturbance at Belendzhik (h=90km corresponds to Φ=595 cc, scaling factor - 0.113 km/cc); c) VLF abnormal component amplitude A_ relative values $A_{\perp}/A_{\parallel}$ during the disturbance.

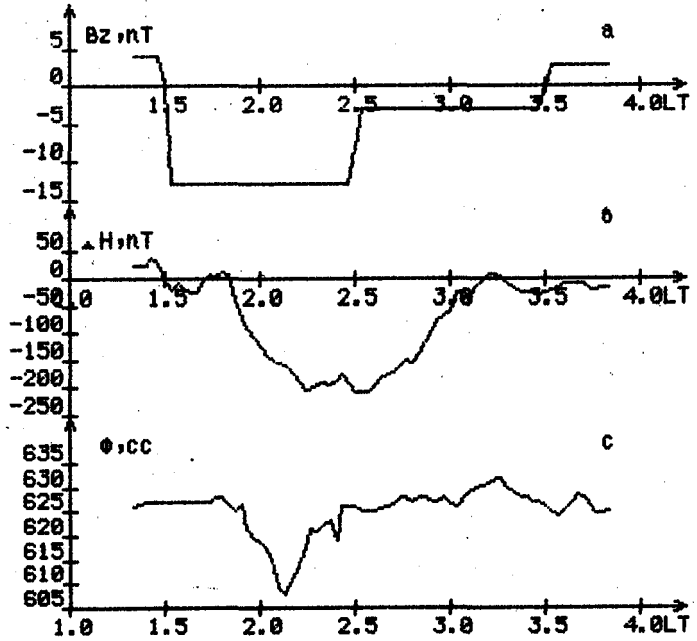

Fig.2
The disturbance of February 25/26, 1980: a) hourly values of the Bz-component of the IMF; b)the behaviour of the H-component of geomagnetic field at Abisko, Sweden; c) VLF phase disturbance in Belendzhik .

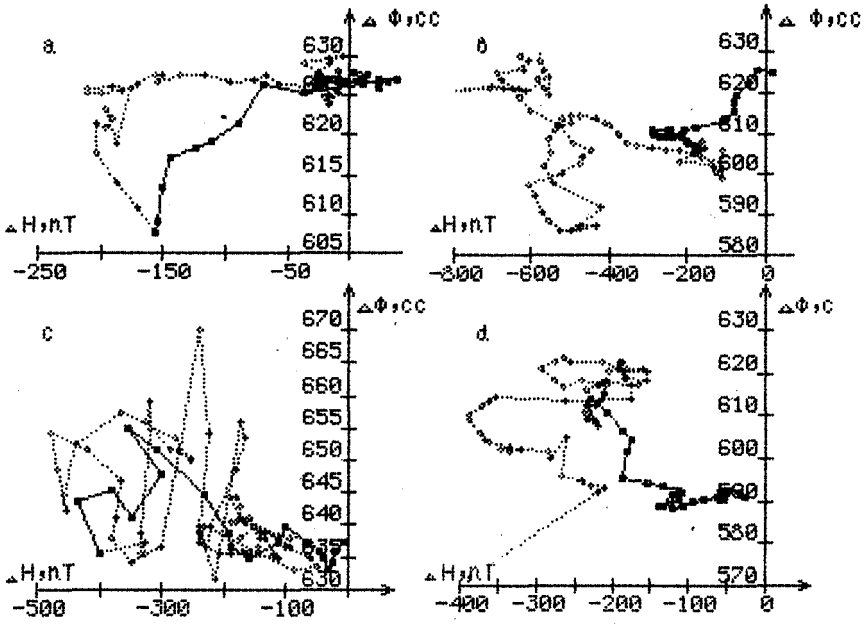

Fig.3
Plots of VLF skywave phase lag Φ at Gelendzhik versus geomagnetic H-component at Abisko:a) February 26,1980 (local date), beginning at 0150 LT of Gelendzhik; b) February 16,1980, 0320 LT; c) February 15, 1980, 2340 LT; d) January 18,1978, 0020 LT.

Table

DATE	LT	A,cc/nT	r
15.02.1980	2240-2310	-0.047	-0.87
18.01.1978	0030-0100	0.031	0.67
18.01.1978	0100-0130	-0.152	-0.62
26.02.1980	0150-0208	0.107	0.89
26.02.1980	0150-0220	0.052	0.51
16.02.1980	0320-0342	0.058	0.94
16.02.1980	0320-0350	0.037	0.46
16.02.1980	0320-0530	0.118	0.48

terms of the running mean with the averaging interval of 50 minutes) reached its maximum value of about 1 km at 2100 UT. On other occasions there was no substantial increase of the short-period fluctuation intensity at VLF during the CEF-event. Fig.2 shows a CEF-event of February 25/26 1980. A rapid turning of Bz southward triggered at 2330 UT a high-latitude substorm accompanied by a shorter bay-like lowering of the reflection height (VLF phase lag decrease) at Gelendzhik. It is worth noting that the large negative hourly value of Bz at 00 UT (-16nT) diminished to -3nT at 01 UT. The change of sign of VLF phase perturbation as compared to the disturbance of February 15 may be, presumably, attributed to the local-time variation of CEF.

To illustrate the correlation between a high-latitude magnetic disturbance and a midlatitude ionospheric reflection height perturbation at VLF, plots of VLF phase $\Phi_\perp$ variation versus H-component variation are given in Fig.3 for 4 night-time CEF-events which had occured at different local times. The dots interconnected by straights to show temporal evolution of the event are separated by two-minute intervals. Bold dots and lines represent the first hour of disturbance. The regression coefficients A for the relation $\Phi_\perp = A*\Delta H + B$ are given in the table for the local dates and time intervals indicated (Gelendzhik local time LT is given). Note that the correlation coefficient r is used here only as a measure of similarity of two waveforms with no statistical meaning being ascribed to it. Inspection of the table shows that for a sudden onset of disturbance $|A|=0.05\div0.1$ with $|r|\approx0.9$ and the two quantities decrease as time window broadens. For gradual disturbances (January 18, 1978 and February 16, 1980) both |A| and |r| tend to be less sensitive to the window opening and in general $|A|\approx0.1\div0.15$ and $|r|\approx0.5\div0.6$.

As for the local-time dependence of the effect in the ionosphere one can suggest that the ionospheric height change tends to be positive before 00 LT and negative after 02 LT, the transition time lying between 0030 and 0130 LT.

DISCUSSION. The observed disturbances in the midlatitude night-time D-region seem to be consistent with the idea of magnetospheric convection electric field influence on the electron density at heights of about 90 km, the tourning of the Bz to the south being the necessary condition. Indeed, an example was shown (ELISEYEV et al., 1988), when a substorm which had occured by positive Bz had not been accompanied by a disturbance at VLF. If we take the high-latitude magnetic data as a replacement for the data on the penetrated electric field we can say that disturbances in the midlatitude D-region commence simultaneously with the CEF enhancement and correlate rather well with the latter at least within the first 20-40 minutes of the event. Sometimes the short-period oscillations intensify during the disturbance and their quasi-period shortens. A surprisingly good correlation was noticed at the recovery stage of disturbance on February 15, 1980 between the small oscillations of VLF skywave phase lag and those of CEF. A similar behaviour of the short-period fluctuations in the F-region could be seen from the data presented by CROWLEY et al (1984) for a disturbance, which followed the Bz polarity change. In general, the events described in this paper for the night-time midlatitude D-region have much in common with the well known CEF-events in the thermosphere and hence are likely to have the same origin.

REFERENCES

Couzens,D.A.,and J.H King,Interplanetary medium data book-Supplement 3A, 1977-1985, NASA Goddard Space Flight Center, Greenbelt, Md., 1986.

Crowley,G.,J.R.Dudeney,A.S.Rodger,and T.B.Jones,Large simultaneous disturbances (LSDs) in the Antarctic ionosphere, J.Atmos.Terr.Phys., 46, 917-925,1984.

Eliseyev,A.Yu.,Yu.V.Kashpar,and A.A.Nikitin,Magnetospheric electric field influence on the midlatitude lower ionosphere, Geomagnetism i Aeronomia, 28, 676-679, 1988.

Hopkins,H.G.,and L.G.Reynolds,An experimental investigation of short-distance ionospheric propagation at low and very low frequencies, Proc. IEE, Pt3, 101, 21-34, 1954

Tanaka,T.,and K.Hirao,Effects of an electric field on the dynamical behavior of the ionosphere and its application to the storm time disturbance of the F-layer, J.Atmos,Terr.Phys., 35, 1443-1452, 1973.

AUTHOR INDEX

	Page
L. Alberca	215
J. V. Arkhipov	236
G. Beig	108
J. Boska	230
J. Bremer	196
N. I. Brezgin	104
G. M. Brown	53
V. Bucha	13
D. K. Chakrabarty	108
S. Chandra	68
M. L. Chanin	27, 33
M. A. Chernigovskaya	164
A. F. Chizhov	104
M. Dameris	49
M. Yu. Danilin	82
A. D. Danilov	183
B. A. de la Morena	215
R. F. Donnelly	1
A. R. Douglass	129
I. G. Dyominov	117, 118
A. Ebel	49, 116
A. Yu. Eliseev	240
G. Entzian	43
N. N. Fomina	47
V. A. Gaidukov	164
H. B. Gayathri	112
L. Hood	76
I. N. Ivanova	96, 104
C. H. Jackman	129
Yu. V. Kashpar	240
E. S. Kazimirovsky	156, 164
G. M. Keating	67
P. Keckhut	33
V. G. Kidiarova	47, 100
G. A. Kokin	104
G. I. Kouznetzov	82
A. A. Krivolutsky	86, 92, 96
L. Krivsky	223
K. Kudela	135
V. N. Kuznetsova	96, 104
V. F. Laikova	236
E. M. Larin	104
J. Lastovicka	119, 210, 215
J. London	9
O. A. Loshkova	92
X.-C. Lu	179
L. N. Mateev	147, 151
P. E. Meade	129
K. Mohanakumar	39, 62
L. P. Morozova	219
N. N. Murzaeva	227
B. Narasimhamurty	112
P. I. Nenovski	151
A. A. Nikitin	240
S. V. Pakhomov	108
D. Pancheva	210, 231
J. Pap	9
B. S. N. Prasad	112
Z. Ts. Rapoport	215
R. Reiter	168
G. J. Rottman	9
G. Satori	192
V. V. Sazonov	104
P. H. Scherrer	53
C. J. E. Schuurmans	22
A. V. Shirochkov	203
O. V. Shtirkov	104
N. G. Skryabin	142
V. A. Soldatov	236
I. I. Sosin	142
J. Taubenheim	43
B. A. Tinsley	53
G. A. Tuchkov	117
A. A. Tyutin	178
P. I. Vellinov	147, 151
G. von Cossart	43
A. M. Zadorozhny	117, 178
L. V. Zelenkova	236
E. I. Zhovty	164
H. C. Zhuang	179

PART 2

COMPARISON OF SATELLITE DERIVED DYNAMICAL QUANTITIES IN THE STRATOSPHERE OF THE SOUTHERN HEMISPHERE

Edited by

Thomas Miles[1] and Alan O'Neill[2,3]

[1]NASA Langley Research Center, Hampton, Virginia, USA

[2]Meteorological Office, Bracknell, UK

[3]Temporary Affiliation: ST Systems Corporation (STX), Hampton, Virginia, USA

MASH Workshop - Williamsburg, Virginia - April 1986

Sponsor: NASA, Washington, D.C.

Workshop Organizers: W. L. Grose and A. O'Neill

Attendees and Contributors:

M. E. Gelman, NOAA, National Meteorological Center, USA
J. C. Gille, National Center for Atmospheric Research, USA
W. L. Grose, NASA Langley Research Center, USA
I. Hirota, Geophysical Institute, Kyoto University, JAPAN
M. H. Hitchman, National Center for Atmospheric Research, USA
D. J. Karoly, Mathematics Department, Monash University, AUSTRALIA
K. Labitzke, Meteorological Institute, Free University Berlin, FRG
T. Miles, NASA Langley Research Center, USA
A. J. Miller, NOAA, National Meteorological Center, USA
A. O'Neill, Meteorological Office, UK
V. D. Pope, Meteorological Office, UK
C. D. Rodgers, Clarendon Laboratory, Oxford University, UK
M. Shiotani, Geophysical Institute, Kyoto University, JAPAN

CONTENTS

1. Introduction . . . . . .
2. Analyses . . . . . .
2.1. Base Level and Tropospheric Analyses . . . . . .
2.2. Satellite Analyses . . . . . .
3. Results. . . . . .
3.1. Quantities Derived From Archived Satellite Analyses During 1979. .
3.2. Impact of Base-Level on Derived Quantities . . . . . .
3.2.1. 1981 Eddy Statistics . . . . . .
3.2.2. 1985 Derived Quantities. . . . . .
4. Conclusions. . . . . .

1. INTRODUCTION

Over the past 10 to 15 years, radiometric measurements from polar orbiting satellites have furnished a wealth of information on the global structure of the middle atmospheric circulation. These data have formed the basis for climatological studies and dynamical investigations. Information on smaller scale structures than can be resolved by satellites is being supplied by radar

and lidar measurements. These activities have been paralleled by increasing efforts to model aspects of the observed circulation using both simplified (mechanistic) models and complex numerical models of the general circulation.

The main focus of these studies has been on the circulation of the Northern Hemisphere; the Southern Hemisphere has not been ignored but, until recently, advances have been comparatively few and far between. Reasons for this imbalance include: (1) impetus to studies of the Northern Hemisphere resulting from much better coverage by radio/rocketsonde network, (2) the quality of operational analyses of the Southern Hemisphere upper troposphere (used to tie on satellite thickness analyses) has been comparatively poor owing to large data-sparse regions, and (3) attention has inevitably been concentrated on one of the most dramatic manifestations of dynamical processes in the middle atmosphere -- the major midwinter warming of the Northern Hemisphere.

In recent years, the routine production of global tropospheric analyses by data assimilation into numerical forecast models has gone some way to improving the quality of analyses for the Southern Hemisphere (satellite measurements have contributed to this improvement). The situation is not entirely satisfactory, but independent analyses (such as those made by the Meteorological Office, Bracknell and the National Meteorological Center, Washington) are in reasonable accord.

It has also been realized that the middle atmosphere of the Southern Hemisphere, despite the absence of major midwinter warmings, is far from quiescent. Very intense, dynamically induced warmings occur in late winter; the intense polar-night vortex may be the seat of instabilities which affect the circulation on a large scale; traveling waves are often clearly seen in the more zonally symmetric circulation of the Southern Hemisphere.

The fact that the circulations of the middle atmosphere of the two hemispheres show marked differences gives dynamical meteorologists the opportunity to study what are, in effect, two different atmospheres. The elucidation of dynamical mechanisms is bound to be furthered by intercomparison. In particular, the tropospheric circulations are different in the two hemispheres, enabling connections of the troposphere with the middle atmosphere to be established more firmly.

At the MAP Assembly in Kyoto (November 23 and 25, 1984), proposals were solicited for new MAP projects. One suggestion was for a study of the dynamics of the Middle Atmosphere in the Southern Hemisphere (MASH), and this has since received the formal approval of the MAP Steering Committee. The MASH project involves a concerted study of the dynamics of the middle atmosphere in the Southern Hemisphere, with emphasis on interhemispheric differences and connections with the troposphere. It will be based on observational data and simulations with numerical models. Parallel studies of radiation, transport, and photochemistry will also be encouraged. The uses of observational data will include:

(a) Intercomparison of observations and analyses obtained by different means. This will be a coordinated study along the lines documented in MAP Handbook 12 for the Northern Hemisphere (contemporaneous satellite data from the LIMS, SAMS and TOVS instruments are available).
(b) Climatological studies of the middle atmospheric circulation. These will focus on the time-mean structure and variances of the circulation together with their seasonal evolution, the structure and temporal variability of large-scale eddies, and the morphology of gravity waves.
(c) Diagnostic and associated theoretical studies will address the evolution of the circulation on both short and seasonal time scales. Topics here will include wave-mean flow interactions and the importance of wave breaking in the Southern Hemisphere (particularly for the dynamics of final warmings), the possible role of instabilities in the strong westerly vortex, the origin of the large-amplitude planetary waves which develop particularly in

early and late winter (e.g., whether developments like blocking in the Northern Hemisphere occur in the troposphere), and the effect of gravity waves on the middle atmosphere.

These investigations will be complemented by studies with numerical models of various levels of sophistication. Broad headings for this work are: (1) experiments with mechanistic models to test dynamical hypotheses, e.g., to determine the influence of the troposphere on the middle atmosphere during final warmings, and (2) longer integrations with numerical models to explore the mechanisms behind the seasonal evolution of the circulation. Features that such models would need to reproduce in the Southern Hemisphere include:

(a) the tendency for large amplitude waves to develop in early and late winter;
(b) the reversed temperature gradient at high latitudes in the upper stratosphere which appears by midwinter;
(c) the poleward and downward movement of zonal mean winds during the final warming;
(d) the traveling wave 2 which contributes much of the variance in the stratosphere.

A series of workshops was held in 1982-1984 which made intercomparisons of Northern Hemisphere stratospheric analyses from several satellite systems (PMP-1 Working Group). The topics considered by these workshops included intercomparison of temperature analyses/measurements from satellites and in situ systems, and assessing the accuracy of derived quantities used in studies of stratospheric dynamics (RODGERS, 1984b; GROSE and RODGERS, 1986).

The first MASH workshop was held in Adelaide on May 18-19, 1987, and proceedings of this meeting will be published in a special issue of PAGEOPH (Vol. 130, in press, 1989). It highlighted some of the inadequacies in our present understanding of the middle atmosphere of the Southern Hemisphere. Three broad areas (among many) requiring much more work are 3-D modeling, troposphere-middle atmosphere coupling, and interhemispheric coupling.

This report summarizes the proceedings from a pre-MASH planning workshop on the intercomparison of Southern Hemisphere observations, analyses and derived dynamical quantities held in Williamsburg, Virginia during April 1986. The aims of this workshop were primarily twofold:

(1) comparison of Southern Hemisphere dynamical quantities derived from various satellite data archives (e.g. from limb scanners and nadir sounders);
(2) assessing the impact of different base-level height information on such derived quantities.

These tasks are viewed as especially important in the Southern Hemisphere because of the paucity of conventional measurements.

A further strong impetus for the MASH program comes from the recent discovery of the springtime ozone hole over Antarctica. Insight gained from validation studies such as the one reported here will contribute to an improved understanding of the role of meteorology in the development and evolution of the hole, in its interannual variability, and in its interhemispheric differences.

The dynamical quantities examined in this workshop included geopotential height, zonal wind, potential vorticity, eddy heat and momentum fluxes, and Eliassen-Palm fluxes. The time periods and data sources constituting the MASH comparisons are summarized in Table 1. Table 1 also includes a list of acronyms which are used throughout the text.

Table 1. MASH INTERCOMPARISON TOPICS AND DATA SOURCES.

Quantities Derived From Archived Satellite Analyses	
Date	January, May 1979
Satellite Analyses	LIMS, NMC, SAMS, UKMO
Base Level Analyses	NMC, CIRA'85, ECMWF
Derived Quantities	U, PV, EPFD

Base Level Impact on Derived Quantities		
Date	June, September 1981	September 1985
Satellite Analyses	UKMO	UKMO
Base Level Analyses	ECMWF, NMC	ECMWF, NMC, UKMO
Derived Quantities	Z, VT, UV	U, PV, EPFD

Derived Quantities

EPFD - Eliassen-Palm Flux Divergence
PV - Potential Vorticity
U - Zonal Wind
UV - Eddy Momentum Flux
VT - Eddy Heat Flux
Z - Geopotential Height

Base Level Height Sources

CIRA - COSPAR Reference Atmosphere (MAP Handbook, Volume 16)
ECMWF - European Center for Medium Range Weather Forecasts, Reading
NMC - National Meteorological Center, Washington
UKMO - United Kingdom Meteorological Office, Bracknell

Satellite Stratospheric Temperature/Thickness Data and Analyses

HIRS - High Resolution Infrared Sounder
LIMS - Limb Infrared Monitor of the Stratosphere
MSU - Microwave Sounding Unit
NESDIS - National Environmental Satellite Data and Information Service
NMC - National Meteorological Center
SAMS - Stratospheric and Mesospheric Sounder
SSU - Stratospheric Sounding Unit
TOVS - TIROS-N Operational Vertical Sounder (HIRS+MSU+SSU)
UKMO - United Kingdom Meteorological Office (Thickness Retrievals)
VTPR - Vertical Temperature Profile Radiometer

2. ANALYSES

The primary objective of the MASH workshop was to compare different Southern Hemisphere satellite-derived quantities and examine the impact of different operational base-level analyses on these derived quantities. Although the satellite-derived quantities are largely based on satellite temperature (thickness) data, for certain dynamical quantities (e.g., potential vorticity maps) the base-level height analysis may contribute significant information throughout the lower-middle stratosphere. This section includes a discussion of the base-level analyses followed by details of the stratospheric satellite instruments and related analyses of temperature, thickness, and geopotential height.

2.1 Base-Level and Tropospheric Analyses

The MASH workshop utilized Southern Hemisphere geopotential height analyses provided by meteorological centers in Reading, Washington, and Bracknell (ECMWF, NMC, and UKMO respectively). These analyses are used for the base-level information at 50 or 100 mb in deriving heights throughout the stratosphere. The three meteorological centers employ broadly similar methods in producing the gridded height analyses. For example, they are produced operationally (i.e. constrained by data cut-off times), use synoptic (radiosonde) and asynoptic (i.e. aircraft, satellite-inferred) upper-air reports, and incorporate background (so-called first-guess) information such as a numerical forecast and/or climatology in the absence of current data. Substantial improvements have occurred in tropospheric global data assimilation, objective analysis procedures, and short-term forecast accuracy since 1979 (BENGTSSON and SHUKLA, 1988), and increasing use has been made of asynoptic meteorological information, e.g. aircraft and satellite data. Nevertheless, difficulties associated with delayed reports and relatively sparse data coverage exist in the Southern Hemisphere. Moreover, differences in quality control and analysis methodology, such as the treatment of isolated, but quite accurate, synoptic reports and the application of spatial smoothing, exist between the three meteorological centers which will influence the accuracy of the archived gridded height analyses. As a result, the Southern Hemisphere tropospheric height analyses are generally regarded as poorer quality compared with Northern Hemisphere analyses (HOLLINGSWORTH et al., 1985; LAMBERT, 1988; TRENBERTH and OLSON, 1988).

The ECMWF and NMC Southern Hemisphere objective analysis procedures have undergone several major changes since their inception in 1978; these are discussed by TRENBERTH and OLSON (1988, and references therein). For example, in May 1980 initialization (removal of unwanted high-frequency components) was applied to the NMC global analyses, and a global spectral forecast model was introduced. [Prior to May 1980, initialization was not applied, and a grid-point numerical forecast model was used.] These changes are known to have resulted in a substantial reduction in noise levels in the NMC final analyses and forecasts (JENNE, private communication, 1984). Further improvements have been made subsequently. The UKMO operational height analysis procedures for the troposphere and lower stratosphere (e.g. 100 mb) have been documented and intercompared with ECMWF and NMC global analyses by HOLLINGSWORTH et al. (1985).

2.2 Satellite Analyses

Southern Hemisphere satellite analyses considered in the MASH workshop consist of archived temperature or thickness analyses for SAMS, LIMS, and TOVS (HIRS+MSU+SSU).

The SAMS and LIMS measurements were made on the Nimbus 7 satellite, while the TOVS measurements/retrievals are from the Tiros-N and NOAA series of operational polar orbiting satellites. SAMS and LIMS data may be viewed as a

research product, whereas TOVS was primarily for operational meteorological requirements, with stratospheric channels included mainly to improve the accuracy of the operational tropospheric temperature soundings.

The limb-scanning SAMS experiment provided temperature retrievals from 15-100 km with a vertical resolution of ~ 8 km using a sequential estimator procedure (RODGERS et al., 1984). The temperature analyses are gridded at a 2.5° latitude interval from 50°S to 70°N from December 1978 to June 1983. Details of the SAMS instrument and validation of temperatures are discussed by WALE and PESKETT (1984) and BARNETT and CORNEY (1984), respectively. Geopotential heights have been obtained using climatological height analyses for the lower stratosphere (BARNETT and CORNEY, 1985).

The LIMS instrument is a limb-scanning radiometer with a vertical resolution of ~ 3 km for the temperature measurements. The LIMS experiment, temperature retrieval and validation are discussed by GILLE and RUSSELL (1984), GILLE et al. (1984a,b), REMSBERG (1986), and MILES et al. (1987). The temperature retrievals were mapped to 1200 UTC using a Kalman filter procedure (REMSBERG et al., 1989) at 4° latitude increments from 64°S to 84°N and at 18 pressure levels from 100 to 0.05 mb, for the period 25 October 1978 - 28 May 1979. Geopotential heights for the LIMS experiment were calculated with 50 mb height base-level analyses from the stratospheric analysis branch at NMC (see below).

The TOVS observing system consists of the HIRS, MSU, and SSU multi-channel radiometers which view at both sides of nadir (i.e. side-scanning) (SMITH et al, 1979; PICK and BROWNSCOMBE, 1981; CLOUGH et al., 1985). The TOVS stratospheric temperature sounding capability consists of 9 channels:

(a) Four HIRS channels located in the lower-middle stratosphere with a vertical resolution of ~ 10-15 km;
(b) Two MSU channels with a vertical resolution of ~ 10 km located near the 90 and 300 mb levels (for nadir viewing);
(c) Three SSU channels centered near the 15, 5, and 1.5 mb levels (for nadir viewing). [Note that prior to June 1979, the top SSU channel was inoperative].

Statistical tests have established that the vertical resolution of the overlapping (nadir-viewing) SSU channels is ~ 10 km (CLOUGH et al., 1985). Side-scanning normal to the sub-orbital track results in near-global meridional sampling (~ 87°N - 87°S) and longitudinal resolution superior to that achieved by the limb-scanning instruments.

The TOVS radiance information is operationally processed by the National Environmental Satellite Data and Information Service (NESDIS) in Washington, D.C. The accuracy (precision and systematic biases) of HIRS, MSU, and SSU radiance measurements and TOVS temperature retrievals for stratospheric levels (100 mb and higher) has been discussed by PHILLIPS et al. (1979), SMITH et al. (1979), SCHLATTER (1981), PICK and BROWNSCOMBE (1981), GELLER et al. (1983), NASH and BROWNSCOMBE (1983), SCHMIDLIN (1984), GELMAN et al. (1986), and NASH and FORRESTER (1986).

In addition to tropospheric analysis/forecast applications, TOVS information is also used for middle atmosphere research efforts at NMC and UKMO, by producing daily global analyses of thickness, temperature, and geopotential height at "standard" pressure levels throughout the stratosphere. Although both stratospheric groups at UKMO and NMC have access to the same TOVS radiance measurements (i.e. from NESDIS), the subsequent production of gridded analyses is somewhat different at these two centers.

The UKMO stratospheric group directly converts TOVS radiances into deep layer-mean thicknesses using a regression procedure applied to a radiosonde/rocketsonde temperature (thickness) climatology for the 100-20, 100-10, 100-5, 100-2, and 100-1 mb layers (PICK and BROWNSCOMBE, 1981; and CLOUGH

et al., 1985). TOVS stratospheric thickness profiles are then interpolated onto a global 5^{o} x 5^{o} grid, and spatial smoothing is applied which retains twelve Fourier wave components in latitude and longitude. Temperatures at specific pressure levels are then obtained through interpolation of the TOVS thickness information. The UKMO geopotential height data used in the MASH workshop consists of stratospheric geopotential heights for the 100, 50, 20, 10, 5, 2, and 1 mb levels. Note, however, the 100 and 50 mb height fields are strictly operational analyses, whereas those from 20 to 1 mb are obtained by stacking the TOVS thicknesses on the operational 100 mb height field. The UKMO 100 and 50 mb operational height analyses were obtained from ECMWF during 1979, NMC during 1980-83, and UKMO since 1984.

The stratospheric analysis group at NMC has produced global analyses of temperature and geopotential height since September 1978 (GELLER et al., 1983; GELMAN et al., 1986). The selection of data for the analyses changed about once per year. Prior to 17 October 1980, NMC used both radiosonde and satellite temperature data (VTPR or TOVS) in the Southern Hemisphere 70 - 10 mb region, and SSU thicknesses only for the 5 - 0.4 mb region. [For the period 24 September 1978 to 23 February 1979, NMC used radiances from the NOAA-5 VTPR instrument.] Since 17 October 1980, however, NMC has used only TOVS data from the various NOAA satellites for all Southern Hemisphere analysis levels (i.e. 70 - 0.4 mb).

The NMC stratospheric analysis differs from UKMO in that NMC uses retrievals produced by NESDIS. The NESDIS temperature retrieval method directly retrieves temperature at 40 pressure levels and uses colocated satellite and in situ data which are updated weekly for the 1000 - 10 mb region (PHILLIPS et al., 1979); above the 10 mb level, however, an historical temperature sample is used because of less frequent in situ data. The NESDIS retrievals are provided to NMC as layer-mean temperature profiles. The operational NMC 100 mb height analyses are used as a base for deriving heights at 70, 50, 30, 10, 5, 2 1, and 0.4 mb. Temperatures at these pressure levels are obtained from linear interpolation of adjacent layer mean temperatures. The NMC stratospheric temperature and height analyses are gridded using a modified Cressman interpolation procedure (FINGER et al., 1965).

3. RESULTS

The scope of the MASH workshop primarily involved a comparison of derived quantities that are of direct relevance to studies of middle atmosphere dynamics. Whereas temperature or thickness analyses represent the basic satellite information, derived quantities are inferred only after considerable manipulation of the data. The initial step in deriving virtually all dynamical quantities for the middle atmosphere consists of hydrostatic integration of satellite temperature profiles above a lower stratosphere base-level geopotential height analysis. Horizontal winds may then be estimated geostrophically through differentiation of the satellite-derived geopotential height distribution. Non-linear quantities such as eddy fluxes of heat and momentum, and the Eliassen-Palm flux divergence may be derived through multiple differentiation of the horizontal wind fields with respect to latitude, longitude, and altitude. The derivation of dynamical quantities from satellite analyses will therefore tend to amplify noise which may be present in the satellite temperature information and the base-level height analyses.

The comparisons presented in this report are for selected dates which are representative of the larger body of data examined during the workshop. After a brief discussion of temperature differences, the intercomparison of dynamical quantities derived from analyses during 1979 is described in Section 3.1. The impact of different base-level height information on derived quantities is addressed in Section 3.2.

Comparison of different satellite temperature analyses in the Southern Hemisphere for January and May 1979 corroborated the findings obtained from previous Northern Hemisphere MAP workshops (RODGERS, 1984a,b; GROSE and RODGERS, 1986). That is, differences between NMC and UKMO zonal-mean cross-sections were less than ± 5K; SAMS-LIMS differences of ± 5 K exhibited a vertical "wavy" structure; UKMO was colder than LIMS in the upper stratosphere by ~ 7 K in January 1979 and ~ 15-20 K in May 1979; and LIMS and SAMS have less zonal structure than NMC and UKMO. [The UKMO upper stratosphere cold bias apparently is related to the failure of the SSU 1.5 mb channel.] Readers are referred to these MAP documents for a detailed account of the temperature comparisons and, additionally, to complementary results in which temperature information (radiances or retrieved profiles) from SAMS, LIMS, MSU, and SSU (TOVS) have been intercompared between satellites or with in situ measurements:

(a) SAMS: BARNETT and CORNEY (1984,1985), DELISI and DUNKERTON (1988);
(b) LIMS: GILLE et al. (1984a,b), HITCHMAN and LEOVY (1986), REMSBERG (1986), HITCHMAN et al. (1987), MILES et al. (1987), DELISI and DUNKERTON (1988), and GROSE et al. (1988);
(c) MSU: YU et al. (1983), NEWMAN and STANFORD (1983);
(d) SSU(TOVS): PICK and BROWNSCOMBE (1981), GELLER et al. (1983), NASH and BROWNSCOMBE (1983), BARNETT and CORNEY (1984), SCHMIDLIN (1984), GELMAN et al. (1986), and NASH and FORESTER (1986);
(e) NMC: NEWMAN and RANDEL (1988) have compared NMC 100 and 30 mb monthly-mean temperature analyses for October and November 1979-1986 with monthly-mean radiosonde measurements over Antarctica from 1957-1984.

3.1 Quantities Derived from Archived Satellite Analyses During 1979

The comparison of dynamical quantities derived from archived satellite analyses is discussed for January and May, 1979. This time period was examined because of the availability of the Nimbus 7 LIMS and SAMS data as well as the commencement of Southern Hemisphere stratospheric analyses by NMC and UKMO. In this section we compare (i) zonal wind cross-sections between these four data sets, and (ii) Eliassen-Palm fluxes and isentropic maps of potential vorticity derived from LIMS and UKMO. May 1979 is the more dynamically active month, so we expect a higher signal-to-noise ratio then. We shall place most attention therefore on the May comparison (also see GROSE and O'NEILL, 1989).

Zonal Wind. Meridional cross-sections of zonal geostrophic wind for LIMS, NMC, SAMS, and UKMO on 26 January 1979 and 19 May 1979 are shown in Figures 1 and 2, respectively. Note that the SAMS thicknesses have not been smoothed in latitude, and the SAMS winds are extrapolated north of 12°S. The four wind cross sections for January 26 contain broadly similar features, with stratospheric easterlies above the mid-latitude upper tropospheric westerlies. Maximum easterly flow occurs in the lower mesosphere, where LIMS and SAMS show fair agreement in wind speeds at 0.1 mb in middle latitudes (-65 to -80 m/s) and in subtropical latitudes (0 to 10 m/s). In the upper stratosphere (near 1 mb) UKMO and LIMS show evidence of a secondary jet maximum near 20°S, which is not present in the SAMS analysis. The NMC wind field exhibits more latitudinal structure in contrast to LIMS, SAMS, and UKMO. For example, at 30 mb the NMC field shows quite large variations in latitude, whereas the UKMO analysis exhibits a more gradual variation. In contrast to the strong easterly flow indicated in the LIMS, SAMS, and UKMO cross-sections at 1 mb and 20°S (-45 to -55 m/s), the NMC analysis shows speeds approaching -20 m/s. In higher southern latitudes (e.g. 60°S) differences of about 10 m/s are found between the NMC wind speed and the LIMS and UKMO analyses near the 1 mb level.

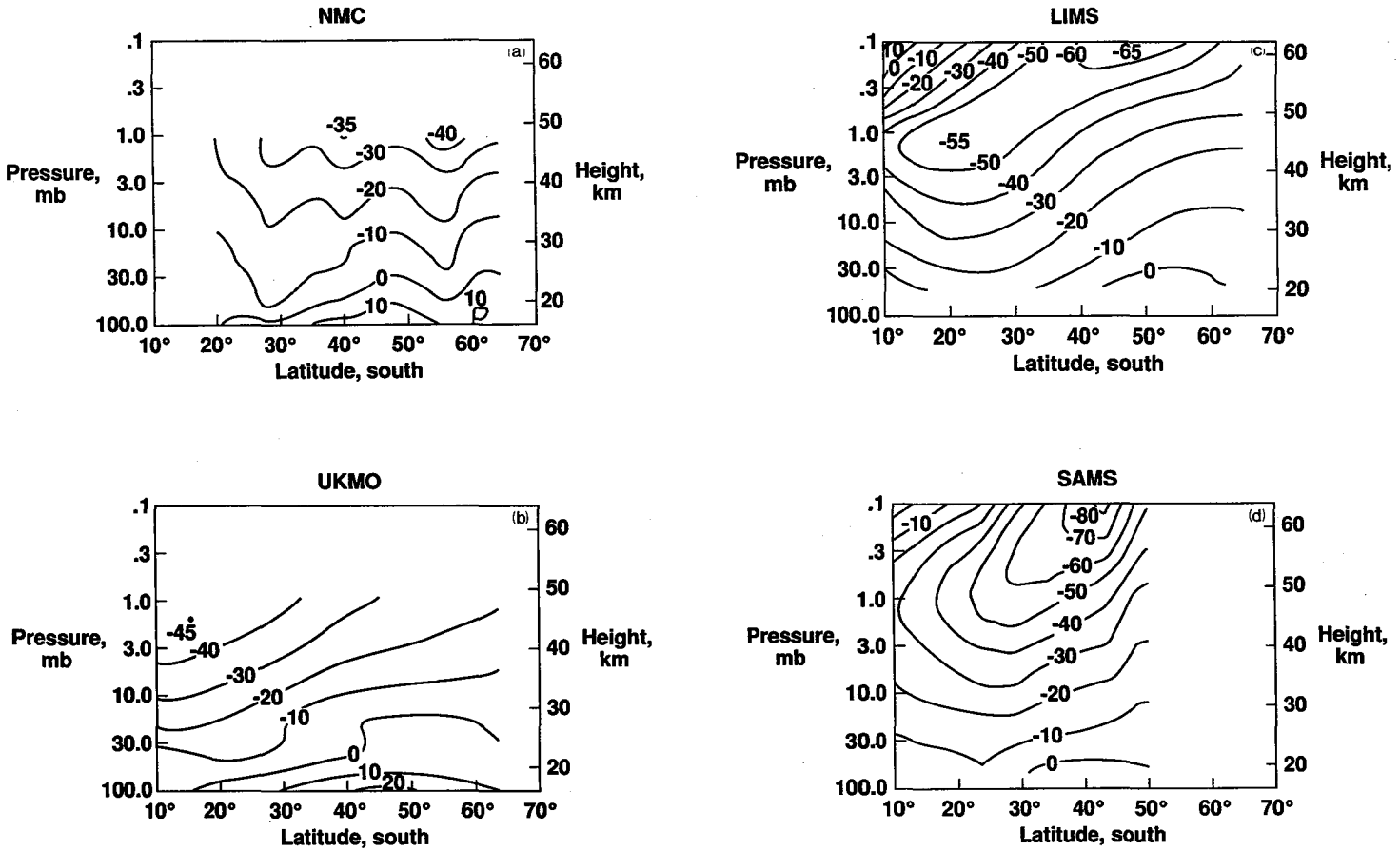

Fig. 1 Zonal-mean geostrophic wind (m s^{-1}) for the southern hemisphere on 26 January 1979. (a) From NMC, (b) from UKMO, (c) from LIMS, and (d) from SAMS.

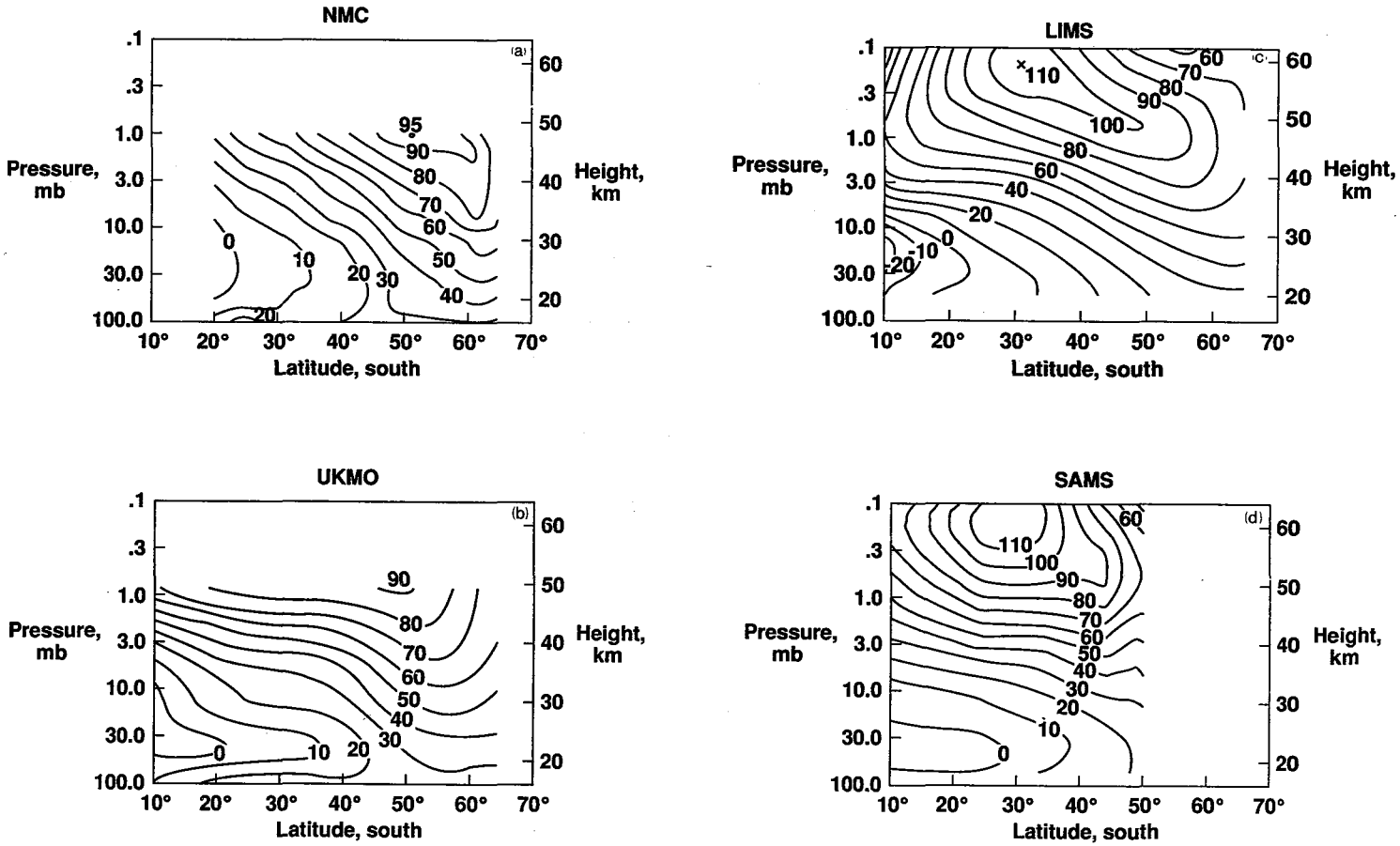

Fig. 2 As for Fig. 1 but for 19 May 1979.

The LIMS and SAMS zonal wind cross sections for 19 May 1979 show good agreement in the location and strength of the westerly jet core in the sub-tropical lower mesosphere, with maximum speeds approaching or exceeding 110 m/s. The LIMS, NMC, and UKMO fields show a jet core axis which tilts poleward with decreasing altitude near 50° - 60°S in the lower-middle stratosphere. The SAMS analysis does not contain this feature to the same extent. In the tropical lower mesosphere, LIMS and SAMS differ by about 50 m/s (e.g. at 10°S, 0.1 mb). In the sub-tropical upper stratosphere (20°-30°S), NMC winds are about 20-30 m/s weaker than for LIMS, SAMS, and UKMO. In the lower stratosphere at 10° - 15°S, the LIMS wind analysis indicates values ~ -20 m/s in contrast to values near zero for SAMS and UKMO. Noticeable differences in vertical wind shear occur between the four analyses in the 10-30 mb layer in subtropical and middle latitudes. The LIMS and SAMS winds at the 50 mb level differ by about 10 m/s at 10°S and also near 45°S, suggesting significant differences in zonal wind at the base-level for the two sets of analyses.

These winds are geostrophic estimates and it is of interest to evaluate to what extent these derived values from satellite data agree with in situ radiosonde and rocketsonde wind speeds obtained from tracking of moving instrument packages. Comparison of LIMS and rocketsonde zonal wind speeds at Ascension Island (~8°S) during January and May 1979 (Fig. 3a) indicates favorable agreement, with LIMS capturing the strong variations with altitude associated with the quasi-biennial and semiannual oscillation. [Note that the LIMS winds used for the rocket comparison are based on a temperature retrieval procedure somewhat different than utilized for the archived LIMS data - see HITCHMAN and LEOVY, 1986.] The equatorial rocket-LIMS differences were found to be similar to those at mid-latitude stations and support the use of satellite geostrophic winds even at low latitudes (also see SMITH and BAILEY, 1985 and GROSE et al., 1988). A similar comparison between UKMO winds and rocket measurements by HIROTA et al. (1983) suggests that although UKMO winds exhibit less vertical structure than individual rocket profiles on a daily basis, agreement is better if time-mean profiles are compared (Figure 3b).

The wind comparisons for 26 January and 19 May 1979 indicate that NMC fields contain more latitudinal "noise" than LIMS, SAMS, and UKMO. Similar differences were found for other dates during 1979 both in meridional sections and on horizontal maps of zonal wind. Although base-level differences may explain part of these differences, it is more probable that latitudinal dependence related to the basic temperature data and/or application of smoothing may be responsible for this difference.

It should be noted, however, that the 1979 comparisons are for analyses produced during the initial phase of southern hemisphere analysis at NMC and UKMO, and the quality of these analyses has improved since then. Nevertheless, the percentage differences identified locally are not insignificant since they imply large differences in vertical and meridional shears, which are of considerable importance in evaluating dynamical quantities such as the refractive index. For certain purposes, it may be advantageous to apply temporal or spatial smoothing to the satellite data (e.g. weekly averages) and the base level height analyses (e.g., HITCHMAN and LEOVY, 1986).

Potential Vorticity. The evaluation of potential vorticity (PV) is made for 24 May 1979 during a period of enhanced planetary wave activity. The comparison consists of LIMS and UKMO PV fields on the 500 K and 850 K isentropic surfaces (near 70 and 10 mb, respectively). PV is a highly differentiated quantity and errors in PV are thus liable to be large. [See GROSE (1984, LIMS) and CLOUGH et al. (1985, TOVS) for details of the PV calculation.].

A contemporaneous set of maps of ozone and nitric acid mixing ratios are available from the LIMS experiment (e.g., LEOVY et al., 1985) and are included for the 24 May 1979 PV comparison. Because these trace gases have photochemical lifetimes which are longer than the time-scale for large-amplitude dynamical

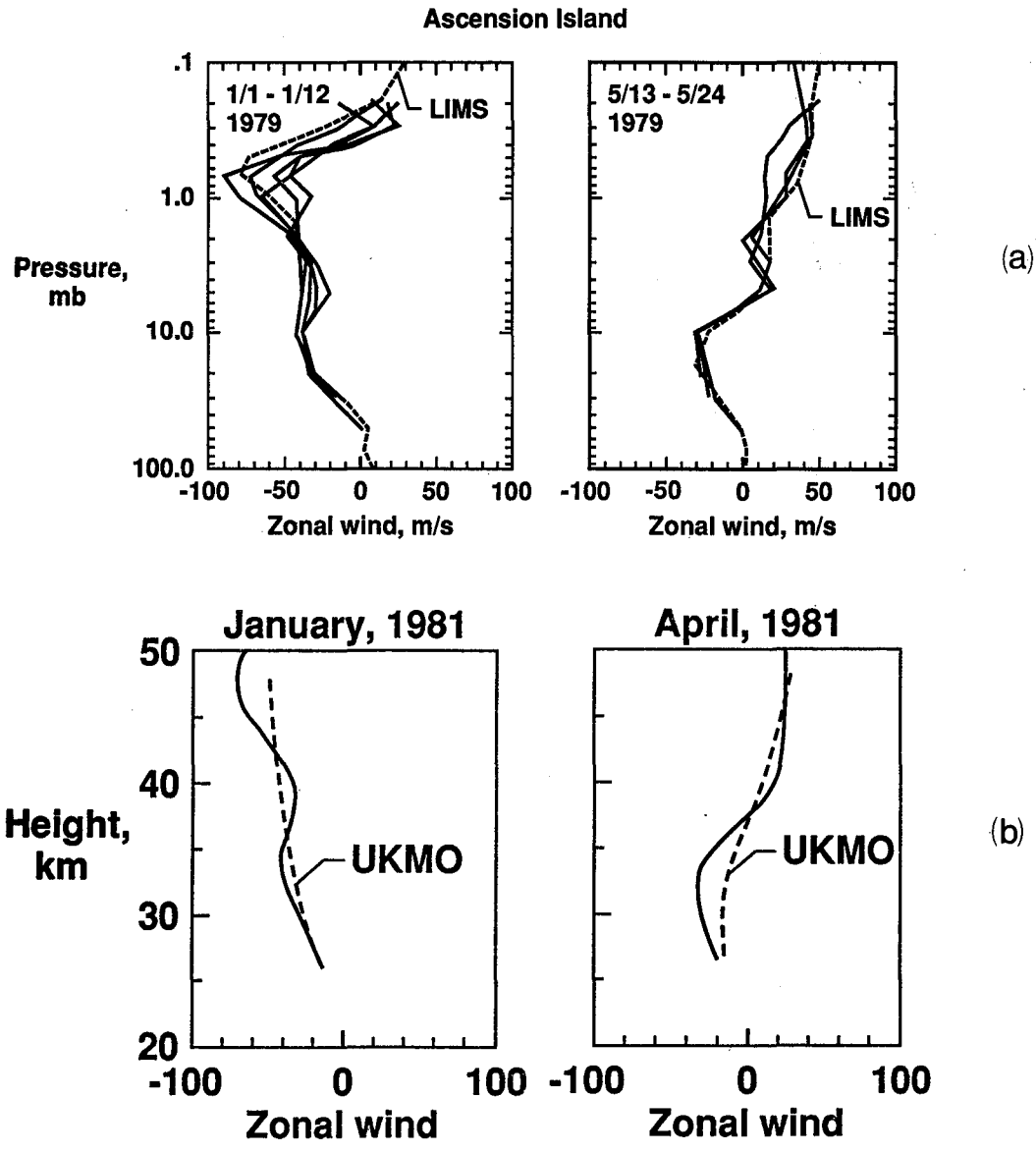

Fig. 3 (a) Twelve-day mean LIMS geostrophic (dashed) and individual rocket profiles (solid) of zonal wind at Ascension Island during 1-12 January 1979 and 13-24 May 1979. (b) Monthly-mean UKMO geostrophic (dashed) and rocket (solid) zonal wind at Ascension Island during January and April 1981. Units: m s^{-1}.

motions, they represent passive tracers which can be used with the PV analyses to infer quasi-conservative large-scale mixing of stratospheric air parcels in the lower-middle stratosphere.

The distribution of the modulus of PV on the 500 K and 850 K surfaces is shown in Figure 4, along with the LIMS analyses of nitric acid and ozone for the 500 K and 850 K surfaces. Although the LIMS and UKMO PV fields exhibit broadly similar features, noticeable localized differences are evident. The 500 K comparison indicates three tongues of high PV (4-5 PV units at 60°S) near 70°-90°E, 150°W, and 30°W which are correlated with three maxima in the nitric acid analysis. A noteworthy feature seen in the LIMS and UKMO PV fields is a reversal in the meridional gradient of PV which occurs in the 110°E - 170°E sector associated with an equatorward displacement of high PV. This change in meridional gradient is also suggested in the 500 K nitric acid field. However, a similar reversal which occurs in the mid-latitude LIMS PV and nitric acid near 70°W has no counterpart in the UKMO field. In subtropical latitudes (e.g. at 30°S), ripples occur in the UKMO field, such as those near 40°W, which are possibly related to artifacts of the methods of observation and derivation of the gridded fields (e.g., CLOUGH et al., 1985).

Several of the features observed at 500 K are evident at the 850K level. For example, LIMS and UKMO show a tongue of high PV near 150°W which is more intense in the UKMO analysis (8 PV units vs. 6 for LIMS). Near 30°W LIMS indicates a broad tongue of high PV, whereas the UKMO field indicates a shorter wavelength tongue of high PV near 10°W. Moreover, the UKMO analysis in this region shows a stronger meridional PV gradient. The low-latitude ripple pattern seen at 500 K is also evident at 850 K, e.g. near 40°W in UKMO. The 850 K PV fields are similar to the LIMS ozone distribution in several respects. For example, the ozone map indicates a tongue of low mixing ratio near 160°W with strong meridional gradients, while a region of weak meridional gradient is present in low latitudes near 110°E.

Although the LIMS and UKMO PV analyses at 500 K and 850 K exhibit qualitative similarities, the UKMO fields generally contain more longitudinal structure than do the LIMS maps. Some of this structure could be real, being on a scale that could be revealed by the good longitudinal resolution afforded by side-scanning on the TOVS instruments. Because of these local differences in PV distribution, potential users should exercise caution for quantitative applications. However, the larger-scale patterns involving distinct trough/ridge features and meridional extrusions of PV do seem to be captured in a fairly reasonable manner in light of the broad agreement with the trace constituent fields. This is particularly true for processes that are dominated by large scales of motion in a deep layer of the atmosphere.

Eliassen-Palm Flux. Meridional cross-sections, from LIMS and UKMO data, of the (quasi-geostrophic) Eliassen-Palm flux divergence on 19 May 1979 are shown in Figure 5 (a scaled form of this quantity is actually plotted as explained in the caption). In the stratosphere, the two terms that constitute this divergence (see Eq. (2.2) in DUNKERTON et al., 1981) are frequently large and of opposite sign, so the divergence is prone to large errors. Indeed, on the day shown, there is no apparent qualitative, let alone quantitative, agreement between the two fields. The LIMS field has convergence over a broad latitudinal band at middle latitudes, whereas the UKMO has divergence. It is likely that the UKMO field is the more suspect of the two, for it shows little continuity from one day to the next around the chosen day; the continuity of the LIMS field is better.

The serious discrepancies noted here between fields of Eliassen-Palm flux divergence are probably attributable to the poorer than normal vertical resolution of the UKMO analyses in the first half of 1979. Afterwards, UKMO analyses should generally be of much better quality (as found by GROSE and RODGERS, 1986), because of better instrument performance and additional data

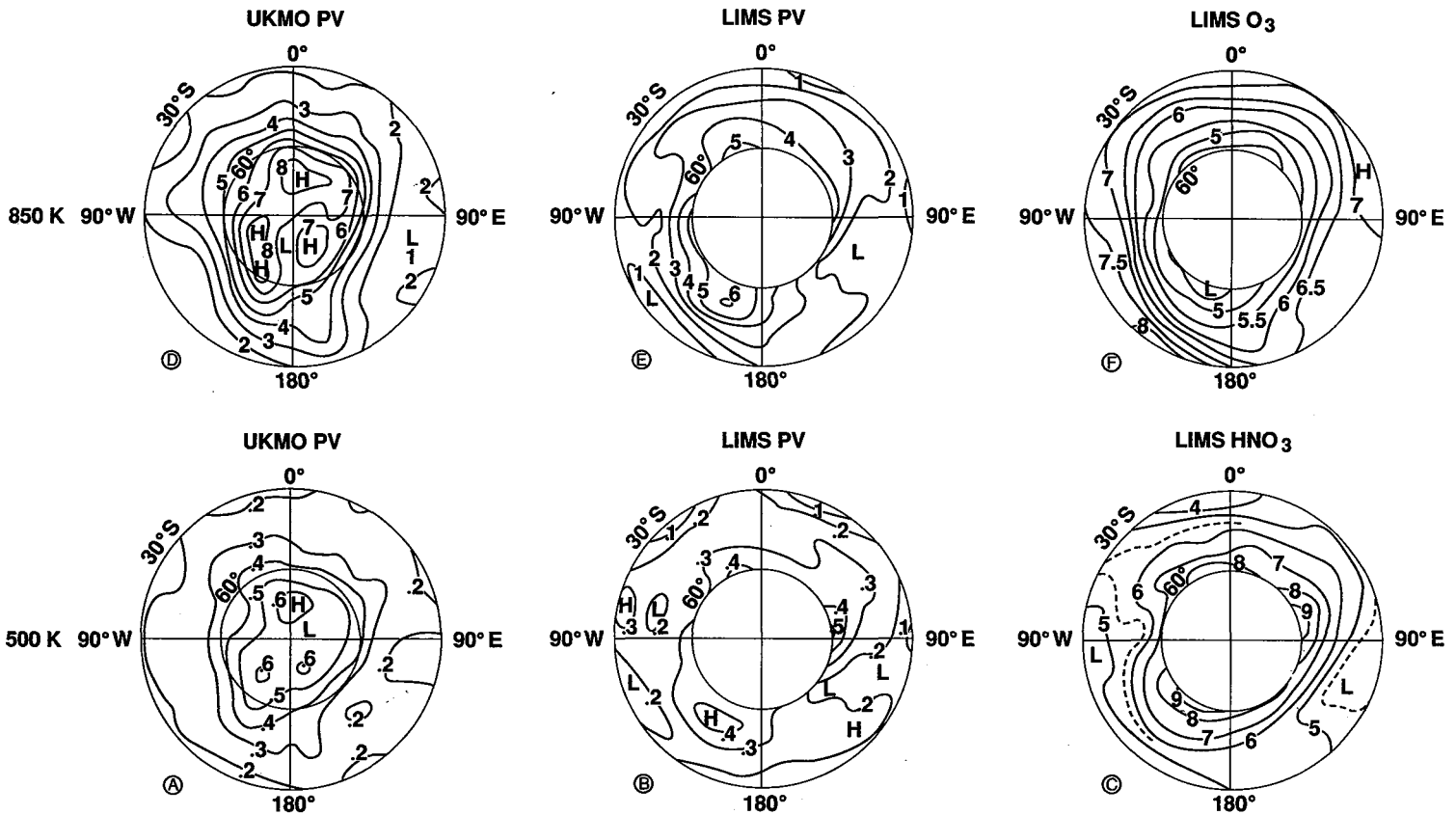

Fig. 4 (a,d) UKMO and (b,e) LIMS maps of the modulus of Ertel's potential vorticity on the 500 K and 850 K isentropic surface for the southern hemisphere on 24 May 1979 (units: 10^{-4} K m^2 kg^{-1} s^{-1}). (c) 500 K nitric acid mixing ratio (ppbv) and (f) 850 K ozone mixing ratio (ppmv) from LIMS on the same day.

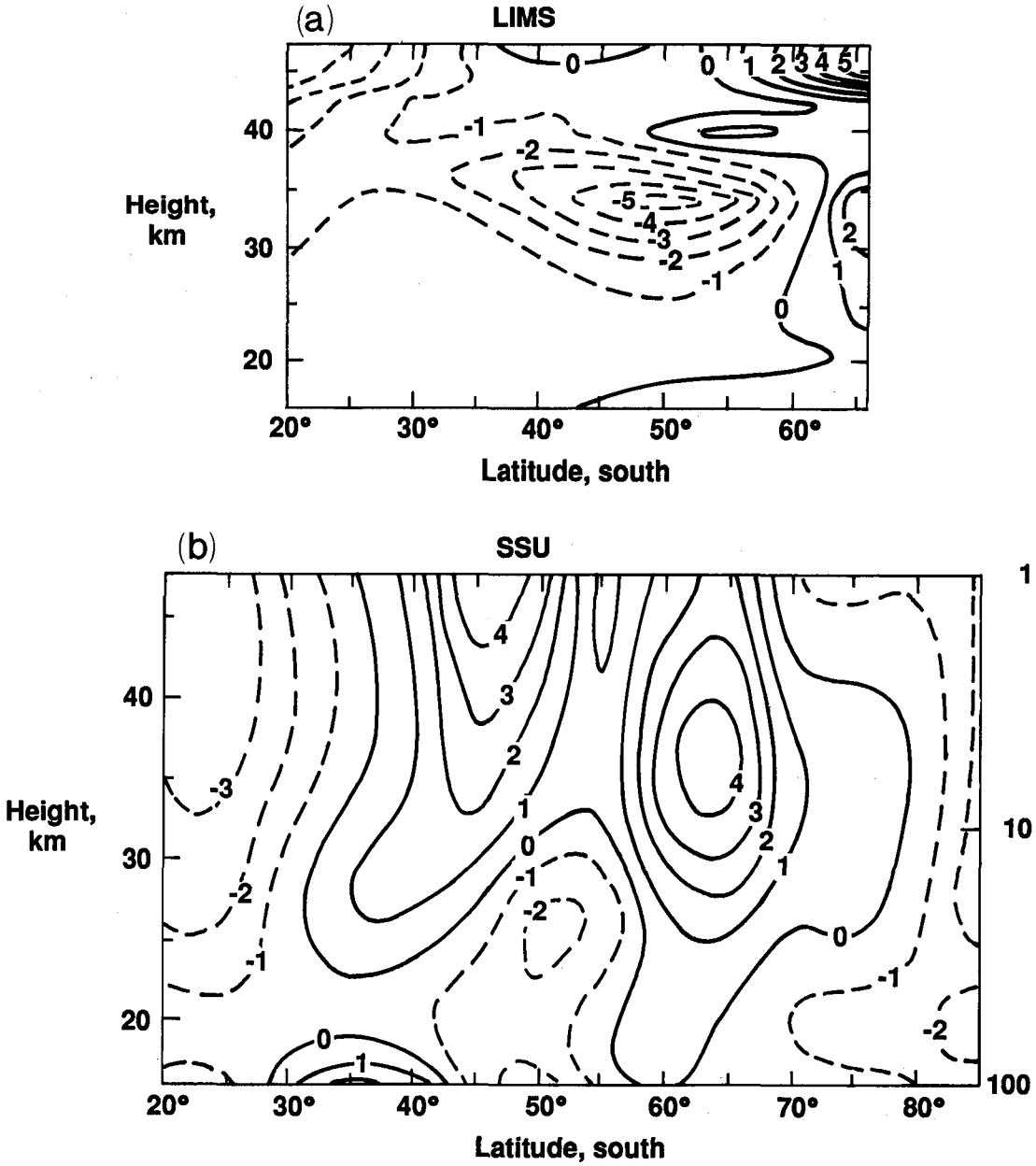

Fig. 5 The divergence of the Eliassen-Palm flux, scaled to give the zonal force per unit mass due to eddies, for the southern hemisphere on 19 May 1979. It is the quantity denoted as D_F by Dunkerton et al. (1981), units: 10^{-5} m s^{-2}. (a) From LIMS, (b) from UKMO. Pecked lines indicate negative values (convergence).

from the HIRS-2 and MSU radiometers. Even so, the vertical resolution of the best possible analyses from these instruments is poorer than from LIMS. As most of the longitudinal variance in the stratosphere is in the longest zonal waves, which LIMS analyses should be able to resolve, side-scanning in the TOVS instruments does not prove to be a significant advantage for the calculation of Eliassen-Palm flux divergence, but it can be for calculations of synoptic maps of PV.

3.2 Impact of Base Level on Derived Quantities

In principle, basic retrieved fields from satellites need be no less accurate in the Southern Hemisphere than they are in the Northern Hemisphere. Indeed the spatially uniform quality of the measurements is one of the main advantages of using satellite data in diagnostic studies. To calculate many quantities of dynamical interest, however, a field of geopotential height at a base level (usually in the lower stratosphere) is also needed. Herein lies the main shortcoming of derived quantities for the Southern Hemisphere: conventional observations of the troposphere and lower stratosphere (e.g., from radiosondes) are sparse. It is not our purpose here to judge the reliability of base level analyses made available by different meteorological centers. Rather, it is to illustrate the differences in derived quantities (eddy flux, zonal wind, potential vorticity, and divergence of the Eliassen-Palm flux) that are produced in the stratosphere when satellite thickness data from one source - in this case the UKMO analyses - are used in conjunction with various base-level analyses of geopotential height at 100 mb.

The impact of different base level analyses is discussed for two periods: (1) June and September, 1981 and (2) September, 1985 (Table 1). In the 1981 comparison (Section 3.2.1), UKMO satellite data are combined with ECMWF and NMC 100 mb base-level height analyses to obtain heights at 50, 20, 10, 5, 2, and 1 mb. Temperatures at each level were derived hydrostatically from the height analyses and geostrophic winds were then calculated. The 1981 comparison investigated the impact on eddy statistics such as the stationary and transient eddy height variances and eddy fluxes of heat and momentum. The 1985 comparison uses the same approach as for 1981, but includes the base-level height analyses from UKMO, and considers the impact on zonal wind, potential vorticity, and Eliassen-Palm flux divergence.

3.2.1 1981 Eddy Statistics

The impact of the different base height analyses for June and September 1981 has been considered by comparing monthly mean fields and daily transient eddy statistics obtained using the ECMWF and NMC base analyses. This comparison was made using horizontal maps at the 100 and 10 mb levels (not shown) and latitude-pressure cross-sections of the zonal mean (also see KAROLY, 1989). Results are discussed separately for stationary and transient eddy features.

Stationary Eddies. Any differences between the ECMWF and NMC height analyses at the 100 mb level occur with the same amplitude at all stratospheric levels. The typical maximum regional differences in the monthly-mean height maps were ~ 100 m. Differences in the zonal- and monthly-mean height fields were smaller, except at high latitudes poleward of 65°S, where the differences in the zonal mean height fields were ~ 100m (not shown).

Regional differences in the mean height field in middle latitudes lead to differences in stationary wave amplitudes and fluxes of heat and momentum. The stationary wave amplitudes are larger in the thickness data in September than in June so that differences in the stationary wave amplitudes due to the different base analyses are more apparent in June than in September. Stationary wave diagnostics for June 1981 are shown in Figures 6, 7, and 8 for the NMC and ECMWF

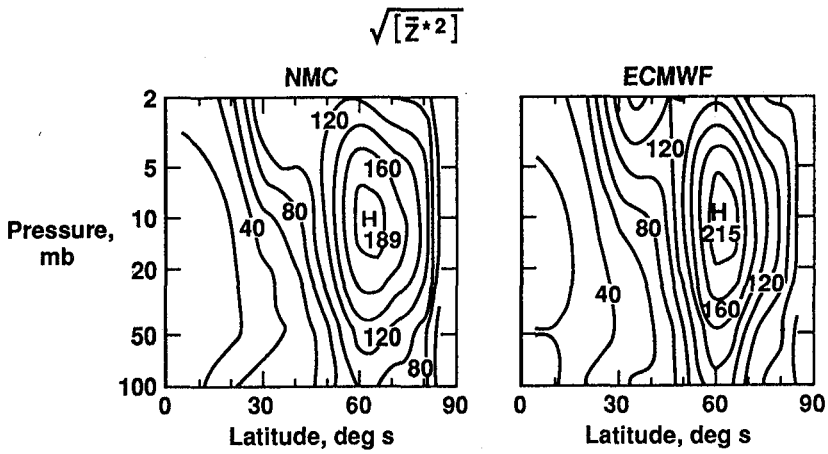

Fig. 6 Stationary eddy r.m.s. zonal variations of geopotential height (m) for the southern hemisphere using NMC (left) and ECMWF (right) base-level analyses of geopotential height at 100 mb for June 1981.

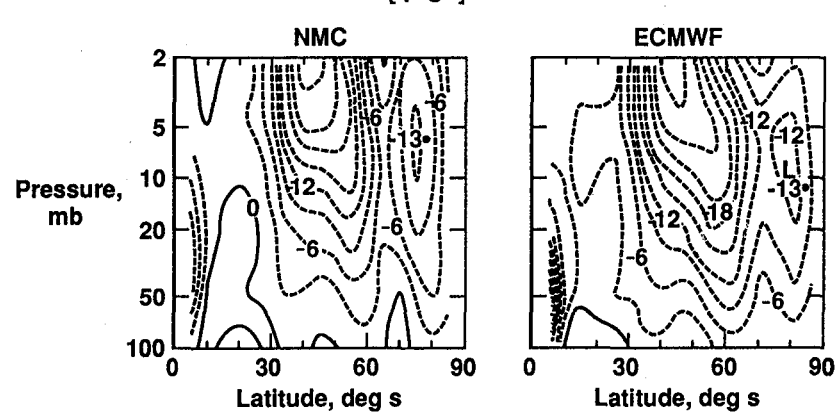

Fig. 7 As for Fig. 6 but for the stationary eddy momentum flux ($m^2\ s^{-2}$).

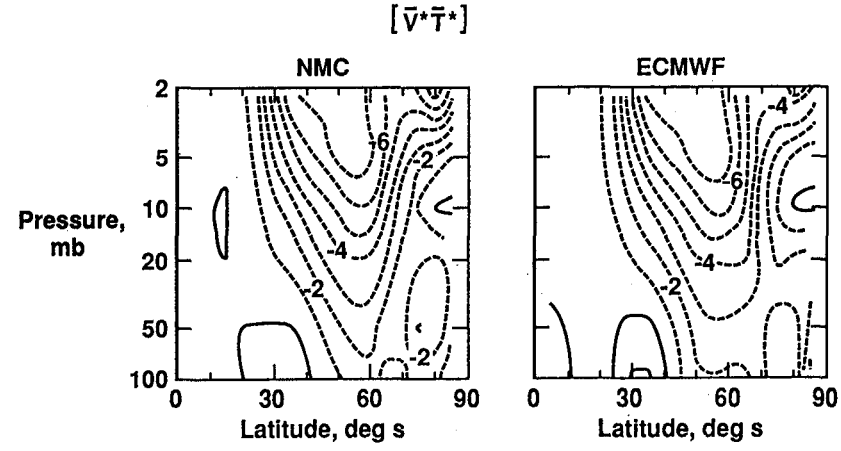

Fig. 8 As for Fig. 6 but for the stationary eddy heat flux (K m s^{-1}).

base analyses. The r.m.s. zonal variations of height show that the ECMWF analyses have larger amplitude stationary waves. The stationary eddy meridional fluxes of momentum and heat are qualitatively similar in structure for both base analyses. However, quantitative differences in momentum flux, in particular, are large at 60°S, with 30% stronger poleward transport for the ECMWF base analyses.

Transient Eddies. Since transient eddy statistics are quadratic, the differences due to the base analyses do not occur with the same amplitude at all levels, but the major differences are similar at all levels. Regional differences (not shown) in amplitude of the transient eddy kinetic energy or height variance are relatively larger than for the stationary eddy fields, but there is reasonable qualititative agreement for the regions of large amplitude transient eddy activity. The horizontal fields from the ECMWF base analyses seem to be more spatially coherent, whereas those from the NMC base analyses have more short-length-scale spatial structure.

For the transient eddy statistics, there is good qualitative agreement for the two base analyses for June and September. The zonal mean daily standard deviation of height for September 1981 is shown in Fig. 9 with the fields obtained using the NMC and ECMWF base analyses and the difference, NMC-ECMWF, on the right. This eddy statistic is very similar for the two analyses, except for large differences which occur at high latitudes, poleward of 70°S. For the horizontal maps of the transient eddy meridional fluxes of momentum and heat there are large regional differences at 100mb (not shown). In terms of the zonal-mean pattern, large differences also occur at high latitudes, poleward of 70°S, for the meridional eddy fluxes (Fig. 10 and 11), whereas differences of 10% in the momentum transport occur in middle latitudes.

Overall, there is qualitative agreement between stationary and transient eddy statistics derived using the two base analyses for the two months, but quantitative differences exist, particularly at high latitudes, which would be very important for budget studies or other derived statistics in the middle-upper stratosphere. Similar differences between ECMWF and NMC high-latitude analyses in the Southern Hemisphere lower stratosphere have been documented by RANDEL et al. (1987), LAMBERT (1988), and NEWMAN and RANDEL (1988).

3.2.2 1985 Derived Quantities

The 1985 base-level impact is evaluated for the ECMWF, NMC, and UKMO base height information combined with the UKMO (TOVS) thickness analyses. Comparisons are presented for zonal mean wind, potential vorticity, and the Eliassen-Palm flux divergence.

Zonal Wind. Three meridional cross-sections of zonal-mean wind on 8 September 1985 are shown in Figure 12 for ECMWF, NMC, and UKMO base-level analyses. These fields include values for the troposphere using operational heights from the three centers. [Note that the NMC heights at 50 mb for the September 1985 comparison are the operational product rather than the stratospheric analysis series (i.e. from 70 - 0.4 mb).] The three wind analyses show a westerly jet in the middle-upper stratosphere which is centered near 55°S and 35 km with maximum speeds in excess of 80 m/s. At low and middle latitudes there is good agreement between the fields. At high latitudes, however, the three fields differ by up to 10-15 m/s at 100 mb (and also at tropospheric levels), the impact of which is noticeable up to the upper stratosphere (e.g., at 80°S). These findings are typical for September 1985.

Potential Vorticity. Three synoptic maps of PV on the 850 K surface on 24 September 1985 are shown in Figure 13 derived using the ECMWF, NMC, and UKMO base-level height information. The fields are generally in good agreement.

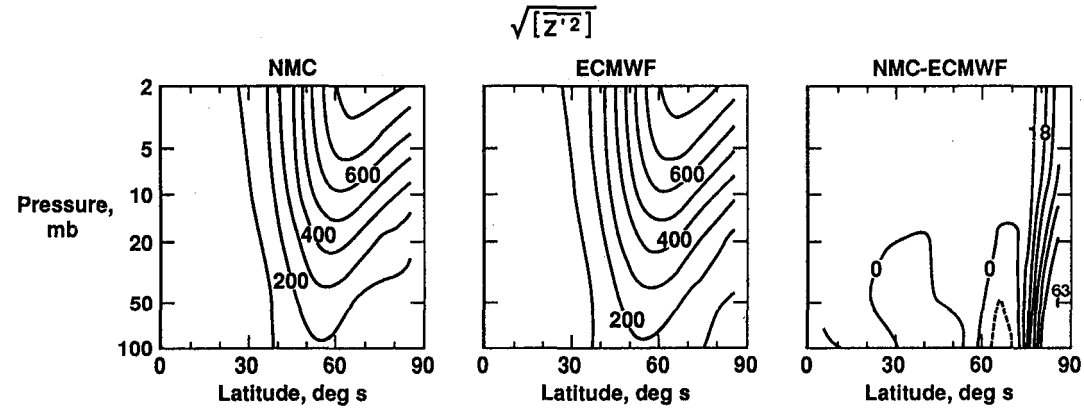

Fig. 9 Transient eddy r.m.s. daily variations of geopotential height (m) for the southern hemisphere using NMC (left) and ECMWF (center) base-level analyses of geopotential height at 100 mb, and the difference NMC-ECMWF (right), for September 1981.

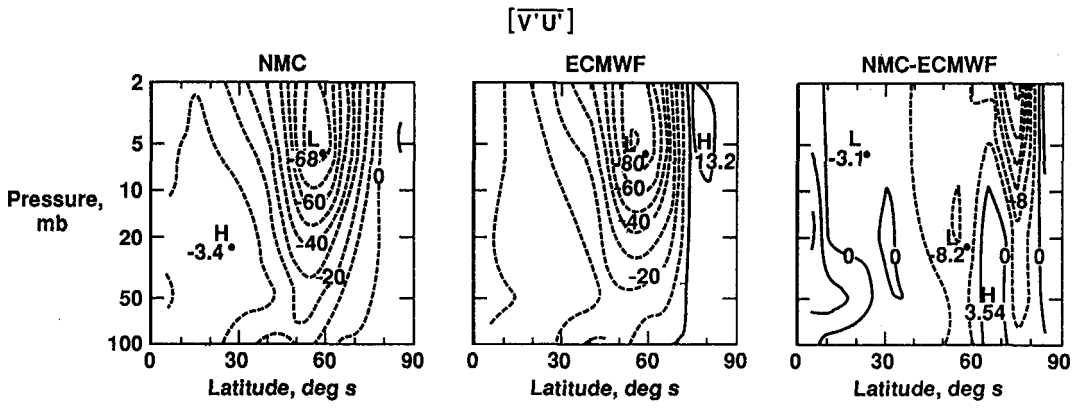

Fig.10 As for Fig. 9 but for the transient eddy momentum flux ($m^2\ s^{-2}$).

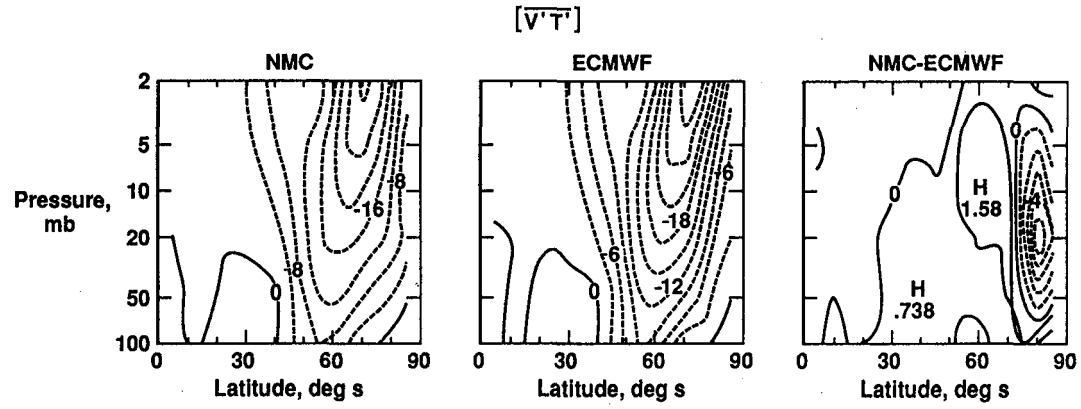

Fig.11 As for Fig. 9 but for the transient eddy heat flux ($K\ m\ s^{-1}$).

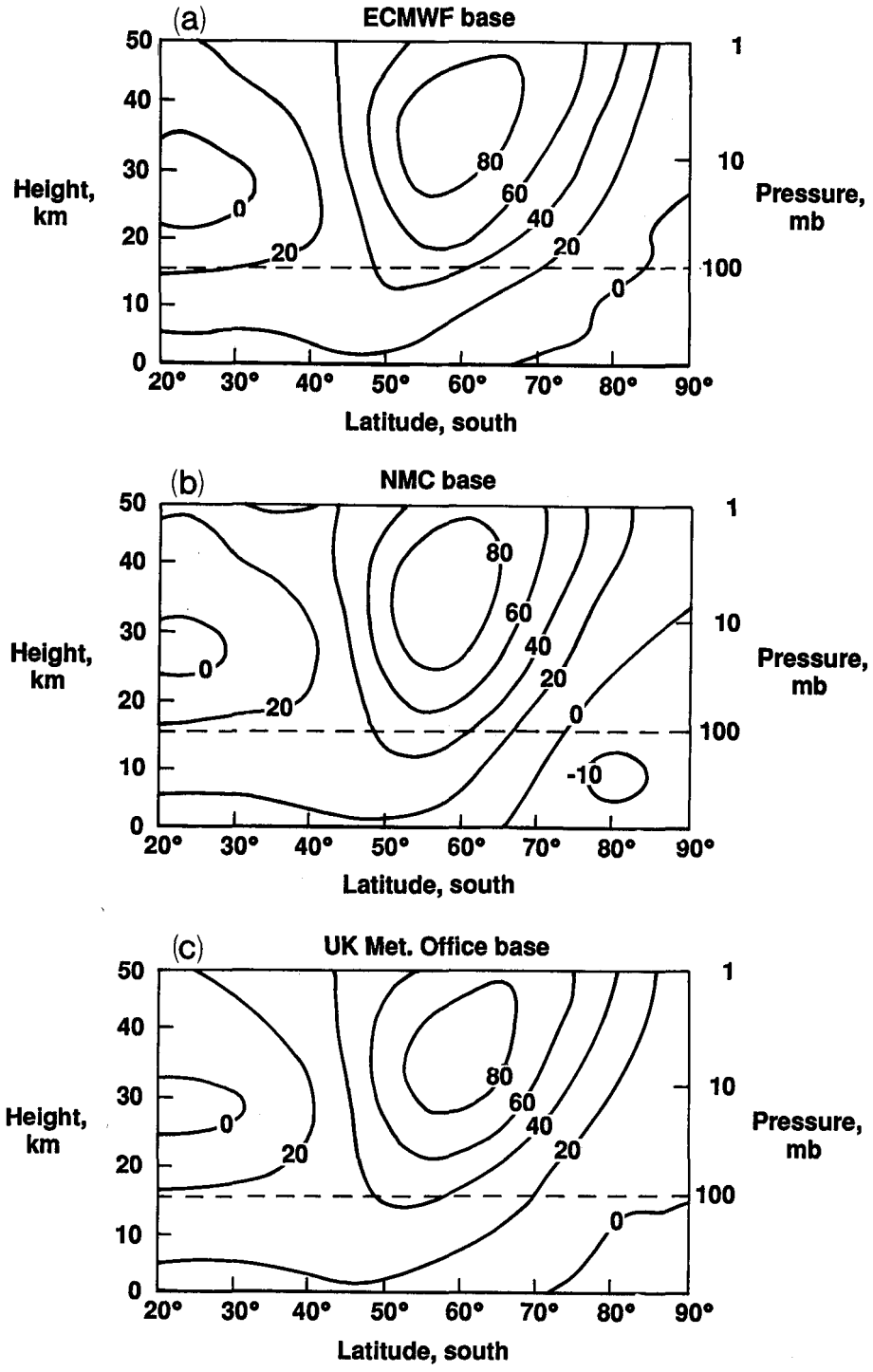

Fig.12 Zonal-mean geostrophic wind (m s^{-1}) for the southern hemisphere on 8 September 1985. Fields constructed using different base-level analyses of geopotential height at 100 mb: (a) from ECMWF, (b) from NMC, (c) from UKMO.

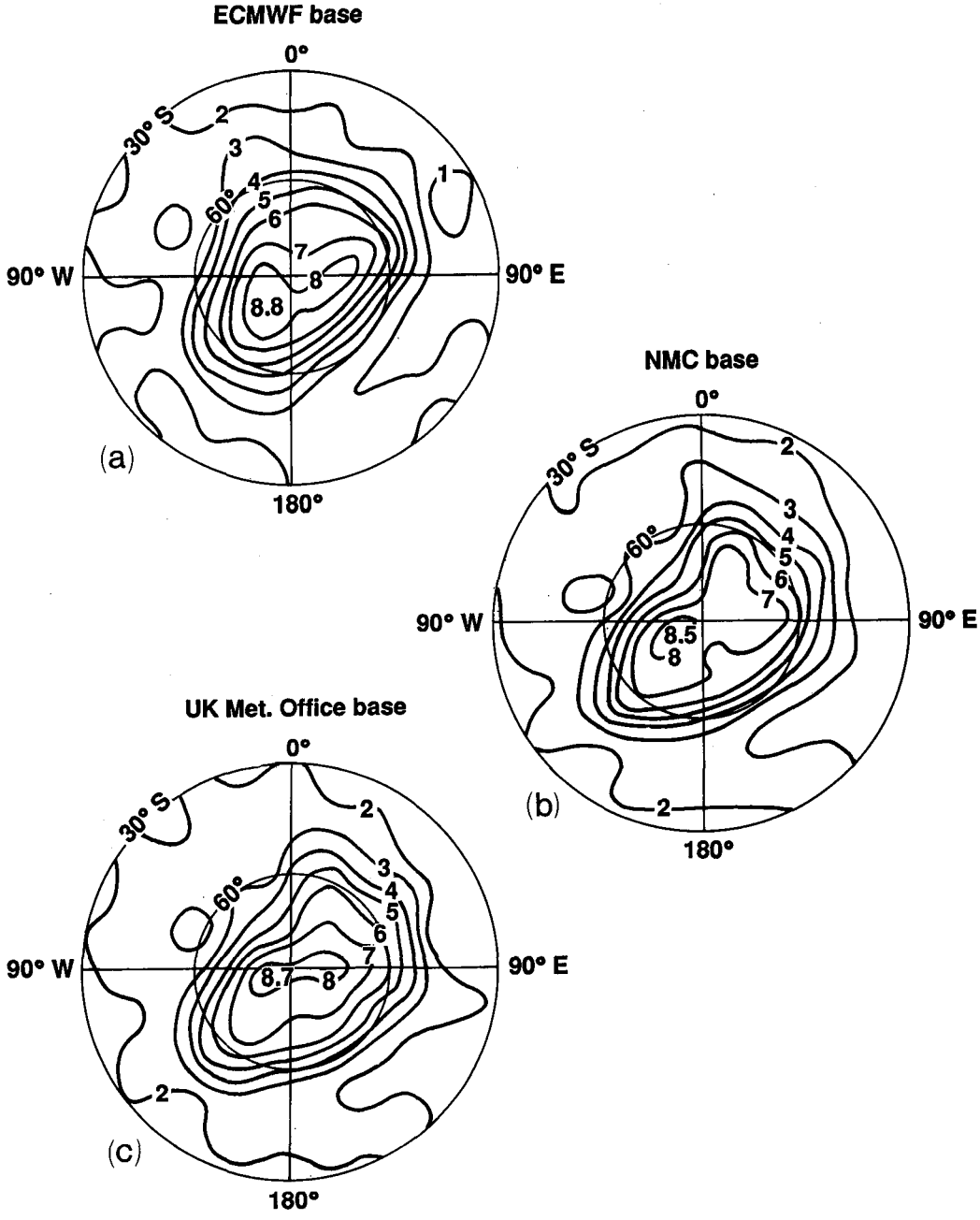

Fig.13 Synoptic maps of the modulus of Ertel's potential vorticity on the 850 K isentropic surface for the southern hemisphere on 24 September 1985 (units: 10^{-4} K m^2 kg^{-1} s^{-1}). Fields constructed using different base-level analyses of geopotential height at 100 mb: (a) from ECMWF, (b) from NMC, (c) from UKMO.

This result is only to be expected since derivatives of the UKMO thickness field (a field the three maps have in common) contribute most to the value of PV. Differences in detail do occur, however, such as the presence of a tongue of high PV near 60°S, 20°E in the NMC and UKMO analyses, which does not appear in the ECMWF analysis. Conversely, at 60°S, 30°W the ECMWF field contains a tongue of high PV which is absent in the NMC and UKMO analyses.

At low latitudes horizontal gradients of the thickness field become small, and those of the geopotential height field at the base level contribute proportionally more to the value of PV. Moreover, gradients of PV are small at low latitudes, so a small difference between base-level analyses can make a big difference to an isopleth's position. Thus although the tongue of locally high PV near 180°E appears on all three maps, it extends further westward for the ECMWF base. Similar differences were found at the 500 K surface (not shown).

Eliassen-Palm Flux. Three meridional cross-sections of the Eliassen-Palm flux divergence on 8 September 1985 are shown in Figure 14 which are derived using the ECMWF, NMC, and UKMO base data. Although the three fields all have divergence in the stratosphere at high latitudes and convergence at middle and sub-polar latitudes, there are significant differences. At high latitudes in the upper stratosphere (e.g., at 80°S), divergence with the ECMWF base is half as large as that with the others. A region of flux divergence exists in the NMC analysis at 55°S, 40 km which is not shown in the ECMWF and UKMO fields. Notice also that there are significant differences at high latitudes in the troposphere.

4. CONCLUSIONS

Overall, examination of the basic meteorological fields (temperatures, winds) derived from measurements by different satellites leads to similar conclusions to those reached in the PMP-1 comparison of data for the Northern Hemisphere. While there is usually qualitative agreement between the different sets of fields, substantial quantitative differences are evident, particularly in high latitudes. Differences in vertical and longitudinal resolution between the limb- and nadir-viewing experiments result in quantitative differences in fields of derived winds, potential vorticity and Eliassen-Palm flux divergence.

There are several techniques that may be used to evaluate the reliability of the information contained in the measurements:

(1) Independent data sets (derived from different instruments and base-level analyses) should, ideally, be used in parallel and studied for consistency.
(2) The temporal continuity of derived fields is often useful in highlighting problems with the data.
(3) Consistency between zonal-mean meridional velocities inferred separately from zonally-averaged momentum and thermodynamic equations provides a powerful constraint (assuming unknown friction can be neglected).
(4) The conservation of potential vorticity over a period of a week or so in the middle stratosphere is an important objective check on the reliability of the analyses.
(5) A good correlation over short periods between some quasi-conservative chemical species (whose concentrations are measured directly) and potential vorticity (a highly derived quantity) is persuasive evidence that the data have at least qualitative value.

It is clear from our study that the fidelity of the base-level analysis is of great importance in calculating derived quantities for the middle atmosphere, especially in the Southern Hemisphere. We have demonstrated this relationship by using a single set of satellite data (from TOVS) with base-level analyses obtained from three meteorological centers (ECMWF, NMC, and UKMO). The

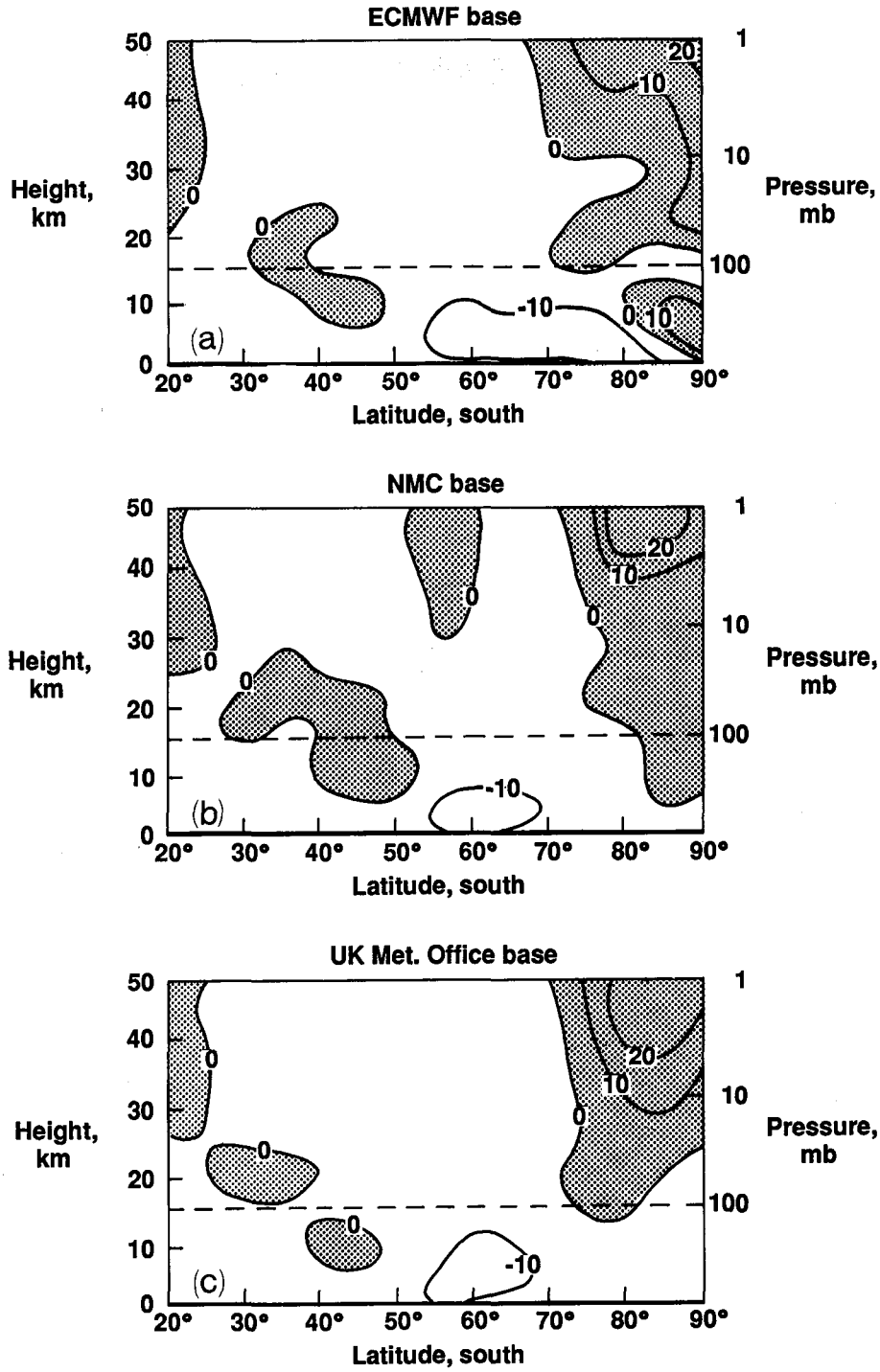

Fig.14 As for Fig. 12 but for divergence of Eliassen-Palm flux, scaled as in Fig.5 (units: 10^{-5}m s^{-2}). Stipling denotes positive values (divergence).

Eliassen-Palm flux divergence is particularly sensitive to the base-level analysis (though it can also be sensitive to the instrument used), as is the potential vorticity at low latitudes where horizontal gradients are weak.

Some effort is needed to improve base level analyses in the Southern Hemisphere. There appear to be particular problems at high latitudes where conventional observations are sparse and infrequent, and spurious features may influence diagnostics throughout the stratosphere. Significant uncertainties in operational analyses of geopotential height over Antarctica have been identified by HOLLINGSWORTH et al. (1985), LAMBERT (1988), and TRENBERTH and OLSON (1988) for tropospheric levels, and similar discrepancies have been observed in the present comparison at 100 mb. Possible reasons for poor quality analyses in this region include sparse radiosonde coverage, steep Antarctic topography, and difficulties in adequately assimilating upper-air reports from isolated stations (e.g., at the South Pole). It is known, for example, that NMC received radiosonde reports from the South Pole station for only 2 days in the month of September 1985. Such telecommunication problems should be resolved.

The steep Antarctic topography may produce errors in the forecast model first-guess fields and, furthermore, will generate gravity wave activity which may produce sampling problems in the radiosonde observations.

Clearly, care should be taken in removing spurious features from the reference-level analyses in the polar region, and ensuring that the operational centers have access to all Antarctic radiosonde station data. Further comparison of radiosonde heights with the final operational analyses should be made specifically for the reference-level (e.g., 100mb). A comparative appraisal of the procedures used to construct the different base-level analyses for the Southern Hemisphere would be of value to Middle Atmosphere researchers. For example, investigation of which station data is incorporated into the base analyses could be made along with evaluating differences in analysis procedures in data-void regions. Such a task may require the use of a data assimilation model and is beyond the scope of the average user of the data; those who produce the analyses are best placed to assess and improve them.

On the basis of the experience gained from the PMP-1 and Williamsburg workshops, we feel it prudent to advise caution in drawing inferences, particularly quantitative ones, from meteorological fields derived from satellite data. Such counsel is certainly apt for the Southern Hemisphere, where coverage of data from sources other than satellites is limited.

ACKNOWLEDGEMENTS

We are grateful to Dixon Butler, NASA Headquarters, Washington, D. C., for providing support for the workshop, William Grose and Nancy Holt of NASA Langley Research Center for local organization of the meeting, Vicky Pope for preliminary collation of data, and Kip Marks for providing Figs. 1(d) and 2(d).

REFERENCES

Barnett, J. J., and M. Corney, Temperature comparisons between the Nimbus 7 SAMS, rocket/radiosondes and the NOAA 6 SSU, J. Geophys. Res., 89, 5294-5302, 1984.

Barnett, J. J., and M. Corney, Temperature data from satellites, MAP Handbook, Vol. 16, pp. 3-11, 1985.

Bengtsson, L., and J. Shukla, Integration of space and in situ observations to study global climate change, Bull. Am. Meteorol. Soc., 69, 1130-1143, 1988.

Clough, S. A., N. S. Grahame, and A. O'Neill, Potential vorticity in the stratosphere derived using data from satellites, Quart. J. Roy. Meteorol. Soc., 111, 335-358, 1985.

Delisi, D. P., and T. J. Dunkerton, Equatorial semiannual oscillation in zonally averaged temperature observed by the Nimbus 7 SAMS and LIMS, J. Geophys. Res., 93, 3899-3904, 1988.

Dunkerton, T., C.-P. F. Hsu, and M. E. McIntyre, Some Eulerian and Lagrangian diagnostics for a model stratospheric warming, J. Atmos. Sci., 38, 819-843, 1981.

Finger, F. G., H. M. Woolf, and C. E. Anderson, A method for objective analysis of stratospheric constant-pressure charts, Mon. Wea. Rev., 93, 619-638, 1965.

Geller, M. A., M.-F. Wu, and M. E. Gelman, Troposphere-stratosphere (surface-55 km) monthly winter general circulation statistics for the northern hemisphere - four year averages, Mon. Wea. Rev., 40, 1334-1352, 1983.

Gelman, M. E., A. J. Miller, K. W. Johnson, and R. M. Nagatani, Detection of long-term trends in global stratospheric temperature from NMC analyses derived from NOAA satellite data, Adv. Space Res., 6, 17-26, 1986.

Gille, J. C., and J. M. Russell III, The Limb Infrared Monitor of the Stratosphere: experiment description, performance, and results, J. Geophys. Res., 89, 5125-5140, 1984.

Gille, J. C., J.M. Russell III, P. L. Bailey, L. L. Gordley, E. E. Remsberg, J. H. Leinesch, W. G. Planet, F. B. House, L. V. Lyjak, and S. A. Beck, Validation of temperature retrievals obtained by the Limb Infrared Monitor of the Stratosphere (LIMS) experiment on Nimbus 7, J. Geophys. Res., 89, 5147-5160, 1984a.

Gille, J. C., P. L. Bailey, and S. A. Beck, A comparison of U.S. and USSR rocketsondes using LIMS satellite temperature sounding as a transfer standard, J. Geophys. Res., 89, 11711-11715, 1984b.

Grose, W. L., Recent advances in understanding stratospheric dynamics and transport processes: application of satellite data to their interpretation, Adv. Space Res., 4, 19-28, 1984.

Grose, W. L., and C. D. Rodgers, Coordinated study of the behavior of the middle atmosphere in winter: monthly mean comparisons of satellite and radiosonde data and derived quantities, MAP Handbook Vol. 21, pp. 79-111, 1986.

Grose, W. L., T. Miles, K. Labitzke, and E. Pantzke, Comparison of LIMS temperatures and geostrophic winds with Berlin radiosonde temperature and wind measurements, J. Geophys. Res., 93, 11217-11226, 1988.

Grose, W. L., and A. O'Neill, Comparison of data and derived quantities for the middle atmosphere of the southern hemisphere, Pure Appl. Geophys., 130, in press, 1989.

Hirota, I., T. Hirooka, and M. Shiotani, Upper stratospheric circulations in the two hemispheres observed by satellites, Quart. J. Roy. Meteorol. Soc., 109, 443-454, 1983.

Hitchman, M. H., and C. B. Leovy, Evolution of the zonal mean state in the equatorial middle atmosphere during October 1978 - May 1979, J. Atmos. Sci., 43, 3159-3176, 1986.

Hitchman, M. H., C. B. Leovy, J. C. Gille, and P. L. Bailey, Quasi-stationary zonally asymmetric circulations in the equatorial lower mesosphere, J. Atmos. Sci., 44, 2219-2236, 1987.

Hollingsworth, A., A. C. Lorenc, M. S. Tracton, K. Arpe, G. Cats, S. Uppala, and P. Kallberg, The response of numerical weather prediction systems to FGGE level IIb data. Part I: Analyses, Quart. J. Roy. Meteorol. Soc., 111, 1-66, 1985.

Karoly, D. J., The impact of base-level analyses on stratospheric circulation statistics for the southern hemisphere, Pure Appl. Geophys., 130, in press, 1989.

Lambert, S. J., A comparison of operational global analyses from the European Centre for Medium Range Weather Forecasts (ECMWF) and the National Meteorological Center (NMC), Tellus, 40A, 272-284, 1988.

Leovy, C. B., C.-R. Sun, M. H. Hitchman, E. E. Remsberg, J. M. Russell III, L. L. Gordley, J. C. Gille, and L. V. Lyjak, Transport of ozone in the middle stratosphere: Evidence for planetary wave breaking, J. Atmos. Sci., 42, 230-244, 1985.

Miles, T., W. L. Grose, J. M. Russell III, and E. E. Remsberg, Comparison of southern hemisphere radiosonde and LIMS temperatures at 100 mb, Quart. J. Roy. Meteorol. Soc., 113, 1382-1386, 1987.

Nash, J., and J. L. Brownscombe, Validation of the stratospheric sounding unit, Adv. Space Res., 2, 59-62, 1983.

Nash, J., and G. F. Forrester, Long-term monitoring of stratospheric temperature trends using radiance measurements obtained by the Tiros-N series of NOAA spacecraft, Adv. Space Res., 6, 37-44, 1986.

Newman, P. A., and J. L. Stanford, Observational characteristics of atmospheric anomalies with short meridional and long zonal scales, J. Atmos. Sci., 40, 2547-2554, 1983.

Newman, P. A., and W. J. Randel, Coherent ozone-dynamical changes during the southern hemisphere spring, 1979-1986, J. Geophys. Res., 93, 12585-12606, 1988.

Phillips, N., L. McMillin, A Gruber, and D. Wark, An evaluation of early operational temperature soundings from Tiros-N, Bull. Amer. Meteorol. Soc., 60, 1188-1197, 1979.

Pick, D. R., and J. L. Brownscombe, Early results based on the stratospheric channels of TOVS on the Tiros-N series of operational satellites, Adv. Space Res., 1, 247-260, 1981.

Randel, W. J., D. E. Stevens, and J. L. Stanford, A study of planetary waves in the southern winter troposphere and stratosphere. Part II: Life cycles, J. Atmos.Sci., 44, 936-949, 1987.

Remsberg, E. E., The accuracy of Nimbus 7 LIMS temperatures in the mesosphere, Geophys. Res. Lett., 13, 311-314, 1986.

Remsberg, E. E., K. V. Haggard, and J. M. Russell III, Description of the Nimbus 7 LIMS MAP archive tape product for middle atmosphere studies, J. Atmos. Ocean. Tech., submitted, 1989.

Rodgers, C. D., Workshops on comparison of data and derived dynamical quantities during northern hemisphere winters, Adv. Space Res, 4, 117-125, 1984a.

Rodgers, C. D., Coordinated study of the behavior of the middle atmosphere in winter (PMP-1), MAP Handbook, Vol. 12, 154 pp., 1984b

Rodgers, C. D., R. L. Jones, and J. J. Barnett, Retrieval of temperature and composition from Nimbus 7 SAMS measurements, J. Geophys. Res., 89, 5280-5286, 1984.

Schlatter, T. W., An assessment of operational Tiros-N temperature retrievals over the United States, Mon. Weath. Rev., 109, 110-119, 1981.

Schmidlin, F. J., Intercomparisons of temperature, density, and wind measurements from in situ and satellite techniques, Adv. Space Res., 4, 101-110, 1984.

Smith, A. K., and P. L. Bailey, Comparison of horizontal winds from the LIMS satellite instrument with rocket measurements, J. Geophys. Res., 90, 3897-3901, 1985.

Smith, W. L., H. M. Woolf, C. M. Hayden, D. Q. Wark, and L. M. McMillin, The TIROS-N operational vertical sounder, Bull. Amer. Meteorol. Soc., 60, 1177-1187, 1979.

Trenberth, K. E. and J. G. Olson, An evaluation and intercomparison of global analyses from the National Meteorological Center and the European Centre for Medium Range Weather Forecasts, Bull. Amer. Meteorol. Soc., 69, 1047-1057, 1988.

Wale, M. J., and G. D. Peskett, Some aspects of the design and behavior of the stratospheric and mesospheric sounder, J. Geophys. Res., 89, 5287-5293, 1984.

Yu, W.-B., R. L. Martin, and J,. L. Stanford, Long and medium-scale waves in the lower stratosphere from satellite-derived microwave measurements, J. Geophys. Res., 88, 8505-8511, 1983.

CUMULATIVE LISTING FOR THE MAP HANDBOOK

Volume	Contents	Publication Date
1	National Plans, PMP-1 , PMP-2, PMP-3 Reports, Approved MAP Projects	June 1981
2	Symposium on Middle Atmosphere Dynamics and Transport	June 1981
3	PMP-5, MSG-1, MSG-2, MSG-3 Reports, Antarctic Middle Atmosphere Project (AMA), EXOS-C Scientific Observations, WMO Report No. 5., Updated Chapter 2 of MAP Planning Document, Condensed Minutes of MAPSC Meetings	November 1981
4	Proceedings of MAP Assembly, Edinburgh, August 1981 Condensed Minutes of MAPSC Meetings, Edinburgh,	April 1982
5	Proceedings of MAP Open Meeting, Hamburg, August 1981, A Catalogue of Dynamic Parameters Describing the Variability of the Middle Stratosphere during the Northern Winters	May 1982
6	MAP Directory	November 1982
7	Acronyms, Condensed Minutes of MAPSC Meetings, Ottawa, May 1982, MAP Projects, National Reports, Committee, PMP, MSG, Workshop Reports, Announcements, Corrigendum	December 1982
8	MAP Project Reports: DYNAMICS, GLOBUS, and SSIM, MSG-7 Report, National Reports: Czechoslovakia, USA	July 1983
9	URSI/SCOSTEP Workshop on Technical Aspects of MST Radar, Urbana, May 1983	December 1983
10	International Symposium on Ground-Based Studies of the Middle Atmosphere, Schwerin, May 1983	May 1984
11	Condensed Minutes of MAPSC Meetings, Hamburg, 1983, Research Recommendations for Increased US Participation in the Middle Atmosphere Program, GRATMAP and MSG-7 Reports	June 1984
12	Coordinated Study of the Behavior of the Middle Atmosphere in Winter (PMP-1) Workshops	July 1984
13	Ground-Based Techniques	November 1984
14	URSI/SCOSTEP Workshop on Technical Aspects of MST Radar, Urbana, May 1984	December 1984
15	Balloon Techniques	June 1985
16	Atmospheric Structure and its Variation in the Region 20 to 120 km: Draft of a New Reference Middle Atmosphere	July 1985
17	Condensed Minutes of MAPSC Meeting, Condensed Minutes of MAP Assembly, MAP Project, MSG, and National Reports	August 1985
18	MAP Symposium, Kyoto, November 1984	December 1985
19	Rocket Techniques	March 1986
20	URSI/SCOSTEP Workshop on Technical and Scientific Aspects of MST Radar, Aguadilla, October 1985	June 1986
21	MAPSC Minutes, ATMAP Workshop, Atmospheric Tides Workshop, MAP/WINE Experimenters Meetings, National Reports: Coordinated Study of the Behavior of the Middle Atmosphere in Winter	July 1986 July 1986
22	Middle Atmosphere Composition Revealed by Satellite Observations	September 1986
23	Condensed Minutes of MAPSC Meetings, Toulouse, June/July 1986	December 1986
24	MAP Directory	May 1987
25	First GLOBMET Symposium, Dushanbe, August 1985	August 1987
26	MAPSC Minutes, Abstracts and Report of Workshop on Noctilucent Clouds, Boulder,	June 1988 October 1985
27	COSPAR Symposium 6, The Middle Atmosphere After MAP,Espoo, July 1988, MAPSC Minutes, Espoo, July 1988; Workshop on Noctilucent Clouds, Tallinn, July 1988	April 1989
28	URSI/SCOSTEP Workshop on Technical and Scientific Aspects of MST Radar, Kyoto, November/December 1988	August 1989
29	International Symposium on Solar Activity Forcing of the Middle Atmosphere, Liblice, Czechoslovakia, April 1989; MASH Workshop, Williamsburg, April 1986	September 1989

CONTENTS

Part 1:

International Symposium on Solar Activity Forcing of the Middle Atmosphere
Liblice, Czechoslovakia, April 1989

Related Papers 1

Quasi-Biennial Oscillations 27

Solar Electromagnetic Radiation Effects 67

Solar Wind and Corpuscular Effects 119

Circulation 156

Atmospheric Electricity 168

Lower Ionosphere 183

Author Index, Part 1 244

Part 2:

MASH Workshop, Williamsburg, 1986 245